

# **Molecular Design, Synthesis, and Evaluation of Chemical Biology Tools**

**Jorin Hoogenboom**

## **Thesis committee**

### **Promotor**

Prof. Dr H. Zuilhof  
Professor of Organic Chemistry  
Wageningen University

### **Co-promotor**

Dr T. Wennekes  
Assistant professor, Chemical Glycobiology  
Utrecht University

### **Other members**

Prof. Dr D. Weijers, Wageningen University  
Prof. Dr A. J. Minnaard, University of Groningen  
Dr E. Ruijter, VU University Amsterdam  
Prof. Dr V. Wittmann, Universität Konstanz, Germany

This research was conducted under the auspices of the Graduate School VLAG (Advanced studies in Food Technology, Agrobiotechnology, Nutrition and Health Sciences).

# **Molecular Design, Synthesis, and Evaluation of Chemical Biology Tools**

**Jorin Hoogenboom**

## **Thesis**

submitted in fulfilment of the requirements for the degree of doctor

at Wageningen University

by the authority of the Rector Magnificus

Prof. Dr A.P.J. Mol,

in the presence of the

Thesis Committee appointed by the Academic Board

to be defended in public

on Friday 17 March 2017

at 4 p.m. in the Aula

Jorin Hoogenboom

Molecular Design, Synthesis and Evaluation of Chemical Biology Tools  
206 pages.

PhD thesis, Wageningen University, Wageningen, NL (2017)

With references, with summary in English

ISBN 978-94-6343-038-8

DOI <http://dx.doi.org/10.18174/400232>



# Table of contents

<b>List of abbreviations</b>	<b>6</b>
<b>Chapter 1:</b> General Introduction	<b>8</b>
<b>Chapter 2:</b> Versatile Scope of a Masked Aldehyde Nitrone in 1,3-Dipolar Cycloadditions	<b>24</b>
<b>Chapter 3:</b> Exploring the Chemistry of Bicyclic Isoxazolidines for the Multicomponent Synthesis of Glycomimetic Building Blocks	<b>48</b>
<b>Chapter 4:</b> Synthesis of a Carbocyclic Activity-Based Probe for Sialidases	<b>78</b>
<b>Chapter 5:</b> Synthesis and Evaluation of Locostatin-Based Chemical Probes towards PEBP-Proteins	<b>106</b>
<b>Chapter 6:</b> Direct Imaging of Glycans in Arabidopsis Roots via Click Labeling of Metabolically Incorporated Azido-Monosaccharides	<b>122</b>
<b>Chapter 7:</b> General Discussion and Future Perspectives	<b>144</b>
<b>Appendix A:</b> Supporting Information for Chapter 2	<b>166</b>
<b>Appendix B:</b> Supporting Information for Chapter 3	<b>170</b>
<b>Appendix C:</b> Supporting Information for Chapter 4	<b>176</b>
<b>Appendix D:</b> Supporting Information for Chapter 5	<b>180</b>
<b>Appendix E:</b> Supporting Information for Chapter 6	<b>184</b>
<b>Appendix F:</b> Supporting Information for Chapter 7	<b>192</b>
<b>Summary</b>	<b>194</b>
<b>Acknowledgements</b>	<b>198</b>
<b>List of Publications</b>	<b>202</b>
<b>About the author</b>	<b>203</b>
<b>Overview of completed training activities</b>	<b>204</b>

## Abbreviations

3CR	three-component reaction	dd	doublet of doublet
ABP	activity-based probe	ddd	doublet of doublet of doublet
ABPP	activity based protein profiling	dddd	doublet of doublet of doublet of doublet
Ac	acetyl	DFT	density functional theory
Ac <sub>3</sub> ArabAz	1,2,3, Tri- <i>O</i> -acetyl-5-azido-5-deoxy-L-arabinofuranose	DiBAL-H	di-isobutylaluminiumhydride
Ac <sub>4</sub> FucAz	1,2,3,4-tetra- <i>O</i> -acetyl-6-azido-L-fucose	DMF	<i>N,N</i> -dimethylformamide
Ac <sub>4</sub> GalNAz	1,3,4,4-tetra- <i>O</i> -acetyl- <i>N</i> -azidoacetyl- $\alpha,\beta$ -D-galactosamine	DMSO	dimethylsulfoxide
Ac <sub>4</sub> GlcNAz	1,3,4,4-tetra- <i>O</i> -acetyl- <i>N</i> -azidoacetyl- $\alpha,\beta$ -D-glucosamine	DNA	deoxyribonucleic acid
Ac <sub>4</sub> ManNAz	1,3,4,4-tetra- <i>O</i> -acetyl- <i>N</i> -azidoacetyl- $\alpha,\beta$ -D-mannosamine	dsRED	<i>Discosoma</i> sp. red fluorescent protein
ADC	antibody-drug conjugate	dt	doublet of triplets
AMP	5-(adamantan-1-yl-methoxy)-pentyl	DTT	dithiothreitol
aq.	aqueous	e.g.	<i>exempli gratia</i> (for example)
Ar	aromatic	EDC	1-ethyl-3-(3-dimethylaminopropyl)carbodiimide
Arab	arabinose	equiv	equivalents
Araf	L-arabinofuranose	ER	endoplasmic reticulum
Arap	L-arabinopyranose	ERT	enzyme replacement therapy
Az	azidoacetyl	ESI	electron spray ionization
BCN	bicyclo[6.1.0]non-4-yne	Et	ethyl
BIOS	biology-oriented synthesis	et al.	<i>et alii</i> (and others)
Bn	benzyl	EtOAc	ethylacetate
Boc	<i>tert</i> -butoxycarbonyl	EtOH	ethanol
bPEBP	bovine PEBP	Fmoc	9H-fluoren-9-ylmethoxycarbonyl
br	broad	FT	FLOWERING LOCUS T
Bu	butyl	FT-IR	fourier transform infrared spectroscopy
Bz	benzoyl	Fuc	fucose
calcd	calculated	g	gram
cat.	catalyst	GalNAc	<i>N</i> -acetyl-D-galactosamine
Cbz	carboxybenzyl	GalNAz	<i>N</i> -azidoacetyl galactosamine
cDNA	complementary DNA	GBA1	glucocerebrosidase 1
CEN	Centrodialis	GBA2	$\beta$ -glucosidase 2
CLV3	CLAVATA3	GC	gas chromatography
Col-0	Columbia	gen.	generation
COSY	correlation spectroscopy	GFP	green fluorescent protein
CSA	camphorsulfonic acid	Glc	glucose
CuAAC	copper(I)-catalyzed alkyne-azide cycloaddition	GlcA	glucuronic acid
d	doublet	GlcNAz	<i>N</i> -azidoacetylglucosamine
DANA	2-deoxy-2,3-dihydro- <i>N</i> -acylneuraminic acid	GlcNCyc	1,3,4,4-tetra- <i>O</i> -acetyl- <i>N</i> -methylcyclopropene- $\alpha,\beta$ -D-glucosamine
DBCO	dibenzocyclooctyne	GST	glutathione S-transferase
DBCO	dibenzocyclooctyne	h	hour
DCM	dichloromethane	HG-II	Hoveyda-Grubbs catalyst 2 <sup>nd</sup> generation

HIV	human immunodeficiency virus	PCT	pharmacologic-chaperone therapy
HOBt	1-hydroxybenzotriazole	Pd/C	palladium on activated charcoal
HPLC	high performance liquid chromatography	PDC	pyridinium dichromate
HRMS	high resolution mass spectrometry	PEBP	phosphatidyl ethanolamine-binding proteins
HSQC	heteronuclear single quantum coherence spectroscopy	PEG	polyethylene glycol
Hz	hertz	Ph	phenyl
IC <sub>50</sub>	inhibitor concentration resulting in 50% of enzyme activity	PI	propidium iodide
invDA	inverse electron demand Diels-Alder	ppm	parts per million
IR	infrared	q	quartet
<i>J</i>	coupling constant	Raney-Ni	Raney-Nickel
kDa	kilo Dalton	RCM	ring-closing metathesis
KDO	3-deoxy-D-manno-oct-2-ulosonic acid	<i>R<sub>f</sub></i>	retardation factor
L	liter(s)	RGP	reversibly glycosylated protein
LD	long day	RKIP	Raf kinase inhibitory protein
LRMS	low resolution mass spectrometry	rt	room temperature
LSD	lysosomal storage disorder	s	singlet
<i>m</i>	<i>meta</i>	sat.	saturated
M	molar(s)	SAWM	Staudinger/aza-Wittig/Mannich
m	multiplet	SAWU	Staudinger/aza-Wittig/Ugi
m/z	mass over charge ratio	SAWU-3CR	Staudinger/aza-Wittig/Ugi three-component reaction
ManNAc	<i>N</i> -acetylmannosamine	SD	short day
Me	methyl	SPAAC	strain promoted azido-alkyne click chemistry
MeOH	methanol	Su	succinimide
mg	milligram(s)	<i>t</i>	tertiary
MHz	megahertz	t	triplet
min	minutes	TBAF	tetra- <i>n</i> -butylammonium fluoride
mL	milliliters(s)	TBDPS	<i>tert</i> -butyldiphenylsilyl
mmol	millimol(s)	<i>t</i> Bu	<i>tert</i> -butyl
MOE	metabolic oligosaccharide engineering	TEMPO	2,2,6,6-tetramethyl-1-piperdinyloxy (free radical)
MS	Murashige and Skoog medium	<i>tert</i>	tertiary
Ms	methanesulfonyl (mesyl)	TES	triethylsilyl
MS	mass spectrometry	TFA	trifluoroacetic acid
NaH	sodium hydride	TFE	2,2,2-trifluoroethanol
NEU1	<i>N</i> -acetyl- $\alpha$ -neuraminidase-1	THF	tetrahydrofuran
NEU2	<i>N</i> -acetyl- $\alpha$ -neuraminidase-2	TLC	thin layer chromatography
NEU3	<i>N</i> -acetyl- $\alpha$ -neuraminidase-3	TMS	trimethylsilyl
NEU4	<i>N</i> -acetyl- $\alpha$ -neuraminidase-4	TMSOTf	trimethylsilyl trifluoromethanesulfonate
Neu5Ac	<i>N</i> -acetylneuraminic acid	Ts	<i>para</i> -toluenesulfonyl (tosyl)
NMR	nuclear magnetic resonance	UAM	UDP-Ara mutase
NOE	nuclear Overhauser effect	UDP	uridine diphosphate
NOESY	nuclear Overhauser enhancement spectroscopy	UXE	UDP-xylose 4-epimerase
<i>o</i>	<i>ortho</i>	UXS	UDP-Xyl Synthase
<i>p</i>	<i>para</i>	WUS	WUSHEL
PCC	pyridinium chlorochromate	Xyl	xylose

# Chapter 1



## General Introduction

This thesis narrates a journey that took place in synthetic organic chemistry, and which had a destination in chemical biology. Before we venture into chemical biology: what is synthetic organic chemistry? Synthetic organic chemistry concerns the engineering of molecules. Engineering resembles chemistry in many ways, as it is concerned with design, manufacture and application of efficient and economical structures. In engineering these structures are typically of the mechanical sort, while in chemistry we think in the same way about molecules. How do we design molecules, how can we produce them, and how do we apply them in an efficient and (economically) justifiable way?

How do we design molecules? Before this question can be answered we should first deal with another question. What do molecules look like? Molecules are obviously too small to see with our own eyes, which meant that in the past scientists had to distinguish molecules based on the physical properties of very, very large quantities of molecules. Furthermore, as advanced techniques were initially not available, early chemists relied on their own senses –like taste, smell and sight– to categorize and identify chemical entities. It is therefore not so surprising that certain assumptions in the past were based solely on these senses. For example, in the 17<sup>th</sup> century an (al)chemist believed that urine, possessing a golden color, contained gold and set out to isolate it.<sup>1</sup> As absurd as this obviously crazy idea is in our modern-day eyes, this process did lead to something completely unexpected, namely the discovery of a new element, phosphorus. This is an example of serendipity, the phenomenon that a critically open-minded person can make important discoveries that he/she was originally not looking for. Many modern-day discoveries occurred through this phenomenon, exemplified by the accidental discovery of polymers, microwaves, penicillin, etc. Even these days we can still be surprised by what kind of molecules exist in nature and how they look. Modern-day chemistry dates back to the nineteenth-century with the synthesis of urea by Frederick Wöhler in 1828 (Figure 1), which like many major discoveries, was accidental.<sup>2</sup>

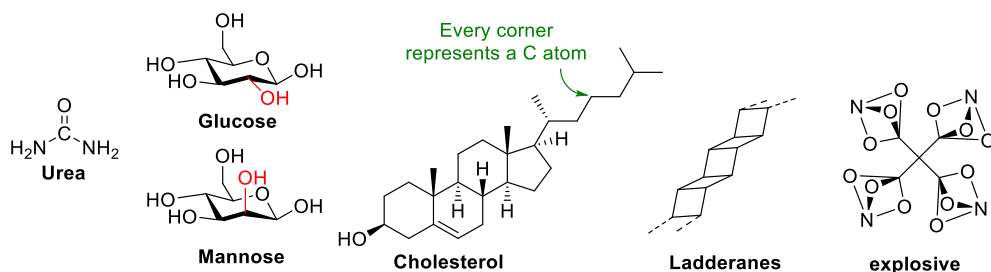
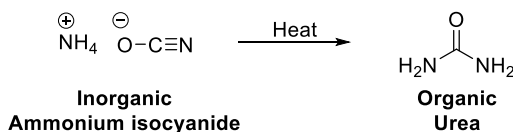


**Figure 1.** A selection of historical accomplishments in the identification and/or synthesis of organic molecules.

Urea was known in 1828 as a classical organic compound, since it was produced by animals. At the time it was believed that *organic* molecules could only be produced by living *organisms*, as contrasted to substances from nonliving, mineral sources, which were termed inorganic molecules.<sup>3</sup> Inorganic substances, such as minerals and metallic elements, were perceived as being much simpler than organic molecules such as sugars, starch and animal fat. These

views were part of the theory of vitalism, which included the premise that inorganic and organic chemistry were governed by opposing forces and that organic molecules could not be synthesized in the laboratory, at least not from inorganic materials. Consequently, at the time scientists were surprised by Wöhler's discovery that an organic molecule, ureum, could be synthesized from an inorganic molecule through "mere chemistry", and could thus duplicate a product of nature (Scheme 1).<sup>3</sup>

**Scheme 1.** The Wöhler synthesis of Urea. The first synthesis of an organic molecule in the laboratory.



The synthesis of urea marked the end of the theory of vitalism and the beginning of the field of synthetic organic chemistry, which deals with the design, analysis and construction of molecules of nature and other organic molecules and materials, i.e., matter in its various forms that contain carbon atoms.<sup>4-5</sup>

Urea, like many of the early synthesized molecules, is planar, so it is not surprising that it was not until the end of the 19<sup>th</sup> century that the scientific community accepted that molecules can have three-dimensional structures. An example of a molecule that is oriented in three dimensions is D-glucose (Figure 1), the primary metabolic fuel in animals. A different sugar, mannose, looks like glucose, but has a single chemical bond that is oriented differently in space (Figure 1). This apparently small change has a big impact on its biological function. Notably, while non-toxic for humans, D-mannose is lethal for honeybees and can blind baby mice.<sup>6-7</sup> The recognition that molecules can have three-dimensional structures and the discovery of more advanced analytical techniques (like NMR spectroscopy), enabled the synthesis of increasingly complex molecules in the 20<sup>th</sup> century such as cholesterol (Figure 1). Scientists have been interested in the structure of cholesterol since 1859, but it proved difficult to acquire the structure of this molecule. Proof of the structure was obtained in large part through the brilliant work of Heinrich Wieland and Adolf Windaus. Ironically, while Adolf Windaus was awarded the 1928 Nobel prize in chemistry for his work on steroids (including cholesterol), the structure of cholesterol he suggested was incorrect.<sup>8-9</sup> The true structure of cholesterol was proposed in 1932,<sup>9-10</sup> but could only be confirmed in 1945 through X-ray crystallography.<sup>11</sup> This technique, based on the scattering of a beam of X-rays, allows scientists to produce three-dimensional structures of crystalline molecules. Furthermore, the development of new analytical techniques in the 20<sup>th</sup> and 21<sup>st</sup> century have finally allowed chemists to 'see' molecules.<sup>12</sup> While molecules are too small to see by eye or any optical microscope, the discovery of advanced probing techniques like atomic force microscopy and scanning tunneling microscopy enabled the visualization of pentacene in a manner that is best described as 'feeling', providing images as shown in Figure 2.

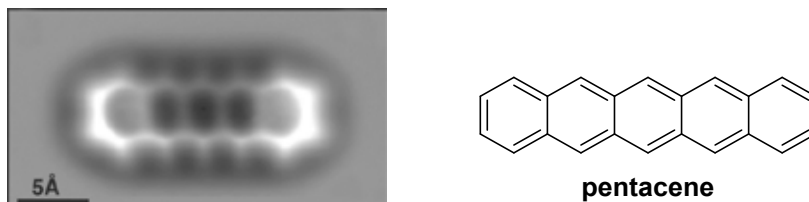


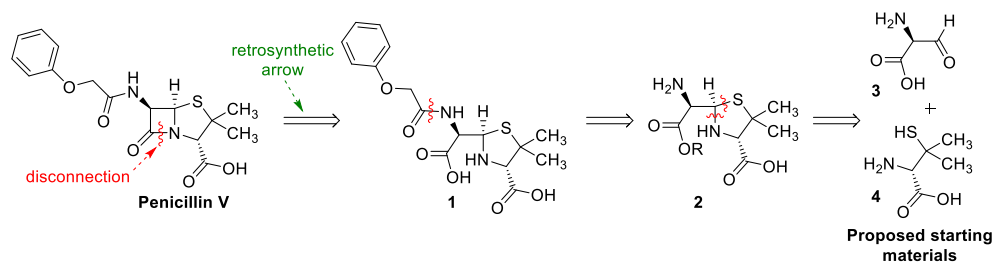
**Figure 2.** An image of the structure of pentacene obtained through atomic force microscopy (left) and a model of pentacene (right).

The plethora of available analytical techniques allows characterization of all but the most complicated molecules. Nevertheless, in the 21<sup>st</sup> century chemists are occasionally still surprised by the discovery of strange natural products, like ladderanes (Figure 1).<sup>13</sup> As such, nature keeps surprising chemists by showing different ways in which atoms can be arranged. Occasionally, however, it is not nature that inspires scientist, but children. For instance, a ten-year-old girl made a model of a completely novel, but also potentially viable molecule in her elementary school science class. This molecule, so-called tetranitratoxycarbon (Figure 1) was predicted to be a highly explosive chemical.<sup>14</sup> Although this molecule has not yet been synthesized, it was calculated that this molecule is probably stable at room temperature.<sup>15</sup> Predictions like these became possible due to the establishment of the basic chemical principles in the past two centuries. These principles are also used in a subdiscipline of chemistry known as synthetic organic chemistry, which deals with the science of constructing molecules, natural or designed, whose primary structural element is carbon. The following paragraphs will emphasize the different aspects of synthetic organic chemistry, starting with design.

## How do we design molecules?

The 2016 Nobel Prize in Chemistry was awarded to Sir J. Fraser Stoddart, Jean-Pierre Sauvage and Bernard L. Feringa for their design and production of molecular machines.<sup>16</sup> Through their work these researchers showed that synthetic organic chemistry does not only enable the engineering of molecules in the figurative sense, but also in the literal sense by engineering mechanical constructs like molecular motors<sup>17-19</sup> and a nanocar<sup>20-22</sup> at the molecular level. How then do synthetic chemists go about “engineering” molecules?

Several strategies exist for the design and synthesis of complex molecules and analogs thereof. Complex molecules are often not only inspired by molecules from nature, but are often also derived from them. The synthesis of these natural products is probably as old as the field of total synthesis, which concerns the complete synthesis of a complex molecule – often a natural product, such as penicillins – from simple, commercially available starting materials. Penicillin V (Scheme 2) is one of the first antibiotics that could be effectively used against many bacterial infections, but how do chemists go about synthesizing a natural product like penicillin V?

**Scheme 2.** A retrosynthetic analysis of penicillin V, essential to the design of complex molecules.

Synthetic design starts with the structure of the target product, which is fixed and unchangeable, and works backwards to identify simple building blocks, the starting materials. This process is known as retrosynthetic analysis. This technique utilizes a dedicated symbol when describing a reaction in reverse, called a retrosynthetic arrow (Scheme 2). Basically, this arrow translates as: ‘it should be possible to make this compound from the next one’. Accordingly, these arrows are used to visualize one or several retrosynthetic analysis steps, which ultimately leads to simple commercially available starting materials as depicted in Scheme 2. Retrosynthetic analysis involves breaking a molecule into its component parts, which is known as a disconnection, and is indicated by a wiggly line as shown above. The first disconnection made in Scheme 2 involves the C-N bond, because this disconnection corresponds to a reliable reaction: amide-bond formation. An amide can be made from a carboxylic acid and an amine, which are both present in intermediate **1**. Key to disconnections is that they should correspond to known and reliable reactions for the formation of the disconnected bond. For example, intermediate **1** can be obtained through another reliable amide-bond formation and the corresponding C-N disconnection provides intermediate **2**. In addition, this intermediate may be obtained through a well-known condensation reaction between an aldehyde and a thiolamine such as **3** and **4**, which were the starting materials used for the first total synthesis of penicillin V.<sup>23-24</sup> The retrosynthesis-guided design of natural products illustrates that synthetic chemistry is above all a creative science, as imagination and inspiration are required to develop short and elegant synthetic routes for complex molecules.

The value of natural products like penicillin makes them a good starting point for the synthesis of analogs that might possess improved properties. The synthesis of analogs of natural products may be enabled through the development of a total synthesis route, since modifications are possible on advanced intermediates. For example, different analogs of penicillin can be obtained by functionalizing intermediate **2** – the original intermediate towards penicillin V – with different ‘carboxylic acids’ (C(=O)OH) to obtain a library of related compounds (**1a-x**) (Scheme 3).<sup>23-24</sup>



NC1C(=O)N(C(=O)O)S1C(C)C (2) + RC(=O)O  $\rightleftharpoons$  NC(=O)R1C(=O)N(C(=O)O)S1C(C)C (1a-x)  $\rightarrow$  Penicillin core

**Penicillin V:** R = Ph-O-CH<sub>2</sub>-  
**Penicillin G:** R = Ph-CH<sub>2</sub>-

obtain these bioactive compounds through total synthesis. For instance, in 2016, Tong and coworkers reported the total synthesis of two styryl lactones - Parvistone D and E - in 18 steps.<sup>31</sup> Later that year Rao et al. reported the synthesis of several styryl lactones, including Parvistone D and E, through an biosynthesis-inspired route, which required only 5 steps with high overall yields (72-75%).<sup>27</sup>

In summary, several strategies exist to design the construction of a desired complex molecule, and the above section described these strategies with representative examples. Still, the design of these molecules raises another question: “How are these molecular designs actually transformed into real materials in a research laboratory”?

## How do we make molecules?

The proper design of a synthetic route for a target compound is only half the work; ultimately reactions have to be carried out to validate and optimize a synthetic route. Although proper literature preparations can prevent many setbacks, it is not uncommon for reactions to fail, which is why chemists usually conduct new reactions on as small a scale as possible. This is so that, should the reaction fail, the costs and risks are limited. Small scale reactions (milligram-gram) to medium-scale (gram-multigram) reactions are typically carried out in round-bottom flasks as depicted in Figure 4.

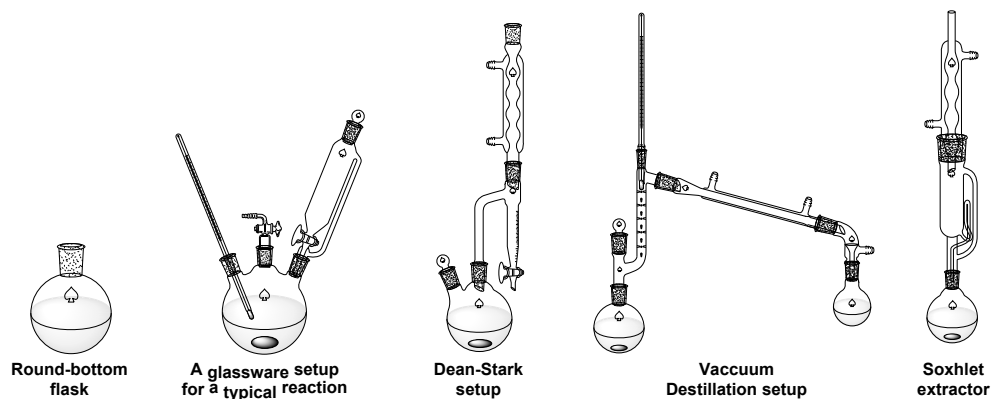


**Figure 4.** Different laboratory setups, illustrating the modular nature of modern-day laboratory glassware.

The reason that these flasks are typically made of glass is because many reactions involve very reactive or corrosive reagents, whereas glass displays a high chemical inertness. Modern day reaction flasks are made of borosilicate glass to make them heat-resistant, allowing quick heating up to +232 degrees Celsius and cooling to temperatures well below freezing. Modern-day glassware is also very modular, which is important since many reactions have to be run under an inert atmosphere of nitrogen or argon, are operated at temperatures other than room temperature and might require addition of reagents without exposing the reaction to

the atmosphere. These requirements are well served by multi-neck round-bottom flasks. For example, a three-neck flask may be connected to an inert atmosphere via a gas inlet, fitted with a dropping funnel or a rubber septum for addition of reagents, and fitted with a thermometer that extends into the reaction solvent (Figure 4).

Once a synthetic experiment has been initiated it is essential to follow the progress of the reaction. The reaction can be monitored in several ways. Analysis of a reaction can be straightforward and may rely on observing simple physical changes (temperature, color, precipitation or dissolution) that signal that a reaction has occurred. However, typically reactions are monitored using different laboratory techniques that separate the reaction mixture into its components (TLC, GC, HPLC) or by using analytical techniques like NMR and mass spectroscopy to analyze reaction progression.

If the analysis of the reaction ideally indicates good product conversion, then next the product needs to be isolated. The main purpose of workup (product isolation) is to remove solvent, excess reagents and sideproducts to enable further handling of the product. Product workup involves at least one, but typically several phases and routinely involves extraction, drying, filtration, and evaporation steps. The execution of these steps requires planning of the workup, since different aspects are important for product isolation. For instance, certain reactions (e.g.  $\text{LiAlH}_4$  reductions) are notorious for their tendency to form emulsions, making product isolation through extraction difficult. However, this problem can be circumvented by using a base during workup. For example, using basic NaOH converts aluminate salts into aluminum oxide, which can be easily filtered off, allowing facile extraction. Alternatively, another strategy to break up aluminum emulsions that does not involve a strong base involves using a solution of Rochelle's salt (sodium potassium tartrate), which is an excellent ligand for aluminum and breaks the aluminum emulsion.

Product workup usually does not produce a single pure compound. It is therefore often necessary to undertake additional purification. Several purification techniques may be carried out depending on the characteristics of the product and the nature of the contaminating substances. For example, distillation allows separation of non-volatile materials from volatiles, and in more detail: of compounds with different boiling points. However, distillation is often not applicable to complex compounds as these might have boiling points that are too high to be practically used, but when it is applicable, distillation can be an excellent purification method. Another purification method is crystallization, which is typically applicable on both small scales and on an industrial scale if the product is a solid and good crystallization conditions can be found. Finally, the workhorse purification technique is column chromatography. This technique is by far the most widely used method of product purification, because it is so general and because it is a natural outgrowth of the analysis of reaction mixtures by TLC. Similar to TLC, column chromatography separates compounds based on their ability to interact with a stationary phase in the column and their solubility in the eluent.

Purification is typically followed by structure elucidation, since it has to be verified whether the product has indeed been synthesized. Alternatively, reactions may provide an unexpected sideproduct and structure determination of this byproduct could aid in elucidating the nature of the corresponding side reaction. Structure elucidation can be undertaken through several techniques such as MS, NMR, IR. Of these, for low-to-intermediate weight organic compounds NMR is more important than all the rest put together, as it is not uncommon in discovery chemistry that new compounds can be identified solely based on NMR data. Mass spectrometry (MS) is a technique that weighs the molecule. The advantage of MS is that it can be routinely coupled to other instruments like HPLC and GC, which allows separation of different isomers or compounds with the same (isobaric) mass. Infrared spectroscopy (IR) has fallen into disuse in some laboratories due to the great advances in NMR and MS techniques. However, some questions are ideally answered through IR. For example, it is relatively straightforward to determine the presence of certain functional groups through IR, such as acid derivatives (ketone, aldehyde, ester, amide) and azides, each possessing a characteristic location in IR spectra. Furthermore, the advantage of IR is that limited to no sample preparation is required. In fact, a sparsely used, but valuable trick is to directly use NMR samples for IR measurements, as the most common NMR solvent ( $\text{CDCl}_3$ ) quickly evaporates leaving a thin film of product.

Reaction optimization is usually required for new reactions and often also for existing literature procedures. The initial outcome of a reaction is often lacking in sufficient yield or in another way (purity, time, convenience). A cliché of the scientific community is “change only one variable at a time”, which is used for deductive reasoning, but in synthetic organic chemistry this advice is much less useful. The reason for this is that synthetic organic chemistry often relies on inductive investigations. In short, inductive investigation reasons from particular observations to general theories. For example, if you observe enough apples falling from trees, you will conclude that apples will always fall to the earth, instead of up or sideways. For chemistry, this kind of investigations can be readily-illustrated through a well-known 3D plot illustrating the outcome of a reaction as a result of two variables (Figure 5). Statistical methods exist to design and interpret experiments involving multiple variables, which could help limit the amount of experiment that have to be performed to find optimal reaction conditions. Changing only one variable at a time could not only be more time-consuming, but could also lead to false assumptions. For example, as shown in Figure 5, an experimenter that would only look at the reaction after 90 minutes would (falsely) conclude that the temperature should not exceed 60 °C to get an optimal yield, since being restricted to only changing the temperature means being limited in the movement along this axis in the plot.

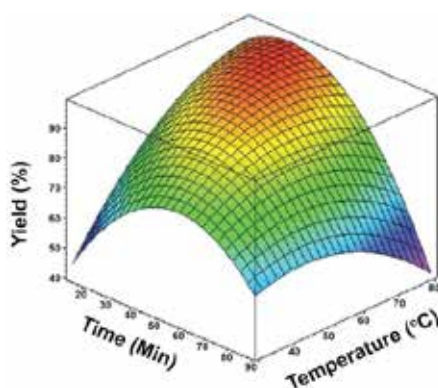


**Figure 5.** A three-dimensional surface plot representing the outcome of many experiments.

## How do we apply molecules? And what is chemical biology?

As important as it is to advance the field of synthetic organic chemistry, equally important is the objective to apply synthesis to obtain unique and functional molecules for biological investigations.<sup>32</sup> Throughout history, total synthesis has aided in the identification and investigation of novel drugs.<sup>5, 33-34</sup> In addition, as described above, existing drugs could be optimized through derivatization by synthesizing a library of related compounds, leading to the development of new drugs (e.g. antibiotics).

Efforts at the interface of synthetic organic chemistry and biology have intensified in the last few decades, which has led to the emergence of new subdisciplines in chemistry and biology. For instance, in addition to the well-established fields of medicinal chemistry and biochemistry a relatively new discipline has developed along the interface of chemistry and biology, chemical biology. The classical definition of this area of research is the use of synthetic organic chemistry to create small-molecule probes of biological processes.<sup>35</sup> Probing biological processes was popularized by Roger Tsien's work on the development of fluorescence-based sensors of calcium concentrations in whole organisms as well as his pioneering use of green-fluorescent proteins, for which he was awarded the 2008 Nobel Prize in chemistry.<sup>36</sup>

Molecular imaging and other novel techniques enabled chemical biologists to learn about biological systems and their properties in ways that scientists from other fields cannot.<sup>37</sup> Furthermore, chemical biology has not only provided new technologies and tools to study new drug targets, but has also affected drug development of the fastest growing class of human drugs, i.e. those based on antibodies.<sup>38-40</sup> Antibodies are Y-shaped proteins produced by our white blood cells to identify and neutralize pathogens such as viruses and bacteria. These antibodies are capable in recognizing and binding a unique molecule – called an antigen – on

these pathogens. This highly selective binding of antigens can also be used to combat cancer, as cancer cells are more likely to develop genetic faults that may give rise to tumor-specific antigens. In other words, antigens can be found on the surface of tumors that are not or hardly present on normal cells.<sup>41</sup> The rise of chemical biology has helped revolutionize the field of cancer chemotherapy by developing new classes of antibody-based drugs known as antibody-drug conjugates (ADCs).<sup>42-44</sup> ADCs represent an innovative therapeutic application that combines the unique, highly specific properties of antibodies that are tumor-specific, with the potent cell-killing activity of cytotoxic small molecule drugs that are too toxic to be used on their own. In linking antibodies with cytotoxic agents, chemical biologist have been able to optimize the features of both components, which has already led to two marketed ADCs in the clinic.<sup>43</sup> Furthermore, the list of ADCs is growing with more than 40 ADCs in various phase of clinical development.<sup>43, 45</sup>

The developments of ADCs and other important contributions have shown that the field of chemical biology has grown beyond its classical definition.<sup>35, 37</sup> However, the broad application of chemical biology tools and technologies has made it difficult for scientist to agree on a precise definition for this field.<sup>35</sup> Still, a fitting if not precise wording of chemical biology was recently presented by prof. Carolyn Bertozzi, a leading investigator in this field,<sup>35</sup> as the area of research in which chemical and biological concepts and tools interact synergistically in the pursuit of new discoveries or technologies.

## **Chemical Biology and activity-based protein profiling**

Aside from the development of novel drugs, chemical biology has also contributed to the identification of novel drug targets and to the development of diagnostic approaches. These developments were enabled through the development of tailor-made organic molecules and biocompatible reactions, which allowed the study of biological systems at the molecular level that elude more conventional methods of biological investigation. For instance, conformational diseases are often caused by mutations affecting protein folding and stability. To accurately diagnose and treat these enzyme-related diseases it is of paramount import to be able to quantify the amount of active enzyme in biological samples. However, while methods exist that can quantify the amount of enzyme expression, this does not automatically translate to the amount of active enzyme. A chemical biology approach that is capable of determining the amount of active enzyme is known as activity-based protein profiling (ABPP) (Figure 6).

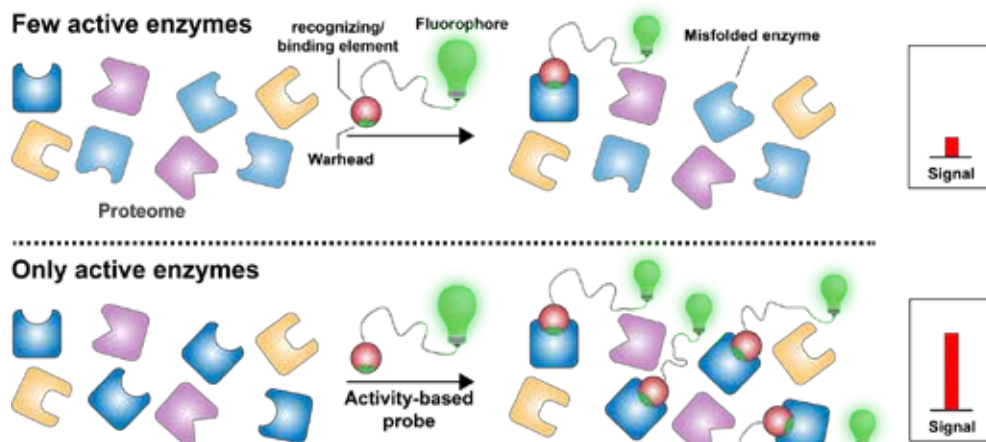


**Figure 6.** Activity-based protein profiling. (ABPP). ABPP probes label only active enzymes, not inactive enzymes or enzymes of a different class. Labeled enzymes are subsequently detected through fluorescence scanning after purification.

This technique employs chemical activity-based probes (ABPs). A common feature in the design of these probes is the presence of an electrophilic ‘warhead’ that can be attacked by nucleophilic functional groups, e.g. amines or thiols, found in the active site of the target protein. Selectivity is not induced by the inherent reactivity of these functional groups, however, but rather by an initial noncovalent recognition and binding step that positions the reactive warhead in close proximity of the active site. ABPP has attracted a lot of attention since the beginning of the 21<sup>st</sup> century. A notable example of the application of ABPP to study a disease that is the result of enzyme deficiency is the development of a very sensitive method to study Gaucher disease.<sup>46</sup> This disease is caused by a deficiency in an enzyme called glucocerebrosidase (GBA) and Overkleeft and coworkers reported on the design, synthesis and application of two fluorescent activity-based probes, which allowed the quantification of active GBA in living mice.<sup>46</sup>

These and similar studies into chemical biology generate increased understanding of biology, which paves the way for drug discovery and development, thereby decisively improving human health and well-being. Synthetic organic chemistry is optimally equipped to develop new tools for chemical biology. For example, the development of novel probes can help to address the study of different, difficult-to-treat diseases.<sup>47–48</sup> Furthermore, the scientific community has witnessed many breakthrough discoveries in chemical biology in its application in bacteria, viruses and mammals, but the plant kingdom, on which all life on earth largely depends, has been left underexplored.<sup>49</sup> Future application of chemical biology in plants could help increase the understanding of the biological processes related to plant health and development.

## Aim of this research

Synthetic organic chemistry has the power to reproduce the most intriguing and valuable molecules of living nature and to synthesize unique variations of them. The synthesis of these valuable natural products and their analogues finds application in biology and in medicine, as these molecules are often employed as leads in drug discovery, and do find application as chemical tools to study biological systems. The focus of this thesis is to develop novel synthetic strategies and technologies to aid the development of biological relevant molecules. Furthermore, this thesis will increasingly focus on the development and application of chemical tools to study biological systems.

## Outline of this thesis

This thesis focusses on the design, synthesis and evaluation of small molecular probes towards the study of proteins and glycans in plant and mammalian cells. Most of these probes are complex glycomimetic small molecules that in many instances are prepared with a nitron-olefin [3+2] cycloaddition as a key step.

The nitron-olefin [3+2] cycloaddition is a powerful tool in synthetic organic chemistry for the synthesis of a wide range of complex molecules. A key feature of this reaction is that it can be used to install three neighboring stereogenic centers in a single step. The power of this feature is illustrated by the synthesis of several classes of natural product such as vitamins<sup>50-51</sup> and alkaloids<sup>52-54</sup> – all complex molecules containing multiple neighboring chiral centers – through the nitron-olefin [3+2] cycloaddition. However, reactions involving small and easily accessible nitrones that show good regio- and stereoselectivity are typically limited in their synthetic applications. In **chapter 2**, we present a new and readily accessible masked aldehyde nitron for the facile synthesis of synthetically versatile cycloadducts.

In this thesis the nitron-olefin [3+2] cycloaddition is also described for the synthesis of glycomimetic building blocks. Glycomimetics such as iminosugars are found in nature and possess a variety of biological activities. The potential of glycomimetics has led to the development of drugs for the treatment of diseases and disorders such as type 2 diabetes, ADHD, Gaucher disease and HIV. **Chapter 3** describes how a versatile cycloadduct – obtained through a nitron-olefin [3+2] cycloaddition – can be modified selectively at each functional position to enable the synthesis of a series of different glycomimetic building blocks. In this way, we were able to make a library of pipercolic acid derivatives – a popular drug motif – via a one-pot Staudinger/aza-Wittig/Ugi three-component reaction.

**Chapter 4** describes the development of a route towards an ABP for the study of the enzymatic activity of neuraminidases. Neuraminidases are a class of enzymes found in a range of organisms including mammals, and their importance is illustrated by the existence



of a neuraminidase-related genetic disease, sialidosis. Similar to a related disease involving enzyme deficiency – Gaucher disease – the development of a neuraminidase-ABP would provide a diagnostic tool to study the activity of neuraminidases, and ultimately help to identify small molecules that could increase the activity of mutant neuraminidase molecules by stabilizing and/or promoting the folding of this enzyme. The synthesis of a carbocyclic neuraminidase ABP was the goal of chapter 4 and was approached by starting with the nitrone-olefin [3+2] cycloaddition as the key step. This reaction provided a bicyclic cycloadduct that was used for the development of a synthetic route that led to a high yielding and practical synthesis of an advanced intermediate possessing the majority of the stereochemistry of the required carbocyclic neuraminidase ABP.

**Chapter 5** describes the synthesis of chemical tools to study phosphatidyl ethanolamine-binding proteins (PEBPs), which is a family of proteins that is found in a variety of organisms including mammals and plants. Among this family is a plant-PEBP known as Flowering Locus T (FT), a vital protein acting as a flowering hormone in plants. No small molecule inhibitors for FT are known, but an inhibitor called locostatin has been reported to bind in the highly conserved ligand binding site of a structurally related PEBP protein in mammals. Based on this conservation and overall structural similarity it was hypothesized that locostatin or derivatives thereof could covalently bind FT and hence influence flowering. In chapter 5 we report the synthesis of novel locostatin-based chemical PEBP probes and evaluate their ability and selectivity towards the binding of FT and a mammalian PEBP.

**Chapter 6** presents another example of how synthetic organic chemistry can be used to develop smart tailor-made tools to study biological systems. Direct molecular imaging of glycans is a technique that has been broadly explored in animals for the past decades. In contrast, imaging of plant glycans has only recently caught the attention of the scientific community, despite that glycosylation is essential to plant health and development. To further expand our knowledge of plant glycobiology by direct imaging of their glycans, there is a need for click chemistry-compatible glycan analogs for other plant monosaccharides. In addition, the metabolic incorporations of monosaccharide analogs by the plant into its glycans reported so far use toxic copper-catalyzed labeling, and future applications would benefit from bio-orthogonal copper-free labeling techniques. Chapter 6 describes the investigation of the metabolic incorporation of five novel monosaccharide probes in *Arabidopsis thaliana* roots and their imaging after fluorescent labeling. Furthermore, we also show, for the first time in metabolic labeling and imaging of plant glycans, the potential of two copper-free click chemistry methods that are bio-orthogonal and lead to more uniform labeling.

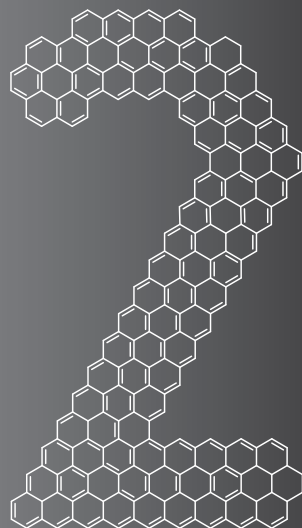
Finally, **chapter 7** contains a general discussion, critically summarizing the body of this thesis and providing insight in the possibilities of future research.

## REFERENCES

1. Bryson, B., *A Short History of Nearly Everything*. **2004**: Broadway Books.
2. Roberts, R.M., *Serendipity: Accidental Discoveries in Science*. **1989**: Wiley.
3. Lipman, T.O. *J. Chem. Educ.* **1964**, *41*, 452.
4. Jonathan Clayden, N.G., Stuart Warren, *Organic Chemistry*. Second Edition ed. **2012**: Oxford University Press.
5. Nicolaou, K.C. *Proceedings of the Royal Society A: Mathematical, Physical and Engineering Science* **2014**, 470.
6. Sharma, V., Ichikawa, M., and Freeze, H.H. *Biochem. Biophys. Res. Commun.* **2014**, *453*, 220.
7. Sharma, V., Nayak, J., DeRossi, C., Charbono, A., Ichikawa, M., Ng, B.G., Grajales-Esquivel, E., Srivastava, A., Wang, L., He, P., Scott, D.A., Russell, J., Contreras, E., Guess, C.M., Krajewski, S., Del Rio-Tsonis, K., and Freeze, H.H. *The FASEB Journal* **2014**, *28*, 1854.
8. Bernal, J.D. *Nature* **1932**, *129*, 277.
9. Bloch, K. *Trends Biochem. Sci* **1982**, *7*, 334.
10. Wieland, H. and Dane, E., Untersuchungen über die Konstitution der Gallensäuren. XXXIX. Mitteilung. Zur Kenntnis der 12-Oxy-cholansäure, in *Hoppe-Seyler's Zeitschrift für physiologische Chemie* **1932**. p. 268.
11. Carlisle, C.H. and Crowfoot, D. *Proc R Soc Lon Ser-A* **1945**, *184*, 64.
12. Gross, L., Mohn, F., Moll, N., Liljeroth, P., and Meyer, G. *Science* **2009**, *325*, 1110.
13. Damste, J.S.S., Strous, M., Rijpstra, W.I.C., Hopmans, E.C., Geenevasen, J.A.J., van Duin, A.C.T., van Niftrik, L.A., and Jetten, M.S.M. *Nature* **2002**, *419*, 708.
14. Zoellner, R.W., Lazen, C.L., and Boehr, K.M. *Computational and Theoretical Chemistry* **2012**, *979*, 33.
15. Buszek, R.J., Lindsay, C.M., and Boatz, J.A. *Propellants, Explosives, Pyrotechnics* **2013**, *38*, 9.
16. The Nobel Prize in Chemistry **2016**.
17. van Delden, R.A., ter Wiel, M.K.J., Pollard, M.M., Vicario, J., Koumura, N., and Feringa, B.L. *Nature* **2005**, *437*, 1337.
18. Koumura, N., Zijlstra, R.W.J., van Delden, R.A., Harada, N., and Feringa, B.L. *Nature* **1999**, *401*, 152.
19. Vachon, J., Carroll, G.T., Pollard, M.M., Mes, E.M., Brouwer, A.M., and Feringa, B.L. *Photochemical & Photobiological Sciences* **2014**, *13*, 241.
20. Shirai, Y., Osgood, A.J., Zhao, Y., Kelly, K.F., and Tour, J.M. *Nano Lett.* **2005**, *5*, 2330.
21. Morin, J.-F., Shirai, Y., and Tour, J.M. *Org. Lett.* **2006**, *8*, 1713.
22. Kudernac, T., Ruangsapichat, N., Parschau, M., Macia, B., Katsonis, N., Harutyunyan, S.R., Ernst, K.-H., and Feringa, B.L. *Nature* **2011**, *479*, 208.
23. Sheehan, J.C. and Henery-Logan, K.R. *J. Am. Chem. Soc.* **1957**, *79*, 1262.
24. Sheehan, J.C. and Henery-Logan, K.R. *J. Am. Chem. Soc.* **1959**, *81*, 3089.
25. Wilson, R.M. and Danishefsky, S.J. *J. Org. Chem.* **2006**, *71*, 8329.
26. Maier, M.E. *Org. Biomol. Chem.* **2015**, *13*, 5302.
27. Ramesh, P. and Rao, T.P. *J. Nat. Prod.* **2016**, *79*, 2060.
28. Blázquez, M.A., Bermejo, A., Zafra-Polo, M.C., and Cortes, D. *Phytochem. Anal* **1999**, *10*, 161.

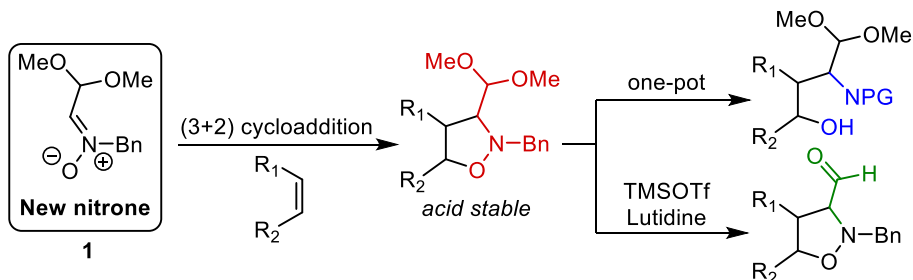
29. Mohd Ridzuan, M.A., Ruenruetai, U., Noor Rain, A., Khozirah, S., and Zakiah, I. *Trop Biomed* **2006**, 23, 140.
30. Mereyala, H. and Joe, M. *Current Medicinal Chemistry - Anti-Cancer Agents* **2001**, 1, 293.
31. Li, Z. and Tong, R. *Synthesis* **2016**, 48, 1630.
32. Nicolaou, K.C. *Chem* **2016**, 1, 331.
33. Nicolaou, K.C. and Snyder, S.A. *Proc. Natl. Acad. Sci. USA* **2004**, 101, 11929.
34. Yun, H., Chou, T.-C., Dong, H., Tian, Y., Li, Y.-m., and Danishefsky, S.J. *J. Org. Chem.* **2005**, 70, 10375.
35. *Nat. Chem. Biol.* **2015**, 11, 378.
36. The Nobel Prize in Chemistry **2008**.
37. *Nat. Chem. Biol.* **2015**, 11, 446.
38. Carter, P.J. *Nat Rev Immunol* **2006**, 6, 343.
39. Reichert, J.M., Rosensweig, C.J., Faden, L.B., and Dewitz, M.C. *Nat Biotech* **2005**, 23, 1073.
40. Jefferis, R. *Expert Opinion on Biological Therapy* **2007**, 7, 1401.
41. Sensi, M. and Anichini, A. *Clinical Cancer Research* **2006**, 12, 5023.
42. Peters, C. and Brown, S. *Biosci. Rep.* **2015**, 35.
43. Jain, N., Smith, S.W., Ghone, S., and Tomczuk, B. *Pharm. Res.* **2015**, 32, 3526.
44. Beck, A., Wagner-Rousset, E., Bussat, M.C., Lokteff, M., Klinguer-Hamour, C., Haeuw, J.F., Goetsch, L., Wurch, T., Van Dorsselaer, A., and Corvaia, N. *Curr. Pharm. Biotechnol.* **2008**, 9, 482.
45. Bakhtiar, R. *Biotechnol. Lett* **2016**, 38, 1655.
46. Witte, M.D., Kallemeijn, W.W., Aten, J., Li, K.Y., Strijland, A., Donker-Koopman, W.E., van den Nieuwendijk, A.M.C.H., Bleijlevens, B., Kramer, G., Florea, B.I., Hooibrink, B., Hollak, C.E.M., Ottenhoff, R., Boot, R.G., van der Marel, G.A., Overkleeft, H.S., and Aerts, J.M.F.G. *Nat. Chem. Biol.* **2010**, 6, 907.
47. Parenti, G., Andria, G., and Valenzano, K.J. *Mol Ther* **2015**, 23, 1138.
48. Suzuki, Y. *Proceedings of the Japan Academy, Series B* **2014**, 90, 145.
49. Sminia, T.J., Zuilhof, H., and Wennekes, T. *Carbohydr. Res.* **2016**, 435, 121.
50. Baggiolini, E.G., Lee, H.L., Pizzolato, G., and Uskokovic, M.R. *J. Am. Chem. Soc.* **1982**, 104, 6460.
51. Kato, Y., Nakano, Y., Sano, H., Tanatani, A., Kobayashi, H., Shimazawa, R., Koshino, H., Hashimoto, Y., and Nagasawa, K. *Bioorg. Med. Chem. Lett.* **2004**, 14, 2579.
52. Shimokawa, J., Shirai, K., Tanatani, A., Hashimoto, Y., and Nagasawa, K. *Angew. Chem. Int. Ed.* **2004**, 43, 1559.
53. Ina, H., Ito, M., and Kibayashi, C. *J. Org. Chem.* **1996**, 61, 1023.
54. Morin, M.S.T. and Arndtsen, B.A. *Org. Lett.* **2014**, 16, 1056.

## Chapter 2



# Versatile Scope of a Masked Aldehyde Nitron in 1,3-Dipolar Cycloadditions

## Abstract



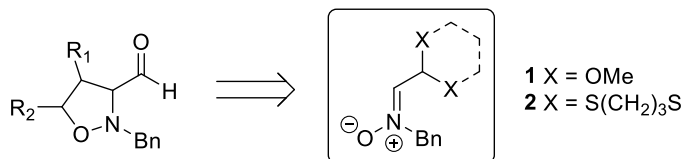
A new masked aldehyde-containing nitron **1** that is easily available through a facile one-step procedure has been developed. It undergoes a [3+2]-thermal cycloaddition with a wide range of dipolarophiles, affording isoxazolidine cycloadducts that are suitable for versatile post-cycloaddition modifications. The acetal-cycloadducts are acid-stable, but allow for acetal hydrolysis under mildly basic conditions. The isoxazolidine-ring can be opened via an efficient one-pot procedure to give amine-protected  $\gamma$ -alcohols that can be further converted to furanose derivatives

Part of this work was published in:

J. Hoogenboom, H. Zuilhof, T. Wennekes,  
*Org. Lett.*, **2015**, *17*, 5550

## Introduction

The nitrone–olefin [3+2] cycloaddition reaction is a powerful tool in organic chemistry for the stepwise construction of the backbone of a wide range of complex molecules.<sup>1</sup> A key feature of this reaction is that it allows for the introduction of three new stereogenic centers in a single step. For example, several classes of alkaloid derivatives<sup>2</sup> and non-natural amino acids<sup>3</sup> that contain multiple neighboring stereogenic centers have been synthesized using a [3+2] cycloaddition as a key step. Most examples of regio- and enantioselective cycloadditions that use structurally small and easily accessible nitrones, however, involve *C*- and/or *N*-aryl-substituted nitrones. This limits the options for subsequent synthetic modification of the cycloaddition product.<sup>4</sup> One of the few examples of easily accessible and simple nitrones that are more suitable for post-cycloaddition modification are  $\alpha$ -amino ester-derived nitrones, possessing a masked carboxylic acid and a deprotectable *N*-substituent.<sup>5</sup> In our ongoing synthetic investigations toward novel glycomimetics for studying phenomena in glycobiology<sup>6</sup> we required a small (masked) aldehyde-containing nitrone. However, to the best of our knowledge no precedent existed for such a compound, so we set out to develop one. We here present a new and readily accessible nitrone **1** (Figure 1) for the facile synthesis of synthetically versatile, masked aldehyde-containing cycloadducts.

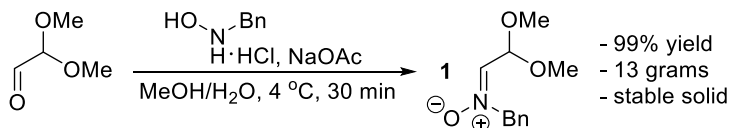


**Figure 1.** Nitrones possessing a masked aldehyde for the synthesis of versatile cycloadducts.

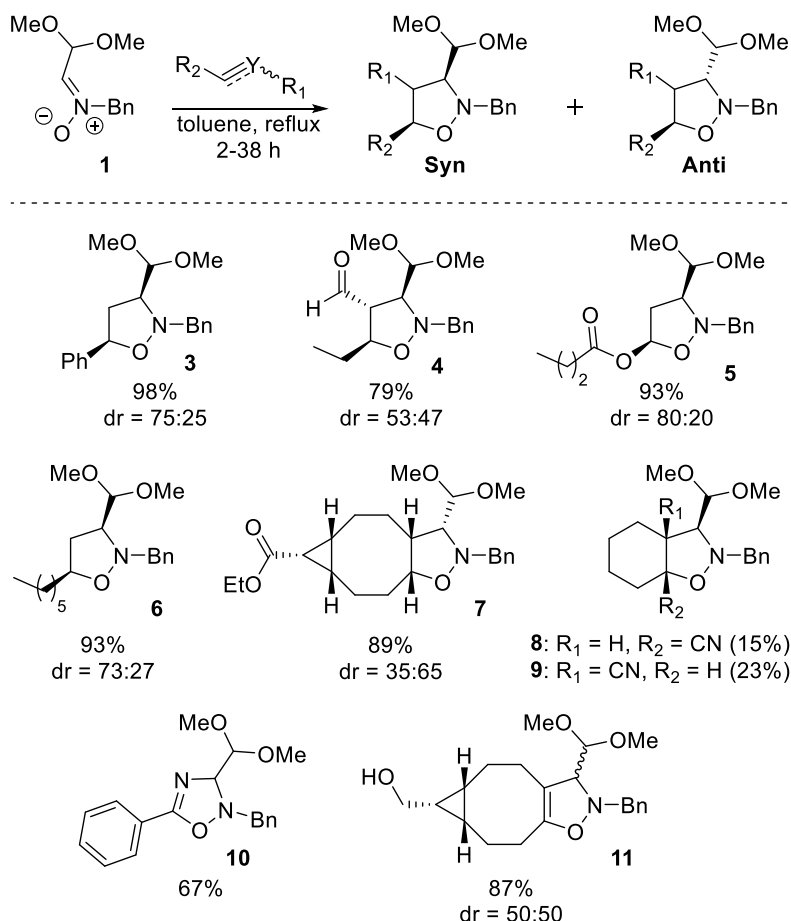
This nitrone displays selective reactivity with a wide range of 1,3-dipolarophiles combined with mild subsequent deprotection and derivatization of the resulting cycloadducts to allow further modification.

Initial efforts focused on the synthesis of nitrone **2**, containing a thioacetal, starting from 1,3-dithiane. We were able to obtain **2** via a two-step procedure in moderate yield. However, nitrone **2** proved to be ineffective for use in nitrone–olefin [3+2] cycloaddition reactions, as the nitrone was not reactive at low temperatures and quickly degraded upon heating (see Appendix A, Scheme S1).

The thermal instability of nitrone **2** in this reaction led us to focus on the synthesis of acetal **1** from readily available *N*-benzylhydroxylamine and dimethoxyacetaldehyde. These compounds reacted readily to give **1** in excellent yield on a multigram scale (Scheme 1). In addition, this reaction does not require a purification step, whereas similar nitrones that are synthesized in this fashion usually require purification through chromatography or crystallization.<sup>5a,7</sup> The purification step could be avoided by performing the reaction at 0 °C and performing a basic workup.

Scheme 1. Synthesis of nitrone **1**

An initial scope study of nitrone **1** in the 1,3-dipolar cycloaddition reaction with a variety of achiral olefins and other dipolarophiles was performed using a general reaction protocol (Scheme 2). The *syn/anti* stereoselectivity of the resulting cycloadducts was assigned using NOESY experiments (For a typical result see Appendix A, Figure S1-2).

Scheme 2. Substrate scope of nitrone **1** with different 1,3-dipolarophiles in [3+2] cycloaddition reactions<sup>a,b</sup>

<sup>a</sup>Isolated yield after column chromatography. <sup>b</sup>*Syn/anti* ratio determined by <sup>1</sup>H NMR and assigned by NOESY.

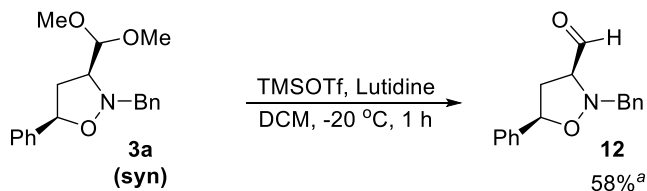
We observed that cycloadditions involving both electron-deficient (providing **3–4**) and electron-rich olefins (providing **5–6**) proceeded rapidly, leading to complete conversion within 2 h at 110 °C in toluene. For a sterically bulky, disubstituted alkene a longer reaction

time (38 h) was required to obtain cycloadduct **7** in good yield. A trisubstituted olefin also showed lower reactivity, but still gave complete conversion to products **8** and **9** after 2 days. The occurrence of two regioisomers (**8** and **9**), instead of the two *syn*- and *anti*-diastereomers observed in most cases, is common for cycloadditions with  $\alpha$ -alkyl trisubstituted olefins.<sup>8</sup>

After these encouraging results for nitrone **1** with olefins, we evaluated several different dipolarophiles such as nitriles and alkynes. First, **1** was reacted with benzonitrile, and selectively gave one major isomer (**10**) in good yield. Next, a cycloaddition with a cyclooctyne yielded cycloaddition product **11** within 5 min at rt. Cyclooctynes have recently been reported to react with nitrones in so-called SPANC click reactions.<sup>9</sup> The nitrones reported in literature for this click reaction with strained alkynes were either cyclic nitrones<sup>9a</sup> or produced cycloadducts possessing *N*-methyl groups,<sup>9b,9c</sup> complicating further modification compared to **11**. The cycloadditions described in Scheme 2 overall show that nitrone **1** allows for the synthesis of a variety of cycloadducts in reasonable to excellent yield, while tolerating a variety of functional groups, including esters, alcohols and aldehydes.

Encouraged by these results, we next attempted to liberate the aldehyde by selectively deprotecting the dimethyl acetal (Scheme 3). Surprisingly, when using typical acidic hydrolysis conditions no conversion was observed even after testing a variety of acidic conditions (e.g., TFA, HCOOH, HClO<sub>4</sub>). We hypothesize that protonation of the nitrogen atom in the isoxazolidine ring in close proximity to the acetal might be suppressing methoxy protonation and thus the acidic hydrolysis.

Scheme 3. Hydrolysis of isoxazolidine acetal **3a**



<sup>a</sup>Crude yield determined by <sup>1</sup>H NMR; isolated yield: 40%.

To validate this hypothesis, several neutral and basic conditions were tested for liberation of the aldehyde.<sup>10</sup> Neutral conditions using iodine, however, led to degradation, and TMS-I gave only minute amounts of product. In contrast, the use of TMSOTf under basic conditions gave the desired product in reasonable yield (Scheme 3). Even though many examples of similar acetal/ketal-substituted isoxazolidines exist in literature,<sup>11</sup> this is the first successful example of acetal hydrolysis on such a substrate.

We also wanted to identify conditions to selectively modify the N–O ring through hydrogenation, followed by an *in situ* protection of the liberated amine with a versatile set of protecting groups (Table 1). An initial hydrogenolysis attempt of substrate **3a** with Pd/C in MeOH under atmospheric pressure (entry 1) resulted in very slow conversion. Complete hydrogenation of **3a** was only observed after 3 days at rt, at which point significant degradation



had occurred. Degradation of **3a** might be caused by partial unwanted hydrogenation of the benzylic C–O bond in the isoxazolidine ring before desired cleavage of the N–O. This side reaction has been reported for similar compounds.<sup>12</sup> We therefore investigated whether the known ability of Raney-Ni to selectively cleave N–O bonds would prevent C–O hydrogenation. Hydrogenolysis with Raney-Ni indeed quantitatively cleaved the N–O bond of substrate **3a** within 1 h and left the C–O and N–Bn bonds intact. However, subsequent *N*-benzyl removal using transfer hydrogenation with refluxing cyclohexene, followed by *in situ* protection with Fmoc-OSu, gave **13** in only 21% yield (entry 2), probably due to thermal degradation of the starting material or intermediate during reflux. It was therefore decided to perform the second hydrogenation step under pressure in a Parr apparatus at rt. This allowed for the removal of the benzyl group in 5 h, and the resulting primary amine could be converted *in situ* to Fmoc-protected amine **13** in 80% yield (entry 3).

**Table 1.** Mild one-pot hydrogenation/protection optimization

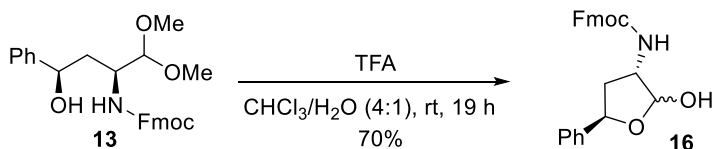
Reaction scheme: **3a** (syn)  $\xrightarrow[\text{one-pot}]{\text{i. Hydrogenation, ii. Protection}}$  **13-15**

entry	conditions <sup>a</sup>	reagent	R/protecting group	yield (%) <sup>b</sup>
1	A	Fmoc-OSu	$\text{H}$ –N–Fmoc ( <b>13</b> )	degr.
2	B	Fmoc-OSu	( <b>13</b> )	24
3	C	Fmoc-OSu	( <b>13</b> )	80
4	C	Boc <sub>2</sub> O	$\text{H}$ –N–Boc ( <b>14</b> )	80
5	C		$\text{N}_3$ –N <sub>3</sub> ( <b>15</b> )	52

<sup>a</sup>Conditions: (A) 10% Pd/C, H<sub>2</sub> (1 bar), MeOH, rt, 3 d; (B) i. Raney-Ni, H<sub>2</sub> (1 bar), THF, rt, 30 min; ii. 10% Pd/C, C<sub>6</sub>H<sub>10</sub>, THF, reflux, 3 h; iii. Fmoc-OSu, NaHCO<sub>3</sub>, THF, H<sub>2</sub>O, 0–20 °C, o/n; (C) i. Raney-Ni, H<sub>2</sub> (1 bar), THF, rt, 1.5 h; ii. Pd/C, H<sub>2</sub> (5 bar), rt, 5 h; iii. for entries 3 and 4: Fmoc-OSu or Boc<sub>2</sub>O, NaHCO<sub>3</sub>, THF, H<sub>2</sub>O, 0–20 °C, o/n; or for entry 5: Diazotransfer reagent, K<sub>2</sub>CO<sub>3</sub>, CuSO<sub>4</sub>·5H<sub>2</sub>O, THF, MeOH, rt, o/n. <sup>b</sup>Isolated yield after purification by column chromatography.

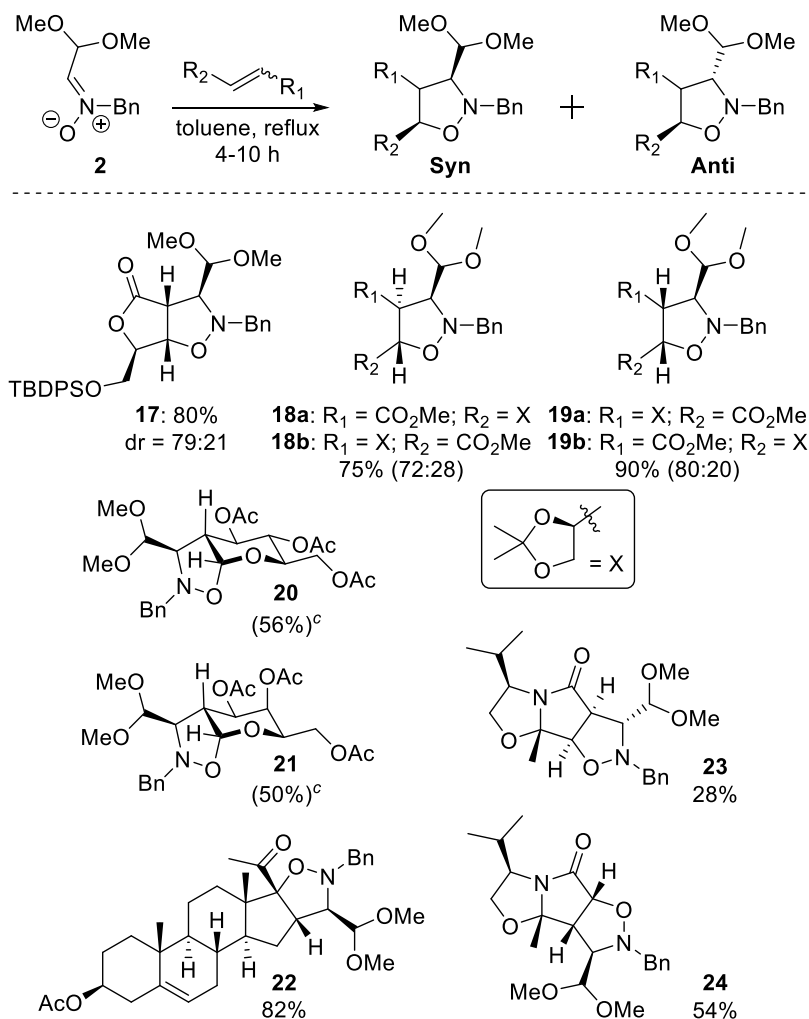
The advantage of this approach is that the whole sequence can be carried out in one pot, since Raney-Nickel can be conveniently removed using a magnet, before adding 10% Pd/C to liberate the primary amine.<sup>13</sup> The optimized conditions of this staged hydrogenation could also be used to install a Boc protecting group (entry 4; **14**) or an azide (entry 5; **15**).

The acetal-masked aldehyde in this ring-opened substrate (**13**) could now be liberated under standard acid hydrolysis conditions to furanose **16** (Scheme 4), indicating that earlier attempts to hydrolyze substrate **3** were indeed hampered by the vicinity of the basic isoxazolidine ring.

Scheme 4. Acid-catalyzed hydrolysis of acetal **13**.

Encouraged by the synthetic versatility of the racemic isoxazolidine substrates, we searched for an asymmetric approach toward these building blocks, since these compounds could represent a promising point for the enantioselective synthesis of functionalized carbohydrate derivatives. The first approach toward chiral isoxazolidine derivatives employed chiral olefins in [3+2] cycloaddition reactions with achiral nitron **1** (Scheme 5); in a second approach (vide infra) chiral derivatives of nitron **1** were reacted with achiral alkenes (Table 2).

The reaction of **1** with a chiral furanone gave bicyclic compound **17**, which is a useful precursor to poly-hydroxylated piperidine derivatives.<sup>14</sup> Compound **17** was obtained in good yield with excellent regioselectivity and good stereoselectivity. Cycloaddition reaction of **1** with two D-mannitol-derived olefins also proved to be stereoselective, providing cycloadducts **18–19**. Interestingly, while the *E*-olefin provided regioisomer **18b** as a minor cycloadduct, the *Z*-olefin provided the analogous regio-isomer **19a** as the major isomer, owing to the attack of the oxygen-atom on the nitron at the  $\alpha$ -position of the  $\alpha,\beta$ -unsaturated alkene.<sup>15</sup> Asymmetric cycloadditions were then carried out with the enol ether in carbohydrate derivatives to obtain cycloadducts **20** and **21**. These cycloaddition reactions with D-glucal- and D-galactal derivatives, which are known for their low reactivity,<sup>16</sup> resulted in only limited conversion of the dipolarophiles after 2 days. We were unable to increase the conversion significantly beyond ~33% by using a high excess of **1** or by increasing the duration of the reaction, since **1** slowly degrades over the course of several days, probably via dimerization as indicated by MS and NMR analysis. As the degradation of **1** by dimerization was thought to be the limiting step we opted to add **1** portion-wise at 165 °C in mesitylene to limit this. Consequently we were able to reach 56% conversion for D-glucal derived **20**, which is good considering there is only one other reported successful cycloaddition of an acyclic nitron on a glycal.<sup>16a</sup> The D-glucal and D-galactal derived cycloadducts were obtained as a single product, illustrating the high regio- and stereoselectivity of these reactions. Furthermore, the unconverted D-glucal and D-galactal derivatives could be recovered through column chromatography. The reaction of nitron **1** with a tri-substituted steroid also proved to be very regio- and stereoselective, providing **22** as a single product in good yield. However, the regio-selectivity of this reaction was reversed compared to other electron-poor dipolarophiles. There is precedent in literature<sup>8a, 17</sup> for similar reversed nitron cycloaddition results and this indicates that steric factors may change the dominant frontier molecular orbital interactions between a nitron and a dipolarophile, thus changing the regiochemical outcome. Finally, the olefin in an enantiopure lactam was reacted with **1**, providing regioisomers **23** and **24** in a total yield of 82%.

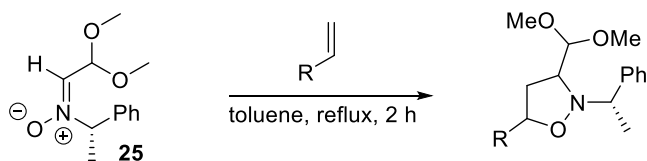
Scheme 5. Scope of **1** in cycloadditions with chiral olefins<sup>a,b</sup>

<sup>a</sup>Isolated yield after column chromatography. <sup>b</sup>*Syn/anti* ratio determined by <sup>1</sup>H NMR and assigned by NOESY. <sup>c</sup>Reaction performed at 165 °C in mesitylene with 5 equiv of **1**.

Surprisingly, although two regio-isomers were formed, none of the other 6 possible stereoisomers were observed. We hypothesize that the two isolated cycloadducts represent the most stable isomers, resulting from the least steric hindrance during the cycloaddition. To validate this hypothesis, the geometries of all eight possible stereo- and regioisomers of the nitrone reaction on the unsaturated lactam were sequentially optimized by molecular mechanics MMFF94 calculations and density functional theory M11-L/6-311+G(d,p) calculations. This indeed yielded the lowest energies for compounds **23** and **24**. All other isomers were less stable, largely due to (significantly) increased steric hindrance (see Appendix A, Scheme S2, Table S1).

Finally, for the second approach, an asymmetric cycloaddition with achiral dipolarophiles was achieved using nitron **25** as a chiral derivative of nitron **1**. Nitron **25** was easily obtained in excellent yield in the same manner as **1**, using (*S*)-*N*-( $\alpha$ -methylbenzyl) hydroxylamine as a chiral precursor, and subsequently employed in several nitron-olefin [3+2] cycloaddition reactions with achiral olefins. These cycloadditions proved to be quite effective, affording the different substrates in very good to excellent yield (Table 2). While the facial selectivity appeared to be moderate, the different major cycloadducts could be isolated in very good yields.

**Table 2.** Scope of chiral nitron **25** in asymmetric cycloadditions reactions with achiral olefins



entry	olefin	diastereomeric ratio <sup>a</sup>	yield (%) <sup>b</sup>
		<i>syn1:syn2:anti1:anti2</i>	
1		52 : 29 : 12 : 7	100
2		51 : 27 : 13 : 9	93
3		47 : 41 : 5 : 7	100

<sup>a</sup>*Syn/anti* ratio determined by <sup>1</sup>H NMR and assigned by NOESY. <sup>b</sup>Isolated yield after column chromatography.

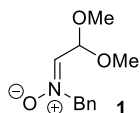
## Conclusion

In summary, a novel nitron **1** containing a masked aldehyde was prepared via a simple and scalable procedure in excellent yield. Using this nitron in [3+2] cycloaddition reactions with a variety of olefins and other dipolarophiles afforded a set of original isoxazolidines in reasonable to excellent overall yields. These cycloadducts can be considered as a masked form of amino aldehydes, making them interesting from a synthetic point of view. The synthetic versatility of these substrates was shown by liberating the masked aldehyde under basic conditions, while the amine could be liberated and immediately protected via an efficient staged one-pot hydrogenolysis procedure. The stability of the masked aldehyde towards acid hydrolysis before ring opening enables facile acid-catalyzed modification of different groups, while still allowing facile acid hydrolysis of the acetal after N-O ring-opening. Finally, a diverse set of chiral olefins led to cycloadducts with high diastereopurity. We are currently pursuing the application of nitrones **1** and **25** in cycloadditions towards several complex glycomimetics,<sup>6</sup> which will be duly reported.

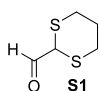
## Experimental section

### General information

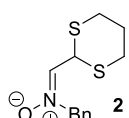
All moisture sensitive reactions were carried out under an argon atmosphere, using oven-dried glassware, unless otherwise stated. Dichloromethane ( $\text{CH}_2\text{Cl}_2$ , Sigma-Aldrich, >99.8%) and toluene (Sigma-Aldrich, >99.8%) were purified over aluminum oxide under argon using a Pure Solv 400 solvent purification system (Innovative Technology, Amesbury, USA). Reagents were obtained from commercial sources and used without further purification unless stated otherwise. Raney-Nickel was bought from Sigma-Aldrich (W.R. Grace and Co. Raney<sup>®</sup>; 2800, as a slurry in  $\text{H}_2\text{O}$ ), which was washed with anhydrous THF three times before use. Palladium on carbon (Pd/C) was bought from Sigma-Aldrich (10 wt. % loading, matrix activated carbon support). Analytical TLC was performed using prepared plates of silica gel (Merck 60 F-254 on aluminium) or aluminum oxide (Fluka 60Å, F-254 on aluminum) and then, according to the functional groups present on the molecules, revealed with UV light or using staining reagents: ninhydrin (5% in EtOH) for amines or basic solution of  $\text{KMnO}_4$  (0.75% in  $\text{H}_2\text{O}$ ) for general staining. Merck silica gel 60 (70–230 mesh) or Fluka aluminium oxide (0.05–0.15 mm particle size, neutral, Brockmann Activity grade I) was used for flash chromatography.  $^1\text{H}$  NMR and  $^{13}\text{C}$  NMR spectra were recorded on a Bruker Avance III 400 spectrometer (observation of  $^1\text{H}$  nucleus 400 MHz, and of  $^{13}\text{C}$  nucleus 100 MHz). Chemical shifts are reported in parts per million (ppm), calibrated on the residual peak of the solvent, whose values are referred to tetramethylsilane ( $\text{TMS}$ ,  $\delta_{\text{TMS}} = 0$ ), as the internal standard.  $^{13}\text{C}$  NMR spectra were performed with proton decoupling. Where indicated, NMR peak assignments were made using COSY and HSQC experiments. Electrospray ionization (ESI) mass analyses were performed on a Finnigan LXQ, while high resolution ESI mass analyses were recorded on a Thermo Scientific Q Exactive High-Resolution mass spectrometer. Infrared analyses were performed on a Bruker FT-IR spectrometer. Optical rotations were measured on a Perkin Elmer 241 polarimeter (Sodium D-line,  $\lambda = 589 \text{ nm}$ ).



**Preparation of nitrone 1:** To a suspension of *N*-benzylhydroxylamine-HCl (10.0 g, 62.7 mmol) in MeOH (30 mL) was added NaOAc (6.68 g, 81.4 mmol, 1.3 equiv). The reaction mixture was cooled in an ice-bath and a 60% solution of 2,2-dimethoxyacetaldehyde in  $\text{H}_2\text{O}$  (10.8 mL, 71.6 mmol, 1.13 equiv) was added dropwise over 5 min. The reaction mixture was stirred for 30 min. at 4 °C and then conc. *in vacuo*. To the residue was added DCM (500 mL) and  $\text{H}_2\text{O}$  (100 mL) and the resulting layers were partitioned. The water-layer was extracted with DCM (100 mL, 2×) and the combined organic layers were washed with sat. aq.  $\text{NaHCO}_3$  (100 mL, 2×) and brine (100 mL), dried ( $\text{MgSO}_4$ ) and conc. *in vacuo*. Affording **1** as a stable<sup>\*</sup> white solid (12.98 g, 99%). <sup>\*</sup>In our handling of the compound, nitrone **1** was stable for 1 year in the –20 °C freezer and for at least several weeks at room temperature.  $^1\text{H}$  NMR (400 MHz, Chloroform-*d*)  $\delta$  7.40 (s, 5H, ArH), 6.70 (d,  $J = 5.5 \text{ Hz}$ , 1H, N=CH), 5.44 (d,  $J = 5.5 \text{ Hz}$ , 1H, (OMe)<sub>2</sub>CH), 4.90 (s, 2H, NCH<sub>2</sub>), 3.41 (s, 6H, 2× OCH<sub>3</sub>).  $^{13}\text{C}$  NMR (101 MHz, Chloroform-*d*)  $\delta$  134.9, 132.2, 129.5, 129.2, 129.0, 97.7, 70.0, 54.5. FT-IR (neat):  $\nu = 2954, 2830, 1595, 1496, 1456 \text{ cm}^{-1}$ . HRMS calcd for  $\text{C}_{11}\text{H}_{15}\text{NO}_3 + \text{Na}^+ [\text{M} + \text{Na}^+]$ : 232.0944. Found. 232.0946.



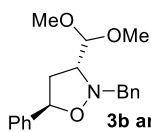
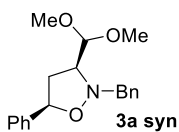
**1,3-Dithiane-2-carbaldehyde (S1):** Prepared according to a literature procedure.<sup>18</sup>  $^1\text{H}$  NMR (400 MHz, Chloroform-*d*)  $\delta$  9.52 (d,  $J = 1.1 \text{ Hz}$ , 1H), 4.09 (s, 1H), 3.03 (ddd,  $J = 14.6, 11.9, 2.8 \text{ Hz}$ , 2H), 2.56 (dddd,  $J = 14.6, 4.9, 3.1, 1.0 \text{ Hz}$ , 2H), 2.23 – 1.78 (m, 2H).



**Preparation of thioacetal nitrone 2:** To a suspension of *N*-benzylhydroxylamine-HCl (1.63 g, 1.02 mmol) in MeOH (10 mL) was added NaOAc (1.10 g, 1.34 mmol, 1.31 equiv). The reaction mixture was stirred for 10 min. at rt, followed by the dropwise addition of 1,3-dithiane-2-carbaldehyde (1.53 g, 1.03 mmol, 1.01 equiv). The resulting light yellow suspension was stirred for 1 h after which DCM (150 mL) and H<sub>2</sub>O (50 mL) were added to the reaction mixture and the resulting layers partitioned. The water-layer was extracted with DCM (50 mL, 2×) and the combined organic layers were washed with brine (50 mL), dried (MgSO<sub>4</sub>) and conc. *in vacuo*. The resulting residue, a sticky yellow solid, was purified by flash column chromatography (4/6/2 to 6/4/2 EtOAc/heptane/DCM), affording **2** as a white solid (1.11 g, 43%). <sup>1</sup>H NMR (400 MHz, Chloroform-*d*) δ 7.40 (s, 5H, ArH), 6.89 (d, *J* = 8.2 Hz, 1H), 5.32 (d, *J* = 8.2 Hz, 1H), 4.93 (s, 2H, NCH<sub>2</sub>), 2.85 (dd, *J* = 6.2, 5.1 Hz, 4H, 2× SCH<sub>2</sub>), 2.16 – 1.91 (m, 2H, CH<sub>2</sub>). <sup>13</sup>C NMR (101 MHz, Chloroform-*d*) δ 134.1, 132.4, 129.3, 129.2, 129.2, 69.7, 37.9, 28.3, 25.3. FT-IR (neat): ν = 3065, 2932, 2901, 1573, 1496, 1455, 1420 cm<sup>-1</sup>. HRMS calcd for C<sub>12</sub>H<sub>15</sub>NOS<sub>2</sub>+Na<sup>+</sup> [M+Na<sup>+</sup>]: 276.0487. Found. 276.0479.

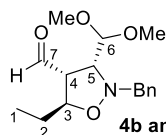
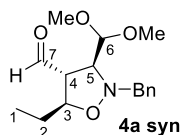
### General procedure A: preparation of cycloadducts.

To a suspension of nitrone **1** (1 mmol) in toluene (1 mL) was added a dipolarophile (2 mmol). The resulting mixture was heated under argon to reflux. After the indicated time, the reaction mixture was concentrated *in vacuo* and the crude material was purified by column chromatography.



#### 2-Benzyl-3-(dimethoxymethyl)-5-phenylisoxazolidine (**3**).

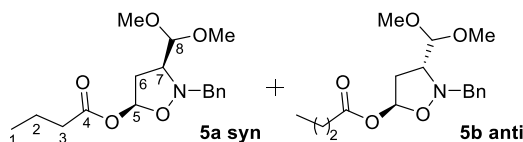
According to general procedure **A** crude **3** was obtained after refluxing for 2 h. The crude product was purified via column chromatography (21-27% Et<sub>2</sub>O in petroleum ether 40-60) afforded **3** as a light yellow oil (2.12 gram, 98%). NMR signals and other experimental data of the major adduct **3a syn**: <sup>1</sup>H NMR (400 MHz, Chloroform-*d*) δ 7.51 – 7.19 (m, 10H, ArH), 5.21 (dd, *J* = 9.0, 6.7 Hz, 1H, OCHPh), 4.32 (d, *J* = 7.0 Hz, 1H, (OMe)<sub>2</sub>CH), 4.20 (d, *J* = 13.3 Hz, 1H, NCH<sub>2</sub>), 4.10 (d, *J* = 13.3 Hz, 1H, NCH<sub>2</sub>), 3.39 (d, *J* = 6.6 Hz, 7H, 2× OCH<sub>3</sub> & NCH), 2.78 (ddd, *J* = 12.8, 8.0, 6.8 Hz, 1H, CH<sub>2</sub>), 2.26 (ddd, *J* = 12.8, 9.0, 6.9 Hz, 1H, CH<sub>2</sub>). <sup>13</sup>C NMR (101 MHz, Chloroform-*d*) δ 139.9, 137.6, 129.5, 128.5, 128.4, 127.9, 127.4, 126.7, 106.8, 78.2, 68.1, 62.3, 55.6, 54.8, 39.9. FT-IR (neat): ν = 3030, 2935, 2831, 1604, 1496, 1454 cm<sup>-1</sup>. HRMS calcd for C<sub>19</sub>H<sub>23</sub>NO<sub>3</sub>+H<sup>+</sup> [M+H<sup>+</sup>]: 314.1751. Found. 314.1738. NMR signals and other experimental data for the minor adduct **3b anti**: <sup>1</sup>H NMR (400 MHz, Chloroform-*d*) δ 7.48 – 7.19 (m, 10H, ArH), 5.04 (dd, *J* = 8.7, 7.2 Hz, 1H, OCHPh), 4.33 (d, *J* = 6.2 Hz, 1H, (OMe)<sub>2</sub>CH), 4.25 (d, *J* = 13.7 Hz, 1H, NCH<sub>2</sub>), 4.12 (d, *J* = 13.6 Hz, 1H, NCH<sub>2</sub>), 3.43 (s, 6H, 2× OCH<sub>3</sub>), 3.31 (ddd, *J* = 9.4, 6.3, 4.7 Hz, 1H, NCH), 2.66 (ddd, *J* = 12.6, 7.2, 4.7 Hz, 1H, CH<sub>2</sub>), 2.30 (dt, *J* = 12.7, 9.1 Hz, 1H, CH<sub>2</sub>). <sup>13</sup>C NMR (101 MHz, Chloroform-*d*) δ 140.7, 137.7, 129.6, 128.5, 128.3, 127.8, 127.3, 126.5, 106.2, 79.1, 67.2, 62.7, 55.7, 54.6, 39.2. FT-IR (neat): ν = 3030, 2931, 2833, 1605, 1496, 1454 cm<sup>-1</sup>. HRMS calcd for C<sub>19</sub>H<sub>23</sub>NO<sub>3</sub>+H<sup>+</sup> [M+H<sup>+</sup>]: 314.1751. Found. 314.1736.



#### 2-Benzyl-3-(dimethoxymethyl)-5-ethylisoxazolidine-4-carbaldehyde (**4**).

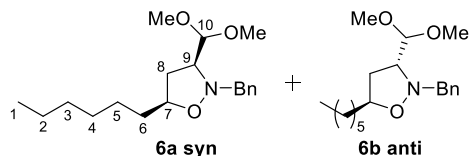
According to general procedure **A** crude **4** was obtained after refluxing for 2 h. The crude product was purified via column chromatography (5-25% EtOAc in petroleum ether 40-60) afforded **4** as a yellow oil (256 mg, 79%). The major adducts could be isolated and separately analysed after a second

purification via column chromatography (Neutral aluminum oxide, 20-80% ether in petroleum ether 40-60). NMR signals and other experimental data of the major adduct **4a syn**:  $^1\text{H}$  NMR (400 MHz, Chloroform-*d*)  $\delta$  9.73 (d,  $J$  = 3.3 Hz, 1H, CHO), 7.44 – 7.21 (m, 5H, ArH), 4.39 (d,  $J$  = 6.5 Hz, 1H, H-6), 4.28 (dt,  $J$  = 8.2, 6.3 Hz, 1H, H-3), 4.10 (d,  $J$  = 13.5 Hz, 1H,  $\text{NCH}_2$ ), 4.01 (d,  $J$  = 13.5 Hz, 1H,  $\text{NCH}_2$ ), 3.51 (dd,  $J$  = 8.9, 6.5 Hz, 1H, H-5), 3.43 – 3.26 (m, 6H,  $\text{OCH}_3$  2 $\times$ ), 3.09 (td,  $J$  = 8.6, 3.3 Hz, 1H, H-4), 1.73 – 1.58 (m, 2H, H-2), 0.93 (t,  $J$  = 7.5 Hz, 3H, H-1).  $^{13}\text{C}$  NMR (101 MHz, Chloroform-*d*)  $\delta$  198.2, 137.0, 129.4, 128.4, 127.5, 104.0, 79.3, 69.7, 62.6, 60.8, 55.6, 55.1, 27.7, 10.4. FT-IR (neat):  $\nu$  = 2965, 2935, 2879, 2836, 1719, 1497, 1435  $\text{cm}^{-1}$ . HRMS calcd for  $\text{C}_{16}\text{H}_{24}\text{NO}_4$  [ $\text{M}+\text{H}^+$ ]: 294.1700. Found: 294.1685. NMR signals and other experimental data for the minor adduct **4b anti**:  $^1\text{H}$  NMR (400 MHz, Chloroform-*d*)  $\delta$  9.81 (d,  $J$  = 1.8 Hz, 1H, CHO), 7.41 – 7.23 (m, 5H, ArH), 4.39 (dt,  $J$  = 7.5, 6.2 Hz, 1H, H-3), 4.25 (d,  $J$  = 6.2 Hz, 1H, H-6), 4.08 (d,  $J$  = 13.0 Hz, 1H,  $\text{NCH}_2$ ), 3.92 (d,  $J$  = 13.0 Hz, 1H,  $\text{NCH}_2$ ), 3.51 (dd,  $J$  = 6.2, 5.2 Hz, 1H, H-5), 3.40 (s, 3H,  $\text{OCH}_3$ ), 3.31 (s, 3H,  $\text{OCH}_3$ ), 3.19 (ddd,  $J$  = 7.3, 5.2, 1.9 Hz, 1H, H-4), 1.79 – 1.62 (m, 2H, H-2), 0.97 (t,  $J$  = 7.4 Hz, 3H, H-1).  $^{13}\text{C}$  NMR (101 MHz, Chloroform-*d*)  $\delta$  199.7, 136.9, 129.4, 128.5, 127.6, 105.7, 78.8, 68.7, 62.8, 61.5, 55.6, 55.4, 26.4, 10.4. FT-IR (neat):  $\nu$  = 2962, 2931, 2878, 2835, 1723, 1497, 1455  $\text{cm}^{-1}$ . HRMS calcd for  $\text{C}_{16}\text{H}_{24}\text{NO}_4$  [ $\text{M}+\text{H}^+$ ]: 294.1700. Found: 294.1686.



**2-Benzyl-3-(dimethoxymethyl)isoxazolidin-5-yl butyrate (5).** According to general procedure **A** crude **5** was obtained after refluxing for 2 h. The crude product was purified via column chromatography (10-20%

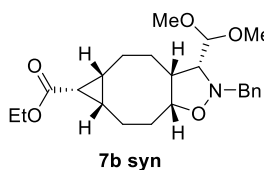
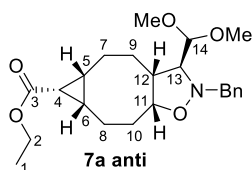
EtOAc in petroleum ether 40-60) afforded **5** as a yellow oil (252 mg, 93%). NMR signals and other experimental data of the major adduct **5a syn**:  $^1\text{H}$  NMR (400 MHz, Chloroform-*d*)  $\delta$  7.42 – 7.35 (m, 2H, ArH), 7.39 – 7.22 (m, 3H, ArH), 6.34 (dd,  $J$  = 6.1, 1.4 Hz, 1H, H-5), 4.44 (d,  $J$  = 7.4 Hz, 1H, H-8), 4.30 (d,  $J$  = 14.3 Hz, 1H,  $\text{NCH}_2$ ), 3.99 (d,  $J$  = 14.3 Hz, 1H,  $\text{NCH}_2$ ), 3.41 (s, 3H,  $\text{OCH}_3$ ), 3.37 (s, 3H,  $\text{OCH}_3$ ), 3.19 (ddd,  $J$  = 9.4, 7.4, 5.4 Hz, 1H, H-7), 2.55 (ddd,  $J$  = 14.1, 9.4, 6.1 Hz, 1H, H-6a), 2.38 – 2.21 (m, 3H, H-6b, H-3), 1.65 (h,  $J$  = 7.5 Hz, 2H, H-2), 0.94 (t,  $J$  = 7.4 Hz, 3H, H-1).  $^{13}\text{C}$  NMR (101 MHz, Chloroform-*d*)  $\delta$  173.1, 129.6, 128.3, 127.5, 105.6, 95.4, 64.7, 62.2, 55.5, 54.0, 38.4, 36.5, 18.3, 13.7. FT-IR (neat):  $\nu$  = 2963, 2876, 2834, 1741, 1497, 1455  $\text{cm}^{-1}$ . HRMS calcd for  $\text{C}_{17}\text{H}_{25}\text{NO}_5$  [ $\text{M}+\text{H}^+$ ]: 324.1805. Found: 324.1791. NMR signals and other experimental data for the minor adduct **5b anti**:  $^1\text{H}$  NMR (400 MHz, Chloroform-*d*)  $\delta$  7.41 – 7.24 (m, 5H, ArH), 6.37 (ddd,  $J$  = 4.6, 1.7, 0.8 Hz, 1H, H-5), 4.23 (d,  $J$  = 6.4 Hz, 1H, H-8), 4.19 (s, 2H,  $\text{NCH}_2$ ), 3.41 (d,  $J$  = 2.8 Hz, 7H, 2 $\times$   $\text{OCH}_3$  & H-7), 2.51 (ddd,  $J$  = 7.7, 5.2, 3.1 Hz, 2H, H-6), 2.31 (t,  $J$  = 7.4 Hz, 2H, H-3), 1.69 (q,  $J$  = 7.4 Hz, 2H, H-2), 0.99 (t,  $J$  = 7.4 Hz, 3H, H-1).  $^{13}\text{C}$  NMR (101 MHz, Chloroform-*d*)  $\delta$  172.5, 137.4, 129.3, 128.4, 127.5, 106.7, 97.5, 65.4, 65.2, 56.0, 55.1, 38.3, 36.6, 18.3, 13.8. FT-IR (neat):  $\nu$  = 2964, 2935, 2834, 1741, 1497, 1455  $\text{cm}^{-1}$ . HRMS calcd for  $\text{C}_{17}\text{H}_{25}\text{NO}_5$  [ $\text{M}+\text{H}^+$ ]: 324.1805. Found: 324.1792.



**2-Benzyl-3-(dimethoxymethyl)-5-hexylisoxazolidine (6).** According to general procedure **A** crude **6** was obtained after refluxing for 2 h. The crude was purified via column chromatography (11-20% EtOAc in petroleum ether 40-60) afforded **6** as a

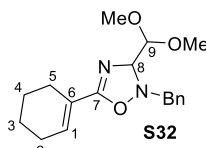
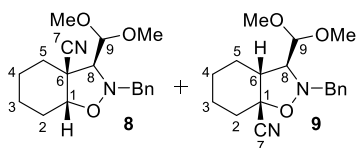
yellow oil (299 mg, 93%). The cycloadducts could not be separated via column chromatography, but it was possible to perform structure elucidation via NMR. FT-IR (neat):  $\nu$  = 2928, 2857, 1496, 1454  $\text{cm}^{-1}$ . HRMS calcd for  $\text{C}_{19}\text{H}_{31}\text{NO}_3+\text{H}^+$  [ $\text{M}+\text{H}^+$ ]: 322.2377. Found: 314. 322.2368. NMR signals of the major adduct **6a syn**  $^1\text{H}$  NMR (400 MHz, Acetonitrile-*d*<sub>3</sub>)  $\delta$  7.48 – 7.16 (m, 5H, ArH), 4.22 – 4.17 (m, 1H, H-7),

4.15 (d,  $J = 7.1$  Hz, 1H, (OMe)<sub>2</sub>CH), 3.97 (d,  $J = 13.5$  Hz, 1H, NCH<sub>2</sub>Ph), 3.86 (d,  $J = 13.6$  Hz, 1H, NCH<sub>2</sub>Ph), 3.34 (s, 3H, OCH<sub>3</sub>), 3.32 (s, 3H, OCH<sub>3</sub>), 3.21 (ddd,  $J = 8.2, 7.1, 6.0$  Hz, 1H, H-9), 2.46 (ddd,  $J = 12.5, 8.3, 6.6$  Hz, 1H, H-8a), 1.74 (dddd,  $J = 12.5, 8.5, 6.1, 1.1$  Hz, 1H, H-8b), 1.61 – 1.39 (m, 2H, H-6), 1.38 – 1.19 (m, 8H, 4xCH<sub>2</sub>), 0.89 (t,  $J = 6.7$  Hz, 3H, H-1). <sup>13</sup>C NMR (101 MHz, Acetonitrile-*d*<sub>3</sub>)  $\delta$  139.8, 130.1, 129.0, 127.9, 107.4, 76.8, 68.7, 62.2, 55.5, 54.7, 37.4, 34.6, 32.5, 30.0, 27.2, 23.3, 14.4. NMR signals for the minor adduct **7b anti**: <sup>1</sup>H NMR (400 MHz, Acetonitrile-*d*<sub>3</sub>)  $\delta$  7.44 – 7.12 (m, 5H, ArH), 4.26 (d,  $J = 6.5$  Hz, 1H, (OMe)<sub>2</sub>CH) 4.23 – 4.19 (d,  $J = 13.9$  Hz, 1H, NCH<sub>2</sub>Ph), 3.83 (m, 1H, H-7), 3.78 (d,  $J = 13.9$  Hz, 1H, NCH<sub>2</sub>Ph), 3.38 (s, 3H, OCH<sub>3</sub>), 3.36 (s, 3H, OCH<sub>3</sub>), 2.27 – 2.21 (m, 1H, H-9), 1.47 (m, 2H, H-6), 1.38 – 1.21 (m, 8H, 4x CH<sub>2</sub>), 0.93 – 0.84 (m, 3H, H-1). <sup>13</sup>C NMR (101 MHz, Acetonitrile-*d*<sub>3</sub>)  $\delta$  140.0, 130.0, 129.0, 127.8, 107.1, 78.1, 68.2, 63.3, 55.8, 54.9, 37.6, 35.5, 32.5, 30.1, 27.0, 23.3, 14.4.



**Ethyl (3aR,5aR,6R,6aS,8aR)-2-benzyl-3-(dimethoxymethyl)decahydro-2H-cyclopropa[5,6]cycloocta[1,2-d]isoxazole-6-carboxylate (7).** According to general procedure A crude **7** was obtained after refluxing for 38 h. The crude was

purified via column chromatography (10–20% EtOAc in petroleum ether 40–60) afforded **7** as a yellow oil (252 mg, 93%). NMR signals and other experimental data of the major adduct **7a anti**: <sup>1</sup>H NMR (400 MHz, Acetonitrile-*d*<sub>3</sub>)  $\delta$  7.37 – 7.19 (m, 5H, ArH), 4.35 (d,  $J = 5.7$  Hz, 1H, H-14), 4.24 (d,  $J = 14.1$  Hz, 1H, NCH<sub>2</sub>), 4.04 (q,  $J = 7.1$  Hz, 2H, H-2), 3.94 (ddd,  $J = 11.8, 6.8, 4.5$  Hz, 1H, H-11), 3.61 (d,  $J = 14.2$  Hz, 1H, NCH<sub>2</sub>), 3.43 (s, 3H, OCH<sub>3</sub>), 3.41 (s, 3H, OCH<sub>3</sub>), 2.58 – 2.46 (m, 2H, H13 & H12), 1.93 – 1.81 (m, 2H), 1.79 – 1.37 (m, 9H), 1.19 (t,  $J = 7.1$  Hz, 3H, H-1). <sup>13</sup>C NMR (101 MHz, Acetonitrile-*d*<sub>3</sub>)  $\delta$  172.7, 140.0, 129.7, 128.9, 127.7, 118.2, 108.1, 80.9, 77.0, 62.9, 60.5, 56.4, 56.1, 52.3, 29.1, 28.7, 27.4, 26.0, 22.7, 22.5, 17.0, 14.7. FT-IR (neat):  $\nu = 2937, 1718, 1496, 1473, 1454$  cm<sup>-1</sup>. HRMS calcd for C<sub>23</sub>H<sub>33</sub>NO<sub>5</sub> + H<sup>+</sup>[M+H<sup>+</sup>]: 404.2431. Found: 404.2432. NMR signals and other experimental data of the minor adduct **7b syn**: <sup>1</sup>H NMR (400 MHz, Chloroform-*d*)  $\delta$  7.45 – 7.19 (m, 5H, ArH), 4.25 – 4.14 (m, 2H, NCH<sub>2</sub> + H-14 OR H-11), 4.10 (q,  $J = 7.1$  Hz, 3H, H-2 + H-14 OR H-11), 3.95 (d,  $J = 13.8$  Hz, 1H, NCH<sub>2</sub>), 3.42 (s, 6H, OCH<sub>3</sub> 2x), 2.82 (ddt,  $J = 12.5, 6.1, 4.1$  Hz, 1H, H-12), 2.70 (dd,  $J = 6.0, 4.4$  Hz, 1H, H-13), 2.23 – 2.12 (m, 1H), 2.12 – 2.03 (m, 1H), 2.03 – 1.64 (m, 7H), 1.55 – 1.36 (m, 2H), 1.25 (t,  $J = 7.1$  Hz, 3H, H-1). <sup>13</sup>C NMR (101 MHz, Chloroform-*d*)  $\delta$  171.9, 138.1, 129.5, 128.3, 127.3, 107.5, 80.0, 74.7, 63.0, 60.0, 56.4, 55.5, 45.1, 28.8, 25.5, 24.1, 22.3, 21.0, 19.4, 18.5, 14.5. FT-IR (neat):  $\nu = 2938, 2876, 1718, 1496, 1453$  cm<sup>-1</sup>. HRMS calcd for C<sub>23</sub>H<sub>33</sub>NO<sub>5</sub> + H<sup>+</sup>[M+H<sup>+</sup>]: 404.2431. Found: 404.2431.

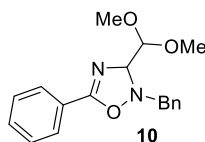


**Cycloaddition of cyclohex-1-ene-1-carbonitrile with nitrone 1.** According to general procedure A; a mixture of crude cycloadducts was obtained after refluxing for 38 h. The crude product was

purified via column chromatography (10–20% EtOAc in petroleum ether 40–60) afforded three major cycloadducts as a yellow oil (171 mg, 53%). NMR signals and other experimental data of the major adduct **8**: <sup>1</sup>H NMR (400 MHz, Chloroform-*d*)  $\delta$  7.35 – 7.16 (m, 5H, ArH), 4.35 – 4.25 (m, 2H, H-9 & NCH<sub>2</sub>), 4.06 (ddd,  $J = 3.9, 2.6, 1.0$  Hz, 1H, H-1), 3.90 (d,  $J = 14.3$  Hz, 1H, NCH<sub>2</sub>), 3.53 (s, 3H, OCH<sub>3</sub>), 3.47 (s, 3H, OCH<sub>3</sub>), 2.83 (d,  $J = 7.1$  Hz, 1H, H-8), 1.99 – 1.88 (m, 1H, H-2a), 1.83 – 1.72 (m, 1H, H-5a), 1.76 – 1.56 (m, 1H, H-2b), 1.58 – 1.16 (m, 5H, H-3 & H-4 & H-5b). <sup>13</sup>C NMR (101 MHz, Chloroform-*d*)  $\delta$  136.5, 129.8, 128.3, 127.6, 119.8, 106.8, 77.1, 75.2, 62.3, 58.4, 56.7, 45.5, 33.1, 24.0, 21.8, 19.9. FT-IR

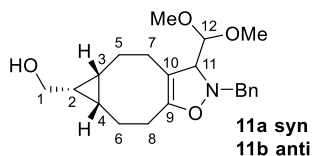


(neat):  $\nu = 2936, 2868, 2835, 1497, 1453 \text{ cm}^{-1}$ . HRMS calcd for  $\text{C}_{18}\text{H}_{24}\text{N}_2\text{O}_3 + \text{H}^+ [\text{M}+\text{H}^+]$ : 317.1860. Found: 317.1852. NMR signals and other experimental data for the minor adduct **9**:  $^1\text{H}$  NMR (400 MHz, Chloroform-*d*)  $\delta$  7.37 – 7.15 (m, 5H, ArH), 4.53 (d,  $J = 7.4 \text{ Hz}$ , 1H, H-9), 4.40 (d,  $J = 15.0 \text{ Hz}$ , 1H,  $\text{NCH}_2$ ), 3.96 (d,  $J = 15.0 \text{ Hz}$ , 1H,  $\text{NCH}_2$ ), 3.46 (s, 3H,  $\text{OCH}_3$ ), 3.38 (s, 3H,  $\text{OCH}_3$ ), 2.74 (dd,  $J = 7.5, 3.0 \text{ Hz}$ , 1H, H-8), 2.54 (ddd,  $J = 10.9, 6.5, 3.0 \text{ Hz}$ , 1H, H-6), 2.14 (dtd,  $J = 14.8, 4.3, 1.4 \text{ Hz}$ , 1H, H-2a), 2.03 – 1.77 (m, 1H, H-2b), 1.74 – 1.62 (m, 1H, H-5a), 1.55 – 1.23 (m, 4H, H-3 & H-4), 1.11 – 0.89 (m, 1H, H-5b).  $^{13}\text{C}$  NMR (101 MHz, Chloroform-*d*)  $\delta$  136.9, 129.0, 128.3, 127.3, 122.1, 107.0, 75.2, 73.4, 61.8, 57.5, 55.3, 48.4, 30.6, 28.6, 22.2, 19.7. FT-IR (neat):  $\nu = 2936, 2864, 2837, 1496, 1452 \text{ cm}^{-1}$ . HRMS calcd for  $\text{C}_{18}\text{H}_{24}\text{N}_2\text{O}_3 + \text{H}^+ [\text{M}+\text{H}^+]$ : 317.1860. Found: 317.1849. NMR signals and other experimental data of the minor adduct **5a**:  $^1\text{H}$  NMR (400 MHz, Chloroform-*d*)  $\delta$  7.41 – 7.13 (m, 5H, ArH), 6.55 (tt,  $J = 3.9, 1.8 \text{ Hz}$ , 1H, H-1), 4.79 (d,  $J = 5.3 \text{ Hz}$ , 1H, H-8), 4.07 – 3.98 (m, 2H, H-9 &  $\text{NCH}_2$ ), 3.84 (d,  $J = 13.1 \text{ Hz}$ , 1H,  $\text{NCH}_2$ ), 3.35 (s, 3H,  $\text{OCH}_3$ ), 3.33 (s, 3H,  $\text{OCH}_3$ ), 2.30 – 2.24 (m, 2H, H-5), 2.10 (dd,  $J = 4.9, 2.3 \text{ Hz}$ , 2H, H-2), 1.66 – 1.41 (m, 4H, H-4 & H-3).  $^{13}\text{C}$  NMR (101 MHz, Chloroform-*d*)  $\delta$  162.9, 137.2, 135.6, 129.4, 128.5, 127.8, 125.1, 105.5, 90.3, 77.4, 63.5, 56.3, 55.6, 25.8, 25.2, 22.1, 21.6. FT-IR (neat):  $\nu = 2936, 2852, 1662, 1497, 1454 \text{ cm}^{-1}$ . HRMS calcd for  $\text{C}_{18}\text{H}_{24}\text{N}_2\text{O}_3 + \text{H}^+ [\text{M}+\text{H}^+]$ : 317.1860. Found: 317.1853.



**2-Benzyl-3-(dimethoxymethyl)-5-phenyl-2,3-dihydro-1,2,4-oxadiazole (10).**

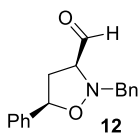
A roundbottom flask containing nitron **1** (1 mmol) in neat benzonitrile (1 mL) was heated under argon to  $110^\circ\text{C}$  for 21 hours. After the indicated time, the reaction mixture was concentrated *in vacuo* and the crude material was purified by column chromatography (6–12% acetone/toluene), affording compound **10** as a light yellow oil (211 mg, 67%).  $^1\text{H}$  NMR (400 MHz, Chloroform-*d*)  $\delta$  7.93 (d,  $J = 7.6 \text{ Hz}$ , 2H, ArH), 7.55 – 7.27 (m, 8H, ArH), 5.02 (d,  $J = 5.2 \text{ Hz}$ , 1H, NCH), 4.25 – 4.17 (m, 2H,  $(\text{OMe})_2\text{CH}$  &  $\text{NCH}_2$ ), 4.03 (d,  $J = 13.2 \text{ Hz}$ , 1H,  $\text{NCH}_2$ ), 3.46 (s, 3H,  $\text{OCH}_3$ ), 3.45 (s, 3H,  $\text{OCH}_3$ ).  $^{13}\text{C}$  NMR (101 MHz, Chloroform-*d*)  $\delta$  162.1, 135.4, 132.1, 129.7, 128.7, 128.6, 128.5, 128.0, 125.5, 105.6, 90.7, 63.8, 56.4, 55.6. FT-IR (neat):  $\nu = 2934, 2833, 1655, 1603, 1581, 1495, 1451 \text{ cm}^{-1}$ . HRMS calcd for  $\text{C}_{18}\text{H}_{20}\text{N}_2\text{O}_3 [\text{M}+\text{H}^+]$ : 313.1547. Found: 313.1545.



**Ethyl (5a*R*,6*R*,6a*S*)-2-benzyl-3-(dimethoxymethyl)-3,4,5,5a,6,6a,7,8-octahydro-2*H*-cyclopropa[5,6]cycloocta[1,2-*d*]isoxazole-6-carboxylate (11).**

To a suspension of nitron **1** (1 mmol) in toluene (1 mL) at rt was added ((1*R*,8*S*,9*S*)-bicyclo[6.1.0]non-4-yn-9-yl)methanol (1.2 mmol). The resulting mixture was stirred for 5 min. and then concentrated *in vacuo*. The residue was purified by column chromatography affording **11** as a yellow oil (314 mg, 87%). NMR signals and other experimental data of the major adduct **11<sup>a</sup>**:  $^1\text{H}$  NMR (400 MHz, Chloroform-*d*)  $\delta$  7.43 – 7.20 (m, 5H, ArH), 4.19 (d,  $J = 6.2 \text{ Hz}$ , 1H, H-12), 4.03 (d,  $J = 12.9 \text{ Hz}$ , 1H,  $\text{NCH}_2$ ), 3.82 (d,  $J = 12.9 \text{ Hz}$ , 1H,  $\text{NCH}_2$ ), 3.72 (d,  $J = 7.8 \text{ Hz}$ , 2H, H-1), 3.63 (d,  $J = 6.2 \text{ Hz}$ , 1H, H-11), 3.39 (s, 3H,  $\text{OCH}_3$ ), 3.34 (s, 3H,  $\text{OCH}_3$ ), 2.54 (ddd,  $J = 16.9, 5.9, 3.2 \text{ Hz}$ , 1H), 2.39 (ddd,  $J = 17.0, 7.7, 5.2 \text{ Hz}$ , 1H), 2.30 – 2.14 (m, 1H), 2.13 – 1.98 (m, 1H), 2.02 – 1.90 (m, 1H), 1.58 (m, 2H), 1.14 (m, 1H), 0.93 (m, 3H).  $^{13}\text{C}$  NMR (101 MHz, Chloroform-*d*)  $\delta$  148.6, 136.6, 129.6, 128.2, 127.4, 107.2, 103.0, 76.4, 62.8, 59.9, 55.9, 55.3, 25.8, 25.7, 22.2, 20.6, 20.3, 18.9, 18.7. FT-IR (neat):  $\nu = 3413, 2920, 1454 \text{ cm}^{-1}$ . HRMS calcd for  $\text{C}_{21}\text{H}_{29}\text{NO}_4 + \text{H}^+ [\text{M}+\text{H}^+]$ : 360.2169. Found: 60.2160. NMR signals and other experimental data of the minor adduct **11<sup>a,b</sup>**:  $^1\text{H}$  NMR (400 MHz, Chloroform-*d*)  $\delta$  7.42 – 7.21 (m, 5H), 4.19 (d,  $J = 6.4 \text{ Hz}$ , 1H), 4.02 (d,  $J = 13.0 \text{ Hz}$ , 1H), 3.82 (d,  $J = 13.0 \text{ Hz}$ , 1H), 3.72 (dd,  $J = 8.2, 2.6 \text{ Hz}$ , 2H), 3.69 – 3.63 (m, 1H), 3.38 (s, 3H), 3.36 (s, 3H), 2.46 – 2.15 (m, 4H), 1.99 (dddd,  $J = 19.0, 8.0, 5.8, 4.3 \text{ Hz}$ , 2H), 1.61 – 1.30 (m, 2H), 1.28 – 1.06 (m, 2H), 1.07 – 0.86 (m, 2H). HRMS calcd for  $\text{C}_{21}\text{H}_{29}\text{NO}_4 + \text{H}^+ [\text{M}+\text{H}^+]$ : 360.2169.

Found: 360.2159. <sup>a</sup>Due to the large distance between the chiral centres it was not possible, even with NOESY, to unambiguously assign *syn/anti* stereochemistry. <sup>b</sup>Upon purification this cycloadduct slowly degrades due to hydrolysis, which prevented full characterization.



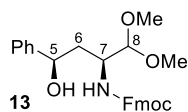
**2-Benzyl-5-phenylisoxazolidine-3-carbaldehyde (12).** To a solution of **3a** (0.260 gram, 0.83 mmol) in dry DCM (1.85 mL) was added 2,6-lutidine (299  $\mu$ L, 2.49 mmol, 3.0 equiv) under argon. The resulting solution was cooled to  $-20^{\circ}\text{C}$  after which TMSOTf (306  $\mu$ L, 1.66 mmol, 2.0 equiv) was added dropwise. The reaction mixture was stirred at  $-20^{\circ}\text{C}$  for 65 min. after which  $\text{H}_2\text{O}$  (8 mL) was added, while allowing the resulting mixture to warm to rt. The mixture was stirred at rt for 15 min followed by the addition of DCM (20 mL). The biphasic system was separated and the waterlayer was extracted with DCM (10 mL, 3x). The combined organic layers were washed with 10% aq.  $\text{NaHSO}_4$  (10 mL), sat. aq.  $\text{NaHCO}_3$  (10 mL) and brine (10 mL). The combined organic layers were then dried ( $\text{MgSO}_4$ ) and conc. *in vacuo*. Affording crude **12** (380 mg, 0.481 mmol, 58%) as a light brown oil. The crude could be purified by column chromatography (0–2% MeCN in DCM; 95% purity), and further purified by a 2<sup>nd</sup> purification by a short silica plug (20% EtOAc in petroleum ether 40–60), affording compound **12** (40%) as a light yellow oil.  $^1\text{H}$  NMR (400 MHz, Chloroform-*d*)  $\delta$  9.63 (d,  $J$  = 2.0 Hz, 1H, CHO), 7.51 – 7.10 (m, 10H, ArH), 5.33 (t,  $J$  = 7.7 Hz, 1H, OCHPh), 4.39 (d,  $J$  = 12.8 Hz, 1H,  $\text{NCH}_2$ ), 4.02 (d,  $J$  = 12.3 Hz, 1H,  $\text{NCH}_2$ ), 3.71 (ddd,  $J$  = 8.6, 4.7, 2.0 Hz, 1H, NCH), 2.93 (dt,  $J$  = 12.3, 8.3 Hz, 1H,  $\text{CH}_2$ ), 2.64 – 2.52 (m, 1H,  $\text{CH}_2$ ).  $^{13}\text{C}$  NMR (101 MHz, Chloroform-*d*)  $\delta$  201.0, 139.0, 136.0, 129.5, 128.8, 128.7, 128.4, 128.1, 126.8, 78.9, 72.5, 61.1, 38.1. FT-IR (neat):  $\nu$  = 3063, 3031, 2899, 2822, 1731, 1604, 1495, 1454  $\text{cm}^{-1}$ . HRMS calcd for  $\text{C}_{17}\text{H}_{17}\text{NO}_2 + \text{H}^+$  [ $\text{M}+\text{H}^+$ ]: 268.1332. Found 268.1325.

### General procedure B for the one-pot hydrogenation/protection sequence

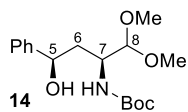
A solution of compound **3a** (**syn**) (0.214 mg, 0.683 mmol) in THF (4 mL) was added to a round-bottom flask containing Raney nickel (0.477 gram). The reaction mixture was put under an hydrogen atmosphere (1 bar; balloon) and stirred vigorously for 90 minutes. The Raney nickel was then removed with a teflon coated magnet and washed with THF (15 mL), THF washing collected in reaction vessel. Pd/C (10% act., 0.211 mg) was then added to this roundbottom flask and the resulting reaction mixture was put under an hydrogen atmosphere (5 bar) and shaken with a Parr-apparatus for 5 hours. The remaining procedure is applicable for general procedure **B1** (for compound **13-14**); The reaction mixture was cooled to  $0^{\circ}\text{C}$  and placed under argon, followed by the addition of  $\text{H}_2\text{O}$  (0.7 mL),  $\text{NaHCO}_3$  (166 mg, 1.98 mmol, 3 equiv) and Fmoc-OSu/  $\text{Boc}_2\text{O}$  (1.98 mmol, 3.0 equiv). The resulting reaction mixture was allowed to warm to rt and stirred o/n after which it was filtered over Celite and the Celite was washed with  $\sim 50^{\circ}\text{C}$  EtOAc. The filtrate was conc. *in vacuo* and the residue was purified by column chromatography.

### General procedure B2 (for compound 15)

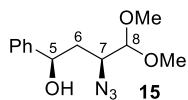
Similar as general procedure **B**, but after hydrogenation with the Parr-apparatus, the reaction mixture was placed under argon, followed by the addition of MeOH (20 mL),  $\text{K}_2\text{CO}_3$  (234 mg, 1.69 mmol, 2.5 equiv) and imidazole-1-sulfonyl azide sulphuric acid salt<sup>19</sup> (0.82 mmol, 1.2 equiv). The resulting reaction mixture was stirred o/n and then filtered over Celite and the Celite washed with  $\sim 50^{\circ}\text{C}$  EtOAc. The filtrate was conc. *in vacuo* and the residue was purified by column chromatography.



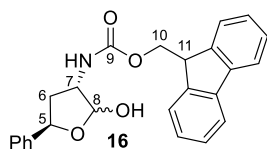
**(9H-Fluoren-9-yl)methyl (4-hydroxy-1,1-dimethoxy-4-phenylbutan-2-yl) carbamate (13).** According to general procedure **B1**, crude **13** was obtained as a yellow oil, which was purified by column chromatography (35-50% EtOAc in petroleum ether 40-60), affording compound **13** (80%) as a yellow oil.  $^1\text{H}$  NMR (400 MHz, Chloroform-*d*)  $\delta$  7.77 (d,  $J$  = 7.6 Hz, 2H, ArH), 7.61 (d,  $J$  = 7.4 Hz, 2H, ArH), 7.45 – 7.29 (m, 8H, ArH), 7.33 – 7.21 (m, 1H, ArH), 5.15 (d,  $J$  = 8.9 Hz, 1H, NH), 4.80 (s, 1H, H-5), 4.42 (d,  $J$  = 7.0 Hz, 2H, Fmoc-CH<sub>2</sub>), 4.23 (q,  $J$  = 6.9, 5.4 Hz, 2H, H-8 & Fmoc-CH), 3.92 (m, 1H, H-7), 3.40 (s, 3H, OCH<sub>3</sub>), 3.38 (s, 3H, OCH<sub>3</sub>), 2.89 (s, 1H, OH), 2.09 (dt,  $J$  = 11.2, 5.1 Hz, 1H, H-6a), 1.95 (dt,  $J$  = 15.2, 8.0 Hz, 1H H-6b).  $^{13}\text{C}$  NMR (101 MHz, Chloroform-*d*)  $\delta$  156.6, 144.4, 144.0, 144.0, 141.4, 128.5, 127.8, 127.6, 127.2, 126.0, 125.2, 120.1, 106.1, 72.2, 66.8, 56.4, 55.9, 50.8, 47.4, 39.1. FT-IR (neat):  $\nu$  = 3401, 2931, 1701, 1515, 1449 cm<sup>-1</sup>. HRMS calcd for C<sub>27</sub>H<sub>29</sub>NO<sub>5</sub> + Na<sup>+</sup> [M+Na<sup>+</sup>]: 470.1939 Found 470.1924.



***t*-Butyl (4-hydroxy-1,1-dimethoxy-4-phenylbutan-2-yl)carbamate (14).** According to general procedure **B1**, crude **14** was obtained as a yellow oil, which was purified by column chromatography (35-50% EtOAc in petroleum ether 40-60), affording compound **14** (80%) as a yellow oil.  $^1\text{H}$  NMR (400 MHz, Chloroform-*d*)  $\delta$  7.43 – 7.30 (m, 4H, ArH), 7.26 (t,  $J$  = 6.9 Hz, 1H, ArH), 4.93 (d,  $J$  = 8.9 Hz, 1H, NH), 4.87 – 4.78 (m, 1H, H-5), 4.24 (d,  $J$  = 3.7 Hz, 1H, H-8), 3.87 (s, 1H, H-7), 3.43 (s, 3H, OCH<sub>3</sub>), 3.38 (s, 3H, OCH<sub>3</sub>), 3.26 (s, 1H, OCH), 2.08 (dt,  $J$  = 14.6, 4.8 Hz, 1H, H-6a), 1.90 (dt,  $J$  = 15.0, 7.9 Hz, 1H, H-6b), 1.46 (s, 9H, *t*Bu).  $^{13}\text{C}$  NMR (101 MHz, Chloroform-*d*)  $\delta$  156.2, 144.6, 128.5, 127.5, 126.0, 106.2, 79.8, 72.3, 56.4, 55.8, 50.4, 39.5, 28.5. FT-IR (neat):  $\nu$  = 3368, 2976, 2932, 2835, 1692, 1506, 1454 cm<sup>-1</sup>. HRMS calcd for C<sub>17</sub>H<sub>27</sub>NO<sub>5</sub> + Na<sup>+</sup> [M+Na<sup>+</sup>]: 348.1781 Found 348.1769.

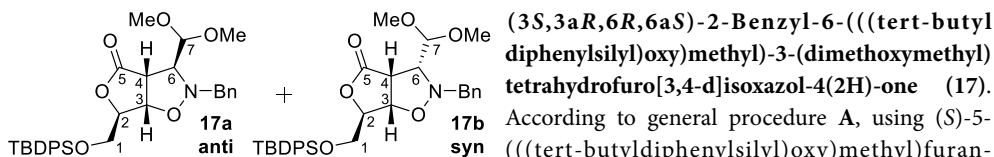


**3-Azido-4,4-dimethoxy-1-phenylbutan-1-ol (15).** According to general procedure **B2**, crude **15** was obtained as a brown oil, which was purified by column chromatography (15-25% EtOAc in petroleum ether 40-60), affording compound **15** (52%) as a yellow oil.  $^1\text{H}$  NMR (400 MHz, Chloroform-*d*)  $\delta$  7.36 (m, 4H, ArH), 7.36 – 7.25 (m, 1H, ArH), 4.85 (t,  $J$  = 6.8 Hz, 1H, H-5), 4.27 (d,  $J$  = 6.0 Hz, 1H, H-8), 3.43 (s, 3H, OCH<sub>3</sub>), 3.35 (s, 3H, OCH<sub>3</sub>), 3.31 (ddd,  $J$  = 9.8, 5.9, 4.2 Hz, 1H, H-7), 2.75 (bs, 1H, OH), 2.00 (ddd,  $J$  = 14.2, 6.4, 4.2 Hz, 1H, H-6a), 1.91 (ddd,  $J$  = 14.3, 9.3, 7.2 Hz, 1H, H-6b).  $^{13}\text{C}$  NMR (101 MHz, Chloroform-*d*)  $\delta$  143.6, 128.7, 128.0, 126.1, 106.5, 72.3, 60.9, 55.6, 54.9, 38.5. FT-IR (neat):  $\nu$  = 3415, 2926, 2837, 2096, 1494, 1454 cm<sup>-1</sup>. HRMS could not be obtained, probably due to the very poor ionising ability of compound **15**, even after testing a wide variety of conditions and additives.

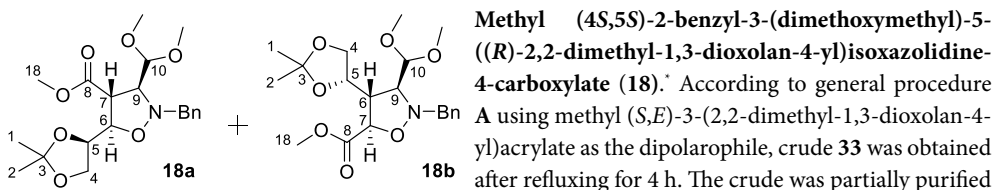


**(9H-Fluoren-9-yl)methyl((3*S'*,5*R'*)-2-hydroxy-5-phenyltetrahydrofuran-3-yl)carbamate (16).** To a mixture of **13** (100 mg, 0.223 mmol) in CHCl<sub>3</sub> (3.2 mL) and H<sub>2</sub>O (0.8 mL) at 0 °C was slowly added TFA (4.0 mL) over 5 minutes. The reaction mixture was stirred at 0 °C for 15 minutes and then allowed to stir at rt for 17h. The reaction mixture was then further diluted by adding additional CHCl<sub>3</sub> (32 mL), H<sub>2</sub>O (8 mL) and TFA (40 mL) and stirred for another 2h, before adding H<sub>2</sub>O and quenching the reaction with NaHCO<sub>3</sub> until pH=7. The reaction mixture was then extracted with DCM (50 mL, 3x). The combined organic layers were washed with sat. aq. NaHCO<sub>3</sub> (50 mL) and brine (50 mL), dried (MgSO<sub>4</sub>) and conc. *in vacuo*, affording 103 mg of a white solid. The crude was purified by column chromatography (30-50% EtOAc in petroleum ether 40-60), affording compound **16** as a 3:1 anomeric mixture (63 mg, 70%) as a yellow oil.  $^1\text{H}$  NMR (400 MHz, Chloroform-*d*)  $\delta$  7.78 (d,  $J$  = 7.6 Hz, 2H, ArH  $\alpha+\beta$ ), 7.61 (d,  $J$  = 7.5 Hz, 2H, ArH  $\alpha+\beta$ ), 7.34 (m, 9H, ArH  $\alpha+\beta$ ), 5.58 (s,

1H, H-8  $\alpha$  or  $\beta$ ), 5.51 – 5.25 (m, 2H, H-8 and H-5  $\alpha$  or  $\beta$ ), 5.20 – 4.84 (m, 1H, H-5  $\alpha$  or  $\beta$ ), 4.60 – 4.32 (m, 3H, H-7 & OCH<sub>2</sub>  $\alpha$  or  $\beta$ ), 4.21 (t,  $J$  = 7.2 Hz, 2H, H-7 & H-11  $\alpha$  or  $\beta$ ), 3.90 (m, OH  $\alpha$  or  $\beta$ ), 2.28 (m, 2H, H-6  $\alpha$  or  $\beta$ ). <sup>13</sup>C NMR (101 MHz, Chloroform-*d*)  $\delta$  156.3, 156.0, 144.0, 143.9, 143.9, 142.2, 141.9, 141.4, 128.6, 128.6, 127.9, 127.8, 127.7, 127.2, 127.2, 126.5, 125.7, 125.2, 125.1, 125.0, 120.2, 120.1, 101.7, 95.8, 81.5, 78.5, 667.0, 66.8, 58.7, 53.2, 47.3, 38.4, 37.7. FT-IR (neat):  $\nu$  = 3335, 2955, 1699, 1541, 1521, 1508, 1450, 1418 cm<sup>-1</sup>. HRMS calcd for C<sub>25</sub>H<sub>23</sub>NO<sub>4</sub> + Na<sup>+</sup> [M+Na<sup>+</sup>]: 424.1519. Found 424.1502.

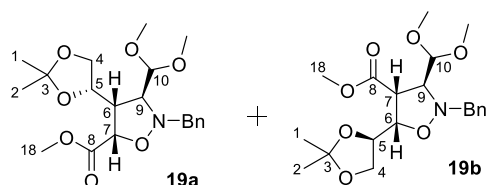


2(5*H*)-one as the dipolarophile, crude **17** was obtained after refluxing for 5 h. The crude was purified via column chromatography (10–15% EtOAc in petroleum ether 40–60) afforded **17** as a light yellow oil (286 mg, 80%). NMR signals and other experimental data of the major adduct **17a anti**: <sup>1</sup>H NMR (400 MHz, Chloroform-*d*)  $\delta$  7.63 (ddd,  $J$  = 8.0, 2.7, 1.5 Hz, 4H, ArH), 7.50 – 7.22 (m, 11H, ArH), 4.71 (d,  $J$  = 6.0 Hz, 1H, H-3), 4.57 (t,  $J$  = 2.3 Hz, 1H, H-2), 4.32 (d,  $J$  = 5.5 Hz, 1H, H-7), 4.16 (d,  $J$  = 13.6 Hz, 1H, NCH<sub>2</sub>), 4.02 (d,  $J$  = 13.5 Hz, 1H, NCH<sub>2</sub>), 3.90 (dd,  $J$  = 11.5, 2.6 Hz, 1H, H-1*a*), 3.82 (dd,  $J$  = 6.0, 2.9 Hz, 1H, H-4), 3.73 (dd,  $J$  = 11.5, 2.0 Hz, 1H, H-1*b*), 3.54 (dd,  $J$  = 5.5, 3.0 Hz, 1H, H-6), 3.46 (s, 3H, OCH<sub>3</sub>), 3.39 (s, 3H, OCH<sub>3</sub>), 1.05 (s, 9H, *t*Bu). <sup>13</sup>C NMR (101 MHz, Chloroform-*d*)  $\delta$  177.6, 137.1, 135.7, 135.6, 132.5, 132.0, 130.2, 129.2, 128.5, 128.1, 127.7, 104.3, 82.4, 80.8, 70.3, 63.9, 62.6, 55.1, 54.0, 52.1, 26.8, 19.2. FT-IR (neat):  $\nu$  = 2931, 2859, 1778, 1455, 1428 cm<sup>-1</sup>. HRMS calcd for C<sub>32</sub>H<sub>39</sub>O<sub>6</sub>NSi + H<sup>+</sup> [M+H<sup>+</sup>]: 562.2547. Found 562.2604. [ $\alpha$ ]<sub>D</sub><sup>20</sup> = -33.0° ( $c$  = 1.00, CHCl<sub>3</sub>). NMR signals and other experimental data of the minor adduct **17b syn**: <sup>1</sup>H NMR (400 MHz, Chloroform-*d*)  $\delta$  7.68 – 7.57 (m, 4H, ArH), 7.48 – 7.22 (m, 11H, ArH), 4.85 (m, 1H, H-3), 4.77 (d,  $J$  = 6.2 Hz, 1H, H-8), 4.50 (m, 1H, H-2), 4.44 (d,  $J$  = 14.3 Hz, 1H, NCH<sub>2</sub>), 3.87 (dd,  $J$  = 11.5, 2.6 Hz, 1H, H-1*a*), 3.81 (d,  $J$  = 14.3 Hz, 1H, NCH<sub>2</sub>), 3.73 (dd,  $J$  = 11.5, 2.1 Hz, 1H, H-1*b*), 3.67 (t,  $J$  = 7.5 Hz, 1H, H-4), 3.52 (s, 3H, OCH<sub>3</sub>), 3.48 (s, 3H, OCH<sub>3</sub>), 3.34 (dd,  $J$  = 7.6, 6.2 Hz, 1H, H-6), 1.03 (s, 9H, *t*Bu). <sup>13</sup>C NMR (101 MHz, Chloroform-*d*)  $\delta$  174.3, 137.4, 135.8, 135.6, 132.8, 132.2, 130.2, 128.9, 128.4, 128.0, 127.4, 103.3, 84.4, 78.4, 68.7, 63.9, 61.1, 56.2, 55.9, 51.6, 26.9, 19.3. FT-IR (neat):  $\nu$  = 2930, 2858, 1775, 1455, 1428 cm<sup>-1</sup>. HRMS calcd for C<sub>32</sub>H<sub>39</sub>O<sub>6</sub>NSi + H<sup>+</sup> [M+H<sup>+</sup>]: 562.2547. Found 562.2605. [ $\alpha$ ]<sub>D</sub><sup>20</sup> = +39.0° ( $c$  = 1.00, CHCl<sub>3</sub>).



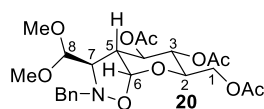
via column chromatography (35–50% Et<sub>2</sub>O in petroleum ether 40–60) affording **33** as a mixture of cycloadducts as a yellow oil (0.297 gram, 75%). The cycloadducts could not be separated via column chromatography, but it was possible to perform structure elucidation via NMR. HRMS calcd for C<sub>20</sub>H<sub>29</sub>NO<sub>7</sub> + Na<sup>+</sup> [M+Na<sup>+</sup>]: 418.1836. Found 418.1825. NMR signals of the major adduct **18a**: <sup>1</sup>H NMR (400 MHz, Chloroform-*d*)  $\delta$  7.40 – 7.22 (m, 5H, ArH), 4.47 (t,  $J$  = 6.7 Hz, 1H, H-6), 4.25 (d,  $J$  = 6.7 Hz, 1H, H-10), 4.20 (td,  $J$  = 6.4, 4.6 Hz, 1H, H-5), 4.12 (d,  $J$  = 12.9 Hz, 1H, NCH<sub>2</sub>), 4.06 (d,  $J$  = 12.9 Hz, 1H, NCH<sub>2</sub>), 4.04 – 4.00 (m, 1H, H-4*a*), 3.88 (dd,  $J$  = 8.8, 4.7 Hz, 1H, H-4*b*), 3.77 (s, 3H, H-18), 3.62 (m, 1H, H-9), 3.45 (m, 1H, H-7), 3.37 (s, 3H, OCH<sub>3</sub>), 3.29 (s, 3H, OCH<sub>3</sub>), 1.41 (s, 3H, H-1), 1.34 (s, 3H, H-2).

NMR signals of the minor adduct **18b**:  $^1\text{H}$  NMR (400 MHz, Chloroform- $d$ )  $\delta$  7.38 – 7.15 (m, 5H, ArH), 4.46 (d,  $J$  = 5.3 Hz, 1H, H-7), 4.26 (ddd,  $J$  = 7.2, 6.4, 4.2 Hz, 1H, H-5), 4.18 – 4.10 (m, 2H, H-10 &  $\text{NCH}_2$ ), 4.06 (d,  $J$  = 14.1 Hz, 1H,  $\text{NCH}_2$ ), 3.81 (dd,  $J$  = 8.5, 6.5 Hz, 1H, H-4a), 3.71 (s, 3H, H-18), 3.67 (dd,  $J$  = 8.6, 7.2 Hz, 1H, H-4b), 3.37 (s, 3H,  $\text{OCH}_3$ ), 3.30 (s, 3H,  $\text{OCH}_3$ ), 3.05 (dt,  $J$  = 5.2, 4.4 Hz, 1H, H-6), 2.97 (dd,  $J$  = 5.9, 4.6 Hz, 1H, H-9), 1.37 (s, 3H, H-1), 1.29 (s, 3H, H-2).  $^{13}\text{C}$  NMR (101 MHz, Chloroform- $d$ )  $\delta$  171.4, 137.0, 129.2, 128.3, 127.4, 109.3, 106.6, 77.2, 75.0, 68.0, 66.9, 60.9, 56.6, 56.1, 52.5, 51.4, 26.7, 25.3.



**Methyl (4*R*,5*S*)-2-benzyl-3-(dimethoxymethyl)-5-((*R*)-2,2-dimethyl-1,3-dioxolan-4-yl)isoxazolidine-4-carboxylate (**19**).** According to general procedure **A**, using methyl (*S*,*Z*)-3-(2,2-dimethyl-1,3-dioxolan-4-yl)acrylate as the dipolarophile, crude **19** was obtained after refluxing

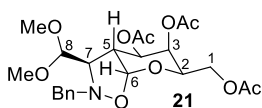
for 4 h. The crude was purified via column chromatography (30-70%  $\text{Et}_2\text{O}$  in petroleum ether 40-60) afforded **19** as a yellow oil (0.324 gram, 82%). NMR signals and other experimental data of the major adduct **19a syn**:  $^1\text{H}$  NMR (400 MHz, Chloroform- $d$ )  $\delta$  7.47 – 7.17 (m, 5H, ArH), 4.65 (d,  $J$  = 7.3 Hz, 1H, H-7), 4.37 (d,  $J$  = 13.2 Hz, 1H,  $\text{NCH}_2$ ), 4.21 (dt,  $J$  = 7.5, 6.2 Hz, 1H, H-5), 4.16 (d,  $J$  = 13.2 Hz, 1H,  $\text{NCH}_2$ ), 4.01 (d,  $J$  = 4.1 Hz, 1H, H-10), 3.89 (dd,  $J$  = 8.3, 6.3 Hz, 1H, H-4a), 3.76 (s, 3H, H-18), 3.62 (dd,  $J$  = 8.2, 7.3 Hz, 1H, H-4b), 3.45 – 3.37 (m, 4H, H-9 &  $\text{OCH}_3$ ), 3.31 (s, 3H,  $\text{OCH}_3$ ), 3.04 (ddd,  $J$  = 7.3, 6.0, 3.3 Hz, 1H, H-6), 1.45 (s, 3H, H-1), 1.32 (s, 3H, H-2).  $^{13}\text{C}$  NMR (101 MHz, Chloroform- $d$ )  $\delta$  169.5, 137.3, 129.8, 129.5, 128.3, 127.4, 108.9, 106.1, 78.1, 73.6, 68.1, 62.7, 56.4, 55.9, 52.0, 49.4, 26.6, 25.2. FT-IR (neat):  $\nu$  = 2986, 2932, 1757, 1734, 1559, 1497, 1455, 1437  $\text{cm}^{-1}$ . HRMS calcd for  $\text{C}_{20}\text{H}_{30}\text{NO}_7 + \text{H}^+$  [ $\text{M} + \text{H}^+$ ]: 396.2017. Found 396.2008. NMR signals and other experimental data of the minor adduct **19b syn**:  $^1\text{H}$  NMR (400 MHz, Methanol- $d_4$ )  $\delta$  7.40 – 7.23 (m, 5H, ArH), 4.32 – 4.21 (m, 2H, H-10 &  $\text{NCH}_2$ ), 4.16 – 4.02 (m, 2H, H-5 & H-6), 4.02 – 3.92 (m, 2H, H-4a &  $\text{NCH}_2$ ), 3.76 (dd,  $J$  = 8.5, 4.9 Hz, 1H, H-4b), 3.69 (s, 3H, H-18), 3.55 – 3.46 (m, 2H, H-7 & H-9), 3.38 (s, 3H,  $\text{OCH}_3$ ), 3.37 (s, 3H,  $\text{OCH}_3$ ), 1.33 (s, 3H, H-2), 1.27 (s, 3H, H-1).  $^{13}\text{C}$  NMR (101 MHz, Methanol- $d_4$ )  $\delta$  173.2, 138.5, 130.5, 129.2, 128.4, 110.6, 106.6, 80.8, 75.2, 72.2, 68.3, 63.2, 56.0, 55.9, 53.2, 52.5, 27.0, 25.6. FT-IR (neat):  $\nu$  = 2988, 2951, 1735, 1497, 1438  $\text{cm}^{-1}$ . HRMS calcd for  $\text{C}_{20}\text{H}_{30}\text{NO}_7 + \text{H}^+$  [ $\text{M} + \text{H}^+$ ]: 396.2017. Found 396.2005.



**(3*R*,3*aR*,4*R*,5*S*,6*R*,7*aR*)-6-(Acetoxymethyl)-2-benzyl-3-(dimethoxymethyl)hexahydro-4*H*-pyrano[3,2-*d*]isoxazole-4,5-diyl diacetate (**20**).** To a round bottom containing 3,4,6-tri-*O*-acetyl-D-glucal (0.272 gr, 1 mmol, 1.00 equiv) was added mesitylene (1.0 mL). The mixture

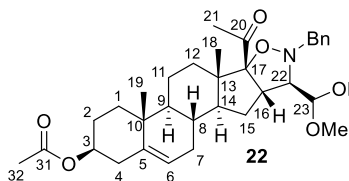
was heated to reflux and nitron **1** (1.05 gr, 5.00 equiv) was added portion-wise over 8 hours via the reflux-condensor. Upon complete addition, the reaction mixture was allowed to reflux for another 2 hours and then allowed to cool to rt. The reaction mixture was conc. *in vacuo*, affording crude **20** as an orange oil (56% conversion according to  $^1\text{H}$  NMR). The crude could be purified up to  $\approx 95\%$  via column chromatography (55-80%  $\text{Et}_2\text{O}$  in petroleum ether 40-60) affording **20** as an orange oil (390 mg).  $^1\text{H}$  NMR (400 MHz, Chloroform- $d$ )  $\delta$  7.44 – 7.26 (m, 5H, ArH), 5.51 (d,  $J$  = 5.1 Hz, 1H, H-6), 5.31 (t,  $J$  = 7.3 Hz, 1H, H-4), 4.98 (t,  $J$  = 7.9 Hz, 1H, H-3), 4.38 – 4.31 (m, 1H, H-1a), 4.29 (d,  $J$  = 13.2 Hz, 1H,  $\text{NCH}_2$ ), 4.23 (d,  $J$  = 13.3 Hz, 1H,  $\text{NCH}_2$ ), 4.16 – 4.05 (m, 2H, H-1b & H-2), 3.98 (d,  $J$  = 5.0 Hz, 1H, H-8), 3.41 (s, 3H,  $\text{OCH}_3$ ), 3.36 (t,  $J$  = 4.8 Hz, 1H, H-7), 3.30 (s, 3H,  $\text{OCH}_3$ ), 2.69 (dt,  $J$  = 6.7, 4.9 Hz, 1H, H-5), 2.08 (s, 3H,  $\text{OAc}$ ), 2.06 (m, 6H, 2 $\times$  $\text{OAc}$ ).  $^{13}\text{C}$  NMR (101 MHz, Chloroform- $d$ )  $\delta$  170.7, 170.2, 169.5, 136.6, 129.5, 128.4, 127.7, 106.2, 98.1, 72.1, 70.6, 68.9, 67.6, 63.4, 62.0, 56.3, 56.1, 46.8, 29.8, 20.9, 20.8. FT-IR (neat):  $\nu$  = 2924, 2851, 1743, 1664, 1497, 1454  $\text{cm}^{-1}$ . HRMS calcd for  $\text{C}_{23}\text{H}_{31}\text{NO}_{10} + \text{Na}^+$  [ $\text{M} + \text{Na}^+$ ]:

504.1840. Found. 504.1829. \*Could not be completely purified, but a relatively pure fraction was obtained for structure determination.



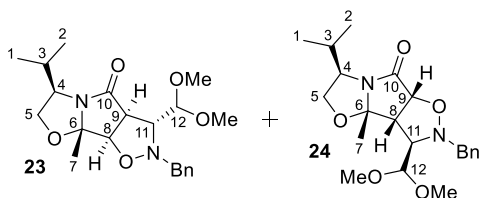
(**3R,3aR,4R,5R,6R,7aR**)-6-(**Acetoxymethyl**)-2-benzyl-3-(**dimethoxymethyl**)hexahydro-4H-pyrano[3,2-d]isoxazole-4,5-diyl diacetate (**21**). To a round bottom containing 3,4,6-tri-*O*-acetyl-D-galactal (0.247 gr, 1 mmol, 1.00 equiv) was added mesitylene (1.0 mL). The mixture

was heated to reflux and nitrone **1** (0.950 gr, 5.00 equiv) was added portion-wise over 8 hours via the reflux-condensor. Upon complete addition, the reaction mixture was allowed to reflux for another 1.5 hours and then allowed to cool to rt. The reaction mixture was conc. *in vacuo*, affording crude **21** as a dark brown oil (50% conversion according to  $^1\text{H}$  NMR). The crude could be partially purified up to  $\approx 95\%$  via column chromatography (58-75%  $\text{Et}_2\text{O}$  in petroleum ether 40-60) affording **21** as an yellow oil.  $^1\text{H}$  NMR (400 MHz, Chloroform-*d*)  $\delta$  7.41 – 7.28 (m, 5H, ArH), 5.54 (d,  $J$  = 4.6 Hz, 1H, H-6), 5.31 (dd,  $J$  = 3.0, 1.8 Hz, 1H, H-3), 5.05 (dd,  $J$  = 9.6, 3.0 Hz, 1H, H-4), 4.31 (td,  $J$  = 6.7, 1.9 Hz, 1H, H-2), 4.26 (d,  $J$  = 13.3 Hz, 1H,  $\text{NCH}_2$ ), 4.16 (d,  $J$  = 13.3 Hz, 1H,  $\text{NCH}_2$ ), 4.11 (dd,  $J$  = 6.7, 2.4 Hz, 2H, H-1), 3.96 (d,  $J$  = 4.7 Hz, 1H, H-8), 3.40 (s, 3H,  $\text{OCH}_3$ ), 3.29 (s, 3H,  $\text{OCH}_3$ ), 3.14 (dd,  $J$  = 4.7, 2.8 Hz, 1H, H-7), 2.66 (ddd,  $J$  = 9.6, 4.6, 2.7 Hz, 1H, H-5), 2.12 (s, 3H, OAc), 2.05 (s, 3H, OAc), 2.03 (s, 3H, OAc).  $^{13}\text{C}$  NMR (101 MHz, Chloroform-*d*)  $\delta$  170.6, 170.4, 170.2, 136.6, 129.6, 128.5, 127.8, 105.8, 98.7, 70.9, 69.9, 69.8, 65.5, 63.7, 61.8, 56.3, 55.7, 42.0, 29.8, 21.0, 20.9. FT-IR (neat):  $\nu$  = 2923, 2850, 1739, 1664, 1497, 1455  $\text{cm}^{-1}$ . HRMS calcd for  $\text{C}_{23}\text{H}_{31}\text{NO}_{10} + \text{Na}^+ [\text{M} + \text{Na}^+]$ : 504.1840. Found. 504.1830.



(**4S,6aR,6bS,8aS,8bR,11R,11aS,12aS,12bR**)-8b-Acetyl-10-benzyl-11-(dimethoxymethyl)-6a,8a-dimethyl-3,4,5,6,6a,6b,7,8,8a,8b,10,11,11a,12,12a,12b-hexadecahydro-1H-naphtho[2',1':4,5]indeno[2,1-d]isoxazol-4-yl acetate (**22**).

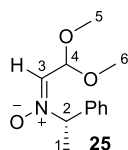
According to general procedure A crude **22** was obtained after refluxing for 5 h. The crude was purified via column chromatography (20-40%  $\text{Et}_2\text{O}$  in petroleum ether 40-60) afforded **22** as a yellow solid (95% purity). The yellow solid could be further purified by suspending the solid in a 10% solution of  $\text{Et}_2\text{O}$  in PE, which, upon decantation, provided **22** as a white solid (0.466 gram, 82%).  $^1\text{H}$  NMR (400 MHz, Chloroform-*d*)  $\delta$  7.46 – 7.14 (m, 5H, ArH), 5.36 (m, 1H, H-6), 4.61 (tdd,  $J$  = 10.5, 6.1, 4.2 Hz, 1H, H-3), 4.37 (d,  $J$  = 14.0 Hz, 1H,  $\text{NCH}_2$ ), 4.22 (d,  $J$  = 7.3 Hz, 1H, H-23), 3.72 (d,  $J$  = 14.0 Hz, 1H,  $\text{NCH}_2$ ), 3.42 (m, 6H,  $\text{OCH}_3 \times 2$ ), 3.32 (m, 1H, H-16), 2.59 (dd,  $J$  = 7.3, 6.0 Hz, 1H, H-22), 2.38 – 2.23 (m, 2H, H-4), 2.03 (s, 3H, H-32), 1.94 (m, 1H), 1.90 – 1.68 (m, 7H), 1.65 – 1.33 (m, 8H), 1.15 (td,  $J$  = 13.9, 13.1, 4.1 Hz, 1H), 0.99 (m, 4H, H-19 + ?), 0.58 (s, 3H, H-18).  $^{13}\text{C}$  NMR (101 MHz, Chloroform-*d*)  $\delta$  211.7, 170.7, 139.7, 138.1, 129.6, 128.0, 127.1, 122.4, 107.2, 99.0, 75.8, 74.0, 61.1, 55.5, 55.4, 50.6, 50.1, 49.7, 45.4, 38.2, 37.1, 36.7, 32.4, 32.1, 31.8, 31.3, 27.9, 26.7, 21.6, 20.6, 19.4, 14.9. FT-IR (neat):  $\nu$  = 2944, 2896, 2833, 1733, 1709, 1497, 1455, 1438  $\text{cm}^{-1}$ . HRMS calcd for  $\text{C}_{34}\text{H}_{47}\text{NO}_6 + \text{H}^+ [\text{M} + \text{H}^+]$ : 566.3476. Found. 566.3456.



**Cycloaddition of (3R,7aS)-3-isopropyl-7a-methyl-2,3-dihydropyrrolo[2,1-b]oxazol-5(7aH)-one with nitrone 1.** According to general procedure A, using (3R,7aS)-3-isopropyl-7a-methyl-2,3-dihydropyrrolo[2,1-b]oxazol-5(7aH)-one as the dipolarophile, crude cycloadducts were obtained after refluxing for 4 h. The crude was purified via



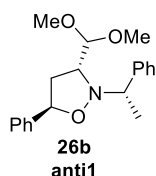
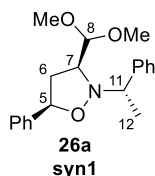
column chromatography (30-70% Et<sub>2</sub>O in petroleum ether 40-60) affording cycloadduct **23** (110 mg, 28%) and **24** (214 mg, 54%) as yellow oils. NMR signals and other experimental data of the major adduct **24**: <sup>1</sup>H NMR (400 MHz, Methanol-*d*<sub>4</sub>) δ 7.49 – 7.13 (m, 5H, ArH), 5.04 (d, *J* = 8.8 Hz, 1H, H-9), 4.56 (dd, *J* = 9.1, 7.7 Hz, 1H, H-5a), 4.15 (d, *J* = 6.0 Hz, 1H, H-12), 4.06 (dd, *J* = 9.1, 7.3 Hz, 1H, H-5b), 3.93 (d, *J* = 12.6 Hz, 1H, NCH<sub>2</sub>), 3.85 (dd, *J* = 6.1, 2.8 Hz, 1H, H-11), 3.69 – 3.58 (m, 2H, H-4 & NCH<sub>2</sub>), 3.46 (m, 1H, H-8), 3.36 (s, 3H, OCH<sub>3</sub>), 3.17 (s, 3H, OCH<sub>3</sub>), 1.78 (m, 1H, H-3), 1.59 (s, 3H, H-7), 1.06 (d, *J* = 6.7 Hz, 3H, H-2), 0.94 (d, *J* = 6.6 Hz, 3H, H-1). <sup>13</sup>C NMR (101 MHz, Methanol-*d*<sub>4</sub>) δ 178.6, 138.2, 130.6, 129.2, 128.5, 105.9, 97.9, 85.3, 72.0, 68.1, 63.7, 63.2, 55.6, 55.5, 54.7, 49.4, 49.2, 48.8, 35.5, 26.5, 21.2, 19.1. FT-IR (neat): ν = 2955, 2922, 2852, 1716, 1455 cm<sup>-1</sup>. HRMS calcd for C<sub>21</sub>H<sub>30</sub>N<sub>2</sub>O<sub>5</sub>+H<sup>+</sup> [M+H<sup>+</sup>]: 391.2227. Found. 391.2214. [α]<sub>D</sub><sup>20</sup> = +48.6° (*c* = 1.00, CHCl<sub>3</sub>). NMR signals and other experimental data for the minor adduct **23**: <sup>1</sup>H NMR (400 MHz, Methanol-*d*<sub>4</sub>) δ 7.35 – 7.21 (m, 5H, ArH), 4.44 (d, *J* = 8.0 Hz, 1H, H-8), 4.37 (d, *J* = 5.6 Hz, 1H, H-12), 4.22 – 4.15 (m, 2H, H-5a & NCH<sub>2</sub>), 4.10 (d, *J* = 13.3 Hz, 1H, NCH<sub>2</sub>), 3.80 (dd, *J* = 8.7, 6.8 Hz, 1H, H-5b), 3.62 (dd, *J* = 8.0, 2.4 Hz, 1H, H-9), 3.60 – 3.51 (m, 2H, H-11 & H-4), 3.41 (s, 3H, OCH<sub>3</sub>), 3.32 (s, 3H, OCH<sub>3</sub>), 1.73 (m, 1H, H-3), 1.35 (s, 3H, H-7), 1.07 (d, *J* = 6.6 Hz, 3H, H-2), 0.90 (d, *J* = 6.6 Hz, 3H, H-1). <sup>13</sup>C NMR (101 MHz, Methanol-*d*<sub>4</sub>) δ 183.5, 138.3, 130.4, 129.3, 128.5, 104.2, 102.3, 82.2, 70.7, 69.6, 66.0, 61.5, 55.0, 54.6, 35.0, 21.5, 19.2, 19.0. FT-IR (neat): ν = 2961, 2930, 1716, 1497, 1466, 1455 cm<sup>-1</sup>. HRMS calcd for C<sub>21</sub>H<sub>30</sub>N<sub>2</sub>O<sub>5</sub>+H<sup>+</sup> [M+H<sup>+</sup>]: 391.2227. Found. 391.2211. [α]<sub>D</sub><sup>20</sup> = +22.6° (*c* = 1.00, CHCl<sub>3</sub>).



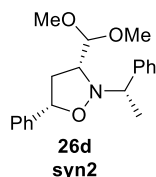
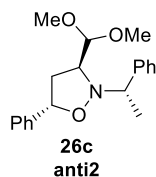
**(S)-2,2-Dimethoxy-N-(1-phenylethyl)ethan-1-imine oxide (25).** To a suspension of (S)-N-(α-methylbenzyl)hydroxylamine oxalate (1.31 gr, 5.78 mmol, 1.00 equiv) in MeOH (3 mL) was added NaOAc (0.95 gram, 11.6 mmol, 2.00 equiv). The mixture was cooled in an ice bath and a 60% solution of 2,2-dimethoxyacetaldehyde in H<sub>2</sub>O (0.99 mL, 6.53 mmol, 1.13 equiv) was added portion-wise. The reaction mixture was stirred for 30 minutes at 4 °C and then conc. *in vacuo*. DCM (50 mL) and H<sub>2</sub>O (10 mL) were added and the resulting layers were partitioned. The water layer was extracted with DCM (20 mL, 10 mL) and the combined organic layers were washed with sat. aq. NaHCO<sub>3</sub> (10 mL, 2×) & brine (10 mL), dried (MgSO<sub>4</sub>) and conc. *in vacuo*, affording compound **25** (1.22 gram, 95%) as a crystalline white solid. <sup>1</sup>H NMR (400 MHz, Chloroform-*d*) δ 7.49 – 7.29 (m, 5H, ArH), 6.79 (d, *J* = 5.4 Hz, 1H, H-3), 5.42 (d, *J* = 5.4 Hz, 1H, H-4), 5.01 (q, *J* = 6.9 Hz, 1H, H-2), 3.41 (s, 3H, H-5), 3.35 (s, 3H, H-6), 1.81 (d, *J* = 6.9 Hz, 3H, H-1). <sup>13</sup>C NMR (101 MHz, Chloroform-*d*) δ 137.8, 133.5, 129.0, 128.9, 127.5, 97.8, 74.5, 54.8, 54.5, 19.1. FT-IR (neat): ν = 2984, 2937, 2831, 1582, 1495, 1453 cm<sup>-1</sup>. HRMS calcd for C<sub>12</sub>H<sub>17</sub>NO<sub>3</sub>+Na<sup>+</sup> [M+Na<sup>+</sup>]: 246.1101. Found. 246.1096. [α]<sub>D</sub><sup>20</sup> = -15.1° (*c* = 1.00, CHCl<sub>3</sub>).

### General procedure C: preparation of cycloadducts.

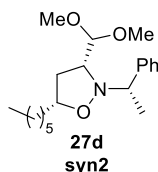
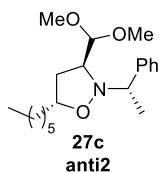
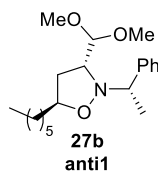
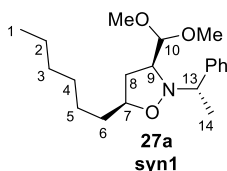
To a suspension of nitron **25** (1 mmol) in toluene (1 mL) was added a dipolarophile (2 mmol). The resulting mixture was heated under argon to reflux. After the indicated time, the reaction mixture was concentrated *in vacuo* and the crude material was purified by column chromatography.



**3-(Dimethoxymethyl)-5-phenyl-2-((S)-1-phenylethyl)isoxazolidine (26).** According to general procedure C crude **26** was obtained after refluxing for 2 h. The crude was purified via column chromatography (18-27% Et<sub>2</sub>O in petroleum ether 40-60) affording **26** as a yellow oil (352 mg, 100%). NMR signals and other experimental data of the major adduct **26 syn1/2**: <sup>1</sup>H NMR



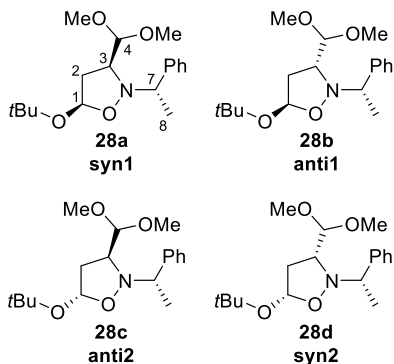
(400 MHz, Chloroform-*d*)  $\delta$  7.48 – 7.25 (m, 10H, ArH), 5.22 (t,  $J$  = 8.2 Hz, 1H, H-5), 4.17 (d,  $J$  = 6.1 Hz, 1H, H-8), 4.04 (q,  $J$  = 6.4 Hz, 1H, H-11), 3.38 (ddd,  $J$  = 8.6, 6.1, 4.3 Hz, 1H, H-7), 3.32 (s, 3H, OCH<sub>3</sub>), 3.08 (s, 3H, OCH<sub>3</sub>), 2.73 (dt,  $J$  = 13.0, 8.3 Hz, 1H, H-6a), 2.28 (ddd,  $J$  = 12.9, 8.5, 4.2 Hz, 1H, H-6b), 1.53 (d,  $J$  = 6.4 Hz, 3H, H-12). <sup>13</sup>C NMR (101 MHz, Chloroform-*d*)  $\delta$  142.9, 140.0, 128.6, 128.5, 128.3, 127.9, 127.7, 126.8, 106.0, 78.7, 66.0, 64.4, 55.5, 54.1, 37.8, 21.4. FT-IR (neat):  $\nu$  = 2932, 2832, 1493, 1454 cm<sup>-1</sup>. HRMS calcd for C<sub>20</sub>H<sub>25</sub>NO<sub>3</sub>+H<sup>+</sup> [M+H<sup>+</sup>]: 328.1907 Found: 328.1900.  $[\alpha]_D^{20}$  = -37.7° ( $c$  = 1.00, CHCl<sub>3</sub>). NMR signals and other experimental data of the minor adduct **26 syn1/2**<sup>a</sup>: <sup>1</sup>H NMR (400 MHz, Methanol-*d*<sub>4</sub>)  $\delta$  7.56 – 7.03 (m, 10H, ArH), 4.76 (dd,  $J$  = 9.6, 6.5 Hz, 1H, H-5), 4.35 (d,  $J$  = 6.9 Hz, 1H, H-8), 4.14 (q,  $J$  = 6.7 Hz, 1H, H-11), 3.63 (dt,  $J$  = 8.0, 6.9 Hz, 1H, H-7), 3.53 (s, 3H, OCH<sub>3</sub>), 3.38 (s, 3H, OCH<sub>3</sub>), 2.68 – 2.53 (m, 1H, H-6a), 2.14 (ddd,  $J$  = 12.6, 9.6, 6.8 Hz, 1H, H-6b), 1.48 (d,  $J$  = 6.8 Hz, 3H, H-12). NMR signals and other experimental data of the minor adduct **26 anti1/2**<sup>a</sup>: <sup>1</sup>H NMR (400 MHz, Methanol-*d*<sub>4</sub>)  $\delta$  7.54 – 6.99 (m, 10H), 5.07 (dd,  $J$  = 10.3, 6.4 Hz, 1H, H-5), 4.01 (q,  $J$  = 6.4 Hz, 1H, H-12), 3.90 (d,  $J$  = 4.7 Hz, 1H, H-8), 3.42 – 3.39 (m, 1H, H-7), 3.35 (s, 3H, OCH<sub>3</sub>), 3.07 (s, 3H, OCH<sub>3</sub>), 2.67 – 2.55 (m, 1H, H-6a), 2.22 (ddd,  $J$  = 12.5, 10.3, 8.9 Hz, 1H, H-6b), 1.54 (d,  $J$  = 6.5 Hz, 3H, H-12). NMR signals and other experimental data of the minor adduct **26 anti1/2**: <sup>1</sup>H NMR (400 MHz, Chloroform-*d*)  $\delta$  7.48 – 7.43 (m, 2H, ArH), 7.37 – 7.19 (m, 8H, ArH), 4.94 (dd,  $J$  = 9.8, 6.5 Hz, 1H, H-5), 4.31 (d,  $J$  = 6.0 Hz, 1H, H-8), 4.18 (q,  $J$  = 6.9 Hz, 1H, H-11), 3.51 (s, 3H, OCH<sub>3</sub>), 3.43 (s, 3H, OCH<sub>3</sub>), 3.37 (ddd,  $J$  = 9.4, 6.0, 3.2 Hz, 1H, H-7), 2.54 (ddd,  $J$  = 12.6, 6.5, 3.2 Hz, 1H, H-6a), 1.92 (dt,  $J$  = 12.6, 9.7 Hz, 1H, H-6b), 1.57 (d,  $J$  = 6.9 Hz, 3H, H-12). <sup>13</sup>C NMR (101 MHz, Chloroform-*d*)  $\delta$  141.1, 140.2, 129.5, 128.4, 128.0, 127.8, 127.3, 126.7, 106.8, 78.8, 64.5, 63.9, 56.5, 54.9, 39.0, 20.6. FT-IR (neat):  $\nu$  = 2954, 2922, 2852, 1493, 1453 cm<sup>-1</sup>. HRMS calcd for C<sub>20</sub>H<sub>25</sub>NO<sub>3</sub>+H<sup>+</sup> [M+H<sup>+</sup>]: 328.1907 Found: 328.1901.  $[\alpha]_D^{20}$  = -11.8° ( $c$  = 1.00, CHCl<sub>3</sub>). <sup>a</sup>Could only be isolated as a mixture of cycloadducts, but it was possible to perform structure elucidation via NMR. <sup>b</sup>*Syn/Anti* stereochemistry was unambiguously assigned, but it was not possible to conclusively assign *syn1/syn2* or *anti1/anti2* stereochemistry even with NOESY.



**3-(Dimethoxymethyl)-5-hexyl-2-((S)-1-phenylethyl)isoxazolidine (27)**. According to general procedure **C** crude **27** was obtained after refluxing for 2 h. The crude was purified via column chromatography (5–10% EtOAc in heptane) afforded **27** as a yellow oil (326 mg, 93%). NMR signals and other experimental data of the major adduct **27 syn1/2**: <sup>1</sup>H NMR (400 MHz, Chloroform-*d*)  $\delta$  7.43 – 7.02 (m, 5H, ArH), 4.11 (ddd,  $J$  = 14.1, 7.6, 6.1 Hz, 1H, H-7), 3.96 (d,  $J$  = 6.4 Hz, 1H, H-10), 3.78 (q,  $J$  = 6.4 Hz, 1H, H-13), 3.23 (s, 3H, OCH<sub>3</sub>), 3.13 (ddd,  $J$  = 8.6, 6.3, 4.0 Hz, 1H, H-9), 2.99 (s, 3H, OCH<sub>3</sub>), 2.30 (ddd,  $J$  = 12.7, 8.6, 7.5 Hz, 1H, H-8a), 1.77 (ddd,  $J$  = 12.4, 8.0, 4.0 Hz, 1H, H-8b), 1.65 – 1.42 (m, 2H, H-6), 1.37 (d,  $J$  = 6.4 Hz, 3H, H-14), 1.36 – 1.14 (m, 8H, 4x CH<sub>2</sub>), 0.90 – 0.74 (m, 3H, H-1). <sup>13</sup>C NMR (101 MHz, Chloroform-*d*)  $\delta$  143.1, 128.5, 128.3, 127.6, 106.0, 76.9, 65.4, 64.0, 55.2, 54.5, 34.8, 34.2, 31.9, 29.4, 26.7, 22.7, 21.4, 14.2. FT-IR (neat):  $\nu$  = 2955, 2929, 2858, 1493, 1454 cm<sup>-1</sup>. HRMS calcd for C<sub>20</sub>H<sub>33</sub>NO<sub>3</sub>+H<sup>+</sup> [M+H<sup>+</sup>]: 336.2533 Found: 336.2525.  $[\alpha]_D^{20}$  = -11.6° ( $c$  = 1.00, CHCl<sub>3</sub>). NMR signals and other experimental data of three minor adducts **27**<sup>a</sup>: <sup>a</sup>Could not be obtained pure, but only as a mixture of cycloadducts. <sup>b</sup>*Syn/Anti* stereochemistry was unambiguously assigned, but it was not possible to



conclusively assign syn1/syn2 or anti1/anti2 stereochemistry even with NOESY.



**5-(*tert*-Butoxy)-3-(dimethoxymethyl)-2-((*S*)-1-phenylethyl)isoxazolidine (28).** According to general procedure **C** crude **28** was obtained after refluxing for 2 h. The crude was purified via column chromatography (22–32% Et<sub>2</sub>O in petroleum ether 40–60) afforded **28** as a yellow oil (309 mg, quant.). NMR signals and other experimental data of the major adduct **28 syn1/2'**: <sup>1</sup>H NMR (400 MHz, Chloroform-*d*) δ 7.39 – 7.21 (m, 5H, ArH), 5.54 (dd, *J* = 6.2, 2.0 Hz, 1H, H-1), 4.45 (d, *J* = 7.9 Hz, 1H, H-4), 3.87 (q, *J* = 6.6 Hz, 1H, H-7), 3.34 (s, 3H, OCH<sub>3</sub>), 3.23 – 3.12 (m, 4H, H-3 & OCH<sub>3</sub>), 2.26 – 2.12 (m, 1H, H-2a), 2.06 (dt, *J* = 13.3, 2.1 Hz, 1H, H-2b), 1.49 (d, *J* = 6.6 Hz, 3H, H-8), 1.25 (s, 9H, *t*Bu). <sup>13</sup>C NMR (101

MHz, Chloroform-*d*) δ 142.7, 128.3, 128.2, 127.5, 105.1, 97.8, 74.5, 65.5, 62.9, 55.4, 53.9, 36.7, 29.0, 20.2. FT-IR (neat): ν = 2974, 2933, 2831, 1493, 1453 cm<sup>-1</sup>. HRMS calcd for C<sub>18</sub>H<sub>29</sub>NO<sub>4</sub> + H<sup>+</sup> [*M*+H<sup>+</sup>]: 324.2169 Found: 324.2156. [α]<sub>D</sub><sup>20</sup> = +71.7° (*c* = 1.00, CHCl<sub>3</sub>). NMR signals and other experimental data of the minor adduct **28 syn1/2'**: <sup>1</sup>H NMR (400 MHz, Chloroform-*d*) δ 7.52 – 7.16 (m, 5H, ArH), 5.23 (dd, *J* = 5.8, 2.5 Hz, 1H, H-1), 4.51 (d, *J* = 7.8 Hz, 1H, H-4), 4.01 (q, *J* = 6.9 Hz, 1H, H-7), 3.53 (s, 3H, OCH<sub>3</sub>), 3.38 (s, 3H, OCH<sub>3</sub>), 3.12 (ddd, *J* = 8.9, 7.8, 4.5 Hz, 1H, H-3), 1.96 (ddd, *J* = 13.2, 4.5, 2.5 Hz, 1H, H-2a), 1.86 (ddd, *J* = 13.1, 8.8, 5.7 Hz, 1H, H-2b), 1.55 (d, *J* = 7.0 Hz, 3H, H-8), 1.21 (s, 9H, *t*Bu). <sup>13</sup>C NMR (101 MHz, Chloroform-*d*) δ 141.3, 129.2, 127.9, 127.2, 106.8, 96.3, 74.3, 64.9, 63.4, 56.1, 54.7, 38.5, 28.9, 20.9. FT-IR (neat): ν = 2974, 2932, 2831, 1494, 1453 cm<sup>-1</sup>. HRMS calcd for C<sub>18</sub>H<sub>29</sub>NO<sub>4</sub> + H<sup>+</sup> [*M*+H<sup>+</sup>]: 324.2169 Found: 324.2155. [α]<sub>D</sub><sup>20</sup> = -87.0° (*c* = 1.00, CHCl<sub>3</sub>). NMR signals and other experimental data of the minor adduct **28 anti1/2'**: <sup>1</sup>H NMR (400 MHz, Chloroform-*d*) δ 7.45 – 7.18 (m, 5H, ArH), 5.34 (dd, *J* = 6.6, 2.9 Hz, 1H, H-1), 4.34 (q, *J* = 6.6 Hz, 1H, H-7), 4.22 (d, *J* = 6.1 Hz, 1H, H-4), 3.69 (ddd, *J* = 8.3, 6.3, 4.0 Hz, 1H, H-3), 3.56 (s, 3H, OCH<sub>3</sub>), 3.46 (s, 3H, OCH<sub>3</sub>), 2.56 (ddd, *J* = 13.7, 6.5, 3.8 Hz, 1H, H-2a), 2.33 (ddd, *J* = 13.7, 8.3, 2.9 Hz, 1H, H-2b), 1.34 (d, *J* = 6.6 Hz, 3H, H-8), 0.97 (s, 9H, *t*Bu). NMR signals and other experimental data of the minor adduct **28 anti1/2'**: <sup>1</sup>H NMR (400 MHz, Chloroform-*d*) δ 7.44 – 7.21 (m, 5H, ArH), 5.53 (dd, *J* = 6.5, 3.3 Hz, 1H, H-1), 4.22 (q, *J* = 6.3 Hz, 1H, H-7), 3.90 (d, *J* = 5.3 Hz, 1H, H-4), 3.32 (m, 4H, OCH<sub>3</sub> & H-3), 3.06 (s, 3H, OCH<sub>3</sub>), 2.52 (ddd, *J* = 13.6, 6.6, 3.5 Hz, 1H, H-2a), 2.30 – 2.16 (m, 1H, H-2b), 1.56 (d, *J* = 6.3 Hz, 3H, H-8), 1.30 (s, 9H, *t*Bu). "Could only be isolated as a mixture of cycloadducts, but it was possible to perform structure elucidation via NMR. 'Syn/Anti stereochemistry was unambiguously assigned, but it was not possible to conclusively assign syn1/syn2 or anti1/anti2 stereochemistry even with NOESY.

## REFERENCES

1. Gothelf, K.V. and Jørgensen, K.A. *Chem. Rev.* **1998**, 98, 863.
2. (a) Shimokawa, J., Shirai, K., Tanatani, A., Hashimoto, Y., and Nagasawa, K. *Angew. Chem. Int. Ed.* **2004**, 43, 1559; (b) Ina, H., Ito, M., and Kibayashi, C. *J. Org. Chem.* **1996**, 61, 1023; (c) Morin, M.S.T. and Arndtsen, B.A. *Org. Lett.* **2014**, 16, 1056.
3. (a) Aouadi, K., Msaddek, M., and Praly, J.-P. *Tetrahedron* **2012**, 68, 1762; (b) Cecioni, S., Aouadi, K., Guiard, J., Parrot, S., Strazielle, N., Blondel, S., Ghersi-Egea, J.-F., Chapelle, C., Denoroy, L., and Praly, J.-P. *Eur. J. Med. Chem.* **2015**, 98, 237.
4. (a) Hashimoto, T. and Maruoka, K. *Chem. Rev.* **2015**, 115, 5366; (b) Stanley, L.M. and Sibi, M.P. *Chem. Rev.* **2008**, 108, 2887.
5. (a) Inouye, Y., Watanabe, Y., Takahashi, S., and Kakisawa, H. *Bull. Chem. Soc. Jpn.* **1979**, 52, 3763; (b) Nguyen, T.B., Beauseigneur, A., Martel, A., Dhal, R., Laurent, M., and Dujardin, G. *J. Org. Chem.* **2010**, 75, 611.
6. (a) Debrassi, A., Ribbera, A., de Vos, W.M., Wennekes, T., and Zuilhof, H. *Langmuir* **2014**, 30, 1311; (b) Branson, T.R., McAllister, T.E., Garcia-Hartjes, J., Fascione, M.A., Ross, J.F., Warriner, S.L., Wennekes, T., Zuilhof, H., and Turnbull, W.B. *Angew. Chem. Int. Ed.* **2014**, 53, 8323; (c) Mattarella, M., Garcia-Hartjes, J., Wennekes, T., Zuilhof, H., and Siegel, J.S. *Org. Biomol. Chem.* **2013**, 11, 4333; (d) Garcia-Hartjes, J., Bernardi, S., Weijers, C.A.G.M., Wennekes, T., Gilbert, M., Sansone, F., Casnati, A., and Zuilhof, H. *Org. Biomol. Chem.* **2013**, 11, 4340; (e) Kallemeijn, W.W., Witte, M.D., Wennekes, T., Aerts, J.M.F.G., and Derek, H., Chapter 4, in *Adv. Carbohydr. Chem. Biochem.* 2014, Academic Press. p. 297; (f) Kim, J.-H., Resende, R., Wennekes, T., Chen, H.-M., Bance, N., Buchini, S., Watts, A.G., Pilling, P., Streltsov, V.A., Petric, M., Liggins, R., Barrett, S., McKimm-Breschkin, J.L., Niikura, M., and Withers, S.G. *Science* **2013**, 340, 71.
7. (a) Nguyen, T.B., Martel, A., Dhal, R., and Dujardin, G. *Synthesis* **2009**, 2009, 3174; (b) Tamura, O., Gotanda, K., Yoshino, J., Morita, Y., Terashima, R., Kikuchi, M., Miyawaki, T., Mita, N., Yamashita, M., Ishibashi, H., and Sakamoto, M. *J. Org. Chem.* **2000**, 65, 8544; (c) Tokunaga, Y., Ihara, M., and Fukumoto, K. *Tetrahedron Lett.* **1996**, 37, 6157.
8. (a) Alibés, R., Busqué, F., de March, P., Figueredo, M., Font, J., and Parella, T. *Tetrahedron* **1998**, 54, 10857; (b) Collon, S., Kouklovsky, C., and Langlois, Y. *Eur. J. Org. Chem.* **2002**, 2002, 3566; (c) Snider, B.B. and Cartaya-Marin, C.P. *J. Org. Chem.* **1984**, 49, 1688.
9. (a) McKay, C.S., Moran, J., and Pezacki, J.P. *Chem. Commun.* **2010**, 46, 931; (b) Dommerholt, J., Schmidt, S., Temming, R., Hendriks, L.J.A., Rutjes, F.P.J.T., van Hest, J.C.M., Lefebvre, D.J., Friedl, P., and van Delft, F.L. *Angew. Chem. Int. Ed.* **2010**, 49, 9422; (c) Sanders, B.C., Friscourt, F., Ledin, P.A., Mbua, N.E., Arumugam, S., Guo, J., Boltje, T.J., Popik, V.V., and Boons, G.-J. *J. Am. Chem. Soc.* **2011**, 133, 949.
10. (a) Fujioka, H., Sawama, Y., Murata, N., Okitsu, T., Kubo, O., Matsuda, S., and Kita, Y. *J. Am. Chem. Soc.* **2004**, 126, 11800; (b) Jung, M.E., Andrus, W.A., and Ornstein, P.L. *Tetrahedron Lett.* **1977**, 18, 4175; (c) Sun, J., Dong, Y., Cao, L., Wang, X., Wang, S., and Hu, Y. *J. Org. Chem.* **2004**, 69, 8932.
11. (a) Ibebeke-Bomangwa, W. and Hootelé, C. *Tetrahedron* **1987**, 43, 935; (b) Yu, J., DePue, J., and Kronenthal, D. *Tetrahedron Lett.* **2004**, 45, 7247; (c) de Meijere, A., von Seebach, M., Kozhushkov, Sergei I., Boese, R., Bläser, D., Cicchi, S., Dimoulas, T., and Brandi, A. *Eur. J. Org. Chem.* **2001**, 2001, 3789.

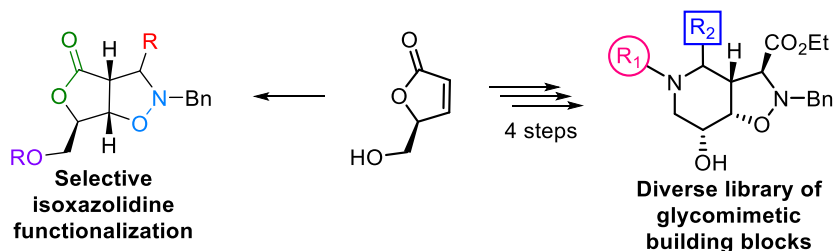
12. Siriwardena, A., Sonawane, D.P., Bande, O.P., Markad, P.R., Yonekawa, S., Tropak, M.B., Ghosh, S., Chopade, B.A., Mahuran, D.J., and Dhavale, D.D. *J. Org. Chem.* **2014**, 79, 4398.
13. *An attempt to perform the hydrogenation with both metals (10% Pd/C & Raney-Ni) at the same time only reached 30% conversion after 5h in the Parr-apparatus (5 bar), after which no further conversion was observed upon longer reaction times.*
14. Ondruš, V., Orság, M., Fišera, L.u., and Prónayová, N.a. *Tetrahedron* **1999**, 55, 10425.
15. (a) *This regioselectivity is explained by the stabilizing attractive interaction between the electron-rich allylic oxygen and the positively charged carbon atom of the dipole of 1. See ref. 16b;* (b) Annunziata, R., Benaglia, M., Cinquini, M., Cozzi, F., and Raimondi, L. *Eur. J. Org. Chem.* **1998**, 1998, 1823.
16. Cardona, F., Valenza, S., Picasso, S., Goti, A., and Brandi, A. *J. Org. Chem.* **1998**, 63, 7311; (b) Cardona, F., Valenza, S., Goti, A., and Brandi, A. *Tetrahedron Lett.* **1997**, 38, 8097.
17. Girdhar, N.K. and Ishar, M.P.S. *Tetrahedron Lett.* **2000**, 41, 7551.
18. Meyers, A.I. and Strickland, R.C. *J. Org. Chem.* **1972**, 37, 2579.
19. Fischer, N., Goddard-Borger, E.D., Greiner, R., Klapötke, T.M., Skelton, B.W., and Stierstorfer, J. *J. Org. Chem.* **2012**, 77, 1760.

## Chapter 3



# Exploring the Chemistry of Bicyclic Isoxazolidines for the Multicomponent Synthesis of Glycomimetic Building Blocks

## Abstract



Starting from a chiral furanone, the nitron–olefin [3+2] cycloaddition can be used to obtain bicyclic isoxazolidines for which we report a set of reactions to selectively modify each functional position. These synthetically versatile bicyclic isoxazolidines allowed us to obtain complex glycomimetic building blocks, like iminosugars, *via* multicomponent chemistry. For example, a library of 20 pipecolic acid derivatives - a recurring motif in various prescription drugs - could be obtained *via* a one-pot Staudinger/aza-Wittig/Ugi three-component reaction of a bicyclic isoxazolidine-derived azido-hemiacetal. Notably, specific pipecolic acids in this library were obtained *via* hydrolysis of an unique tricyclic imide side product of the Ugi reaction. The azido-hemiacetal was also converted into an aza-C-glycoside iminosugar *via* an unprecedented one-pot Staudinger/aza-Wittig/Mannich reaction.

Part of this work was published in:

J. Hoogenboom, H. Zuilhof, M. Lutz, T. Wennekes,  
*J. Org. Chem.*, **2016**, 81, 8826-8836

## Introduction

Glycomimetics such as iminosugars and their derivatives are found in nature and display a wide variety of biological activities. For example, the archetypical glycomimetic 1-deoxynojirimycin (Figure 1), found in the leaves of the mulberry tree<sup>1</sup> and certain species of bacteria,<sup>2</sup> is a glycosidase inhibitor. Since the report of its identification and chemical synthesis in 1967,<sup>3–5</sup> the subsequent decades have witnessed a vast number of studies describing the synthesis and evaluation of biologically active glycomimetics. The value of these synthetic glycomimetics is evidenced by *N*-(hydroxyethyl)-1-deoxynojirimycin (miglitol), a clinically used drug in the treatment of type 2 diabetes<sup>6</sup> that inhibits intestinal glucosidases, and by *N*-butyl-1-deoxynojirimycin (miglustat), a glycosyl transferase inhibitor used in the clinic for the treatment of Gaucher disease.<sup>7,8</sup> Consequently, glycomimetics hold great promise for drug discovery. Key to enabling this is the development of synthetic methodology and novel glycomimetic building blocks to generate comprehensive and structurally diverse libraries of glycomimetics.

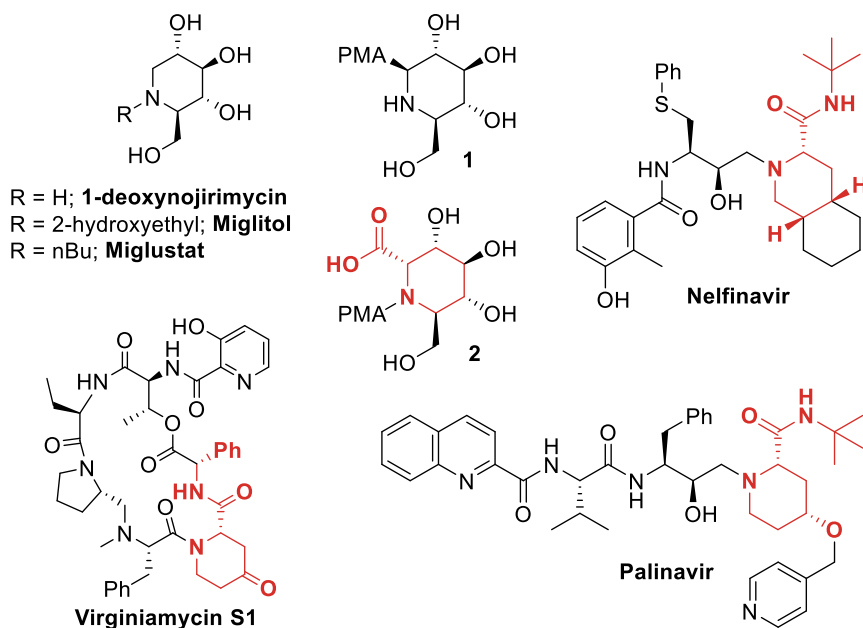


**Figure 1.** 1-Deoxynojirimycin with analogues thereof and notable examples of pipecolic acid derivatives (in red). AMP = 5-(adamantan-1-yl-methoxy)-pentyl.

In our ongoing synthetic investigation toward novel glycomimetics we are, among others, interested in developing aza-*C*-glycoside and pipecolic acid based iminosugars. For example, we have previously reported on **1** and **2** (Figure 1), which are a more potent version of miglustat<sup>9</sup> and a selective inhibitor of GBA2, respectively.<sup>10</sup> These types of iminosugars mimic the glycan and/or the aglycon part and are therefore able to bind and inhibit the active site of specific carbohydrate-active enzymes. They can be constructed in several ways,<sup>11–13</sup>

for example, we have shown previously that cyclic imines can be used in a Staudinger/aza-Wittig/Ugi three-component reaction (SAWU-3CR) to obtain pipecolic acid derivatives.<sup>10</sup> Alternatively, carbohydrate derived cyclic nitrones have also been used to obtain aza-C-glycosides through an 1,3-dipolar cycloaddition reaction.<sup>14,15</sup> However, this cycloaddition reaction has mainly been used to obtain bicyclic iminosugars. In contrast, the Ugi reaction, being a multicomponent reaction, is more suited to create libraries of diverse iminosugars.

The nitron-olefin [3+2] cycloaddition could, in principle, be a useful reaction toward glycomimetic building blocks, since it can be used to install multiple neighboring stereogenic centers with high regio- and stereoselectivity in one step. The reaction has been studied extensively, however, most advances in its application toward high regio- and enantiospecific products provide C-aryl-substituted isoxazolidines that often bear N-aryl groups. These products are synthetically less versatile for elaboration toward glycomimetics.<sup>16,17</sup> One of the few examples of nitrones that do give rise to synthetically versatile cycloadducts are amino-acid derived nitrones **3a,b** (Figure 2). These nitrones bear a deprotectable N-substituent and either a masked carboxylic acid<sup>18,19</sup> or masked aldehyde<sup>20</sup> that enable the synthesis of synthetically versatile isoxazolidines. In addition, the reaction has a large substrate scope, including several sugar-derived olefins. More specifically, olefin-containing D-mannitol-derived furanones **4** and **5** (Figure 2) functioned as the starting point for the current study.<sup>21–24</sup>

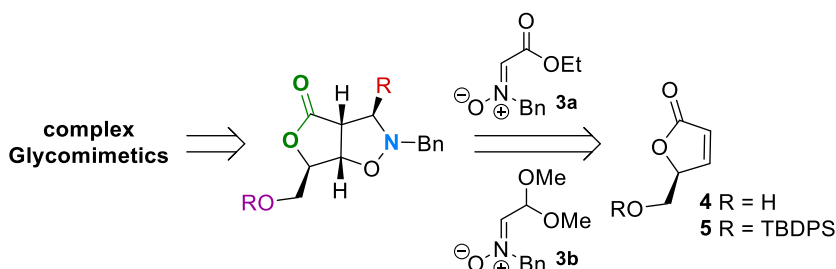


**Figure 2.** Complex glycomimetics may be obtained from bicyclic isoxazolidines, which provide many handles for further functionalization.

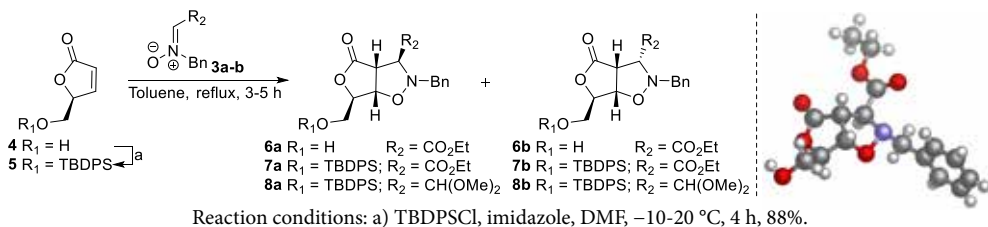
The nitron-olefin [3+2] cycloaddition reaction with **4** and **5** has been reported to proceed with high regio- and diastereoselectivity and to provide a chiral bicyclic isoxazolidine in good yield. We set out to explore the chemistry of these bicyclic isoxazolidines with the aim of creating a versatile chiral intermediate that can be used for the synthesis of glycomimetic building blocks based on pipecolic acid and aza-C-glycosides. Besides the previously mentioned examples of clinically relevant iminosugars, these building blocks also represent important functional motifs in other drugs. Pipecolic acids are a recurring motif in, for example, palinavir, virginiamycin S1, and nelfinavir (Figure 1). These drugs - used as protease inhibitors, antibiotics, or in the treatment of HIV - all contain a piperidine-2-carboxamide motif, and are typically functionalized at the 4-position with either a chiral ether (palinavir), ketone (virginiamycin S1), or as part of a bicyclic system (nelfinavir).

We here show that a versatile bicyclic isoxazolidine cycloadduct can be modified selectively at each functional position and subsequently transformed into a diverse range of pipercolic acid derivatives *via* a one-pot Staudinger/aza-Wittig/Ugi three-component reaction (SAWU-3CR). Finally, starting from the same isoxazolidine intermediate we synthesized an aza-C-glycoside via an unprecedented one-pot Staudinger/aza-Wittig/Mannich (SAWM) reaction.

## Results and Discussion

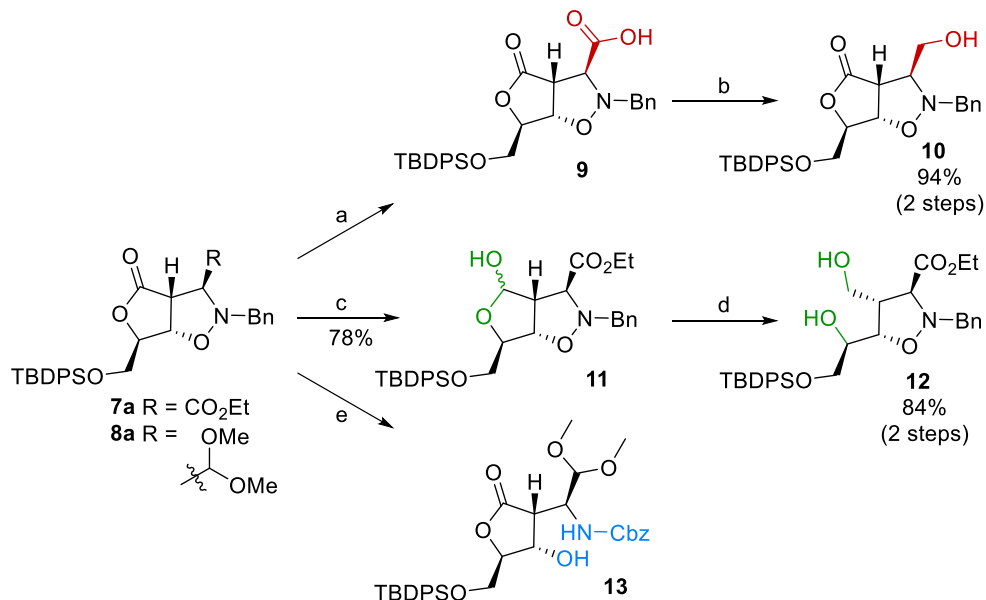
Our initial efforts focused on the product of the nitron-olefin [3+2] cycloaddition between nitron **3a** and furanone **5**, which provides known cycloadduct **7a** (Scheme 1, left). This bicyclic isoxazolidine was first reported by Ondruš et al. but has never been functionalized further.<sup>25</sup> Ondruš and co-workers reported that the selectivity of the cycloaddition reaction can be controlled by changing the *E/Z* ratio of the nitron, allowing the selective synthesis of either the *syn*-**7b** or *anti*-product **7a**. We explored if this selectivity could be further improved and succeeded in increasing the selectivity toward the main *anti*-product **7a** by using toluene as the solvent. By using this solvent compound **7a** was obtained in 68% yield, while providing **7b** (20%) as the minor compound (Scheme 1, left). Thus far, the only reported assignment of the stereochemistry of this major diastereomer was based on NMR coupling constants.<sup>25</sup> We succeeded in crystallizing the closely related cycloadduct **6a** (Scheme 1) – obtained through the reaction between furanone **4** and nitron **3a** – that enabled the unequivocal assignment of the relative stereochemistry by X-ray crystal structure determination (Scheme 1, right and Appendix B, Figure S1-2 + Table S1).

**Scheme 1.** Cycloaddition reaction of furanone **4** and **5** with nitron **3a,b** providing cycloadducts **6–8** (Left). Molecular structure of major *anti*-cycloadduct **6a** in the crystal (Right).



With the cycloaddition reaction optimized and the stereochemistry confirmed, we set out to selectively modify the newly created functional groups in the bicyclic isoxazolidine, namely the exocyclic ester, lactone, and N–O bond. Initial attempts to hydrolyze the ethyl ester of cycloadduct **7a** under both basic (LiOH, ≤51% yield) and acidic conditions (HCl, 39% yield) provided the target carboxylic acid **9**, but only in mediocre yield due to degradation of the TBDPS group. Hydrolysis of the ester under neutral conditions proved more favorable as treatment with Me<sub>3</sub>SnOH gave carboxylic acid **9** in almost quantitative yield (Scheme 2). The carboxylic acid could then be selectively reduced toward primary alcohol **10** in 94% over two steps by reducing an *in situ* formed mixed anhydride with sodium borohydride.



**Scheme 2.** Selective modification of functional positions in bicyclic isoxazolidine **7a** and **8a**.

Reaction conditions: a) Me<sub>3</sub>SnOH, ClCH<sub>2</sub>CH<sub>2</sub>Cl, reflux, 2.5 h; b) isobutyl chloroformate, NaBH<sub>4</sub>, THF, DMF, -15 °C, 75 min., 94% over 2 steps; c) BH<sub>3</sub>-SMe<sub>2</sub>, THF, 4-20 °C, 3.5 h; d) NaBH<sub>4</sub>, MeOH, -3-7 °C, 100 min., 84% over 2 steps; e) i. Raney-nickel, H<sub>2</sub> (1 bar), THF, rt, 7 h; ii. Pd/C, Cyclohexene, THF, reflux, 3 h; iii. CbzCl, NaHCO<sub>3</sub>, THF/H<sub>2</sub>O, rt, 14 h, 45%.

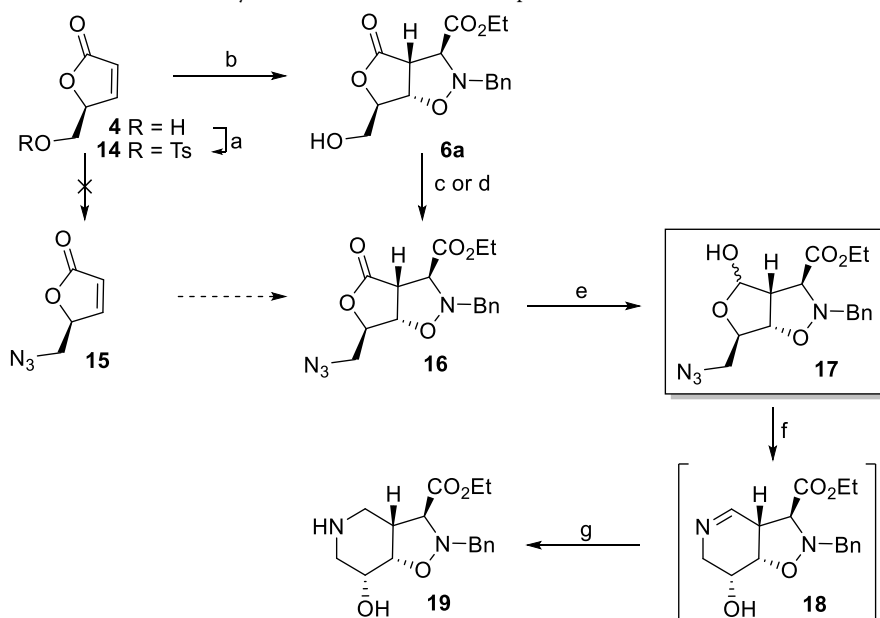
We next focused on selective modification of the lactone in **7a** and observed that its selective reduction is difficult due to the presence of the N-O bond, which is sensitive toward reducing agents. When DiBAL-H, L-Selectride, or NaBH<sub>4</sub> was used as the reducing agent, mixtures of starting material, monoreduction towards the hemiacetal, overreduction toward the diol and additional byproducts were observed. However, when BH<sub>3</sub>-SMe<sub>2</sub> was used as the reducing agent, **7a** could be selectively reduced toward hemiacetal **11** in 78% yield, providing diol **12** (16%) as a minor product. In addition, diol **12** could be obtained in 84% yield over two steps by reducing crude hemiacetal **11** with NaBH<sub>4</sub> in MeOH at 0 °C.

Finally, we investigated cleaving the N-O bond in the isoxazolidine ring through hydrogenation. Initial hydrogenolysis attempts on substrate **7a** with Pd/C or Pd(OH)<sub>2</sub> in MeOH under atmospheric pressure resulted in a very slow conversion. Complete hydrogenation of **7a** was only observed after several days at rt, at which point significant degradation had also occurred. Attempts to accelerate the reaction by using transfer hydrogenation conditions (HCO<sub>2</sub>NH<sub>4</sub>, Pd/C) or staged hydrogenation conditions, which we reported previously for a similar compound,<sup>20</sup> resulted in side product formation, and the target product proved to be unstable during isolation. MS analysis of the formed (side)products indicated that a significant amount of degradation could be attributed to β-elimination side reactions. We hypothesized that replacing one of the two carbonyl groups would prevent this side reaction,

and this spurred the development of our recently published novel nitron **3b** bearing an acetal-masked aldehyde.<sup>20</sup> Cycloaddition of this nitron with furanone **5** provided cycloadduct **8a** in 63% yield. Cycloadduct **8a** was then subjected to a staged hydrogenation with Raney-nickel, followed by a transfer hydrogenation with Pd/C in cyclohexene, to produce the amine that was protected *in situ* as a Cbz-carbamate to provide compound **13** in 45% yield over the three successive transformations.

Encouraged by the versatile synthetic scope, our next aim was to synthesize a small library of functionalized glycomimetic building blocks from a common precursor derived from this bicyclic isoxazolidine. We envisioned that commercially available furanone **4** could be used to obtain azido-hemiacetal **17** in three to four steps (Scheme 3) that in turn could be used in the SAWU-3CR for the synthesis of a small library of pipecolic acid-based iminosugars.<sup>26</sup>

**Scheme 3.** Synthesis of azido-hemiacetal **17**, precursor for the SAWU-3CR.

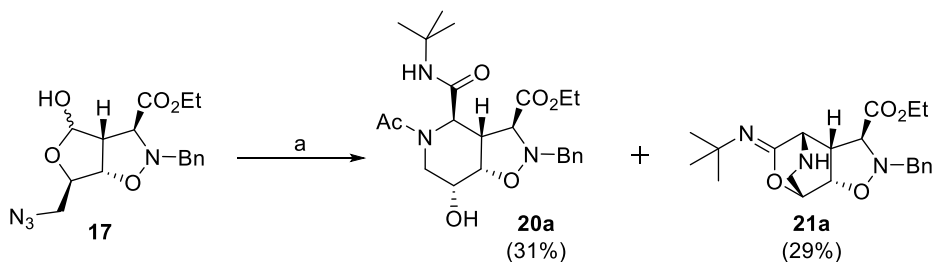


Reaction conditions: a) TsCl, pyridine, DCM,  $-15$ – $-5$  °C, 1 h, 70%; b) nitron **3a**, toluene, reflux, 4.5 h, 55% (**6a**) & 31% (**6b**); c)  $(\text{PhO})_2\text{P}(\text{O})\text{N}_3$ , Diisopropyl azodicarboxylate,  $\text{PPh}_3$ , THF,  $-20$ – $-20$  °C, 1.5 h, 72%; d) i.  $\text{MsCl}$ ,  $\text{Et}_3\text{N}$ , DCM,  $0$  °C, 50 min. ii.  $\text{NaN}_3$ , DMF,  $60$  °C, 90 min., 89% over 2 steps; e)  $\text{BH}_3\text{-SMe}_2$ , THF,  $-4$ – $20$  °C, 7 h, 34%; f)  $\text{PMe}_3$ , THF,  $4$  °C, 3 h; g)  $(\text{AcO})_3\text{BHNHNa}$ , THF,  $4$  °C, 1.5 h, 66% over 2 steps.

We initially focused on synthesizing azido-cycloadduct **16** via azido-furanone **15** (Scheme 3), but it proved impossible to produce intermediate **15** since conversion of **4** into **15** via a Mitsunobu reaction led to degradation. A two-stage reaction toward **15** via tosylate **14** was also unsuccessful. Compound **16** was, however, successfully prepared in 72% yield by installing the azide after the cycloaddition using a Mitsunobu reaction on the previously obtained cycloadduct **6a**. However, this reaction proved less reliable at larger scales, but we could obtain compound **16** reliably at a 19 gram scale in 89% yield by first converting

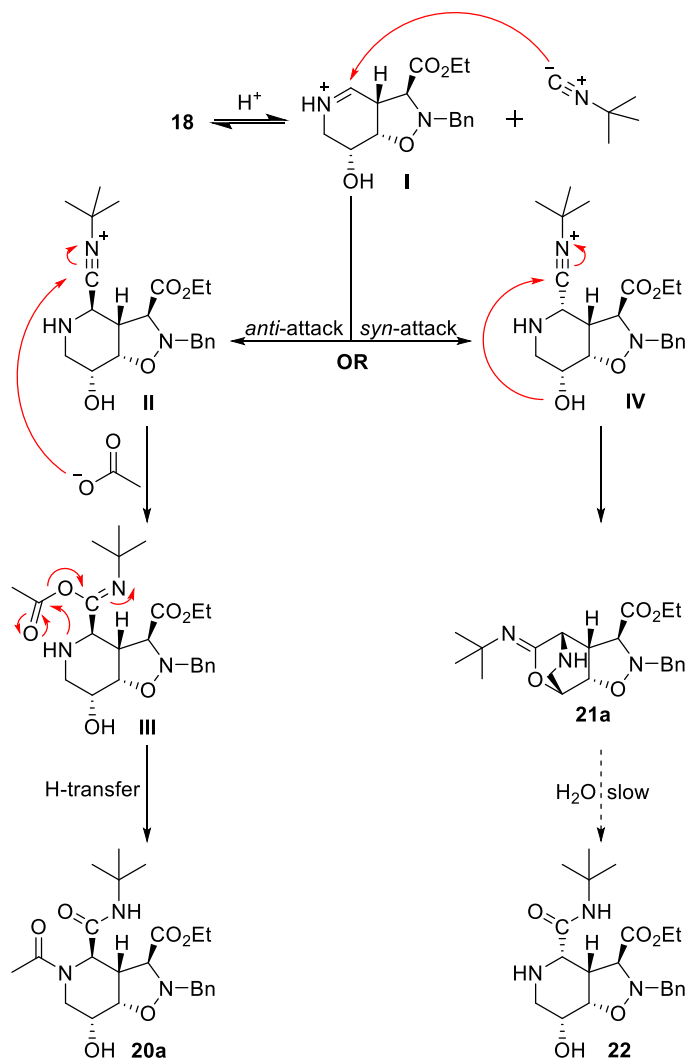
compound **6a** to its mesylate, immediately followed by substitution with  $\text{NaN}_3$ . The lactone in **16** could then be selectively reduced to the target azido-hemiacetal **17** using  $\text{BH}_3\text{-SMe}_2$ . With the key intermediate (**17**) for the SAWU-3CR now in hand, the feasibility of this reaction was investigated by first attempting a tandem one-pot Staudinger/aza-Wittig reaction. Hence, exposing compound **17** to  $\text{PMe}_3$  gave cyclic imine **18** that could be directly converted to iminosugar **19** by reduction with  $\text{NaBH}(\text{OAc})_3$  in the same pot. Encouraged by these results, the complete SAWU-3CR sequence was performed on compound **17** with *tert*-butyl isocyanide and acetic acid to give pipelicolic acid **20a** as the major product (Scheme 4).

**Scheme 4.** The SAWU-3CR with azido-hemiacetal **17**.



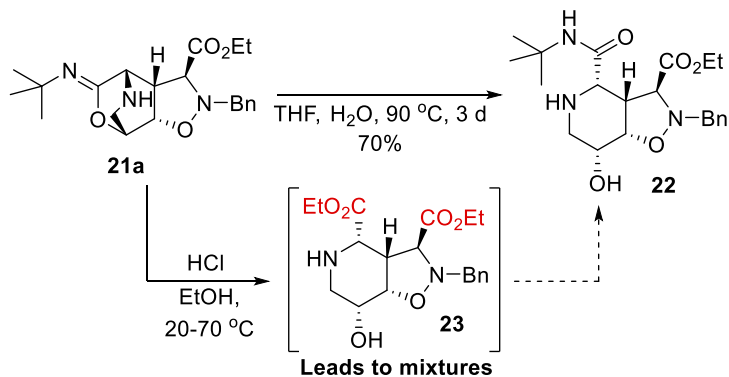
Reaction conditions: a) i.  $\text{PMe}_3$ , EtOH, 4 °C, 3 h; ii. Acetic acid (1.25 equiv), *t*butylisocyanide (1.25 equiv), EtOH/TFE, 0–20 °C, 16 h, 60%, ratio **20a**:**21a** = 51:49.

However, in addition to the expected Ugi product **20a**, another product was also isolated in a considerable yield. Detailed analysis revealed this product to be compound **21a** that contains, to the best of our knowledge, an unprecedented tricyclic imide (Scheme 4). We propose that **21a** results from an intramolecular side reaction during the Ugi reaction. The different products observed in the Ugi-3CR of cyclic imine **18** result from the initial *syn*- or *anti*-attack of the isocyanide after imine protonation (Scheme 5). Compound **20a** is formed by an *anti*-attack by *tert*-butyl isocyanide relative to the free alcohol. The resulting nitrilium ion intermediate **II** then undergoes the expected carboxylate attack and rearrangement seen in Ugi reactions. However, when the reaction proceeds *via* a *syn*-attack of the *tert*-butyl isocyanide, the resulting nitrilium ion (**IV**) can also be attacked intramolecularly via a pseudo-boat conformation by the free alcohol instead of a carboxylate. Such a pseudo-boat conformation places the hydroxy group of **IV** in close proximity of the electrophilic carbon atom of the nitrilium ion, enabling the intramolecular attack. The required pseudo-boat conformation for the formation of cyclic imide **21a** is actually the most stable conformation of the six-membered ring as determined by M11/6-311+g(d,p) density functional calculations (see Appendix B, Figure S3 and Table S2 for details and 3D images of this structure). We propose that this is because of electrostatic stabilizing interactions between the lone pairs of the alcohol O atom and the partially positively charged C atom of the nitrilium group. In comparison, the chair conformations that have either the alcohol or the nitrilium moiety axial are several kcal/mol higher in energy. The resulting tricyclic compound **21a** is surprisingly stable, allowing purification by column chromatography and complete characterization.

**Scheme 5.** Reaction mechanism explaining the formation of *anti*-product **20a** and tricyclic imidate **21a**.

We serendipitously discovered that this side product (**21a**) hydrolyzed selectively over the course of several months toward amide **22**, the complementary pipecolic acid with respect to **20a** (Scheme 5). We initially attempted to reproduce this process in a more practical time frame using acid catalysis, which is typically used to convert imidates to the corresponding amides.<sup>27–29</sup> However, no conversion was observed at lower temperatures (20–25 °C), but the incomplete conversion to product **22** and a similar compound was observed at higher temperatures. We reasoned that the imidate of compound **21a** is first converted to an ethyl ester, similar to other published observations,<sup>30–32</sup> followed by the formation of the amide (Scheme 6). Indeed, by MS analysis the intermediate diester **23** was observed *in situ*, which was eventually converted to either the product **22** or, as we presume, the amide resulting

**Scheme 6.** Acid hydrolysis of imidate **21a** leads to mixtures, while hydrolysis under neutral conditions in THF/H<sub>2</sub>O provides amide **22** in good yield.



from amide bond formation with the original ester of compound **21a**, since the intermediate contains two ethyl esters that are probably equally reactive. Attempting the hydrolysis under basic conditions (NaOH) only led to degradation. However, when the hydrolysis of **21a** was performed under neutral conditions in a THF/water mixture at 90 °C in a closed vessel, product **22** was isolated in 70% yield. These efficient conditions to obtain compound **22** from **21a** made it possible to obtain both pipecolic acid stereoisomers via the SAWU-3CR. Notably, the SAWU-3CR products **20** and **21** display very different retention times during chromatography, which makes purification relatively straightforward.

Next, the scope of the SAWU-3CR was investigated with azido-hemiacetal **17**. To this end, we selected a diverse set of acids and isocyanides and subjected them to the SAWU-3CR with **17** (Table 1). We initially used a large excess of acid and isocyanide (3 equiv; entry 1), but observed that the reaction actually benefited from using the acid and isocyanide in only a minor excess (1.25 equiv; entry 2). These results were obtained by using acetic acid as the carboxylic acid, but when different acids similar were used or better yields were obtained (entries 3–5), indicating that the reaction tolerates a variety of acids. However, when primary, secondary, and aromatic isocyanides were used we observed a significant drop in the reaction yields (entry 6–11). While the corresponding pipecolic acid derivatives **20e–j** could still be isolated in all cases, the tricyclic imidates **21e–j** were obtained in reduced yields or sometimes only observed as trace amounts in the reaction mixtures. It has been reported that unwanted side reactions during Ugi reactions can be suppressed by performing the reaction in the less nucleophilic solvent 2,2,2-trifluoroethanol (TFE) rather than in methanol.<sup>33–36</sup> The use of TFE as the solvent indeed resulted in significantly increased yields for the three selected reactions with a primary (entry 9b), secondary (entry 7b), and an even more challenging aromatic isocyanide (entry 10b) to 74, 79, and 59 % yield, respectively. Notably, the tricyclic imidates (**21f**, **21h**, and **21i**) were now isolated as the major compounds. The observed effect of reaction conditions and components on the initial *syn*- or *anti*-attack of the isocyanides and resulting diastereoselectivity of the Ugi-3CR with cyclic imines has been reported before.<sup>37,38</sup> The complex multistep

**Table 1.** Substrate scope of the SAWU-3CR<sup>a</sup> with hemiacetal **17**

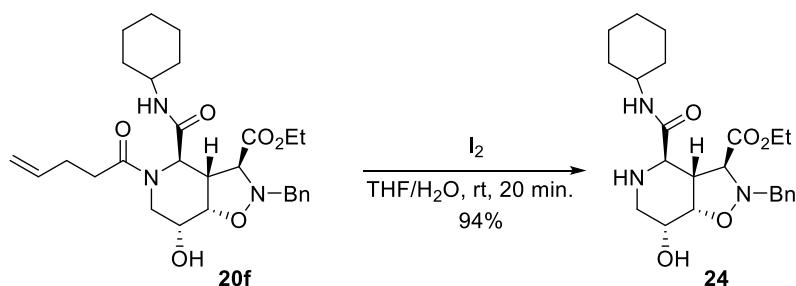
entry	acid	isocyanide	product	yield <sup>b</sup>	ratio
1		$t\text{Bu}-\text{N}^+\equiv\text{C}^-$	<b>20a/21a</b>	53% <sup>c</sup>	56:44
2		$t\text{Bu}-\text{N}^+\equiv\text{C}^-$	<b>20a/21a</b>	60%	51:49
3		$t\text{Bu}-\text{N}^+\equiv\text{C}^-$	<b>20b/21a</b>	65%	46:54
4		$t\text{Bu}-\text{N}^+\equiv\text{C}^-$	<b>20c/21a</b>	76%	36:64
5		$t\text{Bu}-\text{N}^+\equiv\text{C}^-$	<b>20d/21a</b>	68%	48:52
6			<b>20e/21e</b>	54%	53:47
7a			<b>20f/21f</b>	28%	1:0 <sup>d</sup>
7b				79% (TFE)	42:58
8			<b>20g/21g</b>	30%	56:44
9a			<b>20h/21h</b>	20%	82:18
9b				74% (TFE)	33:67
10a			<b>20i/21i</b>	13%	1:0 <sup>d</sup>
10b				59% (TFE)	31:69
11			<b>20j/21i</b>	16%	1:0 <sup>d</sup>

<sup>a</sup> Reaction conditions: a) i.  $\text{PMe}_3$ , EtOH, 4 °C, 3 h; ii. acid (1.25 equiv), isocyanide (1.25 equiv), EtOH/TFE, 0–20 °C, 16 h. <sup>b</sup> Isolated yield. <sup>c</sup> 3.00 equiv of *t*-butylisocyanide and acetic acid were used. <sup>d</sup> NMR showed only trace-amounts of the imide when using EtOH as solvent. TFE = 2,2,2-trifluoroethanol

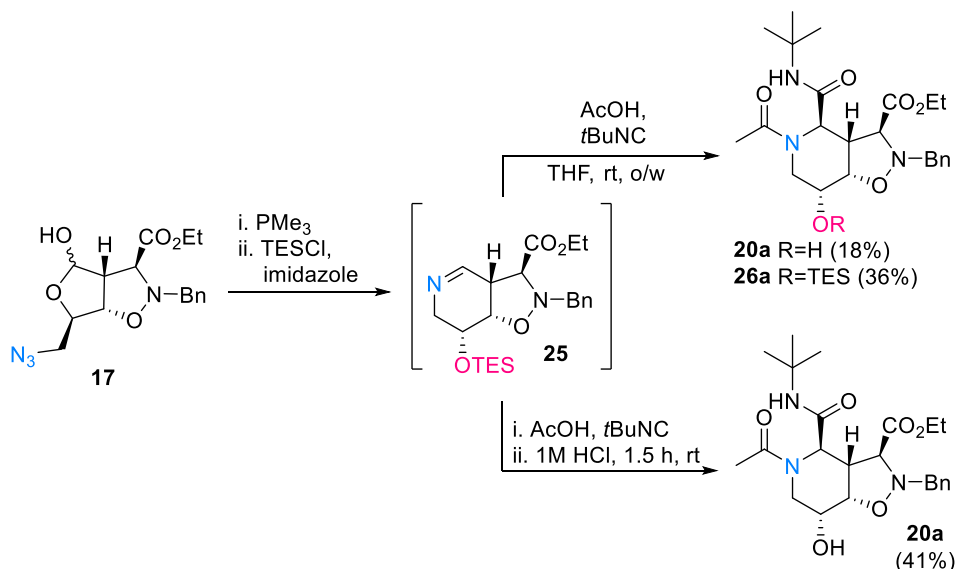
reaction mechanism and intermediates involved in the Ugi-3CR, however, prevent us from explaining the observed differences in the ratio of **20** and **21** when different solvents, carboxylic acids or isocyanides are employed. Remarkably, in a single case (entry 10b), a stable formamidine was isolated in 25% yield that probably resulted from attack of a second 4-methoxyisocyanide on the corresponding imide **21i**, followed by a rearrangement (see Appendix B, Scheme S1-2 for details).

As shown above, imide **21** can be conveniently hydrolyzed to provide the *syn*-product as a free amine, which provides a handle for further modification. Likewise, facile modification of the *anti*-product is also possible, since the 4-pentenoic handle – which is tolerated in the SAWU-3CR reaction – can be removed in almost quantitative yield (Scheme 7).

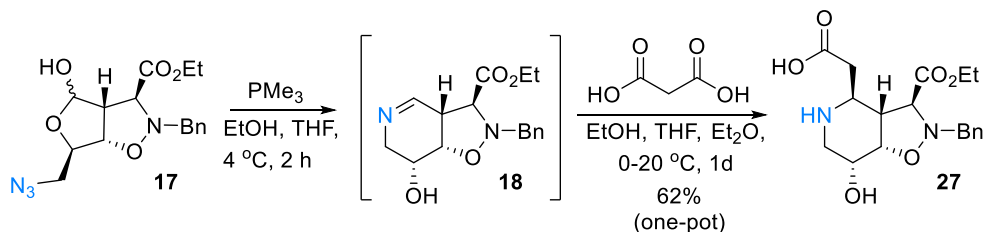
**Scheme 7.** Facile deprotection of *anti*-product **20f** to provide iminosugar **24**



While the synthesis of both diastereomers *via* the SAWU-3CR is ideal for obtaining a diverse library of glycomimetic building blocks, we also wanted to explore the possibility of increasing the selectivity toward one of the SAWU-3CR products. We reasoned that the reaction could be made more selective toward the *anti*-product by introducing a bulky protecting group on the free hydroxyl group thus preventing *syn*-attack of an isocyanide. To this end, a one-pot procedure was developed in which the hydroxyl group that results from the Staudinger/aza-Wittig reaction was protected *in situ* as a TES ether. The crude silyl-protected imine was then subjected to an Ugi reaction to selectively provide only *anti*-products in 53% as a mixture of **26a** and partially TES-deprotected **20a** (Scheme 8). *Anti*-product **20a** could also be obtained as the sole product in 41% by incorporating the TES-deprotection step *in situ*.

**Scheme 8.** *In situ* TES-protection of the cyclic imine results in selective *anti*-product formation

Finally, we investigated if our Staudinger/aza-Wittig derived cyclic imine (**18**) could also be a suitable electrophile in other imine-mediated reactions, analogously to a recent paper describing the Staudinger/aza-Wittig/Grignard reaction.<sup>39</sup> To that end, we chose to investigate the Petasis and Mannich reaction, which both have not yet been used in conjunction with a Staudinger/aza-Wittig-generated imine. While the Petasis reaction did not result in any conversion to the target product in our hands (see experimental section), we were able to modify imine **18** via a Mannich reaction. *In situ* treatment of **18** with malonic acid provided aza-C-glycoside **27** as a pure isomer in 62% yield after crystallization (Scheme 9).

**Scheme 9.** One-pot reaction of the Staudinger/aza-Wittig/Mannich (SAWM) reaction to give compound **27**



## Conclusion

In summary, the nitron-olefin [3+2] cycloaddition reaction can be used to give highly functionalized bicyclic isozazolidine cycloadducts in good yield and stereoselectivity. These cycloadducts are synthetically highly versatile and can be selectively modified at each functional position, which allows for the synthesis of a wide variety of glycomimetic building blocks. In this way, it is possible to make a library of 20 pipecolic acid derivatives and an aza-C-glycoside by converting the bicyclic isozazolidine into an azido-hemiacetal and using this in a one-pot Staudinger/aza-Wittig/Ugi three-component reaction (SAWU-3CR) or an unprecedented Staudinger/aza-Wittig/Mannich reaction reaction. The SAWU-3CR on this azido-hemiacetal also produced an unprecedented tricyclic imidate that can be converted into corresponding pipecolic acid-based glycomimetic compounds.

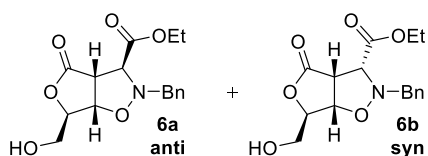
## Experimental Section

### General Information

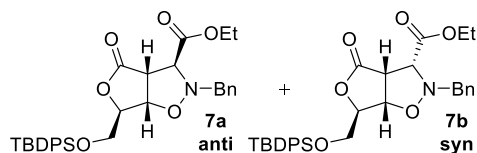
All moisture-sensitive reactions were carried out under an argon atmosphere, using oven-dried glassware, unless otherwise stated. Dichloromethane ( $\text{CH}_2\text{Cl}_2$ , >99.8%) and toluene (>99.8%) were purified over aluminum oxide under argon using a solvent purification system. Reagents were obtained from commercial sources and used without further purification unless stated otherwise. Raney-nickel was purchased from commercial sources (W.R. Grace and Co. Raney<sup>®</sup>; 2800, as a slurry in  $\text{H}_2\text{O}$ ), which was washed with anhydrous THF three times before use. Palladium on carbon (Pd/C) was purchased from commercial sources (10 wt% loading, matrix activated carbon support). Analytical TLC was performed using prepared plates of silica gel (60 F-254 on aluminum) or aluminum oxide (60 Å, F-254 on aluminum) and then, according to the functional groups present on the molecules, revealed with UV light or using staining reagents: ninhydrin (1.5% in *n*-BuOH with 3% AcOH) for amines or basic solution of  $\text{KMnO}_4$  (1.0% in  $\text{H}_2\text{O}$ ) for general staining. Silica gel 60 (70–230 mesh) or aluminum oxide (0.05–0.15 mm particle size, neutral, Brockmann activity grade I) was used for flash chromatography.  $^1\text{H}$  NMR were recorded at 400 and 500 MHz.  $^{13}\text{C}$  NMR spectra were recorded at 100 MHz. Chemical shifts are reported in parts per million (ppm), calibrated on the residual peak of the solvent, whose values are referred to tetramethylsilane (TMS,  $\delta_{\text{TMS}} = 0$ ) as the internal standard or the signal of the deuterated solvent.  $^{13}\text{C}$  NMR spectra were performed with proton decoupling. Where indicated, NMR peak assignments were made using COSY and HSQC experiments. Electrospray ionization (ESI) mass analyses were performed on a mass spectrometer with a linear ion trap mass analyzer, while high-resolution ESI mass analyses were recorded on a Orbitrap high-resolution mass spectrometer. Infrared analyses were performed on a FT-IR spectrometer. Optical rotations were measured on a polarimeter (sodium D line,  $\lambda = 589 \text{ nm}$ ).

X-ray crystal structure determination of **6a**

C<sub>16</sub>H<sub>19</sub>NO<sub>6</sub>, Fw = 321.32, colourless plate, 0.26 × 0.15 × 0.09 mm<sup>3</sup>, monoclinic, P2<sub>1</sub> (no. 4), a = 9.8175(5), b = 5.3650(3), c = 14.4448(6) Å, β = 97.206(3)°, V = 754.82(7) Å<sup>3</sup>, Z = 2, D<sub>x</sub> = 1.414 g/cm<sup>3</sup>, μ = 0.11 mm<sup>-1</sup>. 20768 Reflections were measured on a diffractometer with sealed tube and a monochromator (λ = 0.71073 Å) at a temperature of 150(2) K up to a resolution of (sin θ/λ)<sub>max</sub> = 0.65 Å<sup>-1</sup>. The Eval15 software<sup>40</sup> was used for the integration of the intensities. Multiscan absorption correction and scaling was performed with SADABS<sup>41</sup> (correction range 0.66–0.75). 3459 Reflections were unique (R<sub>int</sub> = 0.044), of which 2916 were observed [I > 2σ(I)]. The structure was solved with Direct Methods using SHELXS-97.<sup>42</sup> Least-squares refinement was performed with SHELXL 2013<sup>43</sup> against F<sup>2</sup> of all reflections. Non-hydrogen atoms were refined freely with anisotropic displacement parameters. All hydrogen atoms were located in difference Fourier maps. The hydroxyl H-atom was refined freely with an isotropic displacement parameter, all other H-atoms were refined with a riding model. 213 Parameters were refined with one restraint (floating origin). R1/wR2 [I > 2σ(I)]: 0.0351 / 0.0733. R1/wR2 [all refl.]: 0.0485 / 0.0783. S = 1.036. The absolute structure could not be determined from anomalous dispersion but has been assigned according to the synthetic procedure. Residual electron density between 0.21 and 0.20 e/Å<sup>3</sup>. Geometry calculations and checking for higher symmetry were performed with the PLATON program.<sup>44</sup>

**Ethyl (3aR,6R,6aS)-2-benzyl-6-(hydroxymethyl)-4-oxohexahydrofuro[3,4-d]isoxazole-3-carboxylate (**6a**).**

Nitrone **3a** (4.83 g, 23.3 mmol, 1.09 equiv) was added to a solution of furanone **4** (2.44 mg, 21.4 mmol, 1.00 equiv) in toluene (10 mL) at 45 °C. The reaction mixture was heated to reflux for 4.5 hours and then conc. *in vacuo*. The residue was purified via column chromatography (30–40% EtOAc in heptane) to afford **6a anti**<sup>a</sup> R<sub>F</sub> = 0.27 (1:1; PE:EtOAc). mp = 83–84 °C. <sup>1</sup>H NMR (400 MHz, Chloroform-*d*) δ 7.44 – 7.04 (m, 5H), 4.73 (d, *J* = 6.4 Hz, 1H), 4.50 (d, *J* = 2.5 Hz, 1H), 4.15 (q, *J* = 7.1 Hz, 2H), 4.05 (q, *J* = 13.8 Hz, 2H), 3.95 – 3.75 (m, 3H), 3.67 (d, *J* = 12.3 Hz, 1H), 2.57 (s, 1H), 1.23 (t, *J* = 7.2 Hz, 3H). NMR signals of the minor adduct **6b syn**<sup>a</sup> R<sub>F</sub> = 0.22 (1:1; PE:EtOAc). mp = 144–145 °C. <sup>1</sup>H NMR (400 MHz, Chloroform-*d*) δ 7.38 – 7.26 (m, 5H), 4.86 (dd, *J* = 7.7, 2.2 Hz, 1H), 4.59 (q, *J* = 2.4 Hz, 1H), 4.32 – 4.19 (m, 3H), 3.94 (ddd, *J* = 12.4, 5.1, 2.5 Hz, 1H), 3.84 (d, *J* = 13.9 Hz, 1H), 3.80 – 3.70 (m, 2H), 3.67 (d, *J* = 7.6 Hz, 1H), 1.82 (dd, *J* = 6.8, 5.2 Hz, 1H), 1.32 (t, *J* = 7.1 Hz, 3H). [α]<sub>D</sub><sup>20</sup> = +115.6 (*c* = 1.00, CHCl<sub>3</sub>). <sup>a</sup>NMR signals in accordance with NMR spectra by Ondruš et al.<sup>25</sup>

**Ethyl (3aR,6R,6aS)-2-benzyl-6-(((tert-butyl)diphenylsilyl)oxy)methyl-4-oxohexahydrofuro[3,4-d]isoxazole-3-carboxylate (**7**).**

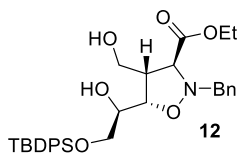
A solution of nitrone **3a** (0.333 g, 1.61 mmol, 1.14 equiv) in toluene (9 mL) was heated to 40 °C for 2 hours, followed by the addition of furanone **2** (0.498 g, 1.41 mmol, 1.0 equiv) and additional toluene (3 mL). The reaction mixture was heated to reflux for 4 hours and then conc. *in vacuo*. The residue was purified via column chromatography (5–15% EtOAc in petroleum ether 40–60) afforded **7a anti** (563 mg, 68%) R<sub>F</sub> = 0.52 (8:2; PE:EtOAc) and **7b** (154 mg, 20%) as a yellow oil. R<sub>F</sub> = 0.44 (8:2; PE:EtOAc). NMR signals of the major adduct **7a anti**<sup>a</sup> <sup>1</sup>H NMR (400 MHz, Chloroform-*d*) δ 7.68 – 7.55 (m, 4H),

7.51 – 7.23 (m, 11H), 4.87 (d,  $J = 6.3$  Hz, 1H), 4.56 (d,  $J = 2.1$  Hz, 1H), 4.26 (q,  $J = 7.2$ , 2H), 4.20 (s, 1H), 4.14 – 4.06 (m, 2H), 3.95 (s, 1H), 3.90 (dd,  $J = 11.6$ , 2.4 Hz, 1H), 3.73 (dd,  $J = 11.6$ , 1.9 Hz, 1H), 2.05 (s, 1H), 1.31 (t,  $J = 7.2$  Hz, 3H), 1.04 (s, 9H). NMR signals of the major adduct **7b syn**:<sup>a</sup> <sup>1</sup>H NMR (400 MHz, Chloroform-*d*)  $\delta$  7.66 – 7.54 (m, 4H), 7.48 – 7.27 (m, 11H), 4.91 (dd,  $J = 7.6$ , 1.7 Hz, 1H), 4.56 (q,  $J = 2.1$  Hz, 1H), 4.35 – 4.24 (m, 3H), 3.92 – 3.76 (m, 3H), 3.76 – 3.66 (m, 2H), 1.34 (t,  $J = 7.1$  Hz, 3H), 1.02 (s, 9H). <sup>a</sup>NMR signals in accordance with NMR spectra by Ondruš et al.<sup>25</sup>

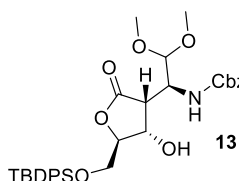
**(3S,3aR,6R,6aS)-2-Benzyl-6-(((tert-butyl-diphenylsilyl)oxy)methyl)-3-(hydroxymethyl)tetrahydrofuro[3,4-d]isoxazol-4(2H)-one (10).** To a solution of ester **7a** (0.443 g, 0.736 mmol, 1.0 equiv) in 1,2-dichloroethane (11 mL) was added  $\text{Me}_3\text{SnOH}$  (0.540 g, 2.99 mmol, 4.06 equiv). The resulting suspension was heated to reflux for 2.5 h and then concentrated under a  $\text{N}_2$  stream and then dissolved in EtOAc (50 mL). The organic layer was washed with 1M aq. HCl (5 mL, 2 $\times$ ), brine (5 mL), dried ( $\text{MgSO}_4$ ) and then conc. *in vacuo*, affording crude compound **9**, which was used without further purification. A small sample of crude **9** was purified by flash column chromatography (5% MeOH in DCM) to obtain an analytically pure sample.  $R_f = 0.43$  (10% MeOH in DCM). <sup>1</sup>H NMR (400 MHz, Chloroform-*d*)  $\delta$  7.62 (ddd,  $J = 8.0$ , 2.6, 1.5 Hz, 4H), 7.49 – 7.30 (m, 11H), 4.83 (d,  $J = 6.5$  Hz, 1H), 4.74 – 4.59 (m, 1H), 4.26 – 4.15 (m, 3H), 4.09 (d,  $J = 13.1$  Hz, 1H), 3.92 (dd,  $J = 11.6$ , 2.6 Hz, 1H), 3.76 (dd,  $J = 11.6$ , 1.9 Hz, 1H), 1.04 (s, 9H). HRMS calcd for  $\text{C}_{30}\text{H}_{32}\text{O}_6\text{NSi} - \text{H}^+$  [ $\text{M} - \text{H}^+$ ]: 530.2004 Found 530.1997. Crude **9** was dissolved in dry THF (18 mL) and added to a flame-dried 3-neck round-bottom flask and cooled to  $-15^\circ\text{C}$ . To this solution was added isobutyl chloroformate (1.07 g, 7.82 mmol, 10.0 equiv), followed by the dropwise addition of a suspension of  $\text{NaBH}_4$  (0.297 g, 7.85 mmol, 10.0 equiv) in DMF (7.0 mL) over 10 minutes. The resulting reaction mixture was stirred at  $-15^\circ\text{C}$  for 75 min. and then quenched with 1M aq. HCl (25 mL). The reaction mixture was extracted with EtOAc (75 mL, 25 mL, 2 $\times$ ). The combined organic layers were washed with brine (25 mL), dried ( $\text{MgSO}_4$ ) and conc. *in vacuo*. The residue was purified by flash column chromatography (20–30% EtOAc in petroleum ether 40–60), affording compound **10** (385 mg, 94% over 2 steps) as a yellow oil, which crystallized upon standing.  $R_f = 0.32$  (7:3; PE:EtOAc). mp =  $109\text{--}110^\circ\text{C}$ . <sup>1</sup>H NMR (400 MHz, Chloroform-*d*)  $\delta$  7.67 – 7.58 (m, 4H), 7.50 – 7.37 (m, 6H), 7.37 – 7.27 (m, 5H), 4.73 (d,  $J = 6.5$  Hz, 1H), 4.59 (t,  $J = 2.2$  Hz, 1H), 4.12 – 4.00 (m, 2H), 3.91 (dd,  $J = 11.5$ , 2.5 Hz, 1H), 3.74 (dd,  $J = 11.6$ , 1.9 Hz, 1H), 3.72 – 3.62 (m, 3H), 3.44 (q,  $J = 3.8$  Hz, 1H), 2.17 (s, 1H), 1.04 (s, 9H). <sup>13</sup>C NMR (101 MHz,  $\text{CDCl}_3$ )  $\delta$  177.5, 136.5, 135.7, 135.6, 132.5, 132.0, 130.3, 130.2, 129.0, 128.7, 128.1, 128.1, 128.0, 83.0, 81.0, 70.6, 64.0, 62.2, 61.6, 52.8, 26.9, 19.2. FT-IR (neat):  $\nu = 3282, 2931, 2859, 1775, 1427\text{ cm}^{-1}$ . HRMS calcd for  $\text{C}_{30}\text{H}_{35}\text{O}_5\text{NSi} + \text{Na}^+$  [ $\text{M} + \text{Na}^+$ ]: 540.2177 Found 540.2162.  $[\alpha]_D^{20} = -32.0$  ( $c = 0.40$ ,  $\text{CHCl}_3$ ).

**Ethyl (3S,3aR,6R,6aS)-2-benzyl-6-(((tert-butyl-diphenylsilyl)oxy)methyl)-4-hydroxyhexahydrofuro[3,4-d]isoxazole-3-carboxylate (11) and ethyl (3S,4S,5S)-2-benzyl-5-((R)-2-(((tert-butyl-diphenylsilyl)oxy)-1-hydroxyethyl)-4-(hydroxymethyl)isoxazolidine-3-carboxylate (12).** To a round-bottom flask containing cycloadduct **7a** (0.404 g, 0.722 mmol, 1.0 equiv) at  $4^\circ\text{C}$  was added a cold ( $4^\circ\text{C}$ ) 2M solution of  $\text{BH}_3\text{-SMe}_2$  in THF (4.00 mL, 8.00 mmol, 11.1 equiv). The mixture was allowed to warm to room temperature and stirred for 3.5 hours and quenched by carefully adding MeOH (0.30 mL). The mixture was concentrated *in vacuo* to afford the crude as a mixture of compound **11** and **12** (0.392 g) as a colorless oil, which was generally used to obtain compound **12** without further purification. Optionally, the crude could be purified by flash column

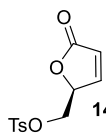
chromatography (30-50% EtOAc in petroleum ether 40-60), affording an anomeric mixture of hemiacetal **11** (320 mg, 78%) as a colorless oil (HRMS calcd for  $C_{32}H_{39}O_6NSi + Na^+$  [M+Na<sup>+</sup>]: 584.2439 Found 584.2429)  $R_f = 0.57$  (7:3; PE:EtOAc) and diol **12** (60 mg, 16%) as a colorless oil.



Hemiacetal **11** (0.100 g, 162 mmol, 1.0 equiv) was dissolved in MeOH (3.0 mL) and cooled to  $-2^\circ\text{C}$ ,  $NaBH_4$  (13.5 mg, 0.357 mmol, 2.0 equiv) was added and the resulting solution was then stirred at  $-3$ – $7^\circ\text{C}$  for 1 h. Additional  $NaBH_4$  (3.4 mg, 0.5 equiv) was added and the reaction mixture was stirred for an additional 40 min., followed by the portion-wise addition of 1M aq. HCl (10 mL). The reaction mixture was extracted with EtOAc (10 mL, 3 $\times$ ) and the combined organic layers were washed with sat. aq.  $NaHCO_3$  solution (10 mL) and brine (10 mL). Then it was dried over  $MgSO_4$  and concentrated *in vacuo*. The resulting oil was purified by flash column chromatography (30-50% EtOAc in petroleum ether 40-60), affording diol **12** (87.2 mg, 87%) as a colorless oil.  $R_f = 0.27$  (7:3; PE:EtOAc).  $^1H$  NMR (400 MHz, Chloroform-*d*)  $\delta$  7.64 (ddt,  $J = 9.8, 6.8, 1.5$  Hz, 4H), 7.50 – 7.30 (m, 6H), 7.24 (s, 5H), 4.18 (dd,  $J = 9.3, 7.1$  Hz, 1H), 4.09 (q,  $J = 7.1$  Hz, 2H), 3.99 (d,  $J = 13.2$  Hz, 1H), 3.96 – 3.87 (m, 3H), 3.83 (dd,  $J = 10.5, 3.2$  Hz, 1H), 3.76 – 3.63 (m, 3H), 3.28 (d,  $J = 4.6$  Hz, 1H), 3.24 – 3.13 (m, 1H), 3.10 (d,  $J = 7.7$  Hz, 1H), 1.22 (t,  $J = 7.2$  Hz, 3H), 1.06 (s, 9H).  $^{13}C$  NMR (101 MHz,  $CDCl_3$ )  $\delta$  170.1, 135.8, 135.7, 135.6, 133.0, 132.7, 130.1, 130.1, 129.7, 128.3, 128.0, 127.7, 78.3, 69.8, 65.5, 62.3, 61.6, 60.6, 52.1, 27.0, 19.4, 14.2. FT-IR (neat):  $\nu = 3385, 2931, 2857, 1738, 1472, 1428\text{ cm}^{-1}$ . HRMS calcd for  $C_{32}H_{41}O_6NSi + H^+$  [M+H<sup>+</sup>]: 564.2776 Found 564.2766.  $[\alpha]_D^{20} = -22.7$  ( $c = 1.00, CHCl_3$ ).

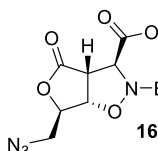


**Benzyl ((S)-1-((3R,4S,5R)-5-(((tert-butyl)diphenylsilyl)oxy)methyl)-4-hydroxy-2-oxotetrahydrofuran-3-yl)-2,2-dimethoxyethyl)carbamate (13).** A solution of cycloadduct **8a** (0.124 g, 0.221 mmol, 1.00 equiv) in dry THF (1.0 mL) was added to a round-bottom flask containing Raney-nickel (0.400 gr). The reaction mixture was placed under and hydrogen atmosphere (1 bar; balloon) and stirred vigorously for 5 h. TLC indicated incomplete conversion at this point so the reaction mixture was transferred to a round-bottom flask containing fresh Raney-nickel (0.500 gram) and stirred under an hydrogen atmosphere (1 bar; balloon) for an additional 2 hours. The reaction mixture was then placed under an argon atmosphere (1 bar) and Pd/C (0.100 gram) was added, followed by cyclohexene (2.5 mL). The resulting mixture was heated to reflux for 3 h and then cooled to  $4^\circ\text{C}$ . Finally,  $H_2O$  (0.6 mL),  $NaHCO_3$  (74 mg, 0.883 mmol, 4.00 equiv) and  $CbzCl$  (0.094 mL, 0.662 mmol, 3.00 equiv) were added sequentially and the resulting reaction mixture was stirred for 14 h, while allowing the mixture to warm to room temperature. The reaction mixture was filtered over Celite, the celite was subsequently washed with THF and the combined filtrate conc. *in vacuo*. The resulting residue was purified by flash column chromatography (20-30% EtOAc in petroleum ether 40-60), affording compound **13** (60.5 mg, 45%) as a yellow oil.  $R_f = 0.23$  (7:3; PE:EtOAc).  $^1H$  NMR (400 MHz, Chloroform-*d*)  $\delta$  7.73 – 7.55 (m, 4H), 7.50 – 7.29 (m, 11H), 5.68 (d,  $J = 8.4$  Hz, 1H), 5.25 – 5.03 (m, 3H), 4.69 (d,  $J = 2.5$  Hz, 1H), 4.48 (dd,  $J = 5.3, 2.5$  Hz, 1H), 4.43 (t,  $J = 2.5$  Hz, 1H), 4.30 (td,  $J = 8.5, 2.4$  Hz, 1H), 3.89 (dd,  $J = 11.8, 2.9$  Hz, 1H), 3.77 (dd,  $J = 11.7, 2.1$  Hz, 1H), 3.50 (s, 3H), 3.47 (s, 3H), 3.45 – 3.39 (m, 1H), 1.02 (s, 9H).  $^{13}C$  NMR (101 MHz,  $CDCl_3$ )  $\delta$  175.2, 157.8, 136.0, 135.8, 135.6, 132.6, 132.0, 130.2, 128.7, 128.5, 128.3, 128.0, 103.5, 85.3, 71.8, 67.6, 63.9, 57.0, 56.9, 50.5, 47.9, 26.8, 19.2. HRMS calcd for  $C_{33}H_{41}O_8NSi + Na^+$  [M+Na<sup>+</sup>]: 630.2494 Found 630.2483.



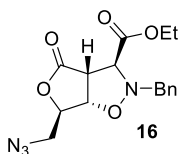
**(S)-5-(5-Oxo-2,5-dihydrofuran-2-yl)methyl 4-methylbenzenesulfonate (14).** To a solution of furanone **4** (215.6 mg, 1.890 mmol, 1.0 equiv) in dry DCM (1.0 mL) at  $-15^{\circ}\text{C}$  was added pyridine (0.377 mL, 4.67 mmol, 2.5 equiv), followed by the portion-wise addition of TsCl (0.540 g, 2.83 mmol, 1.5 equiv). The reaction mixture was stirred at  $-15^{\circ}\text{C}$  and allowed to warm to  $5^{\circ}\text{C}$  over 1 hour. The reaction mixture was diluted with DCM (30 mL) and washed with 1M aq. HCl (10 mL, 3 $\times$ ), sat. aq.  $\text{NaHCO}_3$  (10 mL), brine (10 mL). The organic phase was dried ( $\text{MgSO}_4$ ) and then conc. *in vacuo*. The resulting residue was purified by flash column chromatography (0–100% MeOH in DCM), affording the product **14** (355 mg, 70%) as a colorless oil.  $^1\text{H}$  NMR (400 MHz, Chloroform-*d*)  $\delta$  7.81 – 7.73 (m, 2H), 7.44 (dd,  $J$  = 5.8, 1.6 Hz, 1H), 7.37 (d,  $J$  = 8.0 Hz, 2H), 6.21 (dd,  $J$  = 5.8, 2.1 Hz, 1H), 5.19 (tt,  $J$  = 4.8, 1.9 Hz, 1H), 4.29 – 4.17 (m, 2H), 2.46 (s, 3H).  $^{13}\text{C}$  NMR (101 MHz,  $\text{CDCl}_3$ )  $\delta$  171.7, 151.8, 145.7, 132.2, 130.2, 128.1, 123.9, 79.8, 67.5, 21.8. FT-IR (neat):  $\nu$  = 3100, 2956, 2927, 1756, 1598, 1494, 1452, 1400  $\text{cm}^{-1}$ . HRMS calcd for  $\text{C}_{12}\text{H}_{12}\text{O}_5\text{S} + \text{Na}^+ [\text{M} + \text{Na}^+]$ : 291.0298. Found 291.0290.  $[\alpha]_{\text{D}}^{20} = -46.5$  ( $c$  = 1.00,  $\text{CHCl}_3$ ).

**Ethyl (3S,3aR,6R,6aS)-6-(azidomethyl)-2-benzyl-4-oxohexahydrofuro[3,4-d]isoxazole-3-carboxylate (16).**



Method A:

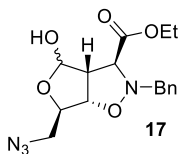
To a solution of cycloadduct **6a** (31.0 mg, 0.0965 mmol, 1.00 equiv) in dry THF (0.5 mL) at  $-20^{\circ}\text{C}$  was added  $\text{PPh}_3$  (50.6 mg, 0.193 mmol, 2.00 equiv), followed by the dropwise addition of diisopropyl azodicarboxylate (38.0  $\mu\text{L}$ , 0.193 mmol, 2.00 equiv) and  $(\text{PhO})_2\text{P}(\text{O})\text{N}_3$  (41.5  $\mu\text{L}$ , 0.193 mmol, 2.00 equiv). The resulting reaction mixture was stirred at  $-20$  to  $-15^{\circ}\text{C}$  for 30 min. and then allowed to warm to room temperature and stirred for 1 hour.  $\text{H}_2\text{O}$  (10 mL) and EtOAc (10 mL) were then added to the reaction mixture and the biphasic system was separated. The water layer was extracted with EtOAc (5 mL, 2 $\times$ ) and the combined organic layers were washed with brine (5 mL), dried ( $\text{MgSO}_4$ ) and then conc. *in vacuo*. The residue was purified by flash column chromatography (2–5% MeOH in DCM), affording compound **16** (24.0 mg, 72%) as a yellow oil.  $R_{\text{F}}$  = 0.44 (7:3; PE:EtOAc).



Method B:

To a solution of cycloadduct **6a** (16.79 g, 52.26 mmol, 1.00 equiv) in DCM (86 mL) at  $0^{\circ}\text{C}$  was added  $\text{Et}_3\text{N}$  (15.35 mL, 110 mmol, 2.10 equiv), followed by the dropwise addition of MsCl (15.35 mL, 110 mmol, 2.10 equiv). The resulting reaction mixture was stirred at  $4^{\circ}\text{C}$  for 50 min.. Sat. aq.  $\text{NaHCO}_3$  (400 mL) was added to the reaction mixture, followed by DCM (1 L). The resulting biphasic system was separated and the water layer was extracted with DCM (2 $\times$ 400 mL, 100 mL) and the combined organic layers were dried ( $\text{MgSO}_4$ ) and then conc. *in vacuo*, affording the crude mesylated intermediate, which was dissolved in DMF (86 mL).  $\text{NaN}_3$  (14.0 g, 215 mmol, 4.00 equiv) was added the reaction mixture was heated to  $60^{\circ}\text{C}$  for 90 min. Additional DMF (50 mL) was added, followed by  $\text{H}_2\text{O}$  (400 mL). The reaction mixture was extracted with  $\text{Et}_2\text{O}$  (1 L, 400 mL, 2 $\times$ 200 mL) and the combined organic layers were washed with 5% aq. LiCl (200 mL, 2 $\times$ ), dried ( $\text{MgSO}_4$ ) and conc. *in vacuo*. The residue was purified by flash column chromatography (10–25% EtOAc in petroleum ether 40–60), affording compound **16** (17.67 g, 89% over 2 steps) as an orange oil.  $R_{\text{F}}$  = 0.44 (7:3; PE:EtOAc).  $^1\text{H}$  NMR (400 MHz, Chloroform-*d*)  $\delta$  7.38 – 7.24 (m, 5H), 4.66 (d,  $J$  = 6.5 Hz, 1H), 4.60 (t,  $J$  = 3.1 Hz, 1H), 4.25 (q,  $J$  = 7.2 Hz, 2H), 4.18 – 4.03 (m, 2H), 4.03 – 3.87 (m, 2H), 3.71 (dd,  $J$  = 13.3, 3.3 Hz, 1H), 3.56 (dd,  $J$  = 13.3, 3.0 Hz, 1H), 1.32 (t,  $J$  = 7.1 Hz, 3H).  $^{13}\text{C}$  NMR (101 MHz,  $\text{CDCl}_3$ )  $\delta$  175.3, 167.9, 136.2, 128.8, 128.5, 127.8, 81.5, 79.8, 69.4, 62.1, 60.3, 52.7, 52.5, 14.2. FT-IR (neat):  $\nu$  = 2983, 2108, 1779, 1734, 1606, 1497, 1455  $\text{cm}^{-1}$ . HRMS calcd for  $\text{C}_{16}\text{H}_{18}\text{O}_5\text{N}_4 + \text{H}^+ [\text{M} + \text{H}^+]$ :

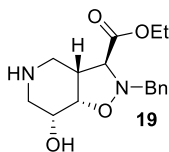
347.1350. Found 347.1344 [ $\alpha$ ]<sub>D</sub><sup>20</sup> = +32.5 ( $c$  = 1.00, CHCl<sub>3</sub>).



**Ethyl (3S,3aR,6R,6aS)-6-(azidomethyl)-2-benzyl-4-hydroxyhexahydrofuro[3,4-d]isoxazole-3-carboxylate (17).** To a round-bottom flask containing lactone

**15** (9.28 g, 26.8 mmol, 1.0 equiv) at 4 °C was added a 4 °C a 2M solution of BH<sub>3</sub>-SMe<sub>2</sub> in THF (110 mL, 220 mmol, 8.2 equiv). The resulting solution was stirred at 4 °C for 15 minutes and then allowed to warm to room temperature and stirred for 7 hours.

The reaction mixture was cooled to 4 °C and quenched by the portion-wise addition of MeOH (200 mL). The reaction mixture was then conc. *in vacuo* and then purified by flash column chromatography (25-50 EtOAc in heptane) affording an anomeric mixture of compound **17** (3.16 g, 34%) as a white solid.  $R_f$  = 0.58 (1:1; PE:EtOAc). mp = 96–98 °C. <sup>1</sup>H NMR (400 MHz, Chloroform-*d*)  $\delta$  7.41 – 7.22 (m, 5H), 5.57 (d,  $J$  = 5.3 Hz, 1H), 4.63 (dd,  $J$  = 7.1, 1.0 Hz, 1H), 4.32 (dd,  $J$  = 7.3, 4.8 Hz, 1H), 4.29 – 4.13 (m, 3H), 3.96 (d,  $J$  = 13.7 Hz, 1H), 3.58 (dd,  $J$  = 12.7, 7.4 Hz, 1H), 3.49 – 3.32 (m, 4H), 1.29 (t,  $J$  = 7.1 Hz, 3H). <sup>13</sup>C NMR (101 MHz, CDCl<sub>3</sub>)  $\delta$  169.0, 136.3, 136.2, 129.1, 128.9, 128.6, 128.4, 128.4, 127.9, 127.8, 103.4, 98.1, 83.9, 83.8, 83.4, 80.5, 70.9, 66.1, 61.8, 61.6, 61.0, 60.7, 55.6, 53.9, 52.5, 14.3, 14.2. FT-IR (neat):  $\nu$  = 3436, 2981, 2936, 2099, 1734, 1497, 1455 cm<sup>-1</sup>. HRMS calcd for C<sub>16</sub>H<sub>20</sub>O<sub>5</sub>N<sub>4</sub> + H<sup>+</sup> [ $M$ +H<sup>+</sup>]: 349.1506. Found 349.1496. [ $\alpha$ ]<sub>D</sub><sup>20</sup> = –54.8 ( $c$  = 1.00, CHCl<sub>3</sub>).



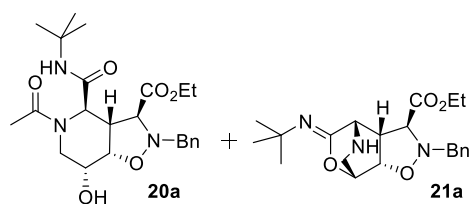
**Ethyl (3S,3aR,7R,7aS)-2-benzyl-7-hydroxyoctahydroisoxazolo[4,5-c]pyridine-3-carboxylate (19).** To a solution of azido-aldehyde **17** (0.106 g, 0.304 mmol, 1 equiv) in dry EtOH (1.6 mL) at 0 °C was added a solution of trimethylphosphine (1M in THF, 0.610 mL, 2 equiv). The reaction mixture was stirred at 0 °C for 3 hours, then concentrated and subsequently co-evaporated with dry toluene (3×). The residue was dissolved in dry THF (1.6 mL) and cooled to 0 °C. (AcO)<sub>3</sub>BHNa (0.184 g, 0.868 mmol, 2.86 equiv) was added and the resulting reaction mixture was stirred for 1.5 h. The reaction was then quenched with sat. aq. NaHCO<sub>3</sub> (20 mL) and then extracted with EtOAc (20 mL, 2×10 mL). The combined organic layers were washed with brine (10 mL), dried (MgSO<sub>4</sub>) and conc. *in vacuo*. The water layer was then additionally extracted with DCM (10 mL, 5×) and the combined organic layers were dried (MgSO<sub>4</sub>) and conc. *in vacuo*. The residues from the EtOAc- and the DCM-extractions were both purified by flash column chromatography (5-10% MeOH in DCM) to afford compound **19** (61.1 mg, 66%) as white crystals.  $R_f$  = 0.14 (10% MeOH in DCM). mp = 120–122 °C. <sup>1</sup>H NMR (400 MHz, Methanol-*d*<sub>4</sub>)  $\delta$  7.47 – 7.22 (m, 5H), 4.36 – 4.25 (m, 2H), 4.21 (d,  $J$  = 13.2 Hz, 1H), 4.06 (q,  $J$  = 7.1 Hz, 2H), 3.82 (ddd,  $J$  = 10.0, 4.8, 3.8 Hz, 1H), 3.41 (d,  $J$  = 3.1 Hz, 1H), 2.81 (dd,  $J$  = 12.7, 5.7 Hz, 2H), 2.77 – 2.63 (m, 2H), 2.38 (dd,  $J$  = 12.7, 9.5 Hz, 1H), 1.16 (t,  $J$  = 7.2 Hz, 3H). <sup>13</sup>C NMR (101 MHz, MeOD)  $\delta$  172.3, 137.0, 131.2, 129.3, 128.8, 78.4, 70.2, 67.6, 63.5, 62.3, 48.1, 47.6, 46.2, 14.4. FT-IR (neat):  $\nu$  = 3308, 2847, 1734, 1498, 1454, 1414 cm<sup>-1</sup>. HRMS calcd for C<sub>16</sub>H<sub>23</sub>O<sub>4</sub>N<sub>2</sub> + H<sup>+</sup> [ $M$ +H<sup>+</sup>]: 307.1652. Found 307.1644. [ $\alpha$ ]<sub>D</sub><sup>20</sup> = –43.0 ( $c$  = 1.00, CHCl<sub>3</sub>).

## General Procedure A & B

To a roundbottom flask containing a 0.18M solution of azido-aldehyde **17** (1 equiv) in dry EtOH at 0 °C was added a solution of trimethylphosphine (1M in THF, 2 equiv). The reaction mixture was stirred at 0 °C for 3 hours, then concentrated and subsequently co-evaporated with dry toluene (3×). The crude cyclic imine was dissolved dry EtOH (0.3M) (procedure **A**) or dry 2,2,2-trifluoroethanol (0.3M) (procedure **B**), divided in the appropriate amount of portions and cooled to 0 °C. Next, the appropriate carboxylic acid (1.25 equiv) and isocyanide (1.25 equiv) were successfully added dropwise

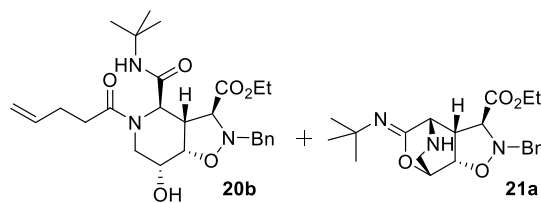


and the resulting reaction mixture was stirred for 20 hours while allowing the mixture to warm to room temperature. Saturated  $\text{NaHCO}_3$  was added to the mixture was extracted with EtOAc (3 $\times$ ). The combined organic layers were washed with sat.  $\text{NaHCO}_3$  and brine, dried ( $\text{MgSO}_4$ ) and conc. *in vacuo*. The SAWU-3-CR products were purified by silica gel flash column chromatography.



**Ethyl (3S,3aR,4R,7R,7aS)-5-acetyl-2-benzyl-4-(tert-butylcarbamoyl)-7-hydroxyoctahydroisoxazolo[4,5-c]pyridine-3-carboxylate (20a)** and **ethyl (3S,3aR,4S,7R,7aS,Z)-2-benzyl-9-(tert-butylimino)octahydro-7,4-(epoxymethano)isoxazolo[4,5-c]pyridine-3-carboxylate (21a)**. According to general procedure A the crude was obtained and

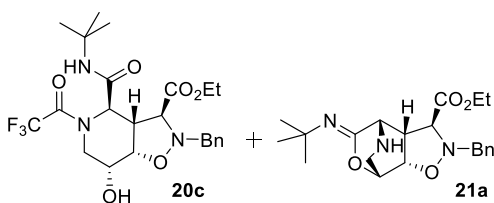
purified via silicagel column chromatography (50-100% EtOAc in heptane then 0-100% EtOH in EtOAc) affording both **20a** (45.7 mg, 31%) and **21a** (40.3 mg, 29%) as light yellow oils. NMR signals and other experimental data of compound **20a**:  $R_F$  = 0.41 (100% EtOAc)  $^1\text{H}$  NMR (400 MHz, Chloroform-*d*)  $\delta$  7.39 – 7.23 (m, 5H), 6.41 (s, 1H), 5.05 (d,  $J$  = 1.4 Hz, 1H), 4.56 (dd,  $J$  = 9.3, 3.6 Hz, 1H), 4.27 (dd,  $J$  = 13.9, 9.1 Hz, 1H), 4.17 (qd,  $J$  = 7.1, 1.6 Hz, 2H), 4.08 – 3.98 (m, 2H), 3.64 (td,  $J$  = 9.4, 1.4 Hz, 1H), 3.36 – 3.20 (m, 2H), 3.18 (s, 1H), 2.53 – 2.44 (m, 1H), 2.05 (s, 3H), 1.31 – 1.21 (s, 12H, *t*Bu &  $\text{COOCH}_2\text{CH}_3$ ).  $^{13}\text{C}$  NMR (101 MHz,  $\text{CDCl}_3$ )  $\delta$  172.8, 169.7, 168.7, 134.9, 130.1, 128.4, 128.0, 73.2, 68.1, 64.5, 61.9, 59.9, 52.5, 51.3, 45.2, 45.1, 28.7, 21.7, 14.2. FT-IR (neat):  $\nu$  = 3333, 2968, 1746, 1685, 1641, 1538, 1455, 1406  $\text{cm}^{-1}$ . HRMS calcd for  $\text{C}_{23}\text{H}_{33}\text{N}_3\text{O}_6 + \text{H}^+$  [M+H $^+$ ]: 448.2442. Found. 448.2425.  $[\alpha]_{\text{D}}^{20}$  = +51.2 ( $c$  = 1.00,  $\text{CHCl}_3$ ). NMR signals and other experimental data of compound **21a**:  $R_F$  = 0.42 (100% EtOH)  $^1\text{H}$  NMR (400 MHz, Chloroform-*d*)  $\delta$  7.44 – 7.36 (m, 2H), 7.39 – 7.30 (m, 2H), 7.35 – 7.24 (m, 1H), 4.55 (ddd,  $J$  = 4.3, 2.3, 0.9 Hz, 1H), 4.34 (d,  $J$  = 13.6 Hz, 1H), 4.29 – 4.17 (m, 2H), 4.21 – 4.10 (m, 1H), 3.81 (d,  $J$  = 13.6 Hz, 1H), 3.52 (d,  $J$  = 3.1 Hz, 1H), 3.39 – 3.23 (m, 3H), 2.88 (dd,  $J$  = 12.1, 0.9 Hz, 1H), 2.22 – 2.02 (m, 1H), 1.36 (s, 9H), 1.29 (t,  $J$  = 7.1 Hz, 3H).  $^{13}\text{C}$  NMR (101 MHz,  $\text{CDCl}_3$ )  $\delta$  169.1, 155.2, 136.9, 129.1, 128.4, 127.6, 75.0, 75.0, 70.3, 69.4, 61.9, 61.7, 53.4, 52.4, 51.1, 42.8, 30.0, 14.3. FT-IR (neat):  $\nu$  = 3378, 3034, 2966, 1741, 1684, 1516, 1477, 1455  $\text{cm}^{-1}$ . HRMS calcd for  $\text{C}_{21}\text{H}_{29}\text{N}_3\text{O}_4 + \text{H}^+$  [M+H $^+$ ]: 388.2231. Found. 388.2223.  $[\alpha]_{\text{D}}^{20}$  = –32.4 ( $c$  = 1.00,  $\text{CHCl}_3$ ).



**Ethyl (3S,3aR,4R,7R,7aS)-2-benzyl-4-(tert-butylcarbamoyl)-7-hydroxy-5-(pent-4-enoyl)octahydroisoxazolo[4,5-c]pyridine-3-carboxylate (20b)** and **ethyl (3S,3aR,4S,7R,7aS,Z)-2-benzyl-9-(tert-butylimino)octahydro-7,4-(epoxymethano)isoxazolo[4,5-c]pyridine-3-carboxylate (21a)**. According to

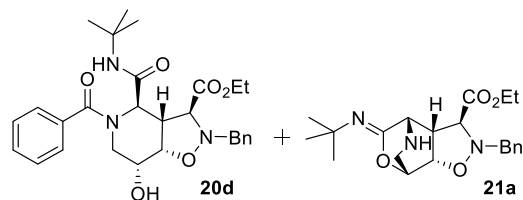
general procedure A the crude was obtained and purified via column chromatography (50-100% EtOAc in heptane then 0-100% EtOH in EtOAc) affording both **20b** (41.4 mg, 30%) and **21a** (39.2 mg, 35%) as yellow oils. NMR signals and other experimental data of compound **20b**:  $R_F$  = 0.76 (100% EtOAc).  $^1\text{H}$  NMR (400 MHz, Chloroform-*d*)  $\delta$  7.39 – 7.27 (m, 5H), 6.43 (s, 1H), 5.93 – 5.78 (m, 1H), 5.14 – 4.98 (m, 3H), 4.57 (dd,  $J$  = 9.3, 3.6 Hz, 1H), 4.30 (d,  $J$  = 14.1 Hz, 1H), 4.18 (qd,  $J$  = 7.2, 2.4 Hz, 2H), 4.11 – 3.98 (m, 2H), 3.70 – 3.61 (m, 1H), 3.40 – 3.22 (m, 2H), 3.17 (s, 1H), 2.56 – 2.27 (m, 5H), 1.31 – 1.24 (m, 12H).  $^{13}\text{C}$  NMR (101 MHz,  $\text{CDCl}_3$ )  $\delta$  174.6, 169.8, 168.6, 137.0, 134.8, 130.1, 128.4, 128.0, 115.8, 73.3, 68.1, 64.6, 61.9, 59.9, 52.7, 51.3, 45.1, 44.7, 32.4, 28.9, 28.7, 14.2. FT-IR (neat):  $\nu$  = 3338, 2976, 1737, 1677,

1635, 1537, 1498, 1454, 1415  $\text{cm}^{-1}$ . HRMS calcd for  $\text{C}_{26}\text{H}_{37}\text{N}_3\text{O}_6 + \text{H}^+ [\text{M} + \text{H}^+]$ : 488.2755. Found. 488.2741.  $[\alpha]_{\text{D}}^{20} = +66.5$  ( $c = 1.00$ ,  $\text{CHCl}_3$ ). NMR signals and other experimental data of compound **21a**:  $R_{\text{F}} = 0.42$  (100% EtOH)  $^1\text{H}$  NMR (400 MHz, Chloroform- $d$ )  $\delta$  7.44 – 7.36 (m, 2H), 7.39 – 7.30 (m, 2H), 7.35 – 7.24 (m, 1H), 4.55 (ddd,  $J = 4.3, 2.3, 0.9$  Hz, 1H), 4.34 (d,  $J = 13.6$  Hz, 1H), 4.29 – 4.17 (m, 2H), 4.21 – 4.10 (m, 1H), 3.81 (d,  $J = 13.6$  Hz, 1H), 3.52 (d,  $J = 3.1$  Hz, 1H), 3.39 – 3.23 (m, 3H), 2.88 (dd,  $J = 12.1, 0.9$  Hz, 1H), 2.22 – 2.02 (m, 1H), 1.36 (s, 9H), 1.29 (t,  $J = 7.1$  Hz, 3H).  $^{13}\text{C}$  NMR (101 MHz,  $\text{CDCl}_3$ )  $\delta$  169.1, 155.2, 136.9, 129.1, 128.4, 127.6, 75.0, 75.0, 70.3, 69.4, 61.9, 61.7, 53.4, 52.4, 51.1, 42.8, 30.0, 14.3. FT-IR (neat):  $\nu = 3378, 3034, 2966, 1741, 1684, 1516, 1477, 1455$   $\text{cm}^{-1}$ . HRMS calcd for  $\text{C}_{21}\text{H}_{29}\text{N}_3\text{O}_4 + \text{H}^+ [\text{M} + \text{H}^+]$ : 388.2231. Found. 388.2223.  $[\alpha]_{\text{D}}^{20} = -32.4$  ( $c = 1.00$ ,  $\text{CHCl}_3$ ).



**Ethyl (3S,3aR,4R,7R,7aS)-2-benzyl-4-(tert-butyl carbamoyl)-7-hydroxy-5-(2,2,2-trifluoroacetyl)octahydroisoxazolo[4,5-c]pyridine-3-carboxylate (20c) and ethyl (3S,3aR,4S,7R,7aS,Z)-2-benzyl-9-(tert-butylimino)octahydro-7,4-(epoxymethano)isoxazolo[4,5-c]pyridine-3-carboxylate (21a).** According to general

procedure **A** the crude was obtained and purified via column chromatography (30-50% EtOAc in heptane then 0-40% EtOH in EtOAc) affording impure **20c** and pure **21a** (70 mg, 49%) as a crystalline solid. Impure **20c** was further purified via column chromatography (20% acetone in toluene) affording **20c** (50.5 mg, 27%) as a colorless oil. NMR signals and other experimental data of compound **20c**:  $R_{\text{F}} = 0.47$  (1:1; PE:EtOAc).  $^1\text{H}$  NMR (400 MHz, Chloroform- $d$ )  $\delta$  7.36 – 7.28 (m, 5H), 6.09 (s, 1H), 4.98 (d,  $J = 1.5$  Hz, 1H), 4.56 (dd,  $J = 9.1, 3.9$  Hz, 1H), 4.32 (d,  $J = 14.2$  Hz, 1H), 4.21 (qd,  $J = 7.2, 6.5, 1.3$  Hz, 2H), 4.12 – 3.98 (m, 2H), 3.67 – 3.58 (m, 2H), 3.36 (s, 1H), 2.25 (s, 1H), 1.35 – 1.27 (m, 12H).  $^{13}\text{C}$  NMR (101 MHz,  $\text{CDCl}_3$ )  $\delta$  168.5, 168.0, 159.6, 159.2, 158.8, 158.4, 135.1, 129.7, 129.4, 128.6, 128.1, 120.6, 117.7, 114.9, 112.0, 72.9, 68.4, 63.6, 62.2, 60.4, 54.3, 51.9, 45.1, 44.1, 28.7, 14.2. FT-IR (neat):  $\nu = 3368, 2975, 1731, 1673, 1526, 1455$   $\text{cm}^{-1}$ . HRMS calcd for  $\text{C}_{23}\text{H}_{30}\text{F}_3\text{N}_3\text{O}_6 + \text{H}^+ [\text{M} + \text{H}^+]$ : 502.2159. Found. 502.2143.  $[\alpha]_{\text{D}}^{20} = +32.7$  ( $c = 0.93$ ,  $\text{CHCl}_3$ ). NMR signals and other experimental data of compound **21a**:  $R_{\text{F}} = 0.42$  (100% EtOH).  $^1\text{H}$  NMR (400 MHz, Chloroform- $d$ )  $\delta$  7.44 – 7.36 (m, 2H), 7.39 – 7.30 (m, 2H), 7.35 – 7.24 (m, 1H), 4.55 (ddd,  $J = 4.3, 2.3, 0.9$  Hz, 1H), 4.34 (d,  $J = 13.6$  Hz, 1H), 4.29 – 4.17 (m, 2H), 4.21 – 4.10 (m, 1H), 3.81 (d,  $J = 13.6$  Hz, 1H), 3.52 (d,  $J = 3.1$  Hz, 1H), 3.39 – 3.23 (m, 3H), 2.88 (dd,  $J = 12.1, 0.9$  Hz, 1H), 2.22 – 2.02 (m, 1H), 1.36 (s, 9H), 1.29 (t,  $J = 7.1$  Hz, 3H).  $^{13}\text{C}$  NMR (101 MHz,  $\text{CDCl}_3$ )  $\delta$  169.1, 155.2, 136.9, 129.1, 128.4, 127.6, 75.0, 75.0, 70.3, 69.4, 61.9, 61.7, 53.4, 52.4, 51.1, 42.8, 30.0, 14.3. FT-IR (neat):  $\nu = 3378, 3034, 2966, 1741, 1684, 1516, 1477, 1455$   $\text{cm}^{-1}$ . HRMS calcd for  $\text{C}_{21}\text{H}_{29}\text{N}_3\text{O}_4 + \text{H}^+ [\text{M} + \text{H}^+]$ : 388.2231. Found. 388.2223.  $[\alpha]_{\text{D}}^{20} = -32.4$  ( $c = 1.00$ ,  $\text{CHCl}_3$ ).

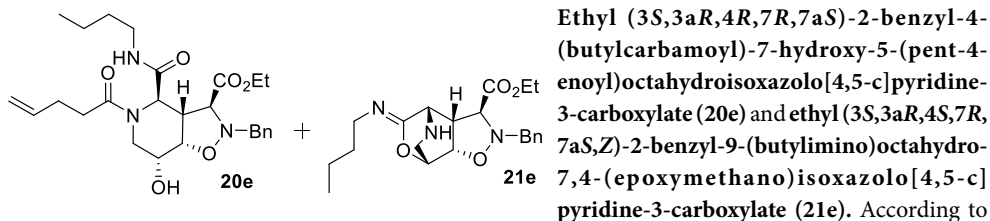


**Ethyl (3S,3aR,4R,7R,7aS)-5-benzoyl-2-benzyl-4-(tert-butylcarbamoyl)-7-hydroxyoctahydroisoxazolo[4,5-c]pyridine-3-carboxylate (20d) and ethyl (3S,3aR,4S,7R,7aS,Z)-2-benzyl-9-(tert-butylimino)octahydro-7,4-(epoxymethano)isoxazolo[4,5-c]pyridine-3-carboxylate (21a).** According to general

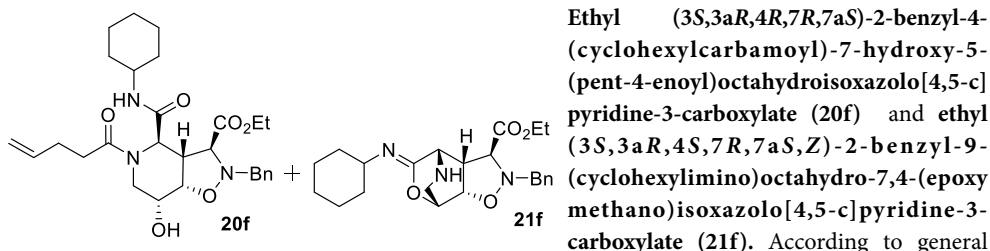
procedure **A** the crude was obtained and purified via column chromatography (50-100% EtOAc in heptane then 0-100% EtOH in EtOAc) affording **20d** (56.4, 33%) as a white turbid oil and **21a** (46.4 mg,



35%) as a yellow oil. NMR signals and other experimental data of compound **20d**:  $R_F = 0.30$  (1:1; PE:EtOAc).  $^1\text{H}$  NMR (400 MHz, Chloroform- $d$ )  $\delta$  7.49 – 7.30 (m, 10H), 6.85 (s, 1H), 5.23 (s, 1H), 4.58 (dd,  $J = 9.1, 4.0$  Hz, 1H), 4.37 (d,  $J = 14.0$  Hz, 1H), 4.21 (q,  $J = 7.2$  Hz, 2H), 4.11 (d,  $J = 14.0$  Hz, 1H), 3.93 – 3.83 (m, 1H), 3.70 (t,  $J = 9.5$  Hz, 1H), 3.63 – 3.43 (m, 2H), 3.11 (d,  $J = 12.9$  Hz, 1H), 2.61 (s, 1H), 1.33 (s, 9H), 1.31 – 1.26 (m, 3H).  $^{13}\text{C}$  NMR (101 MHz,  $\text{CDCl}_3$ )  $\delta$  173.7, 169.5, 168.6, 135.0, 134.7, 130.5, 130.0, 128.5, 127.9, 127.7, 73.7, 67.6, 64.4, 61.9, 60.0, 53.4, 51.3, 46.7, 44.6, 28.8, 14.2. FT-IR (neat):  $\nu = 3304, 2933, 1735, 1681, 1621, 1511, 1414\text{ cm}^{-1}$ . HRMS calcd for  $\text{C}_{28}\text{H}_{35}\text{N}_3\text{O}_6 + \text{H}^+ [\text{M} + \text{H}^+]$ : 510.2599. Found. 510.2587.  $[\alpha]_D^{20} = +71.9$  ( $c = 1.00, \text{CHCl}_3$ ).

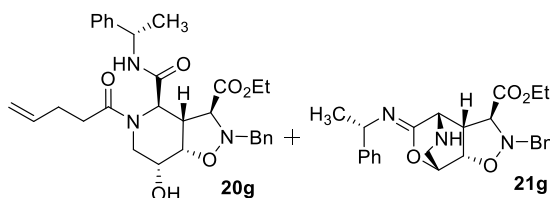


general procedure **A** the crude was obtained and purified via column chromatography (60-100% EtOAc in heptane then 0-100% EtOH in EtOAc) affording both **20e** (47.5 mg, 28%) and **21e** (26%)<sup>a</sup> as yellow oils. NMR signals and other experimental data of compound **20e**:  $R_F = 0.44$  (75% EtOAc in PE).  $^1\text{H}$  NMR (400 MHz, Chloroform- $d$ )  $\delta$  7.41 – 7.21 (m, 5H), 6.60 – 6.45 (m, 1H), 5.85 (ddt,  $J = 16.1, 10.7, 6.0$  Hz, 1H), 5.19 – 4.96 (m, 3H), 4.58 (dd,  $J = 9.3, 3.6$  Hz, 1H), 4.31 (d,  $J = 14.1$  Hz, 1H), 4.17 (qt,  $J = 7.4, 3.7$  Hz, 2H), 4.14 – 3.97 (m, 2H), 3.69 (t,  $J = 9.3$  Hz, 1H), 3.37 – 3.23 (m, 2H), 3.16 (q,  $J = 6.7$  Hz, 3H), 2.48 – 2.24 (m, 5H), 1.42 (p,  $J = 7.2$  Hz, 2H), 1.35 – 1.20 (m, 5H), 0.89 (t,  $J = 7.3$  Hz, 3H).  $^{13}\text{C}$  NMR (101 MHz,  $\text{CDCl}_3$ )  $\delta$  174.6, 170.6, 168.6, 137.1, 134.9, 130.1, 128.4, 128.0, 115.7, 73.2, 68.2, 64.6, 61.9, 59.9, 52.0, 45.3, 44.7, 39.4, 32.5, 31.6, 28.9, 20.1, 14.2, 13.8. FT-IR (neat):  $\nu = 3340, 3034, 2959, 2931, 2873, 1735, 1636, 1529, 1497, 1454, 1415\text{ cm}^{-1}$ . HRMS calcd for  $\text{C}_{26}\text{H}_{38}\text{N}_3\text{O}_6 + \text{H}^+ [\text{M} + \text{H}^+]$ : 488.2755. Found. 488.2745.  $[\alpha]_D^{20} = +51.2$  ( $c = 0.60, \text{CHCl}_3$ ). NMR signals and other experimental data of compound **21e**:  $R_F = 0.27$  (100% EtOH). HRMS calcd for  $\text{C}_{21}\text{H}_{29}\text{N}_3\text{O}_4 + \text{H}^+ [\text{M} + \text{H}^+]$ : 388.2231. Found. 388.2214. <sup>a</sup> The minor product could not be completely purified, but a relatively pure fraction was obtained for structure determination by NMR.



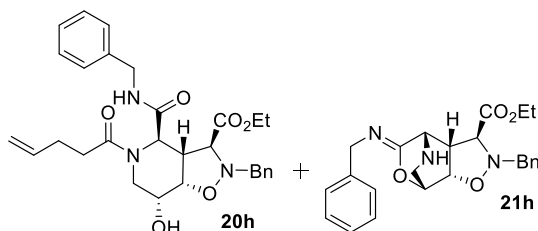
procedure **B** the crude was obtained and purified via column chromatography (50-100% EtOAc in heptane then 0-40% EtOH in EtOAc) affording **20f** (50.6 mg, 34%) as a light yellow oil and **21f** (55.5 mg, 46%) as a yellow oil. NMR signals and other experimental data of compound **20f**:  $R_F = 0.54$  (75% EtOAc in PE).  $^1\text{H}$  NMR (400 MHz, Chloroform- $d$ )  $\delta$  7.37 – 7.27 (m, 5H), 6.43 (d,  $J = 8.1$  Hz, 1H), 5.85 (dddd,  $J = 16.2, 10.7, 5.8, 3.8$  Hz, 1H), 5.18 – 4.99 (m, 3H), 4.57 (dd,  $J = 9.3, 3.6$  Hz, 1H), 4.31 (d,  $J = 14.0$  Hz, 1H), 4.22 – 4.13 (m, 2H), 4.12 – 3.98 (m, 2H), 3.73 – 3.58 (m, 2H), 3.40 – 3.25 (m, 2H), 3.20 (s, 1H), 2.39 (ddt,

$J = 16.7, 13.2, 8.5$  Hz, 5H), 1.89 – 1.80 (m, 1H), 1.80 – 1.72 (m, 1H), 1.70 – 1.52 (m, 4H), 1.38 – 1.22 (m, 6H), 1.22 – 1.03 (m, 3H).  $^{13}\text{C}$  NMR (101 MHz,  $\text{CDCl}_3$ )  $\delta$  174.6, 169.6, 168.7, 137.0, 135.0, 130.0, 128.4, 128.0, 115.8, 73.3, 68.2, 64.6, 61.9, 60.0, 52.1, 48.4, 45.2, 44.7, 32.9, 32.7, 32.5, 28.9, 25.6, 24.7, 14.2. FT-IR (neat):  $\nu = 3338, 2932, 2856, 1735, 1636, 1525, 1452, 1416$   $\text{cm}^{-1}$ . HRMS calcd for  $\text{C}_{28}\text{H}_{39}\text{N}_3\text{O}_6 + \text{H}^+ [\text{M} + \text{H}^+]$ : 514.2912. Found. 514.2898.  $[\alpha]_{\text{D}}^{20} = +42.9$  ( $c = 1.00$ ,  $\text{CHCl}_3$ ). NMR signals and other experimental data of compound **21f**:  $R_{\text{F}} = 0.47$  (100% EtOH).  $^1\text{H}$  NMR (400 MHz, Chloroform- $d$ )  $\delta$  7.30 (m, 5H), 4.55 – 4.43 (m, 1H), 4.27 (d,  $J = 13.8$  Hz, 1H), 4.24 – 4.05 (m, 4H), 3.83 (d,  $J = 13.8$  Hz, 1H), 3.65 – 3.54 (m, 1H), 3.54 – 3.49 (m, 1H), 3.37 – 3.20 (m, 3H), 2.86 (d,  $J = 12.1$  Hz, 1H), 1.82 – 1.70 (m, 4H), 1.63 (d,  $J = 12.7$  Hz, 1H), 1.36 – 1.18 (m, 8H).  $^{13}\text{C}$  NMR (101 MHz,  $\text{CDCl}_3$ )  $\delta$  169.0, 155.9, 136.5, 129.2, 128.3, 127.6, 75.1, 70.5, 68.8, 61.6, 61.3, 53.4, 51.8, 51.2, 42.9, 34.0, 33.7, 25.9, 25.2, 25.1, 14.2. FT-IR (neat):  $\nu = 2928, 2853, 1738, 1689, 1451$   $\text{cm}^{-1}$ . HRMS calcd for  $\text{C}_{23}\text{H}_{31}\text{N}_3\text{O}_4 + \text{H}^+ [\text{M} + \text{H}^+]$ : 414.2387. Found. 414.2391.  $[\alpha]_{\text{D}}^{20} = -24.1$  ( $c = 1.00$ ,  $\text{CHCl}_3$ ).



**Ethyl (3S,3aR,4R,7R,7aS)-2-benzyl-7-hydroxy-5-(pent-4-enoyl)-4-(((S)-1-phenylethyl)carbamoyl)octahydroisoxazolo[4,5-c]pyridine-3-carboxylate (20g) and ethyl (3S,3aR,4S,7R,7aS,Z)-2-benzyl-9-(((S)-1-phenylethyl)imino)octahydro-7,4-(epoxymethano)isoxa-**

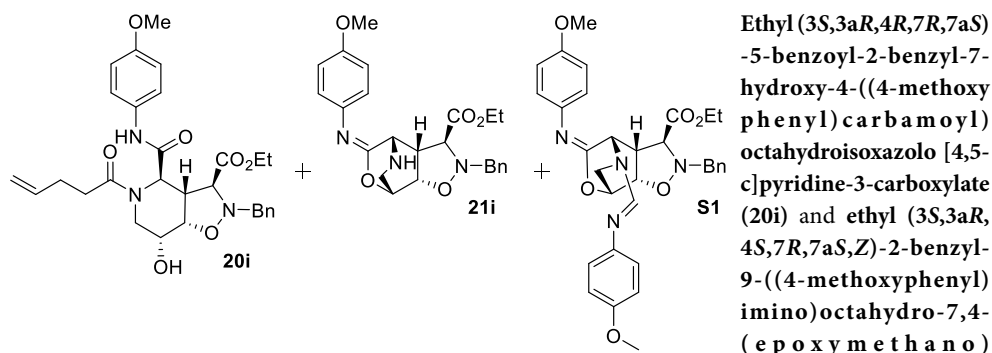
**zolo[4,5-c]pyridine-3-carboxylate (21g).** According to general procedure A the crude was obtained and purified via column chromatography (50–100% EtOAc in heptane then 0–100% EtOH in EtOAc) affording both **20g** (30.1 mg, 17%) and **21g**<sup>a</sup> (19.2 mg, 13%) as yellow oils. NMR signals and other experimental data of compound **20g**:  $R_{\text{F}} = 0.17$  (1:1; PE:EtOAc).  $^1\text{H}$  NMR (400 MHz, Chloroform- $d$ )  $\delta$  7.39 – 7.18 (m, 9H), 7.15 (dd,  $J = 7.2, 1.9$  Hz, 2H), 6.94 (d,  $J = 8.2$  Hz, 1H), 5.89 – 5.73 (m, 1H), 5.20 (d,  $J = 1.4$  Hz, 1H), 5.10 – 4.90 (m, 3H), 4.53 (dd,  $J = 9.2, 3.6$  Hz, 1H), 4.29 (d,  $J = 14.0$  Hz, 1H), 4.24 – 4.13 (m, 2H), 4.02 (d,  $J = 14.0$  Hz, 1H), 3.97 – 3.86 (m, 1H), 3.75 – 3.59 (m, 1H), 3.29 – 3.09 (m, 3H), 2.46 – 2.26 (m, 5H), 1.42 (d,  $J = 7.0$  Hz, 3H), 1.28 (t,  $J = 7.1$  Hz, 4H).  $^{13}\text{C}$  NMR (101 MHz,  $\text{CDCl}_3$ )  $\delta$  174.8, 169.7, 168.6, 143.5, 136.9, 134.9, 130.0, 128.8, 128.4, 127.9, 127.4, 125.7, 115.8, 73.2, 68.2, 64.3, 61.9, 59.9, 52.0, 49.2, 45.0, 44.6, 32.5, 28.8, 22.4, 14.2. FT-IR (neat):  $\nu = 3340, 2959, 2931, 2873, 1735, 1636, 1529, 1497, 1454, 1415$   $\text{cm}^{-1}$ . HRMS calcd for  $\text{C}_{30}\text{H}_{37}\text{N}_3\text{O}_6 + \text{Na}^+ [\text{M} + \text{Na}^+]$ : 558.2575. Found. 558.2567.  $[\alpha]_{\text{D}}^{20} = +64.5$  ( $c = 1.00$ ,  $\text{CHCl}_3$ ). NMR signals and other experimental data of compound **21g**<sup>a</sup>:  $R_{\text{F}} = 0.37$  (100% EtOH). HRMS calcd for  $\text{C}_{25}\text{H}_{29}\text{N}_3\text{O}_4 + \text{H}^+ [\text{M} + \text{H}^+]$ : 436.2231. Found. 436.2211. <sup>a</sup> The minor product could not be completely purified, but a relatively pure fraction was obtained for structure determination by NMR.



**Ethyl (3S,3aR,4R,7R,7aS)-2-benzyl-4-(benzylcarbamoyl)-7-hydroxy-5-(pent-4-enoyl)octahydroisoxazolo[4,5-c]pyridine-3-carboxylate (20h) and ethyl (3S,3aR,4S,7R,7aS,Z)-2-benzyl-9-(benzylimino)octahydro-7,4-(epoxymethano)isoxazolo[4,5-c]pyridine-3-carboxylate (21h).**

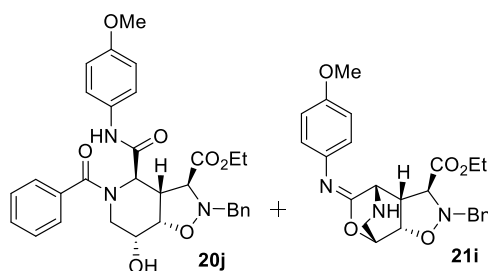
According to general procedure B the crude was obtained and purified via column chromatography (50–100% EtOAc in heptane then 0–100% EtOH

in EtOAc) affording both **20h** (37.1 mg, 24%) and **21h** (61.4 mg, 50%) as yellow oils. NMR signals and other experimental data of compound **20h**:  $R_F = 0.59$  (75% EtOAc in PE).  $^1\text{H}$  NMR (400 MHz, Chloroform- $d$ )  $\delta$  7.41 – 7.21 (m, 8H), 7.21 – 7.12 (m, 2H), 6.94 (t,  $J = 6.0$  Hz, 1H), 5.21 (d,  $J = 1.4$  Hz, 1H), 5.06 – 4.90 (m, 2H), 4.57 (dd,  $J = 9.2, 3.6$  Hz, 1H), 4.45 – 4.24 (m, 3H), 4.24 – 4.13 (m, 2H), 4.13 – 3.98 (m, 2H), 3.72 (td,  $J = 9.3, 1.4$  Hz, 1H), 3.30 (q,  $J = 5.2, 4.3$  Hz, 2H), 3.18 (s, 1H), 2.53 (s, 1H), 2.48 – 2.21 (m, 4H), 1.26 (t,  $J = 7.1$  Hz, 3H).  $^{13}\text{C}$  NMR (101 MHz,  $\text{CDCl}_3$ )  $\delta$  174.7, 170.6, 168.6, 138.0, 136.9, 134.9, 130.1, 128.8, 128.4, 127.9, 127.6, 127.4, 115.7, 73.2, 68.2, 64.5, 61.9, 59.8, 52.0, 45.2, 44.6, 43.6, 32.4, 28.8, 14.2. FT-IR (neat):  $\nu = 3339, 2980, 2929, 1734, 1634, 1524, 1497, 1454, 1416\text{ cm}^{-1}$ . HRMS calcd for  $\text{C}_{29}\text{H}_{35}\text{N}_3\text{O}_6 + \text{Na}^+ [\text{M} + \text{Na}^+]$ : 544.2418. Found: 544.2411.  $[\alpha]_D^{20} = +37.3$  ( $c = 1.00, \text{CHCl}_3$ ). NMR signals and other experimental data of compound **21h**:  $R_F = 0.38$  (100% EtOH).  $^1\text{H}$  NMR (400 MHz, Chloroform- $d$ )  $\delta$  7.43 – 7.20 (m, 10H), 4.62 – 4.54 (m, 1H), 4.50 – 4.34 (m, 2H), 4.27 – 4.07 (m, 4H), 3.71 (d,  $J = 13.9$  Hz, 1H), 3.61 (d,  $J = 3.3$  Hz, 1H), 3.34 – 3.23 (m, 2H), 3.19 (d,  $J = 8.3$  Hz, 1H), 2.89 (d,  $J = 12.1$  Hz, 1H), 1.25 (t,  $J = 7.1$  Hz, 3H).  $^{13}\text{C}$  NMR (101 MHz,  $\text{CDCl}_3$ )  $\delta$  169.0, 157.9, 140.7, 136.3, 129.4, 128.5, 128.3, 128.3, 127.6, 126.7, 75.0, 70.9, 68.4, 61.6, 60.9, 51.8, 51.2, 49.4, 43.0, 14.2. FT-IR (neat):  $\nu = 3030, 2981, 2873, 1737, 1688, 1604, 1496, 1454\text{ cm}^{-1}$ . HRMS calcd for  $\text{C}_{24}\text{H}_{27}\text{N}_3\text{O}_4 + \text{H}^+ [\text{M} + \text{H}^+]$ : 422.2074. Found: 422.2073.  $[\alpha]_D^{20} = -49.5$  ( $c = 0.80, \text{CHCl}_3$ ).



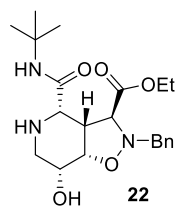
isoxazolo[4,5-c]pyridine-3-carboxylate (**21i**) and ethyl (3S,3aR,4S,7R,7aS,E)-2-benzyl-9-((4-methoxyphenyl)imino)-5-((E)-((4-methoxyphenyl)imino)methyl)octahydro-7,4-(epoxymethano)isoxazolo[4,5-c]pyridine-3-carboxylate (**S1**). According to general procedure **B** the crude was obtained and purified via column chromatography (50-100% EtOAc in heptane then 0-40% EtOH in EtOAc) affording both **20i** (29.0 mg, 18%), **21i** (52.6 mg, 41%) and **S1** (42.9 mg, 25%) as yellow oils. NMR signals and other experimental data of compound **20i**:  $R_F = 0.65$  (75% EtOAc in PE).  $^1\text{H}$  NMR (400 MHz, Chloroform- $d$ )  $\delta$  8.62 (s, 1H, NH), 7.43 – 7.28 (m, 7H), 6.88 – 6.76 (m, 2H), 5.93 – 5.75 (m, 1H), 5.26 (d,  $J = 1.4$  Hz, 1H), 5.16 – 4.95 (m, 2H), 4.65 (dd,  $J = 9.3, 3.6$  Hz, 1H), 4.33 (d,  $J = 14.0$  Hz, 1H), 4.19 (qd,  $J = 7.1, 1.6$  Hz, 3H), 4.05 (d,  $J = 14.0$  Hz, 1H), 3.83 – 3.68 (m, 4H), 3.41 – 3.14 (m, 3H), 2.51 – 2.22 (m, 5H), 1.28 (t,  $J = 7.1$  Hz, 3H).  $^{13}\text{C}$  NMR (101 MHz,  $\text{CDCl}_3$ )  $\delta$  175.3, 168.6, 168.5, 156.6, 136.9, 134.8, 130.8, 130.2, 128.4, 128.0, 121.5, 115.9, 114.3, 73.0, 68.2, 64.6, 62.0, 59.9, 55.6, 53.0, 45.1, 44.7, 32.5, 28.8, 14.2. FT-IR (neat):  $\nu = 3308, 2935, 1738, 1683, 1634, 1512, 1415\text{ cm}^{-1}$ . HRMS calcd for  $\text{C}_{29}\text{H}_{35}\text{N}_3\text{O}_7 + \text{Na}^+ [\text{M} + \text{Na}^+]$ : 560.2367. Found: 560.2360.  $[\alpha]_D^{20} = +64.2$  ( $c = 0.50, \text{CHCl}_3$ ). NMR signals and experimental data of the major adduct **21i**:  $R_F = 0.51$  (100% EtOH).  $^1\text{H}$  NMR (400 MHz, Chloroform- $d$ )  $\delta$  7.38 (d,  $J = 6.7$  Hz, 2H), 7.34 – 7.21 (m, 4H), 7.13 (d,  $J = 8.8$  Hz, 2H), 6.86 (d,  $J = 8.8$  Hz, 2H), 4.61 – 4.54 (m, 1H), 4.37 – 4.26 (m, 2H), 4.26 – 4.12 (m, 2H), 3.90 (d,  $J = 13.8$  Hz, 1H), 3.81 (s, 3H), 3.72 (d,  $J = 3.1$  Hz, 1H), 3.50 – 3.34 (m, 2H), 3.29 (dd,  $J = 12.2, 4.3$  Hz, 1H), 2.92 (d,  $J = 12.1$  Hz, 1H), 1.29 (t,  $J = 7.1$  Hz, 3H).  $^{13}\text{C}$

NMR (101 MHz,  $\text{CDCl}_3$ )  $\delta$  169.0, 157.0, 156.5, 138.4, 136.4, 129.3, 128.4, 127.7, 124.6, 114.0, 75.1, 71.1, 68.9, 61.8, 61.5, 55.6, 52.2, 51.4, 42.8, 14.3. FT-IR (neat):  $\nu$  = 2935, 2836, 1737, 1679, 1606, 1504, 1455  $\text{cm}^{-1}$ . HRMS calcd for  $\text{C}_{24}\text{H}_{28}\text{N}_3\text{O}_5 + \text{H}^+$  [ $\text{M} + \text{H}^+$ ]: 438.2023. Found: 438.2023.  $[\alpha]_{\text{D}}^{20}$  = +135.6 ( $c$  = 0.50,  $\text{CHCl}_3$ ). NMR signals and other experimental data of compound **S1**:  $R_{\text{F}}$  = 0.53 (75% EtOAc in PE).  $^1\text{H}$  NMR (500 MHz, Chloroform- $d$ )  $\delta$  7.72 (s, 1H), 7.37 (d,  $J$  = 7.4 Hz, 2H), 7.29 (dt,  $J$  = 11.6, 6.3 Hz, 3H), 7.21 – 7.12 (m, 2H), 6.96 – 6.89 (m, 2H), 6.90 – 6.82 (m, 4H), 4.87 – 4.73 (m, 1H), 4.41 (d,  $J$  = 8.0 Hz, 1H), 4.40 – 4.31 (m, 2H), 4.29 – 4.18 (m, 2H), 3.97 – 3.86 (m, 2H), 3.82 (s, 3H), 3.79 (s, 3H), 3.56 – 3.43 (m, 3H), 1.31 (t,  $J$  = 7.1 Hz, 3H).  $^{13}\text{C}$  NMR (101 MHz,  $\text{CDCl}_3$ )  $\delta$  168.5, 157.0, 156.4, 152.7, 149.7, 144.1, 137.5, 136.1, 129.3, 128.4, 127.8, 124.9, 121.9, 114.6, 114.1, 75.1, 71.6, 68.1, 62.1, 61.4, 56.4, 55.6, 55.6, 51.7, 44.3, 14.3. FT-IR (neat):  $\nu$  = 2934, 2835, 1736, 1689, 1625, 1577, 1505, 1464, 1426, 1408  $\text{cm}^{-1}$ . HRMS calcd for  $\text{C}_{32}\text{H}_{35}\text{N}_4\text{O}_6 + \text{H}^+$  [ $\text{M} + \text{H}^+$ ]: 571.2551. Found: 571.2548.  $[\alpha]_{\text{D}}^{20}$  = -79.1 ( $c$  = 1.00,  $\text{CHCl}_3$ ).



**Ethyl (3S,3aR,4R,7R,7aS)-2-benzyl-7-hydroxy-4-(((4-methoxyphenyl)carbamoyl)carbamoyl)-5-phenyloctahydroisoxazolo[4,5-c]pyridine-3-carboxylate (20j)** and **ethyl (3S,3aR,4S,7R,7aS,Z)-2-benzyl-9-(((4-methoxyphenyl)imino)octahydro-7,4-(epoxymethano)isoxazolo[4,5-c]pyridine-3-carboxylate (21i)**. According to general procedure A the crude was obtained and purified via column chromatography (50–100%

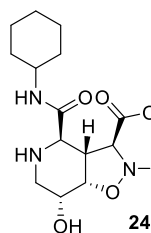
EtOAc in heptane then 0–100% EtOH in EtOAc) affording both **20j** (26.5 mg, 16%) as a yellow oil, while **21i** was only formed in trace amounts under these conditions. NMR signals and other experimental data of compound **20j**:  $R_{\text{F}}$  = 0.21 (1:1; PE:EtOAc).  $^1\text{H}$  NMR (400 MHz, Chloroform- $d$ )  $\delta$  9.10 (s, 1H), 7.52 – 7.33 (m, 12H), 6.86 (d,  $J$  = 8.8 Hz, 2H), 5.44 (s, 1H), 4.68 (dd,  $J$  = 9.1, 4.0 Hz, 1H), 4.43 (d,  $J$  = 14.1 Hz, 1H), 4.25 (q,  $J$  = 6.8 Hz, 2H), 4.16 (d,  $J$  = 14.1 Hz, 1H), 4.02 – 3.91 (m, 1H), 3.85 – 3.76 (m, 4H), 3.70 – 3.47 (m, 2H), 3.13 (dd,  $J$  = 12.9, 3.1 Hz, 1H), 2.39 (s, 1H), 1.31 (t,  $J$  = 7.2 Hz, 3H).  $^{13}\text{C}$  NMR (101 MHz,  $\text{CDCl}_3$ )  $\delta$  174.4, 168.6, 168.2, 156.7, 134.9, 134.2, 131.0, 130.9, 130.2, 128.7, 128.6, 128.2, 128.1, 121.6, 114.4, 73.5, 67.4, 64.5, 62.2, 60.0, 55.7, 53.8, 46.9, 44.7, 14.3. FT-IR (neat):  $\nu$  = 3304, 3064, 2933, 2837, 1735, 1681, 1621, 1601, 1577, 1511, 1454, 1414  $\text{cm}^{-1}$ . HRMS calcd for  $\text{C}_{31}\text{H}_{33}\text{N}_3\text{O}_7 + \text{Na}^+$  [ $\text{M} + \text{Na}^+$ ]: 582.2211. Found: 582.2189.  $[\alpha]_{\text{D}}^{20}$  = +44.8 ( $c$  = 0.50,  $\text{CHCl}_3$ ).



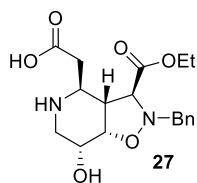
**Ethyl (3S,3aR,4S,7R,7aS)-2-benzyl-4-(tert-butylcarbamoyl)-7-hydroxyoctahydroisoxazolo[4,5-c]pyridine-3-carboxylate (22)**. To a solution of imide **21a** (38.0 mg, 0.098 mmol) in tetrahydrofuran- $d_8$  (2.0 mL) was added  $\text{D}_2\text{O}$  (2.0 mL). The resulting solution was heated in a sealed vessel in an oil bath to 80 °C for 4 h and then heated at 90 °C for 3 days. The reaction mixture was then concentrated *in vacuo* concentrated and co-evaporated with dry toluene to remove excess water. The residue was purified by flash column chromatography (30–50% acetone in toluene),

affording amide **22** (28.0 mg, 70%) as a colorless oil.  $R_{\text{F}}$  = 0.18 (1:1; toluene:acetone).  $^1\text{H}$  NMR (400 MHz, Chloroform- $d$ )  $\delta$  7.30 – 7.18 (m, 5H), 6.64 (s, 1H), 4.23 (dd,  $J$  = 7.0, 4.2 Hz, 1H), 4.15 – 4.03 (m, 3H), 3.98 (d,  $J$  = 13.8 Hz, 1H), 3.77 – 3.68 (m, 1H), 3.61 – 3.52 (m, 2H), 3.37 – 3.29 (m, 1H), 2.98 (dd,  $J$  = 14.2, 3.6 Hz, 1H), 2.51 (dd,  $J$  = 14.2, 2.1 Hz, 1H), 1.25 (s, 9H), 1.18 (t,  $J$  = 7.2 Hz, 3H).  $^{13}\text{C}$  NMR (101 MHz,  $\text{CDCl}_3$ )  $\delta$  169.6, 169.4, 135.8, 129.2, 128.6, 127.9, 76.9, 66.1, 65.3, 61.4, 58.9, 58.7, 51.0, 49.2, 45.8, 28.7, 14.1. FT-IR (neat):  $\nu$  = 3378, 3297, 3034, 2966, 2931, 2874, 1741, 1684, 1515, 1477, 1455  $\text{cm}^{-1}$ .

HRMS calcd for  $C_{21}H_{32}N_3O_5 + H^+$  [M+H<sup>+</sup>]: 406.2336. Found. 406.2334.  $[\alpha]_D^{20} = -72.9$  ( $c = 1.00$ ,  $CHCl_3$ ).



**Ethyl (3S,3aR,4R,7R,7aS)-2-benzyl-4-(cyclohexylcarbamoyl)-7-hydroxyoctahydroisoxazolo[4,5-c]pyridine-3-carboxylate (24).** To a solution of compound **20f** (37.0 mg, 0.072 mmol, 1.0 equiv) in a THF/H<sub>2</sub>O mixture (3:1, 1.4 mL) was added I<sub>2</sub> (54.9 mg, 0.22 mmol, 3.0 equiv). The reaction mixture was stirred for 20 min and then quenched by the addition of 1M aq. Na<sub>2</sub>S<sub>2</sub>O<sub>3</sub> (4 mL) and stirred for 30 min. The reaction mixture was poured into a mixture of 1M aq. Na<sub>2</sub>S<sub>2</sub>O<sub>3</sub>/sat. aq. NaCl (1/1, v/v, 10 mL) and then extracted with EtOAc (4×), dried (MgSO<sub>4</sub>) concentrated *in vacuo*, affording a yellow oil. The residue was purified by flash column chromatography (0–20% EtOH in EtOAc) providing compound **24** (29.9 mg, 94%) as a yellow oil.  $R_F = 0.44$  (20% EtOH in EtOAc). <sup>1</sup>H NMR (400 MHz, Chloroform-*d*)  $\delta$  7.48 – 7.24 (m, 5H), 7.13 (s, 1H), 4.37 (d,  $J = 13.8$  Hz, 1H), 4.33 – 4.20 (m, 2H), 4.18 – 4.06 (m, 2H), 3.98 – 3.80 (m, 2H), 3.79 – 3.64 (m, 2H), 3.64 – 3.51 (m, 1H), 3.32 – 3.19 (m, 1H), 3.00 – 2.86 (m, 2H), 1.94 – 1.78 (m, 2H), 1.78 – 1.65 (m, 2H), 1.65 – 1.52 (m, 1H), 1.40 – 1.10 (m, 8H). <sup>13</sup>C NMR (101 MHz, CDCl<sub>3</sub>)  $\delta$  169.8, 169.4, 135.9, 130.0, 128.6, 128.0, 75.4, 69.3, 64.6, 61.9, 61.7, 56.6, 48.6, 46.3, 45.0, 32.9, 25.5, 24.9, 14.2. FT-IR (neat):  $\nu = 3233, 2931, 2855, 1737, 1654, 1539, 1452$  cm<sup>-1</sup>. HRMS calcd for  $C_{23}H_{33}N_3O_5 + H^+$  [M+H<sup>+</sup>]: 432.2493. Found. 432.2483.  $[\alpha]_D^{20} = -42.5$  ( $c = 0.40$ ,  $CHCl_3$ ).



**2-((3S,3aR,4S,7R,7aS)-2-benzyl-3-(ethoxycarbonyl)-7-hydroxyoctahydroisoxazolo[4,5-c]pyridin-4-yl)acetic acid (27).** To a roundbottom flask containing a solution of azido-aldehyde **17** (0.106 g, 0.287 mmol, 1 equiv) in dry EtOH (1.6 mL) at 0 °C was added a solution of trimethylphosphine (1M in THF, 0.575 mL, 2 equiv). The reaction mixture was stirred at 0 °C for 3 hours and then concentrated and co-evaporated with dry toluene (3×). The residue was dissolved in a 2:1 mixture of dry Et<sub>2</sub>O/THF (3.0 mL) and malonic acid (38.5 mg, 0.370 mmol, 1.29 equiv) was added. The resulting reaction mixture was stirred for 19 h, which resulted in the formation of a sticky oil. The oil was dissolved by the addition of dry EtOH (1.5 mL), providing a yellow solution that quickly formed a white precipitate. This reaction mixture was allowed to stir for another 2 hours, followed by the addition MeOH (5 mL). The resulting solution was conc. *in vacuo*, affording a yellow foam, which purified by trituration with hot THF and subsequent trituration in hot MeOH, affording compound **27** (66.0 mg, 62%) as an off-white solid.  $R_F = 0.10$  (30% MeOH in DCM). <sup>1</sup>H NMR (400 MHz, Methanol-*d*<sub>4</sub>)  $\delta$  7.45 – 7.24 (m, 5H), 4.33 – 4.20 (m, 3H), 4.20 – 4.01 (m, 3H), 3.56 (d,  $J = 2.6$  Hz, 1H), 3.22 (dd,  $J = 12.1, 4.5$  Hz, 1H), 3.00 (dd,  $J = 12.1, 10.4$  Hz, 1H), 2.95 – 2.76 (m, 2H), 2.50 (dd,  $J = 17.3, 3.3$  Hz, 1H), 2.29 (dd,  $J = 17.3, 7.9$  Hz, 1H), 1.21 (t,  $J = 7.1$  Hz, 3H). <sup>13</sup>C NMR (101 MHz, DMSO-*d*<sub>6</sub>)  $\delta$  172.8, 170.4, 136.9, 129.1, 128.0, 127.2, 77.1, 69.5, 66.0, 62.3, 60.5, 53.1, 50.9, 46.1, 37.4, 13.9. FT-IR (neat):  $\nu = 2925, 2869, 1736, 1640, 1557, 1498, 1456, 1420$  cm<sup>-1</sup>. HRMS calcd for  $C_{18}H_{24}N_2O_6 + H^+$  [M+H<sup>+</sup>]: 365.1707. Found. 365.1695.  $[\alpha]_D^{20} = -44.8$  ( $c = 0.50$ ,  $CHCl_3$ ).

### Attempted one-pot Staudinger/aza-Wittig/Petasis reactions

To a roundbottom flask containing a 0.18M solution of azido-aldehyde **17** (1 equiv) in dry EtOH at 0 °C was added a solution of trimethylphosphine (1M in THF, 2 equiv). The reaction mixture was stirred at 0 °C for 3 hours, then concentrated and subsequently co-evaporated with dry toluene (3×). The crude cyclic imine was dissolved dry EtOH (0.2M) or in a 1:1 mixture of EtOH/H<sub>2</sub>O (0.1M) and cooled to

0 °C, followed by the addition of *trans*-2-phenylvinylboronic acid (1.00 equiv). The resulting reaction mixture was stirred at 0 °C for 30 min. and then allowed to warm to room temperature and stirred for 19 h. TLC analysis indicated no conversion at this point. The reaction mixture was heated to 80 °C for 7 h and then cooled to room temperature and conc. *in vacuo*. TLC analysis indicated complete conversion, but analysis by NMR and MS indicated no significant product formation.

### Modified SAWU-3CR procedure with *in situ* alcohol-protection

To a roundbottom containing a solution of azido-aldehyde **17** (0.104 g, 0.299 mmol, 1 equiv) in dry EtOH (1.6 mL) at 0 °C was added a solution of trimethylphosphine (1M in THF, 0.600 mL, 2 equiv). The reaction mixture was stirred at 0 °C for 2 hours and then concentrated and co-evaporated with dry toluene (3×). The residue was dissolved in dry THF (2.5 mL) and imidazole (23.5 mg, 0.345 mmol, 1.15 equiv) was added. The resulting reaction mixture was cooled to 0 °C, followed by the dropwise addition of TESCl (58.0 µL, 0.345 mmol, 1.15 equiv). The reaction mixture was stirred for 45 minutes at 0 °C and then another 50 minutes at room temperature. The mixture was then cooled to 0 °C, followed by the addition of acetic acid (86.0 µL, 1.50 mmol, 5.0 equiv) and *t*butyl isocyanide (170 µL, 1.50 mmol, 5.00 equiv). The resulting mixture was allowed to warm to rt and stirred for 3 days. The reaction was quenched by the addition of sat. aq. NaHCO<sub>3</sub> (5 mL) and EtOAc (20 mL). The biphasic system was separated and the water layer was extracted with EtOAc (10 mL, 2×). The combined organic layers were washed with sat. aq. NaHCO<sub>3</sub> (10 mL), brine (10 mL), dried (MgSO<sub>4</sub>) and then conc. *in vacuo*. The residue was purified by flash column chromatography (20-100% EtOAc in heptane), providing compound **26a** (61.6 mg, 36%) and compound **20a** (23.5 mg, 18%) as yellow oils. NMR signals and other experimental data of compound **26a**:  $R_f$  = 0.28 (7:3; PE:EtOAc). <sup>1</sup>H NMR (400 MHz, Chloroform-*d*) δ 7.42 – 7.20 (m, 5H), 6.36 (s, 1H), 4.95 (s, 1H), 4.44 (dd, *J* = 9.1, 2.9 Hz, 1H), 4.28 – 4.18 (m, 2H), 4.17 – 4.02 (m, 3H), 3.65 (t, *J* = 9.2 Hz, 1H), 3.34 (t, *J* = 10.7 Hz, 1H), 3.19 (dd, *J* = 10.4, 5.6 Hz, 1H), 3.02 – 2.83 (m, 1H), 2.02 (s, 3H), 1.30 – 1.19 (m, 12H), 0.93 (t, *J* = 7.9 Hz, 9H), 0.59 (q, *J* = 8.0 Hz, 6H). <sup>13</sup>C NMR (101 MHz, CDCl<sub>3</sub>) δ 172.8, 170.0, 169.1, 135.0, 130.4, 128.1, 127.7, 73.8, 68.9, 65.3, 61.7, 60.1, 52.6, 51.2, 46.3, 45.6, 28.6, 21.6, 14.2, 6.8, 4.8. FT-IR (neat): ν = 3326, 2958, 2877, 1738, 1681, 1644, 1532, 1455, 1411 cm<sup>-1</sup>. HRMS calcd for C<sub>29</sub>H<sub>48</sub>N<sub>3</sub>O<sub>6</sub>Si+H<sup>+</sup> [M+H<sup>+</sup>]: 562.3307. Found. 562.3281.

### Modified SAWU-3CR procedure with *in situ* alcohol-protection & deprotection

To a roundbottom containing a solution of azido-aldehyde **17** (0.104 g, 0.299 mmol, 1 equiv) in dry EtOH (1.6 mL) at 0 °C was added a solution of trimethylphosphine (1M in THF, 0.598 mL, 2 equiv). The reaction mixture was stirred at 0 °C for 2 hours and then concentrated and co-evaporated with dry toluene (3×). The residue was dissolved in dry THF (2.5 mL) and imidazole (24.0 mg, 0.353 mmol, 1.15 equiv) was added. The resulting reaction mixture was cooled to 0 °C, followed by the dropwise addition of TESCl (60.0 µL, 0.357 mmol, 1.19 equiv). The reaction mixture was stirred for 55 minutes at 0 °C and then another 30 minutes at room temperature. The mixture was then cooled to 0 °C, followed by the addition of *t*butyl isocyanide (170 µL, 1.50 mmol, 5.00 equiv) and acetic acid (86.0 µL, 1.50 mmol, 5.0 equiv). The resulting mixture was allowed to warm to rt and stirred for 17 h. Finally, H<sub>2</sub>O (0.25 mL) and 1M HCl in Et<sub>2</sub>O (1.5 mL) were added and the solution was stirred at rt for 2 h, followed by the addition of sat. aq. NaHCO<sub>3</sub> (5 mL) and EtOAc (20 mL). The biphasic system was separated and the water layer was extracted with EtOAc (10 mL, 2×). The combined organic layers were washed with sat. aq. NaHCO<sub>3</sub> (8 mL), brine (8 mL), dried (MgSO<sub>4</sub>) and then conc. *in vacuo*. The residue was purified by flash column chromatography (50-100% EtOAc in heptane), providing compound **20a** (65.7 mg, 41%) as a yellow oil.

## References

1. Yagi, M., Kouno, T., Aoyagi, Y., and Murai, H. *Nippon Nogeikagaku Kaishi* **1976**, 50, 571.
2. Murao, S. and Miyata, S. *Agric. Biol. Chem.* **1980**, 44, 219.
3. Inouye, S., Tsuruoka, T., Ito, T., and Niida, T. *Tetrahedron* **1968**, 24, 2125.
4. Paulsen, H. *Angew. Chem. Int. Ed.* **1966**, 5, 495.
5. Paulsen, H., Sangster, I., and Heyns, K. *Chem. Ber.* **1967**, 100, 802.
6. Jacob, G.S. *Curr. Opin. Struct. Biol.* **1995**, 5, 605.
7. Butters, T.D., Dwek, R.A., and Platt, F.M. *Chem. Rev.* **2000**, 100, 4683.
8. Platt, F.M., Neises, G.R., Dwek, R.A., and Butters, T.D. *J. Biol. Chem.* **1994**, 269, 8362.
9. Wennekes, T., van den Berg, R.J.B.H.N., Donker, W., van der Marel, G.A., Strijland, A., Aerts, J.M.F.G., and Overkleeft, H.S. *J. Org. Chem.* **2007**, 72, 1088.
10. Wennekes, T., Bongers, K.M., Vogel, K., van den Berg, R.J.B.H.N., Strijland, A., Donker-Koopman, W.E., Aerts, J.M.F.G., van der Marel, G.A., and Overkleeft, H.S. *Eur. J. Org. Chem.* **2012**, 2012, 6420.
11. *Iminosugars: From Synthesis to Therapeutic Applications*; P. Compain and O.R. Martin. Wiley-VCH/ **2007**.
12. Wei, Z. *Curr. Top. Med. Chem.* **2005**, 5, 1363.
13. Wennekes, T., van den Berg, R.J.B.H.N., Boltje, T.J., Donker-Koopman, W.E., Kuijper, B., van der Marel, G.A., Strijland, A., Verhagen, C.P., Aerts, J.M.F.G., and Overkleeft, H.S. *Eur. J. Org. Chem.* **2010**, 2010, 1258.
14. Peer, A. and Vasella, A. *Helv. Chim. Acta* **1999**, 82, 1044.
15. van den Broek, L.A.G.M. *Tetrahedron* **1996**, 52, 4467.
16. Hashimoto, T. and Maruoka, K. *Chem. Rev.* **2015**, 115, 5366.
17. Stanley, L.M. and Sibi, M.P. *Chem. Rev.* **2008**, 108, 2887.
18. Inouye, Y., Watanabe, Y., Takahashi, S., and Kakisawa, H. *Bull. Chem. Soc. Jpn.* **1979**, 52, 3763.
19. Nguyen, T.B., Beauseigneur, A., Martel, A., Dhal, R., Laurent, M., and Dujardin, G. *J. Org. Chem.* **2010**, 75, 611.
20. Hooogenboom, J., Zuilhof, H., and Wennekes, T. *Org. Lett.* **2015**, 17, 5550.
21. Diaz-Rodriguez, A., Sanghvi, Y.S., Fernandez, S., Schinazi, R.F., Theodorakis, E.A., Ferrero, M., and Gotor, V. *Org. Biomol. Chem.* **2009**, 7, 1415.
22. Schmid, C.R., Bryant, J.D., Dowlatzedah, M., Phillips, J.L., Prather, D.E., Schantz, R.D., Sear, N.L., and Vianco, C.S. *J. Org. Chem.* **1991**, 56, 4056.
23. Mann, J. and Weymouth-Wilson, A. *Carbohydr. Res.* **1992**, 216, 511.
24. Fazio, F. and Schneider, M.P. *Tetrahedron: Asymmetry* **2000**, 11, 1869.
25. Ondruš, V., Orság, M., Fišera, L.u., and Prónayová, N.a. *Tetrahedron* **1999**, 55, 10425.
26. Timmer, M.S.M., Risseuw, M.D.P., Verdoes, M., Filippov, D.V., Plaisier, J.R., van der Marel, G.A., Overkleeft, H.S., and van Boom, J.H. *Tetrahedron: Asymmetry* **2005**, 16, 177.
27. Cook, G.R., Shanker, P.S., and Peterson, S.L. *Org. Lett.* **1999**, 1, 615.
28. Endo, A. and Danishefsky, S.J. *J. Am. Chem. Soc.* **2005**, 127, 8298.

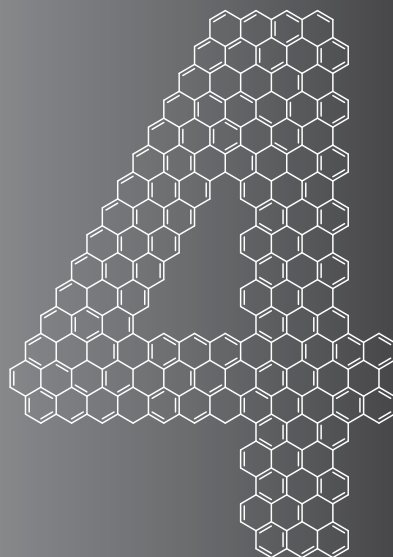


29. Deng, X., Su, J., Zhao, Y., Peng, L.-Y., Li, Y., Yao, Z.-J., and Zhao, Q.-S. *Eur. J. Med. Chem.* **2011**, *46*, 4238.
30. Leca, D., Gaggini, F., Cassayre, J., Loiseleur, O., Pieniazek, S.N., Luft, J.A.R., and Houk, K.N. *J. Org. Chem.* **2007**, *72*, 4284.
31. Schulthess, A.H. and Hansen, H.-J. *Helv. Chim. Acta* **1981**, *64*, 1322.
32. Meise, W. and Mika, U. *Arch. Pharm.* **1989**, *322*, 573.
33. Thompson, M.J. and Chen, B. *J. Org. Chem.* **2009**, *74*, 7084.
34. Kazmaier, U. and Hebach, C. *Synlett* **2003**, *2003*, 1591.
35. Gulevich, A.V., Zhdanko, A.G., Orru, R.V.A., and Nenajdenko, V.G. *Chem. Rev.* **2010**, *110*, 5235.
36. Cristau, P., Vors, J.-P., and Zhu, J. *Org. Lett.* **2001**, *3*, 4079.
37. Katsuyama, A., Matsuda, A., and Ichikawa, S. *Org. Lett.* **2016**, *18*, 2552.
38. Bongers, K.M., Wennekes, T., Filippov, D.V., Lodder, G., van der Marel, G.A., and Overkleeft, H.S. *Eur. J. Org. Chem.* **2008**, *2008*, 3678.
39. Zoidl, M., Gonzalez Santana, A., Torvisco, A., Tysoe, C., Siriwardena, A., Withers, S.G., and Wrodnigg, T.M. *Carbohydr. Res.* **2016**, *429*, 62.
40. G. M. Sheldrick (2008). SADABS and TWINABS. Universität Göttingen, G.
41. Sheldrick, G.M. *Acta Cryst. A* **2008**, *64*, 112.
42. Sheldrick, G.M. *Acta Cryst. C* **2015**, *71*, 3.
43. Spek, A.L. *Acta Cryst. D* **2009**, *65*, 148.





## Chapter 4



# Synthesis of a Carbocyclic Activity-Based Probe for Sialidases



## Introduction

The family of neuraminidase enzymes are involved in the lifecycle of *N*-acetylneuraminic acid (Neu5Ac **1**), which is a monosaccharide that is mainly found in mammals and critical in communication between cells. Currently, four human neuraminidases have been characterized; each being unique in its substrates and subcellular location.<sup>1-6</sup> The functional versatility of this enzyme class denotes its biological significance, as does the existence of a neuraminidase-related genetic disease, sialidosis.<sup>7</sup> Sialidosis is a lysosomal storage disorder (LSD) resulting from a malfunctioning *N*-acetyl- $\alpha$ -neuraminidase-1 (NEU1), which is caused by a mutation in the corresponding NEU1 gene.<sup>1,8,9</sup> Studies of this gene have led to the discovery of 43 known disease-causing mutations of varying severity.<sup>9,10</sup> A 'mild' version of sialidosis, known as type 1 sialidosis, occurs in children and adolescents who, at the age of 20, start to show symptoms involving progressive visual loss and seizures as a result from progressive deterioration of coordinated muscular activities.<sup>10</sup> A more common form of sialidosis, type 2 sialidosis, is even more severe. Infants diagnosed with type 2 sialidosis usually die before reaching the age of five.<sup>11</sup> Currently there is no viable therapy for the treatment of sialidosis patients.

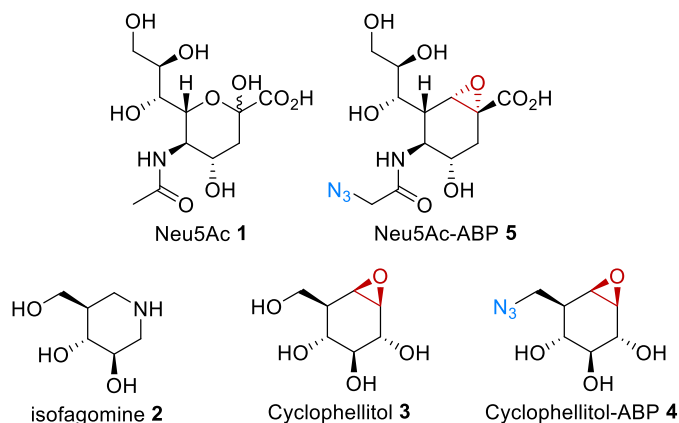


**Figure 1.** Structures of Neu5Ac, isofagomine, cyclophellitol, cyclophellitol-based ABP **4** and Neu5Ac-ABP **5**.

Treatments concerning other enzyme-related LSDs exist and typically involve enzyme replacement therapy (ERT).<sup>12,13</sup> ERT involves treating patients that suffer from enzyme deficiency with recombinant lysosomal hydrolases, and this approach is effective for several LSD patients. However, ERT is not a viable solution for patients suffering from sialidosis due to the unfavorable properties of NEU1, which makes it a difficult target to express and isolate.<sup>10</sup> As such, no ERT therapy is currently available or on the horizon for patients with sialidosis.<sup>10</sup> An alternative approach that has recently received a lot of attention is the so-called small molecule pharmacologic-chaperone therapy (PCT). PCT is a therapy that usually uses small pharmacological molecules, typically iminosugars, to increase enzymatic activity by stabilizing and/or promote folding of mutated proteins. PCT could also be beneficial for sialidosis patients, since NEU1 in cells from sialidosis patients shows improper enzyme folding,

resulting in loss of sialidase activity and subsequent accumulation of sialyl-conjugates within lysosomes. Treatment of sialidosis by stabilizing mutant NEU1 enzymes has recently been explored in two studies involving mice.<sup>14,15</sup> However, these studies involved the challenging and controversial transgenic expression of a chaperone protein to stabilize mutant NEU1.

In contrast to sialidosis, a small molecule PCT treatment has been reported for Gaucher disease. This disease is caused by insufficient activity of a lysosomal  $\beta$ -glucosidase, GBA1. Cells containing this mutated enzyme can be treated with a small molecule, known as isofagomine 2 (Figure 1). This iminosugar is a potent competitive inhibitor interacting with the catalytic pocket of  $\beta$ -glucosidase, which increases the activity by stabilizing and/or promoting the folding of this enzyme.<sup>16-18</sup> Validation of isofagomine activity as a chaperone in PCT was aided greatly by the development of a sensitive  $\beta$ -glucosidase targeting activity-based probe (ABP), compound 4. Early essays to study isofagomine's ability to increase GBA1 activity were quite artificial, as cells were exposed to milimolar concentrations of a fluorogenic substrate at acidic pH,<sup>19</sup> while ABP 4 for the first time allowed monitoring GBA1 activity *in situ*.<sup>20</sup> The structure of ABP 4 and its mechanism-based inactivation of glycosidases is based on the natural product cyclophellitol 3 (Figure 1). Overkleeft et al. developed 4 and showed that this ABP can be used to visualize active GBA1, in a highly sensitive and specific approach.

With treatment options for sialidosis patients being limited, there is keen interest in the discovery of novel mechanisms to restore their neuraminidase activity. Development of a NEU1-ABP would greatly aid in the validation of potential sialidosis PCT targets *in vivo*. More importantly, development of a NEU1-ABP would enable small molecule library screening for leads that can bind the active site of a mutant NEU1 enzyme and promote better folding, thereby hopefully increasing lysosomal trafficking of NEU1 and its enzymatic activity. A few ABPs towards neuraminidases have been developed. These ABPs use different reactive groups (warheads) that allow covalent attachment to the catalytic pocket of the enzyme. These warheads include a photoreactive group (6),<sup>21</sup> a latent ortho-difluoromethylphenyl group (7)<sup>22</sup> and 3-fluorosialyl fluorides (8) (Figure 2).<sup>23</sup>

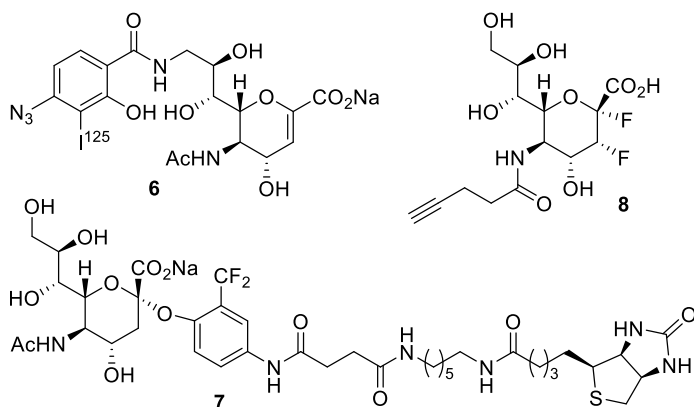
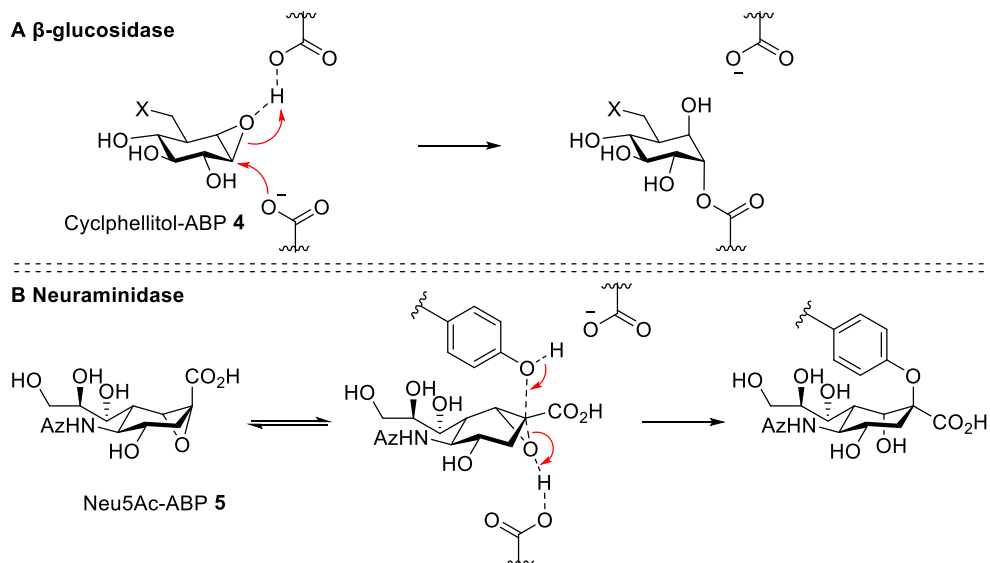


**Figure 2.** Reported neuraminidase ABPs utilizing different warheads as the trapping device.

However, these probes suffer from some drawbacks including nonspecific labeling,<sup>21,22</sup> cell membrane impermeability<sup>21,22</sup> or the requirement of harsh multistep labeling conditions involving toxic copper.<sup>23</sup> Furthermore, while ABP **8** can be applied *in situ*, this requires high concentration of the probe (0.2 mM) compared to the application of an ABP derived from **4** by Overkleeft et al. at much lower concentration (5 nM) due to higher IC<sub>50</sub>-values and the complex labeling.<sup>20,23</sup> A novel ABP towards neuraminidases could be developed that mitigates these problems by replacing these reporters by a small bio-orthogonal azide handle to enable a two-step labeling strategy *via* a strain-promoted click-reaction. The strain-promoted click-reaction is a well-established methodology,<sup>24-27</sup> which does not require toxic copper for labeling, while incorporating a small azide instead of a reporter group is a known strategy to maintain cell-permeability of the usually cell-permeable recognizing groups.<sup>28-31</sup>

With this background in mind, we propose to synthesize carbocyclic ABP **5** that is based on the structure of Neu5Ac and incorporates the characteristics of the highly effective cyclophellitol-based ABP **4**. The absolute stereochemistry of ABP **4** matches that of a  $\beta$ -glucopyranoside moiety, which explains the strong binding of the carbocycle to the active site of retaining  $\beta$ -glucosidases. Upon binding, the epoxide is optimally positioned so that the epoxide can be activated by protonation and opened by attack of a nucleophilic amino acid residue residing in the enzyme active site (Scheme 1A). The nucleophilic attack - involving consecutive protonation and nucleophilic attack of two acidic amino acid residues - is irreversible and is driven by the release of epoxide ring strain upon opening. The irreversible nature of this reaction should result in the formation of a stable ABP-enzyme adduct and thus in activity-based enzyme inactivation. These characteristics can be translated to Neu5Ac-ABP **5**, which would involve the synthesis of a carbocycle with the absolute stereochemistry of Neu5Ac, possessing an endocyclic epoxide (Figure 1). However, while the characteristics can be the same, ABP **5** would be targeted towards an enzyme with a different active site. For example, glucosidases and neuraminidases employ different amino acid residues for the initial nucleophilic attack of the glycosidic bond.<sup>32-34</sup> Still, while the composition of the active site of various neuraminidases is different, the basic displacement mechanisms of  $\beta$ -glucosidase- and neuraminidase substrates are similar and involve a retaining mechanism for both enzymes. For example, the catalytic mechanism of  $\beta$ -glucosidase inactivation with (+)-cyclophellitol has been elucidated in detail and shown to involve a briefly deprotonated glutaminic acid that attacks the substrate (Scheme 1A).

**Scheme 1.** A) Schematic of the irreversible binding of ABP **4** in retaining  $\beta$ -glucosidase and B) schematic of ABP **5** binding in the retaining  $\alpha$ -*N*-acetylneuraminidase, based on the mechanisms of enzymatic hydrolysis of  $\alpha$ -Neu5Ac-glycoconjugates.



In the case of neuraminidases, a covalent bond is formed between a substrate and a highly conserved tyrosine residue positioned directly above the C-2 carbon, where the carboxylate of most retaining glycosidases would be found (Scheme 1B).<sup>32,35-37</sup> The similar trapping of glycomimetics substrates shows that the a carbocyclic epoxide could be used as an ABP for neuraminidase. However, this enzyme also has a different morphology in terms of spatial orientation of amino acid residues. The tight binding of ABP **4** in retaining  $\beta$ -glucosidases does not automatically translate to similar binding of **5** in neuraminidases due to the completely different morphology of these enzyme active sites. Fortunately, extensive studies into structure and mechanism of neuraminidases have provided extensive information about the morphology of the active site of neuraminidases. The active site of especially influenza viral neuraminidase has been especially well studied through the development of different classes of inhibitors. The complementary function of viral and mammalian neuraminidases, requires that the morphology of the catalytic site is similar, which is apparent by the similar inhibition of viral and human neuraminidases by 2-deoxy-2,3-dihydro-*N*-acylneuramini acid (DANA) **9** (Figure 3).<sup>38</sup>

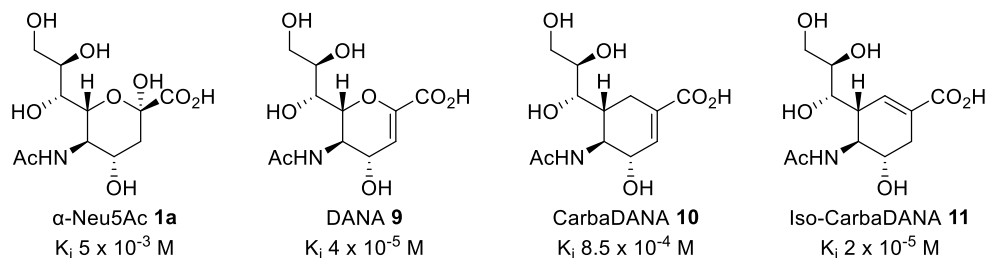


**Figure 3.** Structures of influenza inhibitors with their respective  $IC_{50}$  values towards *Influenza A* neuraminidase.

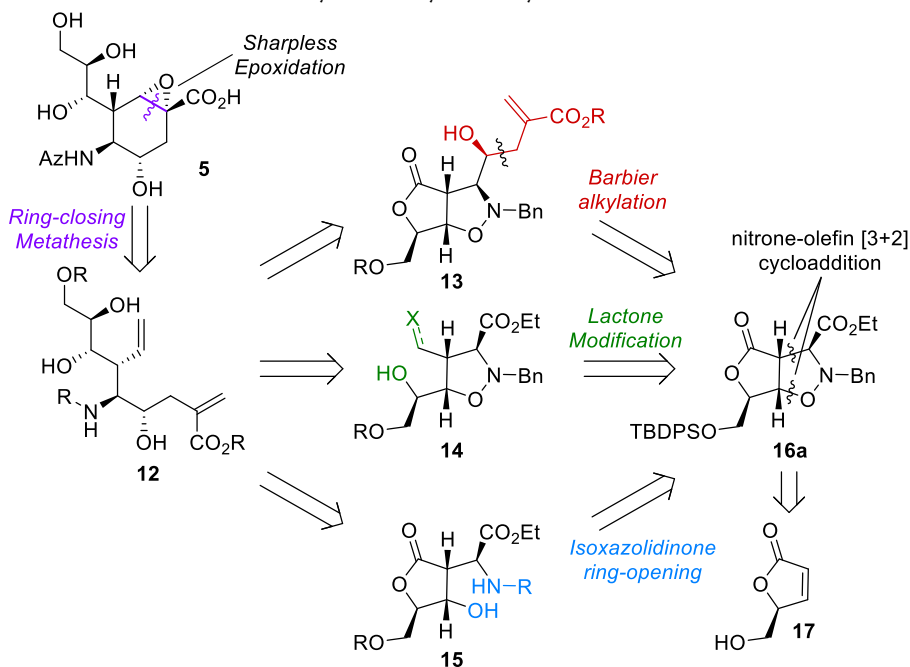
The study of DANA **9** and other inhibitors of influenza showed that the active site contains a relatively high number of charged amino acids, which play a key role in binding and orienting these inhibitors in the active site. In there both α-Neu5Ac **1a** and DANA (Figure 3) are primarily oriented through charge-charge interaction between the C-1 carboxylate group and a positively charged cluster of three arginines.<sup>39,40</sup> Additionally, a range of hydrogen bonding, non-polar and electrostatic interactions - involving the C8-C9 sidechain, the C4 hydroxyl group and the acetamido group on C5 - make important contributions to the overall binding energy. In contrast, the anomeric C2 hydroxyl group plays only a minor role in the overall binding of α-Neu5Ac **1a** in the active site. The minor role of the C2 hydroxyl group is further illustrated by DANA **9**, an inhibitor not possessing a 2-hydroxyl group, which is a much more effective inhibitor of naturally occurring neuraminidase than **1a**. Of particular interest is that the ring oxygen appears to contribute little if any to overall binding of the substrates to the enzyme's active site as reported by Taylor (Neu5Ac **1a**) and Smith (DANA **9**) et al.<sup>39,40</sup> This is further supported by the strong binding of CarbaDANA **10** and Iso-CarbaDANA **11**, both carbocycles, that show stronger binding than Neu5Ac **1a** and, in the case of Iso-CarbaDANA **11**, a two-fold stronger inhibition than DANA **9**.<sup>41</sup> Given these observations, it is our hypothesis that incorporation of an endocyclic epoxide at the C2 position of the carbocycle would still allow active site binding. Furthermore, the presence of the epoxide would then allow irreversible binding of neuraminidases by ABP **5**.<sup>20</sup>

Synthesis of Neu5Ac-ABP **5** would require a late-stage epoxidation of a cyclohexene analog. As depicted in Figure 3, Iso-CarbaDANA **11** would appear to be a good target for late-stage incorporation of the endocyclic epoxide. However, Iso-CarbaDANA **11**, synthesized by Vasella and coworkers,<sup>41</sup> does not accommodate late-stage functionalization of the acetamido, which would be required to introduce an *N*-azidoacetyl group at his position. The introduction of an *N*-azidoacetyl group is required, since ABPs require a clickable handle for imaging and quantification of inactivated enzyme. Furthermore, the synthesis of carbocycle **11** by Vasella et al. is lengthy (19 steps) and low yielding due to the formation of undesired isomers during the synthesis. In fact, the route was designed to give a mixture of intermediates leading to CarbaDANA **10** and Iso-CarbaDANA **11**, providing a precursor to **11** as the minor isomer in low yield.



We therefore aim to develop a novel route towards Neu5Ac-ABP **5** to enable the exploration of this ABP to study the enzymatic activity of neuraminidases such as NEU1. Furthermore, it was envisioned that a practical small molecule screening for PCT treatments would become possible through the synthesis of Neu5Ac-ABP **5**. The proposed route to this ABP involves a late-stage epoxidation and ring-closing metathesis (RCM) to obtain the desired carbocyclic ring (Scheme 2).

**Scheme 2.** Retrosynthesis analysis of the synthesis of Neu5Ac-ABP **5**.



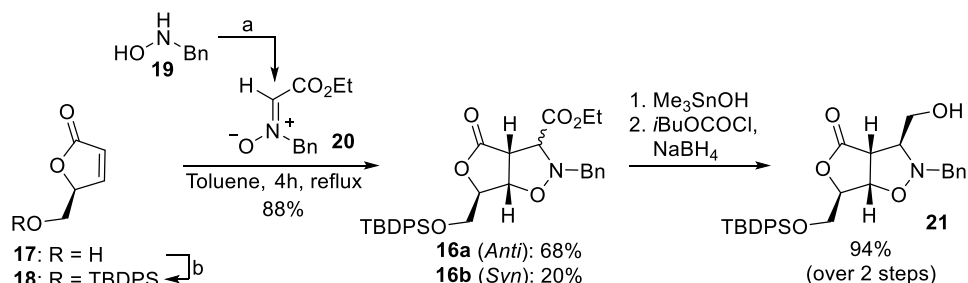
RCM to obtain the cyclohexene-ring for subsequent epoxidation would require linear diene intermediate **12**. This advanced intermediate - possessing 5-consecutive chiral centers - may be obtained *via* bicyclic compound **16a**. This intermediate, possessing the majority of the required stereochemistry can be obtained in one step through a highly regio- and stereoselective nitron-olefin [3+2] cycloaddition.<sup>42</sup> Cycloadduct **16a**, obtained through this cycloaddition reaction, might then be further modified through selective modification of either the exocyclic ester, the lactone, or the N-O-bond, leading to intermediates **13**, **14** or **15** respectively. One of these intermediates should then enable the synthesis of diene **9**, which leads to Neu5Az-ABP **5**.

## Results

The synthesis route towards Neu5Ac-ABP **5** starts with the nitron-olefin [3+2] cycloaddition reaction between a TBDPS-protected furanone **18** and nitron **20**. Both nitron **20**<sup>43</sup> and

furanone **18**<sup>44</sup> are available through a one-step procedure, but furanone **18** was typically prepared from 1,2:5,6-diisopropylidene-D-mannitol in 4 steps for large scale synthesis according to literature procedures.<sup>44,45</sup> With furanone **18** and nitron **20** in hand, the subsequent nitron-olefin [3+2] cycloaddition reaction was optimized as discussed in chapter 3, which selectively provided the desired isoxazolidines **16a** in 68% (Scheme 3)

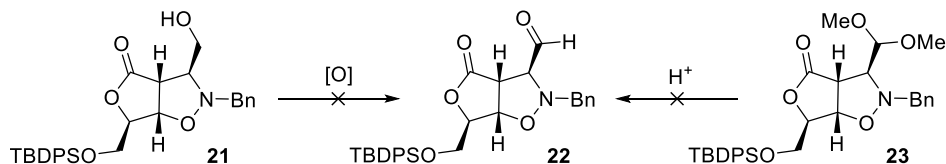
**Scheme 3.** The key-intermediate **16a**, required for the synthesis of Neu5Ac-ABP **5**, was obtained through a nitron-olefin [3+2] cycloaddition, which selectively converted to alcohol **21**.



Reaction conditions: a) ethyl glyoxylate, NaOAc, toluene, MeOH, 3 h, rt, 92%; b) TBDPSCl, imidazole, DMF, -10-20 °C, 4 h, 88%.

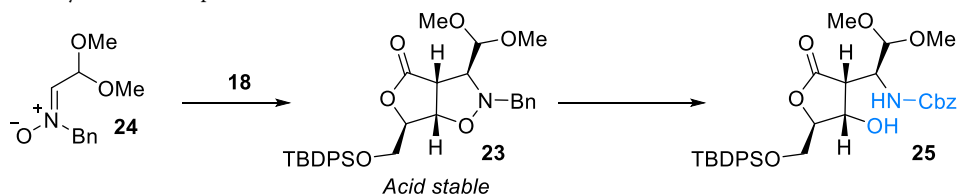
With the first four consecutive chiral centers effectively installed through the optimized cycloaddition reaction, we set out to install the fifth stereogenic center through a Barbier alkylation. This alkylation required converting exocyclic ester **16a** to an aldehyde, which may be obtained through oxidation of the corresponding primary alcohol (**21**). The exocyclic ester **16a** could not be directly reduced towards alcohol **21**, since the lactone is more susceptible towards reducing agents, but the ester could be selectively hydrolyzed. The exocyclic ester **16a** could be hydrolyzed through either basic (LiOH, ≤51% yield) or acidic conditions (HCl, 39% yield), albeit in mediocre yield due to degradation of the TBDPS group. Hydrolysis of ester **16a** under neutral conditions proved more favorable as treatment with Me<sub>3</sub>SnOH gave the corresponding carboxylic acid in almost quantitative yield (Scheme 3). The carboxylic acid could then be reduced by converting this compound *in situ* towards an anhydride with isobutyl chloroformate, followed by reduction with NaBH<sub>4</sub> towards the corresponding primary alcohol **21** in 94% yield over 2 steps. However, converting this alcohol to aldehyde **22** proved to be very difficult. Various attempts were made in oxidizing alcohol **21** towards aldehyde **22**, including Dess-Martin and Swern oxidations (Scheme 4). In addition, attempts were made using PDC, PCC, TEMPO (Anelli's oxidation) and Parikh-Doering oxidation conditions (see Appendix C, Table S1). Nonetheless, no significant aldehyde formation was observed and instead either degradation of **21** or left-over starting material was observed after the reaction.

**Scheme 4.** Aldehyde **22** could not be obtained through oxidation of intermediate **21** or acidic hydrolysis of acetal **23**.



We hypothesized that the inability to oxidize the primary alcohol to an aldehyde might be linked to the close proximity of the of the nitrogen atom in the isoxazolidines-ring. As we reported earlier, a similar isoxazolidines, bearing a masked aldehyde, could not be hydrolyzed under acidic conditions.<sup>46</sup> For example, compound **23** could not be hydrolyzed to aldehyde **22** under acidic conditions. We reasoned that this is due to the close proximity of the isoxazolidines-ring, which might deactivate the acetal, or in this case, the alcohol in oxidative mechanisms towards aldehyde formation. To circumvent this problem, we opted to cleave the N-O ring through hydrogenation. As described in chapter 3, attempts to hydrogenate the isoxazolidine-ring of cycloadduct **16a** were unsuccessful due to the close proximity of two carbonyl-groups that enable  $\beta$ -elimination during the process. We hypothesized that replacing one of the carbonyl groups in the cycloadduct of compound **16a** with an acetal group would prevent significant degradation. To validate that hypothesis we developed novel nitron **24**,<sup>46</sup> which could be transformed into cycloadduct **23** (Scheme 5).

**Scheme 5.** Bicyclic isoxazolidine **23** could be prepared from nitron **24**, which enabled isoxazolidine-ring opening and the synthesis of compound **25**.



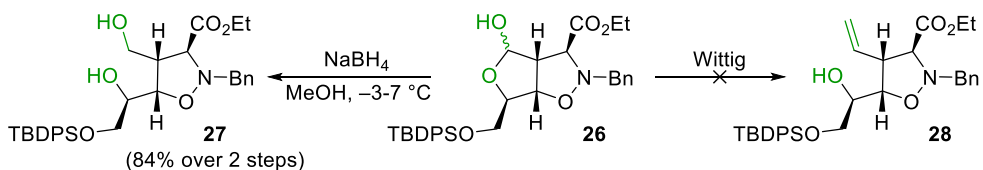
This isoxazolidine, bearing only one carbonyl group was relatively stable upon N-O cleavage through hydrogenation. Indeed, by using a mild one-pot hydrogenation and subsequent protection sequence, compound **25** could be obtained in 45% yield (Scheme 5). In contrast, utilizing the same hydrogenation/protection sequence with compound **16a** resulted in complete degradation (see Appendix C, Table S2). While the opening of the isoxazolidines-ring furnished compound **25** and thereby a potential synthetic pathway towards Neu5Ac-ABP **5**, we ultimately focused on another more promising strategy. In parallel to the cleavage of the N-O bond of the isoxazolidines-ring, the reduction of the lactone of cycloadduct **16a** was studied (Table 1).

**Table 1.** A selection of the different conditions employed of lactone **16a** reduction.

Entry	Reducing agent	Solvent	Temp. (°C)	Combined yield (ratio)
1	DiBALiH	THF	-78	6-52% (1:0)
2	L-selectride	THF	-70	53% (1:0)
3	NaBH <sub>4</sub>	MeOH	20	~30% (0:1)
4	NaBH <sub>4</sub> + ZnCl <sub>2</sub>	MeOH	20	0% (n.a.)
5	BH <sub>3</sub> -SMe <sub>2</sub>	THF	20	93% (84:16)

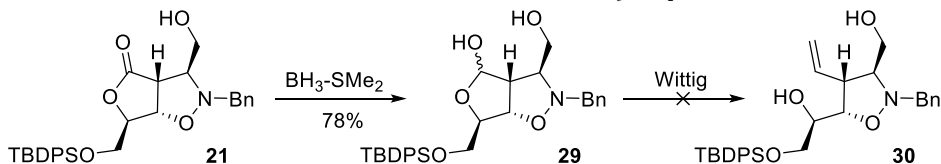
It was observed that the lactone can be selectively reduced in the presence of the exocyclic ester. Still, it proved difficult to find a suitable reducing agent, since the N-O bond was sensitive towards reducing agents, leading to degradation. In addition, when employing DiBAL-H, L-selectride or NaBH<sub>4</sub> as reducing agents, mixtures of starting material, monoreduction towards the hemiacetal, overreduction towards the diol and additional byproducts were observed (Table 1 and Appendix C, Table S3). However, **16a** could be selectively reduced towards hemiacetal **26** in 78% yield by using BH<sub>3</sub>-SMe<sub>2</sub> as the reducing agent, providing diol **27** (16%) as a minor product (entry 5). In addition, diol **27** could be obtained in 84% yield over 2 steps by reducing crude hemiacetal **26** with NaBH<sub>4</sub> in MeOH at 0 °C (Scheme 6).

**Scheme 6.** Hemiacetal **26** could be reduced to diol **27** in very good yield, while Wittig reactions with **26** were unsuccessful.



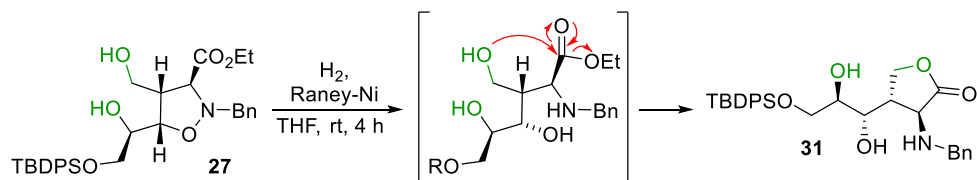
With hemiacetal **26** in hand an attempt was made to convert the hemiacetal to a terminal alkene. However, several attempts to utilize the Wittig reaction – using different bases (KO<sup>t</sup>Bu, *n*BuLi) and phosphonium salts (MeP(Ph)<sub>3</sub>Br & MeP(Ph)<sub>3</sub>I) – were unsuccessful (Scheme 6). Similarly, a Wittig reaction was attempted on hemiacetal **29**, which was obtained through reduction of intermediate **21** with BH<sub>3</sub>-SMe<sub>2</sub> (Scheme 7). However, the Wittig reaction with substrate **29** also led to degradation, similar to the attempts with hemiacetal **26**.

**Scheme 7.** Lactone **21** could be reduced under mild conditions with BH<sub>3</sub>-SMe<sub>2</sub>, but alkene **30** could not be obtained.



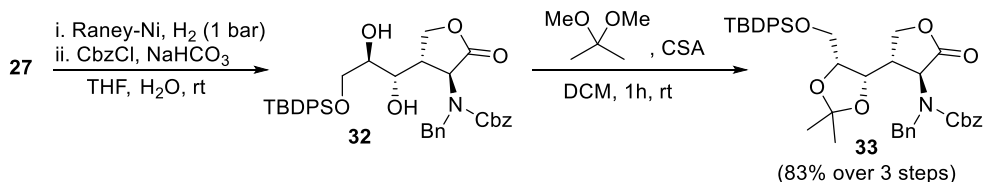
The unsuccessful Wittig reaction in this early stage required a change in strategy. It was therefore decided to focus on cleavage of the N-O bond of intermediate **27**. It was expected that the N-O bond of cycloadduct **27** could be cleaved at this stage even though earlier attempts to open the isoxazolidine-ring were unsuccessful. As we had hypothesized earlier, replacing one of the carbonyl groups may prevent  $\beta$ -elimination during N-O bond cleavage, as exemplified with cycloadduct **23** (Scheme 5). We similarly reasoned that replacing the carbonyl of the lactone would also be beneficial. Indeed, the N-O bond could be selectively cleaved in intermediate **27** by using Raney nickel with atmospheric hydrogen to provide lactone **31** as a result of *in situ* transesterification after hydrogenation of the N-O bond (Scheme 8).

**Scheme 8.** The N-O bond of isoxazolidine **27** can be selectively cleaved with Raney-nickel, followed by transesterification *in situ*, which provides compound **31**.



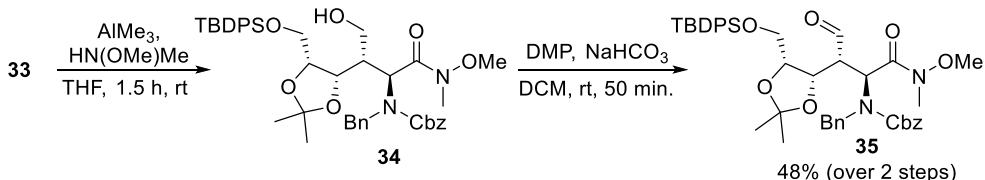
Intermediate **31** could be isolated and purified but it proved to be more efficient to protect this intermediate prior to purification. As such, intermediate **31** was protected *in situ* with Cbz-Cl to mask the secondary amine, followed by the protection of the diol as an isopropylidene acetal using 2,2-dimethoxypropane, affording compound **33** in 83% yield over 3 steps (Scheme 9).

**Scheme 9.** Hydrogenation with Raney-Nickel of diol **27**, followed by *in situ* Cbz-protection and subsequent protection of crude diol **32**, provides intermediate **33** in 83% over 3 steps.



With the now developed efficient methodology - requiring only 2 purifications - to efficiently obtain intermediate **33** from cycloadduct **16a** in hand, our subsequent efforts focused on converting the lactone moiety of compound **33** into Weinreb amide **34**. A first attempt involved a nucleophilic ring opening, using Bodroux conditions. This reaction uses MeO(Me)NH·HCl and an organomagnesium reagent. However, using the conditions for this reaction as reported by Williams et al.<sup>47</sup>, did not provide the desired product. Further efforts to obtain compound **34** focused on conditions using Lewis acids activation of the lactone. It was found that intermediate **33** could be converted efficiently towards compound **34** by using AlMe<sub>3</sub> in combination with MeO(Me)NH·HCl (Scheme 10).

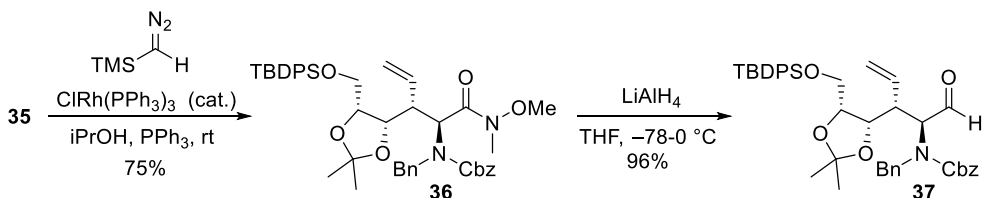
**Scheme 10.** Weinreb **34** could be obtained from lactone **33** by using  $\text{AlMe}_3$  as a Lewis acid. The subsequent oxidation of the primary alcohol provides aldehyde **35** in 48% yield over 2 steps.



However, while compound **34** could be formed it was not possible to purify this compound. Whilst stable on analytical TLC, quantitative cyclization back to the starting material (**33**) was observed during chromatographic purification using various stationary phases (silica, C18, basic alumina). To prevent this cyclization it was decided to omit the purification and perform the subsequent oxidation of the primary alcohol after workup. By oxidizing compound **34** using Dess-Martin periodinane/  $\text{NaHCO}_3$  it was possible to obtain aldehyde **35** in 48% yield over 2 steps together with some recovered **29** (15%) (Scheme 10). Oxidation of crude alcohol **34** using a Swern protocol gave analogous results.

Aldehyde **35** was then used to obtain terminal alkene **36** through a Wittig olefination. Employing standard basic Wittig reaction conditions did indeed yield alkene **36**, albeit in low yield (40%). The low yield and the unreproducible nature of this reaction let us to consider a base-free olefination reaction described by Lebel et al.<sup>48</sup> This rhodium-catalyzed reaction, employing trimethylsilyldiazomethane and triphenylphosphine, produced alkene **36** in good yield (Scheme 11).

**Scheme 11.** A rhodium-catalyzed base-free methylation reaction provides intermediate **36**, which could be reduced to **37**.

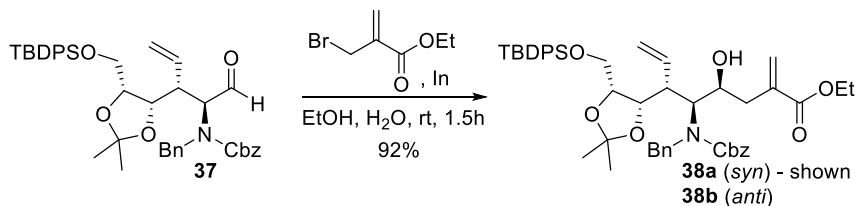


Using this reaction had the added advantage that no extensive efforts had to be made to perform this reaction under anhydrous conditions at low temperatures. Instead this reaction could be performed at room temperature and was generally finished after 75 min, indicated by a reaction mixture that turned dark red accompanied by the sudden rapid evolution of gas ( $\text{N}_2$ ) after circa 1 hour. This relatively stable intermediate **36** was then subjected to  $\text{LiAlH}_4$ , which converted the Weinreb amide to aldehyde **37** in almost quantitative yield (Scheme 11).

Synthesis of aldehyde **37** provided the key precursor to introduce the final portion of the carbon-skeleton and the fifth consecutive chiral center, which could be achieved through a Barbier alkylation. The mild nature of the Barbier alkylation allowed the reaction to be carried out in water and tolerates esters, enabling the direct introduction of a masked carboxylic acid.

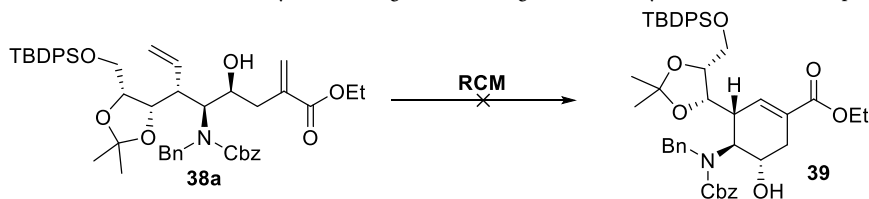
As such, compound **38** could be obtained in 92% yield as a ~3:1 mixture of diastereomers (Scheme 12). Unfortunately, it proved impossible to ascertain the stereochemistry of these two diastereomers due to extensive signal broadening and peak collapsing, preventing complete characterization through NMR. However, this reaction, involving similar substrates, has been reported in a number of cases and typically favors the formation of the *syn*-product, which is the desired stereoisomer in this case.<sup>49-53</sup>

**Scheme 12.** Aldehyde **33** can be successfully alkylated through a Barbier reaction, providing **34** as a diastereomeric mixture.



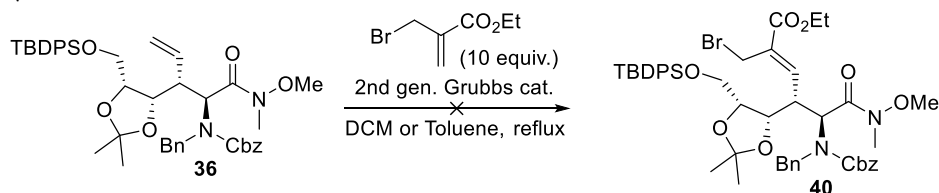
Determining the stereochemistry of compounds **38a-b** may be possible after RCM when a constrained cyclohexene precursor is obtained. It was envisioned that a cyclohexene-precursor could indeed be obtained from diene **38** through a RCM, since RCM reactions involving a conjugated ester diene have been reported in a number of cases.<sup>54-58</sup> Unfortunately, diene **38a** could not be ring-closed to provide cyclohexene **39** using either 2<sup>nd</sup> generation Grubbs catalyst or 2<sup>nd</sup> generation Hoveyda-Grubbs catalyst (Scheme 13).

**Scheme 13.** Diene **38a** could not be cyclized through a RCM using different catalysts, solvents and temperatures.



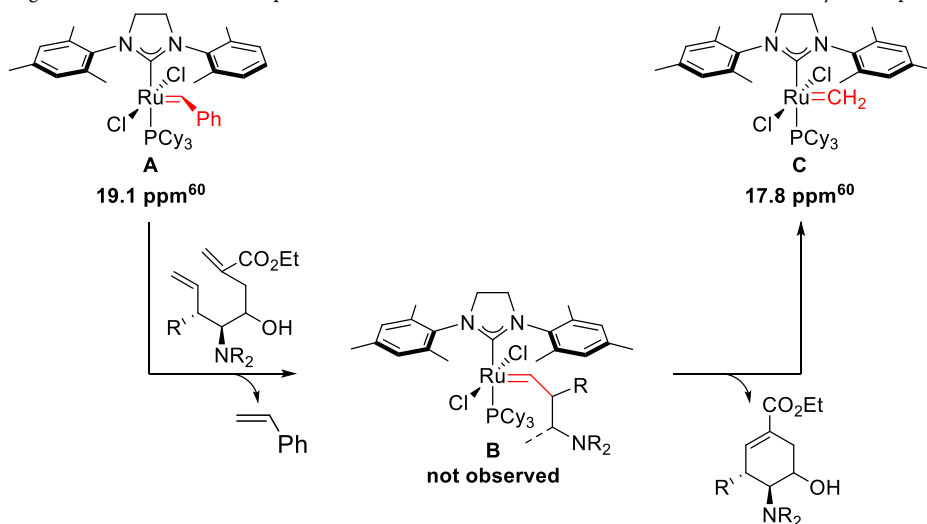
Besides evaluating different catalysts, different solvents ( $\text{DCM}$ ,  $\text{CDCl}_3$ , toluene) and temperatures (20-110 °C) were also screened, but not even trace amounts of compound **39** were observed. Typically, only decomposition pathways were observed, but even those were slow, as compound **38a** was still observed after several days in refluxing toluene. Similarly, a cross-metathesis reaction with intermediate **36** in an attempt to obtain compound **40** - a reaction that is known to be completely *E*-selective<sup>59,60</sup> - did not show significant conversion of the starting material after several days (Scheme 14).

**Scheme 14.** A cross-metathesis reaction attempt with intermediate **36** with a large excess of ethyl 2-(bromomethyl) acrylate.



We hypothesized that the apparent inability of starting materials **36** and **38a** to undergo ring closing metathesis might indicate that the reaction suffers from poor initiation of the RCM catalytic cycle. To validate if poor initiation is really the problem it was necessary to distinguish between two scenarios: one where initiation does not take place, and another where initial initiation takes place but where the ultimately formation of the cyclohexene-ring is the limiting factor (Scheme 15).

**Scheme 15.** 2<sup>nd</sup> Generation Grubbs catalyst (A) and different ruthenium-based catalytic species that are formed during RCM-reactions and the respective low-field <sup>1</sup>H NMR chemical shift of these Ruthenium-alkylidene species.

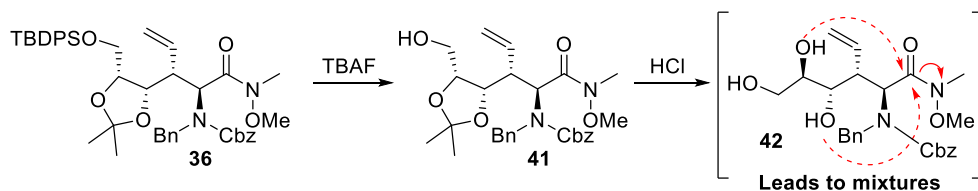


Performing the RCM of **38a** in  $\text{CDCl}_3$  allowed the reaction to be monitored by <sup>1</sup>H NMR, which showed a singlet at 19.1 ppm, corresponding to the benzylidene ( $\text{Ru}=\text{CHPh}$ ) of the 2<sup>nd</sup> generation Grubbs catalyst **A**.<sup>61</sup> Addition of diallyl ether to the reaction mixture containing catalyst **A** and compound **38a**, resulted in the appearance of a singlet peak near 17.8 ppm, corresponding to  $\text{Ru}=\text{CH}_2$ ; the well characterized resting state of the Grubbs catalyst (**C**) after one catalytic cycle.<sup>61</sup> However, no additional Ru-alkylidene peak (**B**) was observed after running the reaction for 75 min at 50 °C. This indicated that the initiation and not necessarily the cyclization itself is the rate-limiting step. We surmised that steric hindrance may prevent initiation. Initiation probably wouldn't take place at the electron-poor conjugated ester olefin, but most likely at the relative electron-rich terminal olefin. This terminal olefin is however,



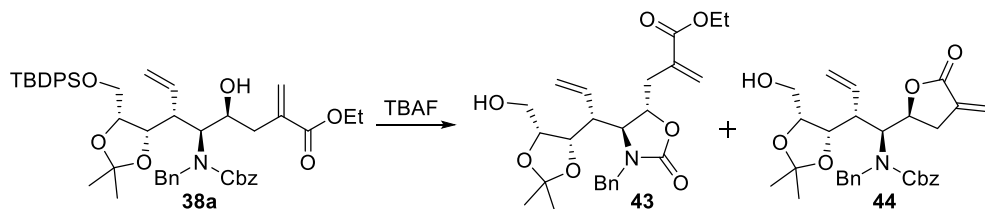
sterically congested due to the close vicinity of multiple protecting groups, among which the bulky TBDPS group. Removing the TBDPS group and the isopropylidene group would decrease the steric hindrance near the terminal alkene for both intermediate **38** and **36**. Accordingly, in a trial experiment intermediate **36** functioned as a model substrate and was subjected to TBAF, which gave crude **41** (Scheme 16). Subjecting this intermediate to acidic conditions did indeed remove the isopropylidene group, but resulted in a complex mixture. Analysis of this mixture showed that byproduct formation mainly results from the previously already observed intramolecular attack of a hydroxyl group with the Weinreb amide as depicted in Scheme 16.

**Scheme 16.** TBDPS-deprotection of intermediate **36**, followed by acid catalyzed acetone deprotection results in a complex mixture due to several transesterification reactions.



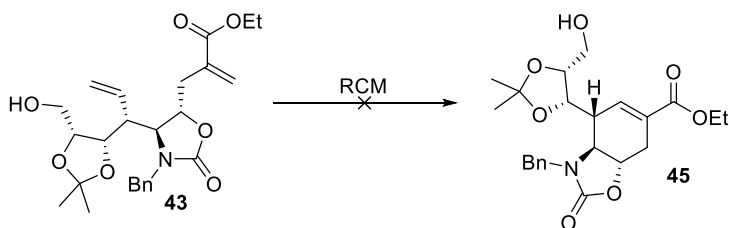
The tendency of intermediate **42** to undergo intramolecular transesterification led us to focus on TBDPS group removal of Barbier product **38a**. However, while the TBDPS group of **38a** was completely removed within 80 min by using TBAF, this resulted in the formation of a number of side products (Scheme 17). Some of these side products could be elucidated and this showed that side product formation, at least partially, resulted from intramolecular transesterification with the ethyl-ester or with the benzyl-carbamate, affording compound **43** and **44**.

**Scheme 17.** The TBAF-mediated TBDPS-deprotection of intermediate **38a** leads to a sideproducts such as **43** and **44**.



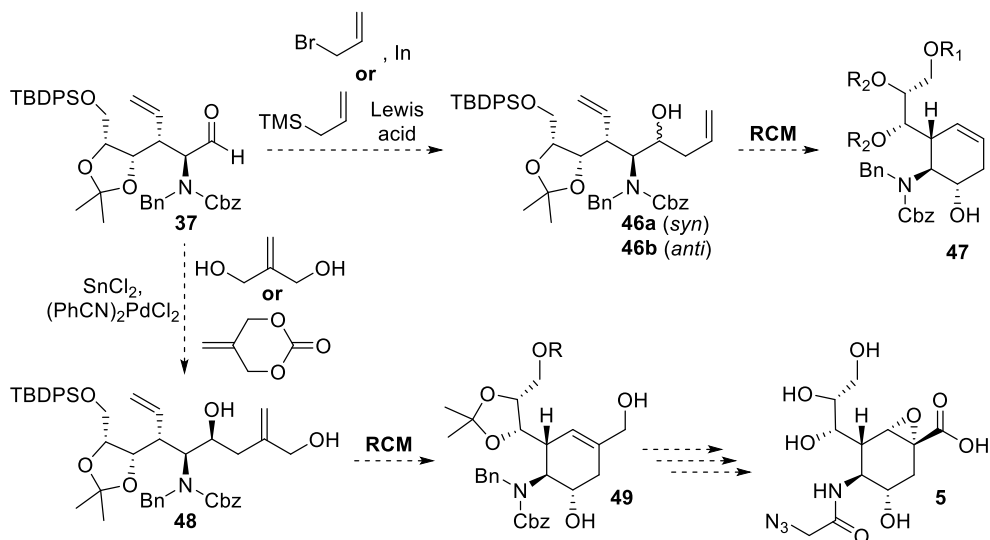
Still, while TBAF deprotection was unselective, it did provide TBDPS-deprotected diene **43**, which could be used in another RCM attempt. Unfortunately, RCM of diene **43** with 2<sup>nd</sup> generation Grubbs catalyst did not provide any detectable (NMR or HRMS) amount of carbocycle **45** (Scheme 18). The failed attempt may be explained by the conformational change imposed by the cyclic carbamate, which positions the two olefins *trans* with respect to each other, which disfavors ring closing. Consequently, while the steric bulk of the TBDPS group was removed, the unfavorable *trans* carbamate may still impede RCM.

**Scheme 18.** A trial attempt at the RCM of TBDPS-protected diene **43** was unsuccessful.



At this point, time constraints prevented further investigation into the development of synthetic pathways towards Neu5Ac-ABP **5**. Further efforts towards the synthesis of this ABP would involve elucidating the aspects that impede successful RCM. Studying this reaction may be aided by investigating a model reaction as depicted in Scheme 19.

**Scheme 19.** Several model reactions to further explore the RCM towards the synthesis of Neu5Ac-ABP **5**.



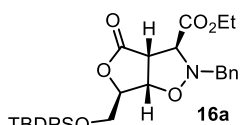
A model reaction would involve the initial alkylation of intermediate **37** with a simple propene-derivative as this would exclude serious electronic effects that could impede with successful RCM. The ring-closing reaction with intermediate **46a** would show if it necessary to perform a deprotection prior to RCM. For example, an unsuccessful RCM with intermediate **46a** would indicate that steric effects impede this reaction, which would mean that the one or more of the sterically demanding protecting groups would have to be removed prior to RCM. On the other hand, a direct successful RCM reaction with intermediate **46a** would indicate that electronic effects of the conjugated ester olefin impede the reaction, necessitating the synthesis of an electron-rich equivalent of intermediate **38a**. Accordingly, the ester of intermediate **38a** may be reduced to the corresponding alcohol **48** or this intermediate may be obtained directly by palladium-catalyzed allylation of intermediate **37** to obtain compound **48** (Scheme 19).<sup>62,63</sup>

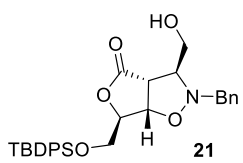
## Conclusion

In this chapter, it is shown that the target linear diene **12** - which possesses five adjacent chiral centers and is a potential key intermediate for the synthesis of target ABP **5** - can be obtained *via* bicyclic compound **16a**. This intermediate is the result of an initial nitrone-olefin [3+2] cycloaddition, which provided a versatile bicyclic intermediate that could be further functionalized. Selective reduction of the lactone of this intermediate enabled further modification to obtain linear diene **38a**. The synthetic route leading to the linear diene was generally high yielding and practical as the synthesis up to diene **38a** required only five purification steps starting from the bicyclic isoxazolidines **16a**. Furthermore, diene **38a** was prepared in an overall yield of 11.3% over 11 steps starting from starting from furanone **18**, which could optionally be prepared from 1,2:5,6-diisopropylidene-D-mannitol in 4 steps (46%). In comparison, the synthesis route developed by Vasella et al. required 18 steps and provided isoCarbaDANA **11** in 1% overall yield.<sup>41</sup> Further developments to obtain target Neu5Ac-ABP **5** would involve finding a synthetic pathway to enable RCM to provide the cyclohexene-ring, followed by the required deprotection steps prior to the final asymmetric Sharpless epoxidation step. The synthesis of Neu5Ac-ABP **5** would then enable the exploration of this ABP as a tool to study the enzymatic activity of neuraminidases, for example in sialidosis.

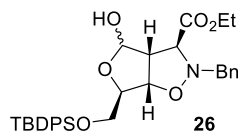
## General Information

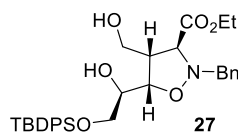
All moisture-sensitive reactions were carried out under an argon atmosphere, using oven-dried glassware, unless otherwise stated. Dichloromethane ( $\text{CH}_2\text{Cl}_2$ , >99.8%) and toluene (>99.8%) were purified over aluminum oxide under argon using a solvent purification system. Reagents were obtained from commercial sources and used without further purification unless stated otherwise. Raney-nickel was purchased from commercial sources (W.R. Grace and Co. Raney<sup>®</sup>; 2800, as a slurry in  $\text{H}_2\text{O}$ ), which was washed with anhydrous THF three times before use. Palladium on carbon (Pd/C) was purchased from commercial sources (10 wt% loading, matrix activated carbon support). Analytical TLC was performed using prepared plates of silica gel (60 F-254 on aluminum) or aluminum oxide (60 Å, F-254 on aluminum) and then, according to the functional groups present on the molecules, revealed with UV light or using staining reagents: ninhydrin (1.5% in *n*-BuOH with 3% AcOH) for amines or basic solution of  $\text{KMnO}_4$  (1.0% in  $\text{H}_2\text{O}$ ) for general staining. Silica gel 60 (70–230 mesh) or aluminum oxide (0.05–0.15 mm particle size, neutral, Brockmann activity grade I) was used for flash chromatography.  $^1\text{H}$  NMR were recorded at 400 and 500 MHz.  $^{13}\text{C}$  NMR spectra were recorded at 100 MHz. Chemical shifts are reported in parts per million (ppm), calibrated on the residual peak of the solvent, whose values are referred to tetramethylsilane (TMS,  $\delta_{\text{TMS}} = 0$ ) as the internal standard or the signal of the deuterated solvent.  $^{13}\text{C}$  NMR spectra were performed with proton decoupling. Where indicated, NMR peak assignments were made using COSY and HSQC experiments. Electrospray ionization (ESI) mass analyses were performed on a mass spectrometer with a linear ion trap mass analyzer, while high-resolution ESI mass analyses were recorded on a Orbitrap high-resolution mass spectrometer. Infrared analyses were performed on a FT-IR spectrometer. Optical rotations were measured on a polarimeter (sodium D line,  $\lambda = 589 \text{ nm}$ ).

 **16a** **Ethyl (3aR,6R,6aS)-2-benzyl-6-(((tert-butyl)diphenylsilyl)oxy)methyl)-4-oxohexahydrofuro[3,4-d]isoxazole-3-carboxylate (16a).** A solution of nitrone **3a** (0.333 g, 1.61 mmol, 1.14 equiv) in toluene (9 mL) was heated to 40 °C for 2 hours, followed by the addition of furanone **2** (0.498 g, 1.41 mmol, 1.0 equiv) and additional toluene (3 mL). The reaction mixture was heated to reflux for 4 hours and then conc. *in vacuo*. The residue was purified via column chromatography (5–15% EtOAc in petroleum ether 40–60) afforded **16a** as a yellow oil (563 mg, 68%)  $R_f = 0.52$  (8:2; PE:EtOAc) and **16b** (154 mg, 20%) as a yellow oil.  $R_f = 0.44$  (8:2; PE:EtOAc). NMR signals of the major adduct **16a anti**:  $^1\text{H}$  NMR (400 MHz, Chloroform-*d*)  $\delta$  7.68 – 7.55 (m, 4H), 7.51 – 7.23 (m, 11H), 4.87 (d,  $J = 6.3 \text{ Hz}$ , 1H), 4.56 (d,  $J = 2.1 \text{ Hz}$ , 1H), 4.26 (q,  $J = 7.2$ , 2H), 4.20 (s, 1H), 4.14 – 4.06 (m, 2H), 3.95 (s, 1H), 3.90 (dd,  $J = 11.6$ , 2.4 Hz, 1H), 3.73 (dd,  $J = 11.6$ , 1.9 Hz, 1H), 2.05 (s, 1H), 1.31 (t,  $J = 7.2 \text{ Hz}$ , 3H), 1.04 (s, 9H). NMR signals of the major adduct **16b syn**:  $^1\text{H}$  NMR (400 MHz, Chloroform-*d*)  $\delta$  7.66 – 7.54 (m, 4H), 7.48 – 7.27 (m, 11H), 4.91 (dd,  $J = 7.6$ , 1.7 Hz, 1H), 4.56 (q,  $J = 2.1 \text{ Hz}$ , 1H), 4.35 – 4.24 (m, 3H), 3.92 – 3.76 (m, 3H), 3.76 – 3.66 (m, 2H), 1.34 (t,  $J = 7.1 \text{ Hz}$ , 3H), 1.02 (s, 9H). <sup>a</sup>NMR signals in accordance with NMR spectra by Ondruš et al.<sup>64</sup>

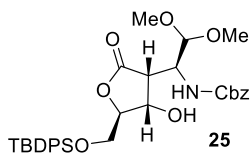
 **21** **(3S,3aR,6R,6aS)-2-Benzyl-6-(((tert-butyl)diphenylsilyl)oxy)methyl)-3-(hydroxymethyl)tetrahydrofuro[3,4-d]isoxazol-4(2H)-one (21).** To a solution of ester **16a** (0.443 g, 0.736 mmol, 1.0 equiv) in 1,2-dichloroethane (11 mL) was added  $\text{Me}_3\text{SnOH}$  (0.540 g, 2.99 mmol, 4.06 equiv). The resulting suspension was heated to reflux for 2.5 h and then concentrated under a  $\text{N}_2$

stream and then dissolved in EtOAc (50 mL). The organic layer was washed with 1M aq. HCl (5 mL, 2×), brine (5 mL), dried (MgSO<sub>4</sub>) and then conc. *in vacuo*, affording crude carboxylic acid **S1**, which was used without further purification. A small sample of crude **S1** was purified by flash column chromatography (5% MeOH in DCM) to obtain an analytically pure sample.  $R_F$  = 0.43 (10% MeOH in DCM). <sup>1</sup>H NMR (400 MHz, Chloroform-*d*)  $\delta$  7.62 (ddd,  $J$  = 8.0, 2.6, 1.5 Hz, 4H), 7.49 – 7.30 (m, 11H), 4.83 (d,  $J$  = 6.5 Hz, 1H), 4.74 – 4.59 (m, 1H), 4.26 – 4.15 (m, 3H), 4.09 (d,  $J$  = 13.1 Hz, 1H), 3.92 (dd,  $J$  = 11.6, 2.6 Hz, 1H), 3.76 (dd,  $J$  = 11.6, 1.9 Hz, 1H), 1.04 (s, 9H). HRMS calcd for C<sub>30</sub>H<sub>32</sub>O<sub>6</sub>NSi + H<sup>+</sup> [M-H<sup>+</sup>]: 530.2004 Found 530.1997. Crude **S1** was dissolved in dry THF (18 mL) and added to a flame-dried 3-neck round-bottom flask and cooled to –15 °C. To this solution was added isobutyl chloroformate (1.07 g, 7.82 mmol, 10.0 equiv), followed by the dropwise addition of a suspension of NaBH<sub>4</sub> (0.297 g, 7.85 mmol, 10.0 equiv) in DMF (7.0 mL) over 10 minutes. The resulting reaction mixture was stirred at –15 °C for 75 min and then quenched with 1M aq. HCl (25 mL). The reaction mixture was extracted with EtOAc (75 mL, 25 mL, 2×). The combined organic layers were washed with brine (25 mL), dried (MgSO<sub>4</sub>) and conc. *in vacuo*. The residue was purified by flash column chromatography (20–30% EtOAc in petroleum ether 40–60), affording compound **21** (385 mg, 94% over 2 steps) as a yellow oil, which crystallized upon standing.  $R_F$  = 0.32 (7:3; PE:EtOAc). mp = 109–110 °C. <sup>1</sup>H NMR (400 MHz, Chloroform-*d*)  $\delta$  7.67 – 7.58 (m, 4H), 7.50 – 7.37 (m, 6H), 7.37 – 7.27 (m, 5H), 4.73 (d,  $J$  = 6.5 Hz, 1H), 4.59 (t,  $J$  = 2.2 Hz, 1H), 4.12 – 4.00 (m, 2H), 3.91 (dd,  $J$  = 11.5, 2.5 Hz, 1H), 3.74 (dd,  $J$  = 11.6, 1.9 Hz, 1H), 3.72 – 3.62 (m, 3H), 3.44 (q,  $J$  = 3.8 Hz, 1H), 2.17 (s, 1H), 1.04 (s, 9H). <sup>13</sup>C NMR (101 MHz, CDCl<sub>3</sub>)  $\delta$  177.5, 136.5, 135.7, 135.6, 132.5, 132.0, 130.3, 130.2, 129.0, 128.7, 128.1, 128.1, 128.0, 83.0, 81.0, 70.6, 64.0, 62.2, 61.6, 52.8, 26.9, 19.2. FT-IR (neat):  $\nu$  = 3282, 2931, 2859, 1775, 1427 cm<sup>–1</sup>. HRMS calcd for C<sub>30</sub>H<sub>35</sub>O<sub>5</sub>NSi + Na<sup>+</sup> [M+Na<sup>+</sup>]: 540.2177 Found 540.2162.  $[\alpha]_D^{20}$  = –32.0 ( $c$  = 0.40, CHCl<sub>3</sub>).

 **Ethyl (3S,3aR,6R,6aS)-2-benzyl-6-(((tert-butyl)diphenylsilyl)oxy)methyl-4-hydroxyhexahydrofuro[3,4-d]isoxazole-3-carboxylate (26).** To a round-bottom flask containing cycloadduct **16a** (0.404 g, 0.722 mmol, 1.0 equiv) at 4 °C was added a cold (4 °C) 2M solution of BH<sub>3</sub>·SMe<sub>2</sub> in THF (4.00 mL, 8.00 mmol, 11.1 equiv). The mixture was allowed to warm to room temperature and stirred for 3.5 hours and quenched by carefully adding MeOH (0.30 mL). The mixture was concentrated *in vacuo* to afford the crude as a mixture of compound **26** and **27** (0.392 g) as a colorless oil, which was generally used to obtain compound **27** without further purification. Optionally, the crude could be purified by flash column chromatography (30–50% EtOAc in petroleum ether 40–60), affording an anomeric mixture of hemiacetal **26** (320 mg, 78%) as a colorless oil (HRMS calcd for C<sub>32</sub>H<sub>39</sub>O<sub>6</sub>NSi + Na<sup>+</sup> [M+Na<sup>+</sup>]: 584.2439 Found 584.2429)  $R_F$  = 0.57 (7:3; PE:EtOAc) and diol **27** (60 mg, 16%) as a colorless oil.

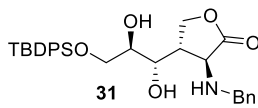
 **Ethyl (3S,4S,5S)-2-benzyl-5-((R)-2-(((tert-butyl)diphenylsilyl)oxy)-1-hydroxyethyl)-4-(hydroxymethyl)isoxazolidine-3-carboxylate (27).** Hemiacetal **26** (0.100 g, 162  $\mu$ mol, 1.0 equiv) was dissolved in MeOH (3.0 mL) and cooled to –2 °C, NaBH<sub>4</sub> (13.5 mg, 0.357 mmol, 2.0 equiv) was added and the resulting solution was then stirred at –3–7 °C for 1 h. Additional NaBH<sub>4</sub> (3.4 mg, 0.5 equiv) was added and the reaction mixture was stirred for an additional 40 min, followed by the portion-wise addition of 1M aq. HCl (10 mL). The reaction mixture was extracted with EtOAc (10 mL, 3×) and the combined organic layers were washed with sat. aq. NaHCO<sub>3</sub> solution (10 mL) and brine (10 mL). Then it was dried over MgSO<sub>4</sub> and concentrated *in vacuo*. The resulting oil was purified by flash column chromatography (30–50% EtOAc in petroleum ether 40–60), affording diol **27** (87.2 mg, 87%) as a

colorless oil.  $R_f$  = 0.27 (7:3; PE:EtOAc).  $^1\text{H}$  NMR (400 MHz, Chloroform- $d$ )  $\delta$  7.64 (ddt,  $J$  = 9.8, 6.8, 1.5 Hz, 4H), 7.50 – 7.30 (m, 6H), 7.24 (s, 5H), 4.18 (dd,  $J$  = 9.3, 7.1 Hz, 1H), 4.09 (q,  $J$  = 7.1 Hz, 2H), 3.99 (d,  $J$  = 13.2 Hz, 1H), 3.96 – 3.87 (m, 3H), 3.83 (dd,  $J$  = 10.5, 3.2 Hz, 1H), 3.76 – 3.63 (m, 3H), 3.28 (d,  $J$  = 4.6 Hz, 1H), 3.24 – 3.13 (m, 1H), 3.10 (d,  $J$  = 7.7 Hz, 1H), 1.22 (t,  $J$  = 7.2 Hz, 3H), 1.06 (s, 9H).  $^{13}\text{C}$  NMR (101 MHz,  $\text{CDCl}_3$ )  $\delta$  170.1, 135.8, 135.7, 135.6, 133.0, 132.7, 130.1, 130.1, 129.7, 128.3, 128.0, 127.7, 78.3, 69.8, 65.5, 62.3, 61.6, 60.6, 52.1, 27.0, 19.4, 14.2. FT-IR (neat):  $\nu$  = 3385, 2931, 2857, 1738, 1472, 1428  $\text{cm}^{-1}$ . HRMS calcd for  $\text{C}_{32}\text{H}_{41}\text{O}_6\text{NSi} + \text{H}^+ [\text{M}+\text{H}^+]$ : 564.2776 Found 564.2766.  $[\alpha]_{\text{D}}^{20}$  = -22.7 ( $c$  = 1.00,  $\text{CHCl}_3$ ).



**Benzyl ((*S*)-1-((3*R*,4*S*,5*R*)-5-(((*tert*-butyldiphenylsilyl)oxy)methyl)-4-hydroxy-2-oxotetrahydrofuran-3-yl)-2,2-dimethoxyethyl)carbamate (25).** A solution of cycloadduct **23** (0.124 g, 0.221 mmol, 1.00 equiv) in dry THF (1.0 mL) was added to a round-bottom flask containing Raney-nickel (0.400 gr). The reaction mixture was placed under and hydrogen atmosphere

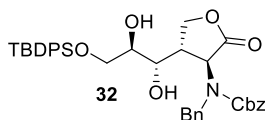
(1 bar; balloon) and stirred vigorously for 5 h. TLC indicated incomplete conversion at this point so the reaction mixture was transferred to a round-bottom flask containing fresh Raney-nickel (0.500 gram) and stirred under an hydrogen atmosphere (1 bar; balloon) for an additional 2 hours. The reaction mixture was then placed under an argon atmosphere (1 bar) and Pd/C (0.100 gram) was added, followed by cyclohexene (2.5 mL). The resulting mixture was heated to reflux for 3 h and then cooled to 4 °C. Finally,  $\text{H}_2\text{O}$  (0.6 mL),  $\text{NaHCO}_3$  (74 mg, 0.883 mmol, 4.00 equiv) and  $\text{CbzCl}$  (0.094 mL, 0.662 mmol, 3.00 equiv) were added sequentially and the resulting reaction mixture was stirred for 14 h, while allowing the mixture to warm to room temperature. The reaction mixture was filtered over Celite, the celite was subsequently washed with THF and the combined filtrate conc. *in vacuo*. The resulting residue was purified by flash column chromatography (20-30% EtOAc in petroleum ether 40-60), affording compound **25** (60.5 mg, 45%) as a yellow oil.  $R_f$  = 0.23 (7:3; PE:EtOAc).  $^1\text{H}$  NMR (400 MHz, Chloroform- $d$ )  $\delta$  7.73 – 7.55 (m, 4H), 7.50 – 7.29 (m, 11H), 5.68 (d,  $J$  = 8.4 Hz, 1H), 5.25 – 5.03 (m, 3H), 4.69 (d,  $J$  = 2.5 Hz, 1H), 4.48 (dd,  $J$  = 5.3, 2.5 Hz, 1H), 4.43 (t,  $J$  = 2.5 Hz, 1H), 4.30 (td,  $J$  = 8.5, 2.4 Hz, 1H), 3.89 (dd,  $J$  = 11.8, 2.9 Hz, 1H), 3.77 (dd,  $J$  = 11.7, 2.1 Hz, 1H), 3.50 (s, 3H), 3.47 (s, 3H), 3.45 – 3.39 (m, 1H), 1.02 (s, 9H).  $^{13}\text{C}$  NMR (101 MHz,  $\text{CDCl}_3$ )  $\delta$  175.2, 157.8, 136.0, 135.8, 135.6, 132.6, 132.0, 130.2, 128.7, 128.5, 128.3, 128.0, 103.5, 85.3, 71.8, 67.6, 63.9, 57.0, 56.9, 50.5, 47.9, 26.8, 19.2. HRMS calcd for  $\text{C}_{33}\text{H}_{41}\text{O}_8\text{NSi} + \text{Na}^+ [\text{M}+\text{Na}^+]$ : 630.2494 Found 630.2483.



**(3*S*,4*S*)-3-(Benzylamino)-4-((1*S*,2*R*)-3-(((*tert*-butyldiphenylsilyl)oxy)-1,2-dihydroxypropyl)dihydrofuran-2(3*H*)-one (31).** To a roundbottom flask containing Raney-Ni (12.0 gram), washed beforehand with dry THF (2 $\times$ ), was added a solution of diol **27** (6.12 g, 9.39 mmol, 1.00 equiv) in THF

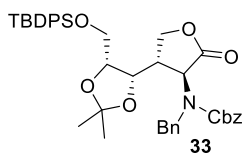
(90 mL). The resulting mixture was vigorously stirred under an  $\text{H}_2$  atmosphere (balloon) for 4 hours. Conversion to compound **31** was monitored by  $^1\text{H}$  NMR by taking a small sample which, after conc. *in vacuo*, indicated complete conversion. TLC-analysis is not recommended. The  $\text{H}_2$  atmosphere was replaced with an argon atmosphere and the next reaction step was generally carried out *in situ*. Optionally, the crude could be purified by filtering the reaction mixture over a Celite plug and the resulting filtrate was conc. *in vacuo*. The crude compound can then be purified by means of flash column chromatography (3 % MeOH and 1%  $\text{Et}_3\text{N}$  in DCM) to afford compound **31** as an amorphous white solid.  $^1\text{H}$  NMR (400MHz,  $\text{CDCl}_3$ ):  $\delta$  7.66 - 7.57 (m, 4H), 7.46 - 7.32 (m, 6H), 7.31 - 7.17 (m, 5H), 4.50 (dd,  $J$  = 9.6, 8.1 Hz, 1H), 4.18 (d,  $J$  = 11.9 Hz, 1H), 4.10 (t,  $J$  = 10.1 Hz, 1H), 3.87 (dd,  $J$  = 10.3, 4.4 Hz,

1H), 3.81 - 3.69 (m, 3H), 3.68 - 3.54 (m, 1H), 3.48 (d,  $J = 11.8$  Hz, 1H), 2.58 (ddt,  $J = 11.9, 10.5, 8.1$  Hz, 1H), 1.03 (s, 9H);  $^{13}\text{C}$ -NMR (101MHz,  $\text{CDCl}_3$ ):  $\delta$  177.3 (C=O), 138.3, 135.8, 132.4, 130.6, 129.0, 128.3, 128.1, 77.9, 72.3, 68.7, 68.4, 58.20, 50.7, 46.9, 27.1, 19.42; HRMS calcd for  $\text{C}_{30}\text{H}_{37}\text{NO}_5\text{Si} + \text{H}^+$  [ $\text{M} + \text{H}^+$ ]: 520.2514 Found 520.2487.



**Benzyl benzyl((3S,4S)-4-((1S,2R)-3-((tert-butyldiphenylsilyl)oxy)-1,2-dihydroxypropyl)-2-oxotetrahydrofuran-3-yl)carbamate (32).** As

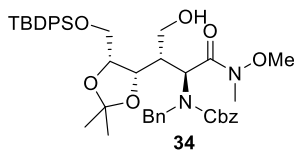
mentioned before, compound **32** was typically prepared by converting freshly prepared lactone **31** *in situ* towards compound **32**. To a roundbottom flask containing Raney-Ni (12.0 gr), washed beforehand with dry THF (2 $\times$ ), was added a solution of diol **27** (6.12 g, 9.39 mmol, 1.00 equiv) in THF (90 mL). The resulting mixture was vigorously stirred under an  $\text{H}_2$  atmosphere (balloon) for 4 hours. Conversion to compound **31** was monitored by  $^1\text{H}$  NMR by taking a small sample which, after conc. *in vacuo*, indicated complete conversion. TLC-analysis is not recommended. The  $\text{H}_2$  atmosphere was replaced with an argon atmosphere and  $\text{H}_2\text{O}$  (48 mL),  $\text{NaHCO}_3$  (2.9 g, 34.5 mmol 3.67 equiv) and  $\text{CbzCl}$  (4.95 mL, 34.6 mmol, 3.69 equiv) were sequentially added. The resulting reaction mixture was stirred for 18 hours, followed by the addition of sat. aq.  $\text{NaHCO}_3$  (150 mL). The mixture was pulled over a Celite plug, which was then washed with additional THF. To the resulting filtrate was added EtOAc (500 mL) and the biphasic system was separated. The water-layer was extracted with EtOAc (250 mL, 200 mL) and the combined organic layers were washed with brine (200 mL), dried ( $\text{MgSO}_4$ ) and conc. *in vacuo*, affording 8.49 gram of a dark pink oil, which was generally used without further purification. Optionally, the crude could be purified by flash column chromatography (10 $\rightarrow$ 30% EtOAc in PE) to yield compound **32** as a white amorphous solid.  $R_f = 0.23$  (7:3; PE:EtOAc).  $^1\text{H}$  NMR (400 MHz,  $\text{CDCl}_3$ ):  $\delta$  7.62 (d,  $J = 7.4$  Hz, 4H), 7.53 - 7.11 (m, 18H), 5.19 (s, 2H), 4.79 (d,  $J = 15.4$  Hz, 1H), 4.71 (d,  $J = 5.6$  Hz, 1H), 4.48 (d,  $J = 15.9$  Hz, 1H), 4.26 (t,  $J = 8.6$  Hz, 1H), 4.22 - 4.07 (m, 1H), 4.03 (d,  $J = 9.3$  Hz, 1H), 3.67 - 3.50 (m, 1H), 3.30 (d,  $J = 41.3$  Hz, 2H), 3.06 (s, 1H), 2.72 (s, 1H), 1.06 (s, 9H);  $^{13}\text{C}$ -NMR (101MHz,  $\text{CDCl}_3$ ):  $\delta$  = 173.24, 156.82, 137.7, 135.5, 132.6, 130.2, 128.7, 128.6, 128.3, 128.2, 128.1, 128.0, 127.9, 127.8, 72.0, 68.3, 67.3, 65.0, 57.3, 56.9, 50.2, 41.9, 41.7, 29.7, 26.9, 19.2, 14.2; LRMS calcd for  $\text{C}_{38}\text{H}_{43}\text{NO}_7\text{Si} + \text{Na}^+$  [ $\text{M} + \text{Na}^+$ ]: 676.27 Found 676.50. \*NMR characterization suffered from peak broadening and peak splitting due to the formation of rotamers.



**Benzyl benzyl((3S,4S)-4-((4S,5R)-5-(((tert-butyldiphenylsilyl)oxy)methyl)-2,2-dimethyl-1,3-dioxolan-4-yl)-2-oxotetrahydrofuran-3-yl)carbamate (33).** Crude compound **32** was dissolved in DCM (25 mL), followed by the addition of 2,2-dimethoxypropane (5.55 mL, 45.3 mmol, 4.8 equiv) and camphorsulfonic acid (42.0 mg, 0.181 mmol, 0.019 equiv). The

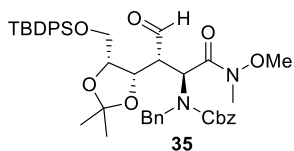
resulting reaction mixture was stirred for 80 min and then conc. *in vacuo*, affording an orange oil. The crude oil was purified by flash column chromatography (10 $\rightarrow$ 20 EtOAc in petroleum ether 40-60), affording compound **33** (5.46 g, 84% over 3 steps). \*  $R_f = 0.70$  (7:3; PE:EtOAc).  $^1\text{H}$  NMR (400MHz,  $\text{CDCl}_3$ ):  $\delta$  7.60 - 7.44 (m, 4H), 7.43 - 7.17 (m, 16H), 5.21 - 5.08 (m, 2H), 4.85 (d,  $J = 15.5$  Hz, 1H), 4.32 (d,  $J = 15.4$  Hz, 1H), 4.21 - 3.77 (m, 4H), 3.56 - 3.48 (m, 1H), 3.20 - 3.02 (m, 2H), 1.27 - 1.03 (m, 6H), 0.96 (d,  $J = 6.9$  Hz, 9H);  $^{13}\text{C}$ -NMR (101MHz,  $\text{CDCl}_3$ ):  $\delta$  173.24, 156.82, 137.74, 135.49, 132.60, 130.15, 128.74, 128.6, 128.3, 128.2, 128.1, 128.0, 127.9, 127.8, 72.0, 68.3, 67.3, 65.0, 57.3, 56.9, 50.2, 41.9, 41.7, 29.7, 26.9, 19.2, 14.2. FT-IR (neat):  $\nu = 2932, 2858, 1782, 1700, 1497, 1456, 1427\text{ cm}^{-1}$ . LRMS calcd. for  $\text{C}_{41}\text{H}_{47}\text{NO}_7\text{Si} + \text{Na}^+$  [ $\text{M} + \text{Na}^+$ ]: 716.30. Found: 716.50. \*NMR characterization suffered from peak broadening and peak splitting due to the formation of rotamers.





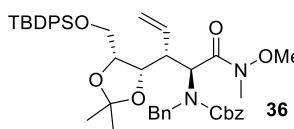
**Benzyl benzyl((2S,3S)-3-(((4S,5R)-5-(((tert-butyl)diphenylsilyl)oxy)methyl)-2,2-dimethyl-1,3-dioxolan-4-yl)-4-hydroxy-1-(methoxy(methyl)amino)-1-oxobutan-2-yl)carbamate (34).** A suspension of (MeO)NHMe.HCl (0.433 g, 4.44 mmol, 3.08 equiv) in dry DCM (7.5 mL) was cooled to  $-78^{\circ}\text{C}$ , followed by the dropwise addition

of a solution of 2M  $\text{AlMe}_3$  in toluene (2.2 mL, 4.40 mmol, 3.06 equiv) over 5 min. The reaction mixture was allowed to warm to  $-30^{\circ}\text{C}$  over 75 min. The reaction mixture was cooled to  $-40^{\circ}\text{C}$  and a solution of compound **33** in dry DCM (5 mL) was added dropwise over 5 min. The resulting reaction mixture was stirred at  $-40^{\circ}\text{C}$  for 20 minutes. The cooling bath was removed and the reaction mixture was allowed to warm to room temperature and stirred for 165 min and then poured in 50 mL sat. potassium sodium tartrate (50 mL). The resulting mixture was filtered over a plug of Celite, which was washed with additional DCM (75 mL). The resulting biphasic system was separated and the water layer was extracted with DCM (50 mL, 25 mL). The combined organic layers were dried ( $\text{MgSO}_4$ ) and conc. *in vacuo*, affording crude **34**,  $R_f = 0.20$  (7:3; PE:EtOAc), which was used without further purification.



**Benzyl benzyl((2S,3R)-3-(((4S,5R)-5-(((tert-butyl)diphenylsilyl)oxy)methyl)-2,2-dimethyl-1,3-dioxolan-4-yl)-1-(methoxy(methyl)amino)-1,4-dioxobutan-2-yl)carbamate (35).** Crude **34** was dissolved in DCM (30 mL) and cooled to  $0^{\circ}\text{C}$ , followed by the addition of  $\text{NaHCO}_3$  (1.93 g, 16 equiv) and Dess-Martin periodinane (1.23 g, 2.90 mmol, 2.0

equiv). The reaction mixture was stirred at  $0^{\circ}\text{C}$  for 55 min and was then diluted with  $\text{Et}_2\text{O}$  (100 mL) and poured in sat. aq.  $\text{NaHCO}_3$  containing 12 gram  $\text{Na}_2\text{S}_2\text{O}_3$  (75 mL). This biphasic system was stirred at rt for 5 min, followed by the separation of the layers. The water layer was extracted with  $\text{Et}_2\text{O}$  (3 $\times$ 100 mL) and the combined organic layers were washed with brine (80 mL), dried ( $\text{MgSO}_4$ ) and conc. *in vacuo*. The residue was purified by flash column chromatography (12 $\rightarrow$ 30% EtOAc in petroleum ether 40-60), affording compound **35** (572 mg, 48% over 2 steps; 63% brsm) as a yellow oil. \*  $R_f = 0.61$  (7:3; PE:EtOAc).  $^1\text{H}$  NMR (400 MHz, Chloroform- $d$ )  $\delta$  9.71 (s, 1H), 7.75 – 7.59 (m, 4H), 7.49 – 7.03 (m, 17H), 5.73 (d,  $J = 11.2$  Hz, 1H), 5.26 (dd,  $J = 12.4, 2.9$  Hz, 1H), 5.21 – 5.05 (m, 1H), 4.49 (d,  $J = 15.4$  Hz, 1H), 4.43 – 4.26 (m, 1H), 4.20 (d,  $J = 6.5$  Hz, 1H), 4.17 – 3.94 (m, 2H), 3.79 – 3.63 (m, 4H), 3.42 (s, 2H), 2.76 (d,  $J = 6.9$  Hz, 3H), 1.27 (d,  $J = 16.0$  Hz, 4H), 1.17 (d,  $J = 20.1$  Hz, 4H), 1.09 (d,  $J = 7.8$  Hz, 9H).  $^{13}\text{C}$ -NMR (101MHz,  $\text{CDCl}_3$ ):  $\delta$  200.8, 200.6, 169.4, 169.1, 157.0, 156.4, 137.9, 137.8, 136.4, 136.3, 136.2, 136.0, 135.8, 135.7, 132.9, 132.9, 132.8, 130.1, 130.0, 128.5, 128.3, 128.2, 128.1, 128.0, 127.9, 127.9, 127.4, 127.3, 127.1, 108.7, 77.1, 77.0, 74.1, 74.0, 68.1, 68.0, 63.0, 62.8, 61.8, 61.4, 53.9, 49.1, 48.8, 47.2, 47.0, 31.9, 27.3, 27.1, 26.9, 26.8, 24.6, 19.3. FT-IR (neat):  $\nu = 2934, 2860, 1698, 1660, 1428, 1411\text{ cm}^{-1}$ . HRMS calcd for  $\text{C}_{43}\text{H}_{54}\text{N}_2\text{O}_8\text{Si} + \text{Na}^+$  [ $\text{M} + \text{Na}^+$ ]: 777.3547. Found 777.3519. \*NMR characterization suffered from peak broadening and peak splitting due to the formation of rotamers.



**Benzyl benzyl((2S,3R)-3-(((4S,5R)-5-(((tert-butyl)diphenylsilyl)oxy)methyl)-2,2-dimethyl-1,3-dioxolan-4-yl)-1-(methoxy(methyl)amino)-1-oxopent-4-en-2-yl)carbamate (36).** To a red solution of  $\text{RhCl}(\text{PPh}_3)_3$  (22.5 mg, 0.0243 mmol, 0.06 equiv),  $\text{PPh}_3$  (239 mg, 0.911 mmol, 2.25 equiv) and 2-propanol (73.0  $\mu\text{L}$ , 0.953 mmol, 2.35 equiv) in

dry THF (1.3 mL) was added a solution of aldehyde **35** (304 mg, 0.405 mmol, 1.00 equiv) in dry THF (4.3 mL). To the resulting light orange solution was added dropwise a solution of  $\text{TMSCHN}_2$  (2M in  $\text{Et}_2\text{O}$ , 0.60 mL, 3.0 equiv). The reaction mixture was stirred at rt for 1.5. [Precipitation and gas-evolution

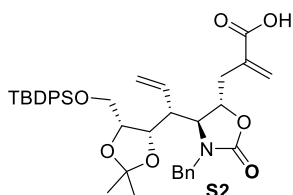


started to occur after circa 1 h and TLC-analysis indicated complete conversion after 75 min.] H<sub>2</sub>O (60 mL) and DCM (60 mL) were added to the reaction mixture and the resulting biphasic system was separated. The water layer was extracted with DCM (2×50mL) and the combined organic layers were washed with brine (40 mL), dried (MgSO<sub>4</sub>) and conc. *in vacuo*. The residue was purified by flash column chromatography (10→20% EtOAc in heptane [crude applied to column as a mixture in DCM/heptane], affording compound **36** (237 mg, 75%) as a yellow oil.\*  $R_F = 0.34$  (8:2; PE:EtOAc). <sup>1</sup>H NMR (400MHz, CDCl<sub>3</sub>): δ 7.73 - 7.53 (m, 5H), 7.50 - 6.95 (m, 17H), 5.87 - 5.65 (m, 1H), 5.56 + 5.38 (2xd, J = 11.2 Hz, 1H), 5.25 - 4.87 (m, 4H), 4.86 - 4.28 (m, 2H), 4.18 - 3.80 (m, 2H), 3.76 - 3.48 (m, 3H), 3.38 - 2.99 (m, 3H), 2.77 (d, J = 44.7 Hz, 3H), 1.32 (s, 3H), 1.15 (s, 3H), 1.02 (d, J = 10.1 Hz, 9H). <sup>13</sup>C-NMR (101MHz, CDCl<sub>3</sub>): δ 168.5, 155.4, 137.0, 134.1, 132.0, 128.1, 126.8, 126.6, 126.4, 126.2, 125.4, 118.9, 106.3, 76.4, 72.4, 66.3, 61.3, 60.3, 53.9, 45.4, 39.6, 30.4, 25.4, 23.1, 17.7. LRMS calcd for C<sub>44</sub>H<sub>54</sub>N<sub>2</sub>O<sub>7</sub>Si+Na<sup>+</sup> [M+Na<sup>+</sup>]: 773.36. Found 773.50. \*NMR characterization suffered from peak broadening and peak splitting due to the formation of rotamers.

**37** **Benzyl benzyl((2S,3R)-3-(((4S,5R)-5-(((tert-butylidiphenylsilyl)oxy)methyl)-2,2-dimethyl-1,3-dioxolan-4-yl)-1-oxopent-4-en-2-yl)carbamate (37).** A roundbottom flask containing Weinreb amine **36** (219 mg 0.292 mmol, 1.00 equiv) and a stirring bar was co-evaporated with dry toluene (3×). The flask was put under argon and dry THF (7.0 mL) and molsieves 3Å were added. The solution was cooled to -78 °C, followed by the dropwise addition of 1M LiAlH<sub>4</sub> (333 μL, 1.14 equiv). The roundbottom flask was then put in an ice bath and stirred at 0 °C for 20 min. Finally, the reaction mixture was cooled to -78 °C and then quenched by the rapid addition of sat. aq. NH<sub>4</sub>Cl (2.0 mL), followed by the addition of EtOAc (10 mL). The mixture was allowed to warm to room temperature and then stirred at rt for 30 min. Finally, H<sub>2</sub>O (10 mL) and additional EtOAc (20 mL) were added and the biphasic system was separated. The water layer was extracted with EtOAc (20 mL, 2×) and the combined organic layers were washed with sat. aq. NaHCO<sub>3</sub> (15 mL), brine (15 mL), dried (MgSO<sub>4</sub>) and conc. *in vacuo*, affording pure aldehyde **37** (194 mg, 96%) as a yellow oil.\*  $R_F = 0.53$  (15% Et<sub>2</sub>O in PE). <sup>1</sup>H NMR (400 MHz, Chloroform-*d*) δ 9.55 (s, 1H), 9.27 (s, 1H), 7.77 - 7.54 (m, 5H), 7.52 - 7.15 (m, 20H), 5.98 - 5.75 (m, 1H), 5.23 - 4.78 (m, 6H), 4.39 - 4.12 (m, 3H), 3.97 - 3.84 (m, 1H), 3.83 - 3.59 (m, 2H), 3.49 (d, J = 4.7 Hz, 2H), 1.42 (s, 3H), 1.30 (s, 3H), 1.07 (s, 9H). <sup>13</sup>C NMR (101 MHz, CDCl<sub>3</sub>) δ 197.6, 197.2, 156.0, 137.3, 136.2, 135.8, 135.7, 135.3, 133.6, 133.4, 129.8, 129.8, 128.7, 128.7, 128.6, 128.4, 128.3, 128.2, 128.1, 128.0, 127.8, 127.8, 127.7, 127.0, 120.5, 108.0, 78.5, 74.8, 68.1, 67.9, 67.5, 62.7, 53.1, 42.4, 42.0, 27.1, 27.0, 26.7, 24.7, 19.3. FT-IR (neat): ν = 2932, 2858, 1731, 1697, 1497, 1456, 1427 cm<sup>-1</sup>. HRMS calcd for C<sub>42</sub>H<sub>49</sub>NO<sub>6</sub>Si+Na<sup>+</sup> [M+Na<sup>+</sup>]: 714.3221. Found 714.3196. \*NMR characterization suffered from peak broadening and peak splitting due to the formation of rotamers.

**38a,b** **Ethyl (5S,6R)-5-(benzyl((benzyloxy)carbonyl)amino)-6-(((4S,5R)-5-(((tert-butylidiphenylsilyl)oxy)methyl)-2,2-dimethyl-1,3-dioxolan-4-yl)-4-hydroxy-2-methyleneoct-7-enoate (38).** To a solution of aldehyde **37** (378 mg, 0.547 mmol, 1.00 equiv) in a mixture of EtOH (9.0 mL) and H<sub>2</sub>O (1.0 mL) at 0 °C was added ethyl-2-(bromomethyl)acrylate (227 μL, 1.64 mmol, 3.00 equiv) and indium powder (157 mg, 1.37 mmol, 2.50 equiv). The resulting mixture was stirred under argon for 5 min and then sonicated at 20-35 °C for 45 min. During the sonication process the indium, initially a fine powder, started to form grey lumps. Conversion to compound **38** was monitored by TLC ( $R_F$

aldehyde **37** = 0.44;  $R_f$  compound **38** = 0.32, in 15% EtOAc in PE, KMnO<sub>4</sub> stain), and shown to be incomplete (~90%). Accordingly, additional indium powder (44.0 mg, 0.383 mmol, 0.70 equiv) was added to the reaction mixture, which was then sonicated for an additional 75 min, after which TLC indicated complete conversion. The reaction mixture was conc. *in vacuo*, and co-evaporated with toluene to remove the remaining water. EtOAc was then added and the suspension was filtered over a thin layer of Celite and washed with additional EtOAc. The collected eluent was conc. *in vacuo*, affording an orange oil, which was purified by flash column chromatography (14→20% EtOAc in petroleum ether 40-60), affording compound **38** (408 mg, 92%, d.r. = ~3:1) as a partially separated mixture of diastereomers of major compound **38a** and minor compound **38b**. \*NMR signals and other experimental data of the major adduct **38a**:  $R_f$  = 0.22 (15% Et<sub>2</sub>O in PE). <sup>1</sup>H NMR (500 MHz, Chloroform-*d*)  $\delta$  7.65 (dd,  $J$  = 12.4, 6.9 Hz, 4H, ArH), 7.48 – 7.14 (m, 16H, ArH), 6.08 (s, 1H, H-12a), 5.90 – 5.70 (m, 1H, H-10), 5.39 (s, 1H, H-12b), 5.35 – 5.16 (m, 2H, Cbz-CH<sub>2</sub>), 5.16 – 4.88 (m, 3H, H-11, BnCH<sub>2</sub>), 4.88 – 4.67 (m, 1H, Bn-CH<sub>2</sub>), 4.41 – 4.36 (m, 1H, H-5), 4.15 – 4.10 (m, 2H, H-13), 4.10 – 4.04 (m, 2H, H-7), 4.02 – 3.89 (m, 1H, H-4), 3.81 – 3.67 (m, 2H, H-8), 3.57 (dd,  $J$  = 10.5, 7.2 Hz, 1H, H-9), 3.53 – 3.38 (m, 1H, H-9, H-6), 2.93 (t,  $J$  = 10.3 Hz, 1H, H-6), 1.36 – 1.30 (m, 3H, CCH<sub>3</sub>), 1.28 – 1.14 (m, 5H, OCH<sub>2</sub>CH<sub>3</sub> & CCH<sub>3</sub>), 1.10 – 1.02 (m, 9H, *t*Bu). <sup>13</sup>C NMR (101 MHz, CDCl<sub>3</sub>)  $\delta$  167.5, 167.1, 158.6, 157.7, 139.8, 137.8, 137.6, 137.2, 136.3, 136.1, 136.0, 135.8, 135.8, 135.7, 134.7, 133.7, 129.8, 129.7, 129.6, 128.8, 128.7, 128.6, 128.5, 128.5, 128.4, 128.1, 128.0, 127.9, 127.9, 127.8, 127.8, 127.7, 127.7, 127.3, 126.8, 120.6, 119.3, 107.8, 107.6, 78.7, 78.4, 75.7, 75.3, 75.0, 70.4, 68.5, 68.1, 67.8, 66.7, 63.0, 62.9, 61.2, 61.0, 60.4, 55.1, 48.4, 42.4, 41.8, 38.3, 37.5, 29.8, 27.1, 26.8, 26.7, 24.8, 19.3, 14.3, 14.2. FT-IR (neat):  $\nu$  = 2932, 2858, 1731, 1697, 1497, 1456, 1427 cm<sup>-1</sup>. HRMS calcd for C<sub>48</sub>H<sub>59</sub>NO<sub>8</sub>Si+Na<sup>+</sup> [M+Na<sup>+</sup>]: 828.3902. Found 828.3881. \*NMR characterization suffered from peak broadening and peak splitting due to the formation of rotamers. Minor compound **38b**:  $R_f$  = 0.14 (15% Et<sub>2</sub>O in PE).



**2-(((4*S*,5*S*)-3-Benzyl-4-((*R*)-1-(((4*S*,5*R*)-5-(((*tert*-butyldiphenylsilyl)oxy)methyl)-2,2-dimethyl-1,3-dioxolan-4-yl)allyl)-2-oxo-oxazolidin-5-yl)methyl)acrylic acid (**S2**).** To a solution of compound **38a** in EtOH (1.0 mL) at 0 °C was added 5N aq. NaOH (0.2 mL). The reaction mixture stirred at rt and monitored by TLC analysis. TLC analysis showed complete disappearance of starting material within 2 min to an intermediate, which all but disappeared within 45 min. After

stirring for 1.5 h the reaction was quenched by the addition of sat. aq. NH<sub>4</sub>Cl (10 mL). The resulting mixture was extracted with EtOAc (10 mL, 5 mL, 2×). The combined organic layers were washed with sat. aq. NaHCO<sub>3</sub> (8.0 mL), brine (8.0 mL), dried (MgSO<sub>4</sub>) and conc. *in vacuo*, affording crude **S2**. \*  $R_f$  = 0.29 (6:4; PE:EtOAc). <sup>1</sup>H NMR (400 MHz, Chloroform-*d*)  $\delta$  7.68 – 7.58 (m, 4H), 7.51 – 7.14 (m, 11H), 6.28 (s, 1H), 5.98 – 5.82 (m, 1H), 5.42 (s, 1H), 5.18 (t,  $J$  = 10.0 Hz, 2H), 5.03 – 4.86 (m, 2H), 4.79 (td,  $J$  = 6.8, 2.6 Hz, 1H), 4.27 (td,  $J$  = 7.5, 5.3 Hz, 1H), 4.03 (dd,  $J$  = 7.1, 1.6 Hz, 1H), 3.97 – 3.84 (m, 2H), 3.77 (ddd,  $J$  = 10.5, 5.5, 2.3 Hz, 1H), 3.52 – 3.45 (m, 1H), 3.23 (dt,  $J$  = 4.8, 3.0 Hz, 1H), 2.85 – 2.74 (m, 1H), 2.60 (dd,  $J$  = 13.8, 6.4 Hz, 1H), 2.25 (dd,  $J$  = 13.8, 6.8 Hz, 1H), 1.38 (s, 3H), 1.27 (s, 3H), 1.11 (s, 9H). HRMS calcd for C<sub>48</sub>H<sub>59</sub>NO<sub>8</sub>Si+Na<sup>+</sup> [M+Na<sup>+</sup>]: 692.3014. Found 692.3000. \*Tentative NMR-spectra derived from a crude sample.

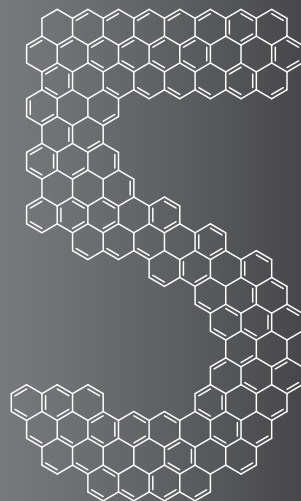
## References

1. Bonten, E., van der Spoel, A., Fornerod, M., Grosveld, G., and d'Azzo, A. *Genes & development* **1996**, *10*, 3156.
2. Pshezhetsky, A.V., Richard, C., Michaud, L., Igdoura, S., Wang, S., Elsliger, M.A., Qu, J., Leclerc, D., Gravel, R., Dallaire, L., and Potier, M. *Nature genetics* **1997**, *15*, 316.
3. Monti, E., Preti, A., Rossi, E., Ballabio, A., and Borsani, G. *Genomics* **1999**, *57*, 137.
4. Monti, E., Bassi, M.T., Papini, N., Riboni, M., Manzoni, M., Venerando, B., Croci, G., Preti, A., Ballabio, A., Tettamanti, G., and Borsani, G. *Biochem. J* **2000**, *349*, 343.
5. Monti, E., Bassi, M.T., Bresciani, R., Civini, S., Croci, G.L., Papini, N., Riboni, M., Zanchetti, G., Ballabio, A., Preti, A., Tettamanti, G., Venerando, B., and Borsani, G. *Genomics* **2004**, *83*, 445.
6. Yamaguchi, K., Hata, K., Koseki, K., Shiozaki, K., Akita, H., Wada, T., Moriya, S., and Miyagi, T. *Biochem. J* **2005**, *390*, 85.
7. Cantz, M., Gehler, J., and Spranger, J. *Biochem. Biophys. Res. Commun.* **1977**, *74*, 732.
8. Bonten, E.J., Arts, W.F., Beck, M., Covanis, A., Donati, M.A., Parini, R., Zammarchi, E., and d'Azzo, A. *Human molecular genetics* **2000**, *9*, 2715.
9. Seyrantepe, V., Poupetova, H., Froissart, R., Zobot, M.T., Maire, I., and Pshezhetsky, A.V. *Human mutation* **2003**, *22*, 343.
10. d'Azzo, A., Machado, E., and Annunziata, I. *Expert opinion on orphan drugs* **2015**, *3*, 491.
11. Caciotti, A., Di Rocco, M., Filocamo, M., Grossi, S., Traverso, F., d'Azzo, A., Cavicchi, C., Messeri, A., Guerrini, R., Zammarchi, E., Donati, M.A., and Morrone, A. *Journal of Neurology* **2009**, *256*, 1911.
12. Barton, N.W., Brady, R.O., Dambrosia, J.M., Di Bisceglie, A.M., Doppelt, S.H., Hill, S.C., Mankin, H.J., Murray, G.J., Parker, R.I., Argoff, C.E., and et al. *The New England journal of medicine* **1991**, *324*, 1464.
13. Grabowski, G.A., Barton, N.W., Pastores, G., Dambrosia, J.M., Banerjee, T.K., McKee, M.A., Parker, C., Schiffmann, R., Hill, S.C., and Brady, R.O. *Annals of internal medicine* **1995**, *122*, 33.
14. O'Leary, E.M. and Igdoura, S.A. *Molecular genetics and metabolism* **2012**, *107*, 173.
15. Bonten, E.J., Yogalingam, G., Hu, H., Gomero, E., van de Vlekkert, D., and d'Azzo, A. *Biochimica et Biophysica Acta (BBA) - Molecular Basis of Disease* **2013**, *1832*, 1784.
16. Steet, R.A., Chung, S., Wustman, B., Powe, A., Do, H., and Kornfeld, S.A. *Proc. Natl. Acad. Sci. USA* **2006**, *103*, 13813.
17. Kornhaber, G.J., Tropak, M.B., Maegawa, G.H., Tuske, S.J., Coales, S.J., Mahuran, D.J., and Hamuro, Y. *ChemBioChem* **2008**, *9*, 2643.
18. Shen, J.S., Edwards, N.J., Hong, Y.B., and Murray, G.J. *Biochem. Biophys. Res. Commun.* **2008**, *369*, 1071.
19. Yu, Z., Sawkar, A.R., Whalen, L.J., Wong, C.-H., and Kelly, J.W. *J. Med. Chem.* **2007**, *50*, 94.
20. Witte, M.D., Kallemeijn, W.W., Aten, J., Li, K.-Y., Strijland, A., Donker-Koopman, W.E., van den Nieuwendijk, A.M.C.H., Bleijlevens, B., Kramer, G., Florea, B.I., Hooibrink, B., Hollak, C.E.M., Ottenhoff, R., Boot, R.G., van der Marel, G.A., Overkleeft, H.S., and Aerts, J.M.F.G. **2010**, *6*, 907.
21. van der Horst, G.T., Mancini, G.M., Brossmer, R., Rose, U., and Verheijen, F.W. *J. Biol. Chem.* **1990**,

- 265, 10801.
22. Lu, C.-P., Ren, C.-T., Lai, Y.-N., Wu, S.-H., Wang, W.-M., Chen, J.-Y., and Lo, L.-C. *Angew. Chem. Int. Ed.* **2005**, *44*, 6888.
23. Tsai, C.S., Yen, H.Y., Lin, M.I., Tsai, T.I., Wang, S.Y., Huang, W.I., Hsu, T.L., Cheng, Y.S.E., Fang, J.M., and Wong, C.H. *Proc. Natl. Acad. Sci. USA* **2013**, *110*, 2466.
24. Agard, N.J., Prescher, J.A., and Bertozzi, C.R. *J. Am. Chem. Soc.* **2004**, *126*, 15046.
25. Dommerholt, J., van Rooijen, O., Borrmann, A., Guerra, C.F., Bickelhaupt, F.M., and van Delft, F.L. *Nat. Commun.* **2014**, *5*.
26. Debets, M.F., van Berkel, S.S., Schoffelen, S., Rutjes, F.P.J.T., van Hest, J.C.M., and van Delft, F.L. *Chem. Commun.* **2010**, *46*, 97.
27. Yao, J.Z., Uttamapinant, C., Poloukhtine, A., Baskin, J.M., Codelli, J.A., Sletten, E.M., Bertozzi, C.R., Popik, V.V., and Ting, A.Y. *J. Am. Chem. Soc.* **2012**, *134*, 3720.
28. Voadlo, D.J., Hang, H.C., Kim, E.-J., Hanover, J.A., and Bertozzi, C.R. *Proceedings of the National Academy of Sciences* **2003**, *100*, 9116.
29. Kele, P., Li, X., Link, M., Nagy, K., Herner, A., Lorincz, K., Beni, S., and Wolfbeis, O.S. *Org. Biomol. Chem.* **2009**, *7*, 3486.
30. Willems, L.I., Li, N., Florea, B.I., Ruben, M., van der Marel, G.A., and Overkleef, H.S. *Angew. Chem. Int. Ed.* **2012**, *51*, 4431.
31. Laughlin, S.T., Baskin, J.M., Amacher, S.L., and Bertozzi, C.R. *Science* **2008**, *320*, 664.
32. Voadlo, D.J. and Davies, G.J. *Curr. Opin. Chem. Biol.* **2008**, *12*, 539.
33. Koshland, D.E. *Biol. Rev.* **1953**, *28*, 416.
34. Stick, R.V. and Williams, S.J., *Carbohydrates: The Essential Molecules of Life (Second Edition)*. Elsevier/ Oxford, **2009**.
35. Watts, A.G., Damager, I., Amaya, M.L., Buschiazzi, A., Alzari, P., Frasch, A.C., and Withers, S.G. *J. Am. Chem. Soc.* **2003**, *125*, 7532.
36. Watts, A.G., Oppezzo, P., Withers, S.G., Alzari, P.M., and Buschiazzi, A. *J. Biol. Chem.* **2006**, *281*, 4149.
37. Watts, A.G. and Withers, S.G. *Can. J. Chem.* **2004**, *82*, 1581.
38. von Itzstein, M., Wu, W.Y., Kok, G.B., Pegg, M.S., Dyason, J.C., Jin, B., Phan, T.V., Smythe, M.L., White, H.F., Oliver, S.W., Colman, P.M., Varghese, J.N., Ryan, D.M., Woods, J.M., Bethell, R.C., Hotham, V.J., Cameron, J.M., and Penn, C.R. *Nature* **1993**, *363*, 418.
39. Taylor, N.R. and Vonitzstein, M. *J. Med. Chem.* **1994**, *37*, 616.
40. Smith, B.J., Colman, P.M., Von Itzstein, M., Danylec, B., and Varghese, J.N. *Protein Sci.* **2001**, *10*, 689.
41. Vorwerk, S. and Vasella, A. *Angew. Chem. Int. Edit.* **1998**, *37*, 1732.
42. Ondruš, V., Orság, M., Fišera, L.u., and Prónayová, N.a. *Tetrahedron* **1999**, *55*, 10425.
43. Nguyen, T.B., Martel, A., Dhal, R., and Dujardin, G. *Synthesis* **2009**, *2009*, 3174.
44. Ghosh, A.K., Leshchenko, S., and Noetzel, M. *J. Org. Chem.* **2004**, *69*, 7822.
45. Schmid, C.R., Bryant, J.D., Dowlatzedah, M., Phillips, J.L., Prather, D.E., Schantz, R.D., Sear, N.L., and Vianco, C.S. *J. Org. Chem.* **1991**, *56*, 4056.

46. Hoogenboom, J., Zuilhof, H., and Wennekes, T. *Org. Lett.* **2015**, 17, 5550.
47. Williams, J.M., Jobson, R.B., Yasuda, N., Marchesini, G., Dolling, U.-H., and Grabowski, E.J.J. *Tetrahedron Lett.* **1995**, 36, 5461.
48. Lebel, H. and Paquet, V. *J. Am. Chem. Soc.* **2004**, 126, 320.
49. Matthies, S., Stallforth, P., and Seeberger, P.H. *J. Am. Chem. Soc.* **2015**, 137, 2848.
50. Chng, S.-S., Hoang, T.-G., Wayne Lee, W.-W., Tham, M.-P., Ling, H.Y., and Loh, T.-P. *Tetrahedron Lett.* **2004**, 45, 9501.
51. Chan, T.-H. and Lee, M.-C. *J. Org. Chem.* **1995**, 60, 4228.
52. Chappell, M.D. and Halcomb, R.L. *Org. Lett.* **2000**, 2, 2003.
53. Steurer, S. and Podlech, J. *Eur. J. Org. Chem.* **1999**, 1551.
54. Hyldtoft, L. and Madsen, R. *J. Am. Chem. Soc.* **2000**, 122, 8444.
55. Oh, H.-S. and Kang, H.-Y. *J. Org. Chem.* **2012**, 77, 8792.
56. Tripathi, S., Shaikh, A.C., and Chen, C. *Org. Biomol. Chem.* **2011**, 9, 7306.
57. Grim, J.C., Garber, K.C.A., and Kiessling, L.L. *Org. Lett.* **2011**, 13, 3790.
58. Kancharla, P.K., Doddi, V.R., Kokatla, H., and Vankar, Y.D. *Tetrahedron Lett.* **2009**, 50, 6951.
59. Nagata, K., Itoh, T., Fukuoka, H., Nakamura, S., and Ohsawa, A. *Heterocycles* **2005**, 65, 1283.
60. Aouzal, R. and Prunet, J. *Org. Biomol. Chem.* **2009**, 7, 3594.
61. Nelson, D.J., Carboni, D., Ashworth, I.W., and Percy, J.M. *J. Org. Chem.* **2011**, 76, 8386.
62. Kang, S.-K., Park, D.-C., Park, C.-H., and Jang, S.-B. *Synth. Commun.* **1995**, 25, 1359.
63. Masuyama, Y., Kagawa, M., and Kurusu, Y. *Chem. Commun.* **1996**, 1585.
64. Ondruš, V., Orság, M., Fišera, L.u., and Prónayová, N.a. *Tetrahedron* **1999**, 55, 10425.

## Chapter 5



# Synthesis and Evaluation of Locostatin-Based Chemical Probes towards PEBP-Proteins

## Abstract

Phosphatidyl ethanolamine-binding proteins (PEBPs) are implicated in various critical physiological processes in all eukaryotes. Among them is FLOWERING LOCUS T (FT), the protein recently discovered as the vital flowering hormone in plants. Small molecule inhibitors and activators of FT could provide control over plant flowering and are therefore an interesting target for industrial agriculture. No small molecule inhibitors or activators are known for FT, but for a structurally similar PEBP, RKIP, an inhibitor called locostatin has been reported to covalently bind in the RKIP ligand binding pocket. Herein, we report the synthesis of novel locostatin-based chemical PEBP probes and evaluate their ability and selectivity towards the binding of FT and RKIP.

Part of this work was published in:

J. Hoogenboom, M. Fiers, R. Immink, H. Zuilhof, T. Wennekes,  
*Tetrahedron Lett.*, **2016**, 57, 2406

## Introduction

The phosphatidyl ethanolamine-binding protein (PEBP) family comprises over 400 members from a variety of organisms, including plants, bacteria, yeast and mammals.<sup>1</sup> The PEBP family is thus a highly conserved group of proteins, that fulfill a plethora of different functions. Recently, a new functional addition to the PEBP family was made due to the search towards ‘florigen’. Florigen is a crucial, long sought substance that relays a signal from the leaves to the growing tip of a plant, known as the shoot apical meristem, to induce flowering. The extensive hunt for florigen has led to the discovery of FLOWERING LOCUS T (FT) as the flowering inducing agent belonging to the PEBP family of proteins in the model plant *Arabidopsis thaliana*.<sup>2,3</sup> As a PEBP, FT also possesses the two notable features common to all PEBPs, namely (1) a compact globular structure, which provides ample surface area for interaction with other proteins and (2) a ligand binding pocket.<sup>1</sup> The crystal structures of PEBPs from rat, human, bovine and plant material reveal the evolutionary highly conserved nature of the PEBP ligand binding pocket.<sup>4</sup> For example, the very similar spatial arrangement of the amino acid residues in the ligand binding pocket of the FT-like protein Centrodialis (CEN) from Antirrhinum and bovine PEBP (bPEBP) is depicted in Figure 1.

The ligand binding pocket in FT is interesting as a potential target for the development of small molecules that can activate or inhibit the functioning of FT. In view of the importance of FT as the key flowering-inducing protein, the applications for such compounds in plant science and industry are obvious.

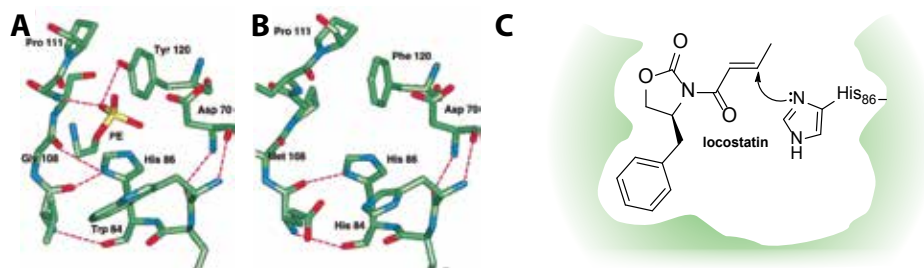


**Figure 1.** Top: conserved residues of the PEBP ligand binding pocket in crystal structure of bPEBP (A) with bound phosphoryl group (PE) and FT-like protein CEN (B).<sup>5</sup> (C) Putative binding mechanism of locostatin in the ligand binding pocket of the PEBP, RKIP.<sup>10,17</sup>

Currently, no small molecule inhibitor is known that can selectively bind FT. In contrast, several small molecule inhibitors have been identified for the Raf Kinase Inhibitory Protein (RKIP), a structurally similar mammalian PEBP. RKIP has been well studied as a potential therapeutic target involved in pathophysiological processes including diabetic nephropathy,<sup>6</sup> Alzheimer's disease<sup>7-9</sup> and immunotherapy against human cancer.<sup>10-13</sup> The extensive study of RKIP has also led to the discovery of locostatin (Figure 1), named after its ability to inhibit cellular locomotion in multiple systems.<sup>10</sup> Besides claims about its potential therapeutic value,<sup>10-12, 14-16</sup> locostatin's mode of action has been reported to involve covalent and irreversible

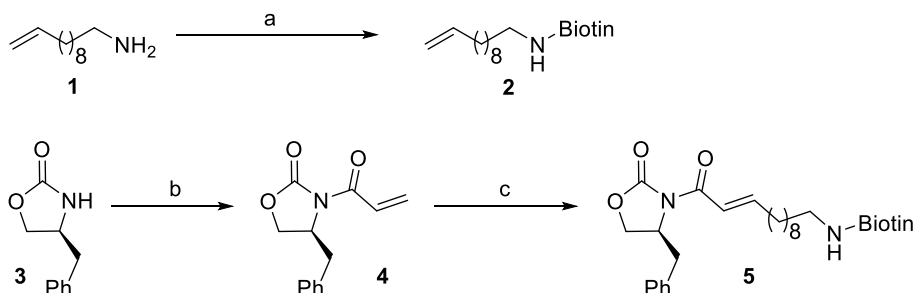


binding of the RKIP ligand binding pocket.<sup>10,14,17</sup> The pocket contains a highly conserved histidine residue (His86) that was reported to act as a nucleophile on the Michael acceptor in locostatin<sup>17</sup> and which is also present in bPEBP, CEN and FT (Figure 1). Because of this conservation and the overall structural similarity of the binding pocket, we hypothesized that FT might also be covalently bound by locostatin in a similar fashion and block the mode of action of FT, and hence influence flowering. We therefore set out to investigate if locostatin affects the flowering-inducing properties of FT and by developing a set of novel locostatin-based chemical probes, if it selectively binds FT in its ligand binding pocket.

We started by studying the effect of locostatin on the flowering time of *Arabidopsis thaliana* Col0. We initially tested different concentrations of locostatin and noticed that this compound is toxic for Arabidopsis at higher concentrations (Appendix D, Figure S1). Based on this pilot experiment a 25  $\mu$ M locostatin solution in H<sub>2</sub>O was used in a flowering time experiment. Although here we found some very early flowering plants, no significant flowering stimulating or repressing activity was observed at population level (Appendix D, Figure S2). The only significant effect was that locostatin negatively affected root development of the plants (Appendix D, Figure S1). It is improbable that locostatin is affecting the roots due to interaction with FT, since the FT gene is not expressed in roots.<sup>18</sup> A saturated version of locostatin did not have a significant effect on the root development (Appendix D, Figure S3), indicating the crucial role of the reactive Michael acceptor of locostatin for its activity.

Despite the fact that no FT-related phenotypes could be observed in the plants treated with locostatin, we decided to investigate whether FT can be targeted by locostatin, based on the conservation of the PEBP ligand binding pocket and previous binding studies for locostatin and RKIP.<sup>10,14,17</sup> In order to visualize the covalent modification of FT by locostatin, novel chemical probe analogues of locostatin were designed. We aimed to modify the Michael acceptor tail of locostatin, since it has been previously reported for RKIP that this part of locostatin remains covalently bound to the PEBP protein, while the oxazolidinone-moiety may dissociate over time through hydrolysis.<sup>17</sup> In addition, a structure-activity relationship study of locostatin with RKIP has shown that structural modification of this part is tolerated.<sup>10</sup>

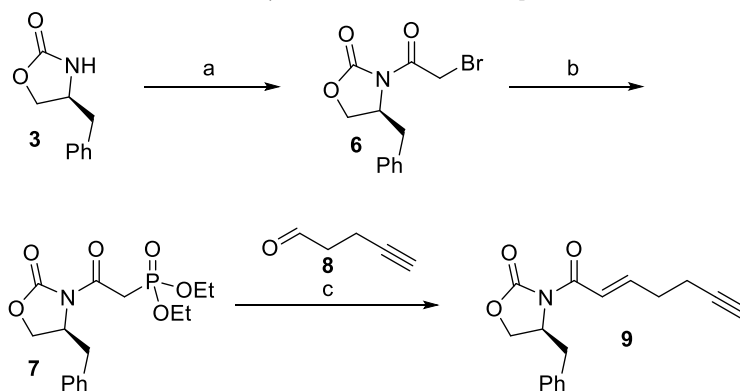
**Scheme 1.** Synthesis of locostatin-probe 5



Reaction conditions: a) EDC, HOBT, D-Biotin, DMF, rt, 1 d, 85%; b) *n*-BuLi, acryloyl chloride, THF,  $-78^{\circ}\text{C}$ , 1 h, 17%; c) 2, Hg-II, AcOH,  $40^{\circ}\text{C}$ , 1 d, 26%.

We aimed to synthesize target locostatin-based chemical probe **5** by starting with commercially available 1-amino-10-undecene **1**, which was coupled to biotin in good yield (Scheme 1). The resulting alkene **2** was then reacted with known compound **4** *via* a cross-metathesis reaction. Initial attempts to carry out this reaction with the 2<sup>nd</sup> generation Grubbs catalyst were unsuccessful, but we were able to obtain compound **5** by using the more stable 2<sup>nd</sup> generation Hoveyda-Grubbs catalyst in AcOH, which exclusively gave the *E*-isomer. Not surprisingly, this compound turned out to possess only limited water-solubility so we also set out to develop more water-soluble versions. To this end we aimed to synthesize locostatin analogue **9** (Scheme 2) and PEGylated compound **13** (Scheme 3), which could then be coupled to a PEGylated Biotin group through a Cu(I)-catalyzed alkyne-azide click reaction.<sup>19</sup>

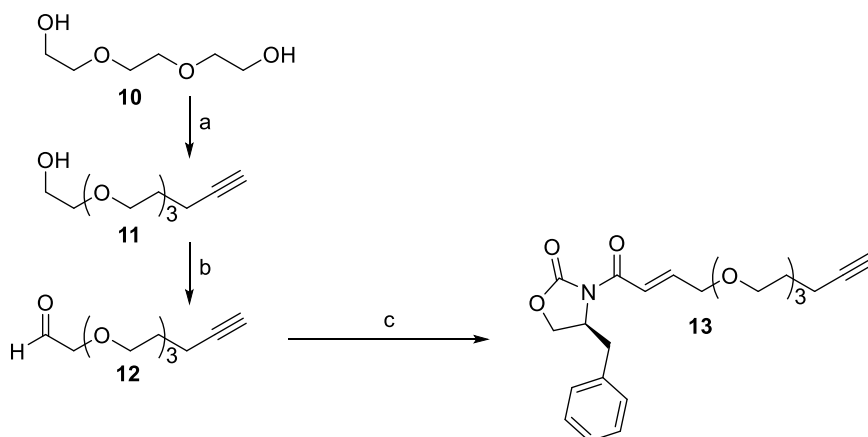
**Scheme 2.** Synthesis of click-enabled compound **9**.



Reaction conditions: a) bromoacetyl bromide, *n*-BuLi, THF,  $-78^{\circ}\text{C}$ , 1 h, 70%; b)  $\text{P}(\text{OEt})_3$ , neat,  $50^{\circ}\text{C}$ , 16 h, 100%; c) **8**, NaH, THF, rt, 1 h, 74%.

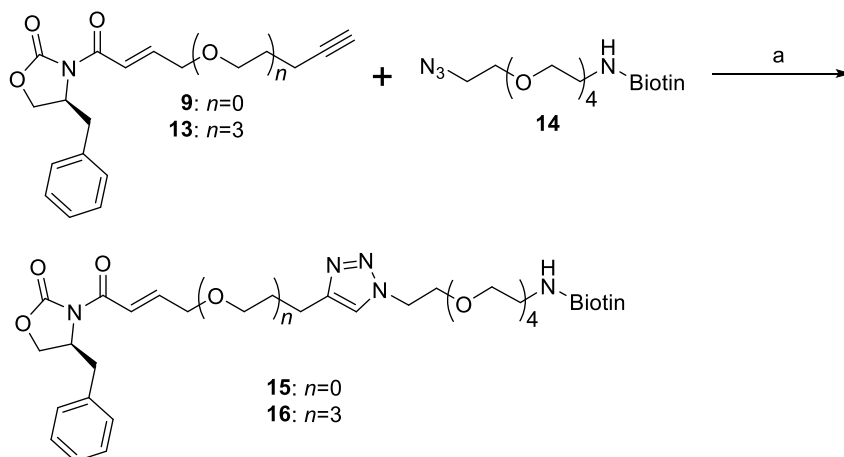
Compound **9** could be obtained from (*S*)-4-benzyloxazolidin-2-one **3**, which was acrylated in good yield with 2-bromoacetyl bromide and then converted to phosphonate **7** through an Arbuzov reaction in almost quantitative yield. The resulting intermediate was reacted through a Horner-Wadsworth-Emmons reaction with aldehyde **8**, providing the *E*-isomer as the major isomer that could be purified to provide compound **9** in 74% yield.

The other required building block, compound **13**, could be obtained from triethylene glycol, which was first alkylated to provide intermediate **11** (Scheme 3). Intermediate **11** was then oxidized *via* a Swern protocol to aldehyde **12**. This aldehyde was reacted with intermediate **7** through another Horner-Wadsworth-Emmons reaction to give compound **13**.

**Scheme 3.** Synthesis of PEGylated intermediate **13**.

Reaction conditions: a) NaH, 5-chloro-1-pentyne, THF, 60 °C, 16 h, 60%; b) Oxalyl chloride, DMSO, DCM, -78 °C, Et<sub>3</sub>N, 1 h, 47% c) NaH, 7, THF, DCM, rt, 1 h, 26%.

With both compound **13** and compound **9** in hand we set out to couple them to a PEGylated biotin **14** through a CuAAC click reaction, which was achieved in reasonable yield (Scheme 4).

**Scheme 4.** Synthesis of locostatin-probes **15** and **16**.

Reaction conditions: a) CuSO<sub>4</sub>, Sodium ascorbate, DMF, H<sub>2</sub>O, 64% (for **15**) or 68% (for **16**).

With probes **5**, **15** and **16** in hand, we set out to validate if these locostatin-based chemical probes could covalently bind FT. For this purpose FT was expressed *in vitro* and the protein mixture containing this FT was incubated with locostatin-probe **5** for 24 h at 37 °C (Appendix D, Figure S4), similar to the conditions employed earlier by Beshir and co-workers<sup>17</sup> for locostatin and RKIP. However, instead of selective labeling of FT we observed that the probe seemed to label the majority of the proteins in the cell lysate. Similarly, when we used locostatin-probes **15** and **16** under milder conditions: 2 h at 4 °C or room temperature, we

again did not see any selectivity for FT even at lower concentrations (Figure 2A and Appendix D, S4). Nevertheless, it was unclear if this was due to poor selectivity or due to low expression levels of FT in our system.

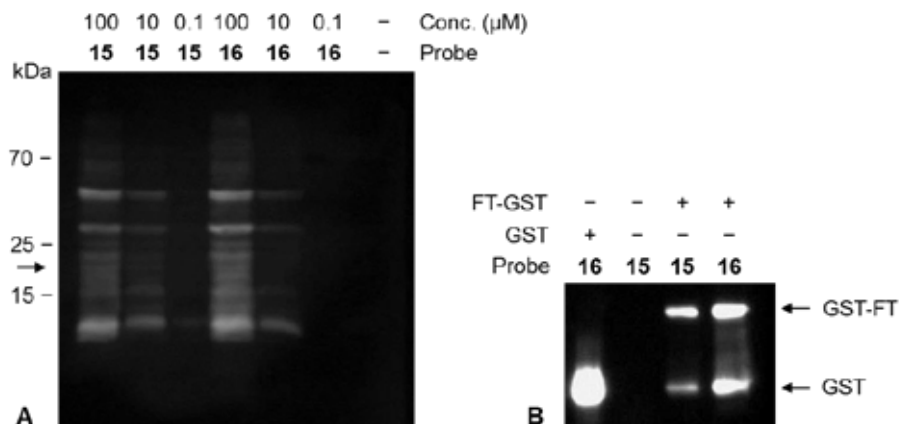


**Figure 2.** A) Binding of probe **15** and **16** at room temperature for 2 h with *in vitro* expressed FT; B) Binding of 40  $\mu\text{M}$  probe **15** and **16** with purified GST-FT and residual GST; binding of 200  $\mu\text{M}$  probe **15** with GST. Arrow indicates proximate position where FT is expected.

To that end, we expressed FT, fused to Glutathione S-Transferase (GST), in *Escherichia coli* and purified this fusion protein using affinity chromatography. The *N*-terminal GST fusion was used as an affinity tag. We then incubated GST-FT with locostatin probes **15** and **16**. Upon incubating GST-FT with probes **15** and **16** we found that both probes were able to successfully bind GST-FT (Figure 2B). However, we observed that the probes also bound residual cleaved GST to a similar extent (Figure 2B and Appendix D, Figure S5). This proved that locostatin-based probes **15** and **16** were not selectively binding FT. It also seemed to indicate that the Michael acceptor motif in locostatin is capable of reacting with the various nucleophiles present on any given protein.

In the past it has been reported that a tritium-labeled locostatin analogue was able to selectively label RKIP in MDCK cell extracts.<sup>10</sup> We therefore next investigated if 1) our locostatin-based chemical probes could also bind RKIP, and 2) if they display selectivity towards RKIP. As such, we incubated recombinant RKIP with locostatin probe **15** with or without 2 mM DTT. Although DTT has been used by others in incubation steps of locostatin with RKIP, we expected that the nucleophilic thiol of DTT might deactivate our locostatin-based chemical probes.<sup>10,17</sup> As expected we indeed observed that binding of our locostatin-based probe **15** proceeded much better in the absence of DTT (Figure 3A). Similarly, locostatin probe **5** was also able to bind RKIP, but not quantitatively, probably due to a lower effective concentration of the probe as a result of its lower water solubility (Appendix D, Figure S6).

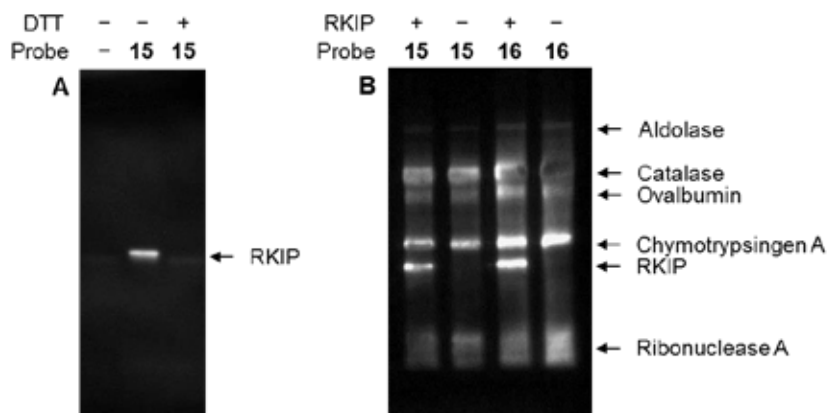


**Figure 3.** A) Evaluation of binding of 2.38  $\mu\text{M}$  RKIP by 200  $\mu\text{M}$  locostatin probe **15** for 6 h at 37  $^{\circ}\text{C}$  with or without 2 mM DTT; B) evaluation of selectivity of locostatin probes **15** and **16** towards 5 reference proteins (2.38  $\mu\text{M}$ ) with or without 2.38  $\mu\text{M}$  RKIP for 1 h at rt.

Finally, we tried to visualize the selectivity of our locostatin probes towards RKIP by introducing equimolar amounts of commonly used, non-PEBP, reference proteins to a buffered solution with or without RKIP. We observed that locostatin-based chemical probes **15** and **16** seem to bind RKIP and the other negative control proteins more or less to the same extent (Figure 3B and Appendix D, S7). In addition, the selectivity did not improve by performing the incubation for a shorter time at reduced temperatures. These results are in line with a recent study of locostatin towards a bacterial PEBP present in *Mycobacterium tuberculosis*, where the authors speculate that locostatin probably inhibits targets.<sup>20</sup>

## Conclusions

We successfully synthesized novel locostatin-based chemical probes. These probes enabled us to study the locostatin binding selectivity in cell lysates and protein mixtures, which provided surprising and important new insights into the selectivity of locostatin. While our locostatin-based probes can covalently bind both FT and RKIP, we have shown that these probes are not selective and can also bind a multitude of non-PEBP proteins. In addition, the apparent toxicity of locostatin towards plants and lack of selectivity of locostatin-based chemical probes towards FT indicate that locostatin is not a suitable lead compound towards novel small molecule binders of FT and flowering time-modulating compounds.

Locostatin is currently sold commercially by many vendors as a small molecule inhibitor of cell migration through its supposed selective inhibition of RKIP. In addition, potential pharmacological applications<sup>10-12,14-16</sup> have been attributed to locostatin. However, our findings here highlight that future research into locostatin and its analogues and their use as inhibitors of RKIP and other PEBP targets should take into account that locostatin has limited selectivity towards these proteins.

## General information and methods

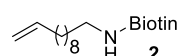
All moisture sensitive reactions were carried out under an argon atmosphere, using oven-dried glassware, unless otherwise stated. Dichloromethane ( $\text{CH}_2\text{Cl}_2$ , Sigma-Aldrich, >99.8%) and toluene (Sigma-Aldrich, >99.8%) were purified over aluminum oxide under argon using a Pure Solv 400 solvent purification system (Innovative Technology, Amesbury, USA). Reagents were obtained from commercial sources and used without further purification unless stated otherwise. Analytical TLC was performed using prepared plates of silica gel (Merck 60 F-254 on aluminium) or aluminum oxide (Fluka 60Å, F-254 on aluminum) and then, according to the functional groups present on the molecules, revealed with UV light or using staining reagents: ninhydrin (5% in EtOH) for amines or basic solution of  $\text{KMnO}_4$  (0.75% in  $\text{H}_2\text{O}$ ) for general staining. Merck silica gel 60 (70–230 mesh) or Fluka aluminium oxide (0.05–0.15 mm particle size, neutral, Brockmann Activity grade I) was used for flash chromatography.  $^1\text{H}$  NMR and  $^{13}\text{C}$  NMR spectra were recorded on a Bruker Avance III 400 spectrometer (observation of  $^1\text{H}$  nucleus 400 MHz, and of  $^{13}\text{C}$  nucleus 100 MHz). Chemical shifts are reported in parts per million (ppm), calibrated on the residual peak of the solvent, whose values are referred to tetramethylsilane (TMS,  $\delta_{\text{TMS}} = 0$ ), as the internal standard.  $^{13}\text{C}$  NMR spectra were performed with proton decoupling. Where indicated, NMR peak assignments were made using COSY and HSQC experiments. Electrospray ionization (ESI) mass analyses were performed on a Finnigan LXQ, while high resolution ESI mass analyses were recorded on a Thermo Scientific Q Exactive High-Resolution mass spectrometer. Infrared analyses were performed on a Bruker FT-IR spectrometer. Optical rotations were measured on a Perkin Elmer 241 polarimeter (Sodium D-line,  $\lambda = 589 \text{ nm}$ ).

### Growth of *Arabidopsis Thaliana*

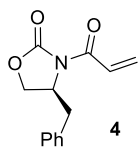
For the flowering time experiments, plants were grown under SD conditions, which comprises 8 h of light per day. Seeds were germinated on rock wool plugs and watered with Hyponex nutrition [1g/L]. After 6 days of growth 0.25 mL of locostatin [100 mM] was added per litre of Hyponex solution for watering the plants, resulting in 25  $\mu\text{M}$  of locostatin, or DMSO as a control. Plants were watered twice a week and were scored positive as soon as the plants were bolting visually. For *in vitro* experiments plants were grown on  $\frac{1}{2}$  MS media with 1% sucrose under LD (Long Day, 16 h of light) conditions with 25–50  $\mu\text{M}$  locostatin or DMSO as a control.

### In vitro expression of FT.

The cDNA of *Arabidopsis* FT was cloned in the pSPUTK vector and this construct was used for the *in vitro* expression of FT using the TnT® SP6 High-Yield Wheat Germ Protein Expression System (Promega), according to the protocol of the manufacturer.

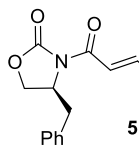
 5-((3aS,4S,6aR)-2-Oxohexahydro-1H-thieno[3,4-d]imidazol-4-yl)-N-(undec-10-en-1-yl)pentanamide (2). To a solution of Biotin (0.837 gram, 3.43 mmol, 1.0 equiv) in DMF (40 mL) was added *N*-(3-dimethylaminopropyl)-*N'*-ethylcarbodiimide hydrochloride (0.657 gram, 3.43 mmol, 1.0 equiv) and 1-hydroxybenzotriazole hydrate (0.695 gram, 5.14 mmol, 1.5 equiv), followed by diisopropylethylamine (2.5 mL, 4.2 equiv). The reaction mixture was stirred at room temperature for 15 min, followed by the addition of a solution of 1-amino-10-undecene (0.200, 1.18 mmol, 1.15 equiv) in DMF (10 mL). The resulting solution was stirred overnight and then conc. under high vacuum. The residue was then purified by column chromatography (5–10% MeOH in DCM)

affording compound **2** (1.15 gram, 85%) as a white solid.  $^1\text{H}$  NMR (400 MHz,  $\text{DMSO}-d_6$ )  $\delta$  7.68 (t,  $J$  = 5.6 Hz, 1H), 6.39 (s, 1H), 6.33 (s, 1H), 5.78 (ddt,  $J$  = 16.9, 10.2, 6.6 Hz, 1H), 5.03 – 4.88 (m, 2H), 4.29 (dd,  $J$  = 7.7, 5.1 Hz, 1H), 4.11 (ddd,  $J$  = 7.3, 4.4, 1.8 Hz, 1H), 3.08 (ddd,  $J$  = 8.5, 6.1, 4.3 Hz, 1H), 2.99 (q,  $J$  = 6.6 Hz, 2H), 2.81 (dd,  $J$  = 12.4, 5.1 Hz, 1H), 2.57 (d,  $J$  = 12.4 Hz, 1H), 2.07 – 1.94 (m, 4H), 1.60 (ddt,  $J$  = 12.4, 9.4, 6.2 Hz, 1H), 1.54 – 1.39 (m, 3H), 1.39 – 1.21 (m, 16H).  $^{13}\text{C}$  NMR (101 MHz,  $\text{DMSO}$ )  $\delta$  171.7, 162.7, 138.8, 114.6, 61.0, 59.2, 55.4, 39.8, 38.3, 35.2, 33.1, 29.1, 28.9, 28.8, 28.7, 28.5, 28.2, 28.0, 26.4, 25.3. HRMS calcd for  $\text{C}_{21}\text{H}_{37}\text{N}_3\text{O}_2\text{SNa}[\text{M}+\text{Na}^+]$ : 418.2499. Found: 418.2511



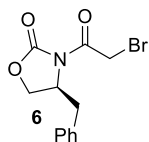
**(S)-3-Acryloyl-4-benzylloxazolidin-2-one (4).** To a solution of (S)-4-benzyl-2-oxazolidinone (10.0 gram, 56.4 mmol, 1.0 equiv) in THF (200 mL) at  $-78^\circ\text{C}$  was added dropwise a solution of *n*BuLi (1.6M in hexanes, 40.6 mL, 1.1 equiv) over 30 min. The reaction mixture was stirred for 30 min, followed by the addition of a solution of acryloyl chloride (5.48 mL, 67.7 mmol, 1.2 equiv) in THF (100 mL) over 20 minutes. The reaction

mixture was stirred at  $-78^\circ\text{C}$  for 1h and then quenched with sat. aq.  $\text{NH}_4\text{Cl}$  (40 mL).  $\text{H}_2\text{O}$  (600 mL) was added and the reaction mixture was extracted with  $\text{Et}_2\text{O}$  (500 mL, 3 $\times$ ). The combined organic layers were filtered, then dried ( $\text{Na}_2\text{SO}_4$ ) and conc. *in vacuo*. The resulting brown oil was purified by column chromatography (5–60%  $\text{EtOAc}$  in heptane), affording compound **4** (2.2 gram, 17%) as white crystals.  $^1\text{H}$  NMR (400 MHz,  $\text{Chloroform}-d$ )  $\delta$  7.54 (dd,  $J$  = 17.0, 10.4 Hz, 1H), 7.41 – 7.34 (m, 2H), 7.34 – 7.21 (m, 3H), 6.64 (dd,  $J$  = 17.0, 1.8 Hz, 1H), 5.97 (dd,  $J$  = 10.4, 1.8 Hz, 1H), 4.77 (ddt,  $J$  = 9.6, 7.4, 3.3 Hz, 1H), 4.31 – 4.18 (m, 2H), 3.38 (dd,  $J$  = 13.4, 3.3 Hz, 1H), 2.84 (dd,  $J$  = 13.4, 9.6 Hz, 1H). The physical data are in agreement with the literature values.<sup>21</sup>



**N-((E)-12-((S)-4-Benzyl-2-oxooxazolidin-3-yl)-12-oxododec-10-en-1-yl)-5-((3aS,4S,6aR)-2-oxohexahydro-1H-thieno[3,4-d]imidazol-4-yl)pentanamide (5).** To a solution of compound **3** (60.0 mg, 0.152 mmol, 1.0 equiv) in  $\text{AcOH}$  (5.0 mL) at  $30^\circ\text{C}$  was added compound **4** (53.0 mg, 0.228 mmol, 1.5 equiv), followed by Hoveyda-Grubbs Catalyst 2<sup>nd</sup> Generation

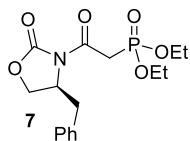
(0.014 gram, 0.022 mmol, 0.15 equiv). The reaction mixture was stirred overnight at  $30^\circ\text{C}$  and then conc. *in vacuo*. The residue was purified by column chromatography (4–10%  $\text{MeOH}$  in  $\text{DCM}$ ) affording compound **5** (24 mg, 26.4%) as a white solid.  $^1\text{H}$  NMR (400 MHz,  $\text{DMSO}-d_6$ )  $\delta$  7.69 (t,  $J$  = 5.6 Hz, 1H), 7.36 – 6.96 (m, 7H), 6.39 (s, 1H), 6.33 (s, 1H), 4.70 (tt,  $J$  = 7.9, 3.1 Hz, 1H), 4.38 – 4.25 (m, 2H), 4.17 (dd,  $J$  = 8.8, 2.9 Hz, 1H), 4.11 (ddd,  $J$  = 7.2, 4.6, 1.8 Hz, 1H), 3.12 – 3.03 (m, 1H), 3.03 – 2.88 (m, 4H), 2.80 (dd,  $J$  = 12.4, 5.1 Hz, 1H), 2.57 (d,  $J$  = 12.4 Hz, 1H), 2.25 (q,  $J$  = 7.0 Hz, 2H), 2.03 (t,  $J$  = 7.4 Hz, 2H), 1.67 – 1.37 (m, 5H), 1.39 – 1.19 (m, 15H).  $^{13}\text{C}$  NMR (101 MHz,  $\text{CDCl}_3$ )  $\delta$  173.1, 165.3, 153.6, 152.1, 135.5, 129.6, 129.1, 127.4, 120.5, 77.5, 77.2, 76.8, 66.3, 62.0, 60.3, 55.7, 55.5, 40.7, 39.7, 38.1, 36.2, 32.8, 29.8, 29.5, 29.4, 29.2, 28.3, 28.3, 28.2, 27.0, 25.8. HRMS calcd for  $\text{C}_{32}\text{H}_{47}\text{N}_4\text{O}_5[\text{M}+\text{H}^+]$ : 599.3262. Found: 599.3249



**(S)-4-Benzyl-3-(2-bromoacetyl)oxazolidin-2-one (6).** To a solution of (S)-4-benzyl-2-oxazolidinone in dry THF (20.0 mL) at  $-78^\circ\text{C}$  was added a solution of *n*BuLi (1.6M in hexanes, 4.0 mL, 6.40 mmol, 1.1 equiv). To the resulting solution was added dropwise a solution of bromoacetyl bromide (0.51 mL, 5.64 mmol, 1.0 equiv). The reaction mixture was stirred at  $-78^\circ\text{C}$  for 30 min and then allowed to warm to rt. The reaction mixture was stirred at rt for 15 min and then quenched with sat. aq.  $\text{NH}_4\text{Cl}$  (3.0 mL) and  $\text{H}_2\text{O}$  (60 mL). The

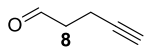


mixture was extracted with Et<sub>2</sub>O (30 mL, 3×), dried (MgSO<sub>4</sub>) and conc. *in vacuo*. The residue was purified by column chromatography (10–25% EtOAc in heptane) affording compound **6** (1.18 gram, 70.3%) as a blue oil. <sup>1</sup>H NMR (400 MHz, Chloroform-*d*) δ 7.38 – 7.18 (m, 5H), 4.71 (ddt, *J* = 9.6, 7.6, 3.3 Hz, 1H), 4.54 (d, *J* = 2.9 Hz, 2H), 4.33 – 4.18 (m, 2H), 3.34 (dd, *J* = 13.4, 3.4 Hz, 1H), 2.81 (dd, *J* = 13.4, 9.5 Hz, 1H). The physical data are in agreement with the literature values.<sup>22</sup>



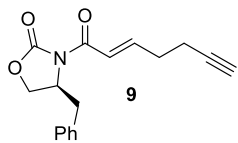
**Diethyl (S)-(2-(4-benzyl-2-oxooxazolidin-3-yl)-2-oxoethyl)phosphonate (7).**

Bromoacetate **6** (0.404 gram, 1.36 mmol, 1.0 equiv) and triethyl phosphite (1.13 gram, 6.78 mmol, 5.0 equiv) were heated together at 55 °C with stirring for 16 hours. The mixture was cooled and the excess triethyl phosphite was removed under high vacuum by heating until 70 °C, affording compound **7** (481 mg, 100%) as a clear yellow oil. <sup>1</sup>H NMR (400 MHz, Chloroform-*d*) δ 7.40 – 7.15 (m, 5H), 4.71 (ddt, *J* = 10.4, 6.9, 3.2 Hz, 1H), 4.27 – 4.12 (m, 6H), 3.86 (dd, *J* = 21.9, 14.2 Hz, 1H), 3.75 (dd, *J* = 22.1, 14.2 Hz, 1H), 3.36 (dd, *J* = 13.5, 3.4 Hz, 1H), 2.76 (dd, *J* = 13.4, 9.9 Hz, 1H), 1.36 (t, *J* = 7.1 Hz, 6H). The physical data are in agreement with the literature values.<sup>23</sup>



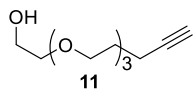
**Pent-4-ynal (8).**

A solution of DMSO (0.93 mL, 13.1 mmol, 2.19 equiv) in dry DCM (2.0 mL) was added over 10 minutes to a stirred solution of oxalyl chloride (0.57 mL, 6.73 mmol, 1.13 eq) in CH<sub>2</sub>Cl<sub>2</sub> (12.5 mL) at -78 °C. After addition, the reaction was stirred for 15 minutes, followed by the dropwise addition of 4-pentynol (0.502 gram, 5.97 mmol, 1.0 equiv) over 10 minutes. The resulting mixture was stirred for 1 hour at -78 °C. Lastly, Et<sub>3</sub>N (4.13 mL, 5.0 equiv) was added and the reaction stirred for another hour at -78 °C before allowing the reaction to warm to room temperature. The reaction mixture was quenched by the addition of water (12.5) and subsequently extracted with DCM (8 mL, 3×). The combined organic layers were washed with 1M HCl in saturated aq. NaCl (8 mL, 4×), sat. aq. NaHCO<sub>3</sub> (10 mL). The aqueous layers were back extracted with CH<sub>2</sub>Cl<sub>2</sub> (10 mL). Combined organic layers were washed with brine (10 mL), dried (MgSO<sub>4</sub>), filtered and concentrated with a rotary evaporator at 30 °C at 300 mbar to provide crude pent-4-ynal **8** (4.75 mmol, 80%) as a ±50% solution in DCM, which was used without further purification. <sup>1</sup>H NMR (400 MHz, Chloroform-*d*) δ 9.79 (s, 1H), 2.69 (t, *J* = 7.4 Hz, 1H), 2.50 (dt, *J* = 7.3, 2.5 Hz, 2H), 1.98 (t, *J* = 2.7 Hz, 1H). The physical data are in agreement with the literature values.<sup>24</sup>

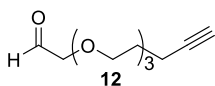


**(S,E)-4-Benzyl-3-(hept-2-en-6-ynoyl)oxazolidin-2-one (9).**

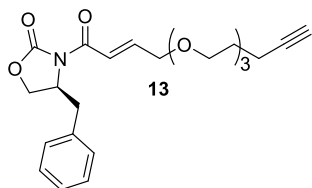
A solution of compound **7** (0.550 gram, 1.54 mmol, 1.2 equiv) in dry THF (5.0 mL) was added to a suspension of NaH (60% in mineral oil, 57.0 mg, 1.43 mmol, 1.1 equiv) in dry THF (7.5 mL). The reaction mixture was stirred for 5 minutes at rt. A solution of crude **8** (±50% in DCM, 0.226 gram, 1.38 mmol, 1.0 equiv) was added dropwise. The resulting mixture was stirred at rt for 1 hour. Et<sub>2</sub>O (20 mL) was added to the reaction mixture the mixture was washed with H<sub>2</sub>O (5 mL, 2×). The waterlayer was extracted with DCM (4 mL, 2×) and the combined organic layers were washed with brine (5 mL), dried (MgSO<sub>4</sub>) and conc. *in vacuo*. The residue was purified by column chromatography 20–24% EtOAc in heptane), affording compound **9** (288 mg, 73.7%) as a white crystalline solid. <sup>1</sup>H NMR (400 MHz, CDCl<sub>3</sub>) δ 7.40 – 7.14 (m, 7H), 4.73 (ddt, *J* = 10.7, 7.0, 3.2 Hz, 1H), 4.26 – 4.12 (m, 2H), 3.34 (dd, *J* = 13.4, 3.3 Hz, 1H), 2.80 (dd, *J* = 13.4, 9.5 Hz, 1H), 2.54 (qd, *J* = 6.7, 1.4 Hz, 2H), 2.40 (td, *J* = 7.0, 2.8 Hz, 2H), 2.02 (t, *J* = 2.6 Hz, 1H). <sup>13</sup>C NMR (101 MHz, CDCl<sub>3</sub>) δ 164.9, 153.5, 148.8, 135.5, 129.6, 129.1, 127.5, 121.7, 82.7, 77.5, 77.2, 76.8, 69.7, 66.3, 55.5, 38.0, 31.6, 17.7. HRMS calcd for C<sub>17</sub>H<sub>17</sub>NO<sub>3</sub>Na[M+Na<sup>+</sup>]: 306.1101. Found: 306.1096



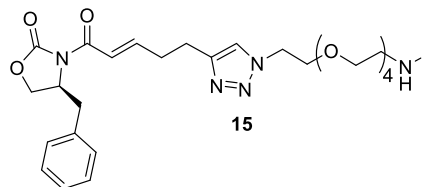
**2-(2-(2-(Pent-4-yn-1-yloxy)ethoxy)ethoxy)ethan-1-ol (11).** To a suspension of NaH (60% in mineral oil, 0.780 gram, 19.5 mmol, 2.0 equiv) in dry THF (10 mL) at 60 °C was added triethylene glycerol (6.51 mL, 48.8 mmol, 5 equiv). The mixture was stirred at 60 °C for 1 hour, followed by the addition of 5-chloro-1-pentyne. The reaction mixture was stirred overnight at 60 °C. The reaction was quenched with AcOH (1.0 mL) and stirred for 5 min and then further diluted with THF (10 mL) and then filtered. The residue was washed with THF (20 mL) and the combined organic layers were conc. *in vacuo*. The residue was purified by column chromatography 75-100% EtOAc in heptane, affording compound **11** (1.27 mg, 60%) as a brown oil. <sup>1</sup>H NMR (400 MHz, Chloroform-*d*) δ 3.75 – 3.51 (m, 14H), 2.62 (bs, 1H, OH), 2.28 (td, *J* = 7.1, 2.7 Hz, 2H), 1.93 (t, *J* = 2.7 Hz, 1H), 1.79 (p, *J* = 6.7 Hz, 2H). <sup>13</sup>C NMR (101 MHz, CDCl<sub>3</sub>) δ 84.0, 77.5, 77.2, 76.8, 72.6, 70.7, 70.6, 70.4, 70.3, 69.7, 68.6, 61.8, 28.5, 15.2. HRMS calcd for C<sub>11</sub>H<sub>20</sub>O<sub>4</sub>Na[M+Na<sup>+</sup>]: 239.1254. Found: 239.1254



**2-(2-(2-(Pent-4-yn-1-yloxy)ethoxy)ethoxy)acetaldehyde (12).** A solution of oxalyl chloride (0.128 gram, 1.50 mmol, 1.5 equiv) in dry DCM (10 mL) under argon was cooled to at -78 °C and a solution of DMSO (0.143 gram, 2.00 mmol, 2.0 equiv) in dry DCM (1.0 mL) was added dropwise. After addition, the reaction was stirred for a 20 minutes, followed by the dropwise addition of compound **11** (0.220 gram, 1.02 mmol, 1.0 equiv) over 10 minutes. The resulting mixture was stirred for 20 min at -78 °C. Lastly, Et<sub>3</sub>N (0.550 mL, 4.00 mmol, 4.0 equiv) was added and the reaction mixture was allowed to warm to room temperature. The reaction mixture was filtered and then conc. *in vacuo*, affording a crude compound **12** (0.476 mmol, 47%) as a ±16% solution in DMSO/Et<sub>3</sub>N, which was used without further purification. <sup>1</sup>H NMR (400 MHz, Chloroform-*d*) δ 9.73 (s, 1H), 4.15 (s, 2H), 3.76 – 3.67 (m, 4H), 3.67 – 3.61 (m, 2H), 3.59 (dt, *J* = 5.9, 2.0 Hz, 2H), 3.55 (t, *J* = 6.2 Hz, 2H), 2.27 (td, *J* = 7.0, 2.7 Hz, 2H), 1.92 (t, *J* = 2.6 Hz, 1H), 1.78 (p, *J* = 6.9 Hz, 2H).



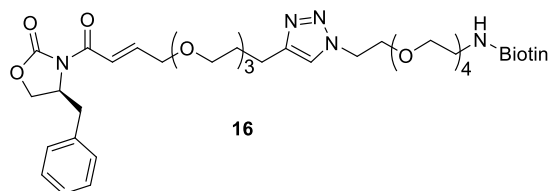
**(S,E)-4-benzyl-3-(4-(2-(2-(pent-4-yn-1-yloxy)ethoxy)ethoxy)but-2-enoyl)oxazolidin-2-one (13).** A solution of compound **7** (0.203 gram, 0.572 mmol, 1.2 equiv) in dry THF (5.0 mL) was added to a suspension of NaH (60% in mineral oil, 21.0 mg, 0.873 mmol, 1.1 equiv) in dry THF (5.0 mL). The reaction mixture was stirred for 10 minutes at rt. A solution of crude compound **12** (0.476 mmol, 1.0 equiv) in a mixture of dry THF (4.0 mL) and dry DCM (10.0 mL) was added. The resulting mixture was stirred at rt for 1 hour and then conc. *in vacuo*. The residue was purified by column chromatography (2.5-5% MeOH in DCM) and subsequently by Reverse phase column chromatography (40-60% MeCN in H<sub>2</sub>O), affording compound **13** (45.4 mg, 23.0%) as a yellow oil. <sup>1</sup>H NMR (400 MHz, Chloroform-*d*) δ 7.47 (dt, *J* = 15.5, 1.9 Hz, 1H), 7.38 – 7.12 (m, 6H), 4.73 (ddt, *J* = 9.5, 7.5, 3.3 Hz, 1H), 4.29 (dd, *J* = 4.6, 1.9 Hz, 2H), 4.26 – 4.13 (m, 2H), 3.75 – 3.65 (m, 6H), 3.65 – 3.60 (m, 2H), 3.57 (t, *J* = 6.2 Hz, 2H), 3.34 (dd, *J* = 13.4, 3.4 Hz, 1H), 2.80 (dd, *J* = 13.4, 9.5 Hz, 1H), 2.29 (td, *J* = 7.1, 2.7 Hz, 2H), 1.94 (t, *J* = 2.7 Hz, 1H), 1.80 (p, *J* = 6.7 Hz, 2H). <sup>13</sup>C NMR (101 MHz, CDCl<sub>3</sub>) δ 164.8, 153.4, 146.6, 135.4, 129.6, 129.1, 127.5, 120.6, 84.2, 70.9, 70.8, 70.5, 70.4, 70.4, 69.7, 68.5, 66.3, 55.4, 38.0, 28.7, 15.3. HRMS calcd for C<sub>23</sub>H<sub>29</sub>NO<sub>6</sub>Na[M+Na<sup>+</sup>]: 438.1887. Found: 438.1880



15

***N*-(14-(4-((*E*)-5-((*S*)-4-Benzyl-2-oxooxazolidin-3-yl)-5-oxopent-3-en-1-yl)-1H-1,2,3-triazol-1-yl)-3,6,9,12-tetraoxatetradecyl)-5-(((3*aS*,4*S*,6*aR*)-2-oxohexahydro-1H-thieno[3,4-*d*]imidazol-4-yl)pentanamide (15).** To a solution of alkyne **9** (20.5 mg, 0.0724 mmol, 1.0 equiv) in DMF (0.3 mL) was slowly added a solution of Biotin-PEG4-Azide (35.5

mg, 0.0727 mmol, 1 equiv) in H<sub>2</sub>O (0.3 mL), followed by (+)-sodium-L-ascorbate (37.0 mg, 0.187 mmol, 2.5 equiv). To the resulting suspension was added CuSO<sub>4</sub> (1.5 mg, 0.0094 mmol, 0.1 equiv) together with additional H<sub>2</sub>O (0.3 mL) and DMF (0.3 mL). The reaction mixture was stirred overnight at rt and subsequently freeze-dried. The residue was purified by column chromatography (2.5-10% MeOH in DCM) affording compound **15** (35.8 mg, 64.1%) as a colorless oil. <sup>1</sup>H NMR (400 MHz, Chloroform-*d*) δ 7.53 (s, 1H), 7.36 – 7.11 (m, 7H), 6.83 (t, *J* = 5.6 Hz, 1H), 6.45 (s, 1H), 5.61 (s, 1H), 4.71 (ddt, *J* = 9.5, 7.7, 3.2 Hz, 1H), 4.56 – 4.40 (m, 3H), 4.32 – 4.24 (m, 1H), 4.24 – 4.10 (m, 2H), 3.85 (t, *J* = 5.2 Hz, 2H), 3.66 – 3.57 (m, 12H), 3.53 (t, *J* = 5.0 Hz, 2H), 3.44 – 3.34 (m, 2H), 3.30 (dd, *J* = 13.4, 3.3 Hz, 1H), 3.11 (td, *J* = 7.3, 4.4 Hz, 1H), 2.98 – 2.83 (m, 3H), 2.78 (dd, *J* = 13.4, 9.5 Hz, 1H), 2.74 – 2.65 (m, 3H), 2.19 (t, *J* = 7.4 Hz, 2H), 1.77 – 1.56 (m, 4H), 1.46 – 1.34 (m, 2H). <sup>13</sup>C NMR (101 MHz, CDCl<sub>3</sub>) δ 173.4, 165.0, 163.9, 153.6, 149.9, 146.5, 135.5, 129.6, 129.1, 127.5, 122.3, 121.3, 70.7, 70.6, 70.6, 70.2, 70.1, 69.7, 66.3, 61.9, 60.3, 55.7, 55.4, 50.3, 40.7, 39.3, 38.0, 36.0, 32.3, 28.3, 28.2, 25.7, 24.4. HRMS calcd for C<sub>37</sub>H<sub>53</sub>N<sub>7</sub>O<sub>9</sub>SNa[M+Na<sup>+</sup>]: 794.3518. Found: 794.3507



16

***N*-(14-(4-(3-(2-(((*Z*)-4-((*S*)-4-Benzyl-2-oxooxazolidin-3-yl)-4-oxobut-2-en-1-yl)oxy)ethoxy)ethoxy)propyl)-1H-1,2,3-triazol-1-yl)-3,6,9,12-tetraoxatetradecyl)-5-(((3*aS*,4*S*,6*aR*)-2-oxohexahydro-1H-thieno[3,4-*d*]imidazol-4-yl)pentanamide (16).** To a solution of alkyne **13** (128 mg,

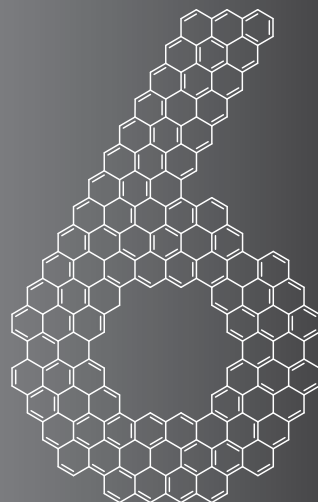
0.308 mmol, 1.0 equiv) in DMF (1.3 mL) was slowly added a solution of Biotin-PEG4-Azide (0.147 mg, 0.301 mmol, 0.98 equiv) in H<sub>2</sub>O (1.3 mL), followed by (+)-sodium-L-ascorbate (153 mg, 0.772 mmol, 2.5 equiv). To the resulting suspension was added CuSO<sub>4</sub> (7.5 mg, 0.047 mmol, 0.15 equiv). The reaction mixture was stirred overnight at rt and subsequently freeze-dried. The residue was purified by reverse-phase column chromatography (40-55% MeCN in H<sub>2</sub>O) affording compound **16** (35.8 mg, 68%) as a yellow oil. <sup>1</sup>H NMR (400 MHz, Chloroform-*d*) δ 7.54 – 7.39 (m, 2H), 7.39 – 7.11 (m, 6H), 6.46 (s, 1H), 5.62 (s, 1H), 4.85 (s, 1H), 4.73 (ddt, *J* = 10.3, 7.1, 3.2 Hz, 1H), 4.55 – 4.43 (m, 3H), 4.36 – 4.27 (m, 2H), 4.27 – 4.12 (m, 2H), 3.87 (t, *J* = 5.2 Hz, 2H), 3.75 – 3.65 (m, 6H), 3.65 – 3.58 (m, 13H), 3.58 – 3.47 (m, 4H), 3.43 (q, *J* = 5.2 Hz, 2H), 3.33 (dd, *J* = 13.4, 3.3 Hz, 1H), 3.15 (td, *J* = 7.2, 4.5 Hz, 1H), 2.97 – 2.69 (m, 5H), 2.22 (t, *J* = 7.0 Hz, 2H), 1.96 (p, *J* = 6.8 Hz, 2H), 1.80 – 1.56 (m, 6H), 1.45 (p, *J* = 7.6 Hz, 2H). <sup>13</sup>C NMR (101 MHz, CDCl<sub>3</sub>) δ 173.4, 164.7, 163.9, 153.4, 146.5, 136.1, 135.4, 129.5, 129.1, 127.4, 122.2, 120.6, 70.9, 70.7, 70.6, 70.6, 70.5, 70.5, 70.5, 70.4, 70.3, 70.2, 70.1, 69.7, 66.3, 61.9, 60.3, 55.6, 55.4, 53.9, 50.2, 41.6, 40.6, 39.3, 37.9, 36.0, 29.5, 28.3, 28.2, 25.7, 22.4. HRMS calcd for C<sub>43</sub>H<sub>65</sub>N<sub>7</sub>O<sub>12</sub>SNa[M+Na<sup>+</sup>]: 926.4304. Found: 926.4308

## References

1. Granovsky, A.E. and Rosner, M.R. *Cell Res.* **2008**, *18*, 452.
2. Lifschitz, E., Eviatar, T., Rozman, A., Shalit, A., Goldshmidt, A., Amsellem, Z., Alvarez, J.P., and Eshed, Y. *Proc. Natl. Acad. Sci. USA* **2006**, *103*, 6398.
3. Corbesier, L., Vincent, C., Jang, S., Fornara, F., Fan, Q., Searle, I., Giakountis, A., Farrona, S., Gissot, L., Turnbull, C., and Coupland, G. *Science* **2007**, *316*, 1030.
4. Banfield, M.J. and Brady, R.L. *J. Mol. Biol.* **2000**, *297*, 1159.
5. Serre, L., Vallée, B., Bureaud, N., Schoentgen, F., and Zelwer, C. *Structure* **1998**, *6*, 1255.
6. Keller, E.T., Fu, Z., and Brennan, M. *Biochem. Pharmacol.* **2004**, *68*, 1049.
7. Sultana, R., Perluigi, M., and Butterfield, D.A. *Acta Neuropathologica* **2009**, *118*, 131.
8. Yuasa, H., Ojika, K., Mitake, S., Katada, E., Matsukawa, N., Otsuka, Y., Fujimori, O., and Hirano, A. *Developmental Brain Research* **2001**, *127*, 1.
9. Al-Mulla, F., Bitar, M.S., Taqi, Z., and Yeung, K.C. *J. Cell. Physiol.* **2013**, *228*, 1688.
10. Zhu, S., Mc Henry, K.T., Lane, W.S., and Fenteany, G. *Chemistry & biology* **2005**, *12*, 981.
11. Rudnitskaya, A.N., Eddy, N.A., Fenteany, G., and Gascon, J.A. *J. Phys. Chem. B* **2012**, 10176.
12. Ménoret, A., McAleer, J.P., Ngoi, S.-M., Ray, S., Eddy, N.A., Fenteany, G., Lee, S.-J., Rossi, R.J., Mukherji, B., Allen, D.L., Chakraborty, N.G., and Vella, A.T. *The Journal of Immunology* **2009**, *183*, 7489.
13. Mc Henry, K.T., Ankala, S.V., Ghosh, A.K., and Fenteany, G. *ChemBioChem* **2002**, *3*, 1105.
14. Shemon, A.N., Eves, E.M., Clark, M.C., Heil, G., Granovsky, A., Zeng, L., Imamoto, A., Koide, S., and Rosner, M.R. *PLoS ONE* **2009**, *4*, e6028.
15. Ciarmela, P., Marzioni, D., Islam, M.S., Gray, P.C., Terracciano, L., Lorenzi, T., Todros, T., Petraglia, F., and Castellucci, M. *J. Cell. Physiol.* **2012**, *227*, 1821.
16. Best, O.G., Pyke, T., Crassini, K., Stevenson, W.S., and Mulligan, S.P. *Blood* **2014**, *124*, 3326.
17. Beshir, A.B., Argueta, C.E., Menikarachchi, L.C., Gascón, J.A., and Fenteany, G. *For Immunopathol Dis Therap.* **2011**, *2*, 47.
18. Farrona, S., Thorpe, F.L., Engelhorn, J., Adrian, J., Dong, X., Sarid-Krebs, L., Goodrich, J., and Turck, F. *The Plant Cell* **2011**, *23*, 3204.
19. Rostovtsev, V.V., Green, L.G., Fokin, V.V., and Sharpless, K.B. *Angew. Chem. Int. Ed.* **2002**, *41*, 2596.
20. Eulenburg, G., Higman, V.A., Diehl, A., Wilmanns, M., and Holton, S.J. *FEBS Lett.* **2013**, *587*, 2936.
21. Evans, D.A., Chapman, K.T., and Bisaha, J. *J. Am. Chem. Soc.* **1988**, *110*, 1238.
22. Evans, D.A. and Weber, A.E. *J. Am. Chem. Soc.* **1987**, *109*, 7151.
23. Aldrich, L.N., Berry, C.B., Bates, B.S., Konkol, L.C., So, M., and Lindsley, C.W. *Eur. J. Org. Chem.* **2013**, *2013*, 4215.

24. Adams, T.C., Dupont, A.C., Carter, J.P., Kachur, J.F., Guzewska, M.E., Rzeszutarski, W.J., Farmer, S.G., Noronha-Blob, L., and Kaiser, C. *J. Med. Chem.* **1991**, *34*, 1585.

## Chapter 6



# Direct Imaging of Glycans in Arabidopsis Roots via Click Labeling of Metabolically Incorporated Azido-Monosaccharides

Part of this work was published in:

J. Hoogenboom, N. Berghuis, D. Cramer, R. Geurts, H. Zuilhof, T. Wennekes,  
*BMC Plant Biology*, **2016**, 16, 220

## Abstract

### Background

Carbohydrates, also called glycans, play a crucial but not fully understood role in plant health and development. The non-template driven formation of glycans makes it impossible to image them in vivo with genetically encoded fluorescent tags and related molecular biology approaches. A solution to this problem is the use of tailor-made glycan analogs that are metabolically incorporated by the plant into its glycans. These metabolically incorporated probes can be visualized, but techniques documented so far use toxic copper-catalyzed labeling. To further expand our knowledge of plant glycobiology by direct imaging of its glycans via this method, there is need for novel click-compatible glycan analogs for plants that can be bioorthogonally labelled via copper-free techniques.

### Results

*Arabidopsis* seedlings were incubated with azido-containing monosaccharide analogs of *N*-acetylglucosamine, *N*-acetylgalactosamine, L-fucose, and L-arabinofuranose. These azido-monosaccharides were metabolically incorporated in plant cell wall glycans of *Arabidopsis* seedlings. Control experiments indicated active metabolic incorporation of the azido-monosaccharide analogs into glycans rather than through non-specific absorption of the glycan analogs onto the plant cell wall. Successful copper-free labeling reactions were performed, namely an inverse-electron demand Diels-Alder cycloaddition reaction using an incorporated *N*-acetylglucosamine analog, and a strain-promoted azide-alkyne click reaction. All evaluated azido-monosaccharide analogs were observed to be non-toxic at the used concentrations under normal growth conditions.

### Conclusions

Our results for the metabolic incorporation and fluorescent labeling of these azido-monosaccharide analogs expand the possibilities for studying plant glycans by direct imaging. Overall we successfully evaluated five azido-monosaccharide analogs for their ability to be metabolically incorporated in *Arabidopsis* roots and their imaging after fluorescent labeling. This expands the molecular toolbox for direct glycan imaging in plants, from three to eight glycan analogs, which enables more extensive future studies of spatiotemporal glycan dynamics in a wide variety of plant tissues and species. We also show, for the first time in metabolic labeling and imaging of plant glycans, the potential of two copper-free click chemistry methods that are bio-orthogonal and lead to more uniform labeling. These improved labeling methods can be generalized and extended to already existing and future click chemistry-enabled monosaccharide analogs in *Arabidopsis*.

## Background

All plant cells are covered by a dense layer of carbohydrates (glycans), called the glycocalyx. It is the glycocalyx that is first encountered by other cells, including microbes. Glycans are also found on more than 50% of plant proteins as an important post-translational modification that directly influences protein functioning.<sup>1</sup> Hence it is not surprising that glycans play essential roles in a myriad of biological processes in all stages of plant development, such as cell-cell communication,<sup>2</sup> control of metabolism, growth, stress response<sup>3</sup> and external signalling, thereby also tied to the rhizosphere.<sup>4-6</sup> Glycans thus play a crucial but not well understood role in plant health and disease. Developing techniques to better study plant glycans and increase our understanding of and control over their role is an essential next step in plant sciences.

Due to the non-template driven formation of glycans it is not possible to use genetically encoded protein-based fluorescent tags to image and study glycans directly. Externally added protein-based probes, usually fluorescently-labeled lectins, image the glycans indirectly and are only able to image glycans exposed on the most outer layer of the cell surface glycocalyx.<sup>7-8</sup>

Another approach, however, exists that allows the direct imaging of plant glycans. Glycans, especially in plants, usually have highly complex and diverse structures containing monosaccharides such as glucose, N-acetylglucosamine, galactose, L-arabinose, xylose, L-fucose and 3-deoxy-D-manno-oct-2-ulonic acid (KDO).<sup>9-11</sup> Besides their de novo biosynthesis, these monosaccharides and their derivatives can also be recycled by plant cells.<sup>12</sup> Through uptake of extracellular monosaccharides and by intracellular catabolism of complex plant glycans, these monosaccharides can be recycled through the glycan salvage pathways. Using this recycling pathway the monosaccharides again end up in plant cell-surface glycans and its glycoproteins.<sup>13</sup> Glycans and their conjugates are biosynthesized by glycosyltransferases present in the Golgi apparatus and endoplasmic reticulum (ER). The composition and levels of glycans in the glycocalyx and in proteins depends on the presence and levels of these enzymes and their activated monosaccharide donor substrates.<sup>12</sup>

The metabolic incorporation of monosaccharide analogs with a latent imaging tag via these pathways would allow for the direct imaging of plant glycans (Fig. 1).<sup>12</sup> These incorporated monosaccharide analogs can be visualized and studied through a tag that enables click chemistry, which allows for rapid, specific and versatile covalent labeling of plant glycans with a fluorescent reporter molecule.<sup>14-15</sup> This technique is called Metabolic Oligosaccharide Engineering (MOE) and it has already been widely applied for studying glycobiology in various organisms, with the notable exception of plants.<sup>16</sup> Indeed, only in 2012, the first application of MOE with click-compatible monosaccharide analogs in plants was reported by Anderson et al. in which fucosylated plant glycans were fluorescently imaged in *Arabidopsis thaliana* (Col-0) seedlings.<sup>17</sup> Two other click-compatible monosaccharide analogs were reported recently, namely, 6-deoxy-alkynyl-glucose that incorporates in *Arabidopsis* root hair



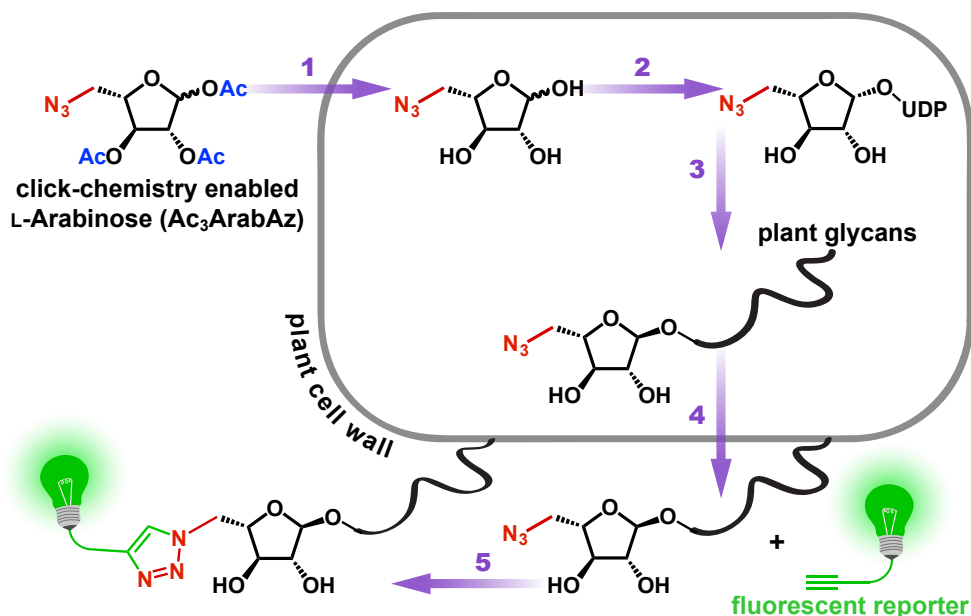


**Figure 1.** Metabolic labeling of Arabidopsis cell wall-glycans with azido-monosaccharides. Arabidopsis is grown on MS containing an azido-monosaccharide such as Ac<sub>3</sub>ArabAz, which is taken up through the cell wall followed by hydrolysis of the acetyl (Ac) groups by intracellular esterases (1). The resulting ArabAz enters the glycan salvage pathway and is converted to an azido-nucleotide sugar donor (2) that allows its incorporation by glycosyltransferases into plant glycans (3) that end up in plant cell-surface glycans and its glycoproteins (4). Finally, the incorporated glycan can be imaged after a click-reaction with a fluorescent reporter group (5).

tips,<sup>18</sup> and 8-azido-8-deoxy-KDO, a probe analogous to KDO that is present in the cell wall pectic polysaccharide, rhamnogalacturonan II.<sup>19</sup> To further expand our knowledge of plant glycobiology by direct imaging of glycans, there is need for click chemistry-compatible glycan analogs for other plant monosaccharides. In addition, the click chemistry compatible glycan analogs in plants documented so far were labeled using toxic copper-labeling, and future applications would benefit from bio-orthogonal copper-free labeling techniques.

We investigated five glycans: *N*-acetyl-D-glucosamine, L-fucose and L-arabinose - which are all known to be present in the glycocalyx of Arabidopsis<sup>11,20</sup> - and *N*-acetyl-D-galactosamine (GalNAc) and *N*-acetyl-D-mannosamine. While the latter two glycans are not known to be present in plant glycans, it was recently discovered that UDP-GalNAc is present and transported in the ER of Arabidopsis,<sup>21</sup> indicating that GalNAc is metabolized by plants. In this technical advance paper we expand the monosaccharide analog toolbox (Fig. 2) for metabolic labeling of glycans in Arabidopsis seedlings. Furthermore, the glycan analogs reported so far in plants use a Cu(I)-catalyzed cycloaddition, however, this is cytotoxic for Arabidopsis<sup>22</sup> and microbes in soils<sup>23</sup> making this method less suitable for long-term and more complex experiments with living plants. Therefore we investigated the possibilities of bio-orthogonal copper-free click reactions in Arabidopsis roots.

## Results and discussion

### Azido-monosaccharides are not toxic at experimental concentrations

To determine if Arabidopsis seedlings behave differently under normal growth conditions when incubated with our non-natural azido-containing monosaccharide analogs (Fig. 2), their toxicity was evaluated. Earlier reports of metabolic labeling of plant seedlings with monosaccharide analogs have evaluated toxicity by measuring the root length of 8-day old seedlings on MS plates.<sup>22,24</sup> This toxicity evaluation exposes plant seedlings for several days to high levels of azido-monosaccharides, while the metabolic incorporation experiments are carried out at similar or lower concentrations in a fraction of that time (typically 4-24 hours). Accordingly, seedlings were exposed for 8 days to the azido-monosaccharides at concentrations that were used in the different metabolic incorporation experiments (10, 25 and 100  $\mu$ M). When compared to seedlings grown on agarose plates with only MS medium, no significant difference was observed (Appendix E, Figure S1). This shows that azido-monosaccharides do not significantly influence the growth and metabolic processes in Arabidopsis.

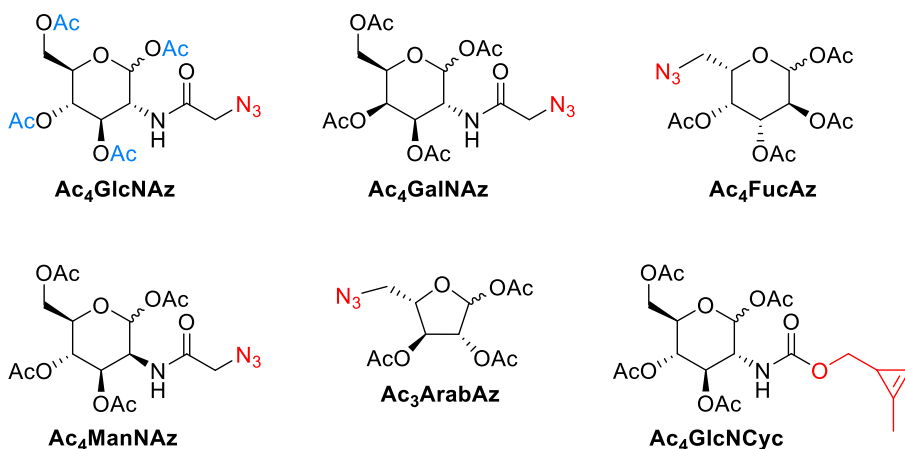


**Figure 2.** Chemical structure of click chemistry-enabled monosaccharide analogs that were used in this study.

### Ac<sub>4</sub>GlcNAz, Ac<sub>3</sub>ArabAz and Ac<sub>4</sub>FucAz are incorporated in root cell walls of differentiating Arabidopsis

*N*-acetylglucosamine is commonly present in *N*-glycans of plant cell walls<sup>11,20</sup> and is important for *N*-glycan formation, since it is the first monosaccharide attached to glycoproteins.<sup>25</sup> Therefore metabolic click-mediated labeling of Arabidopsis cell walls was investigated with a *N*-acetyl-glucosamine analog containing a clickable azide (Ac<sub>4</sub>GlcNAz; Fig. 2). Ac<sub>4</sub>GlcNAz was synthesized according to a procedure of Bertozzi and co-workers.<sup>26</sup> Ac<sub>4</sub>GlcNAz was dissolved in a ½ MS medium and used to incubate four day-old Arabidopsis (Col-0) seedlings. The seedlings were incubated with 10, 25, 50 or 100  $\mu$ M Ac<sub>4</sub>GlcNAz and control seedlings

were incubated with 0.01% DMSO. After 24 h, seedlings were washed and then transferred for 45 min to a solution containing Alexa Fluor® 488-alkyne and a Click-iT kit solution for the copper-catalyzed labeling. After the labeling and the subsequent washing steps, fluorescence intensity of cell walls was monitored by confocal microscopy. Seedlings incubated with 25  $\mu\text{M}$   $\text{Ac}_4\text{GlcNAz}$  showed optimal labeling (Fig. 3a & Appendix E, Figure S2). Increased labeling could be reached at higher concentrations, but was not required (Appendix E, Figure S2-3). Control seedlings (Fig. 3e) treated with 0.01% DMSO did not show auto-fluorescence background signals under these conditions and therefore 25  $\mu\text{M}$  was used for further labeling experiments with  $\text{Ac}_4\text{GlcNAz}$ .

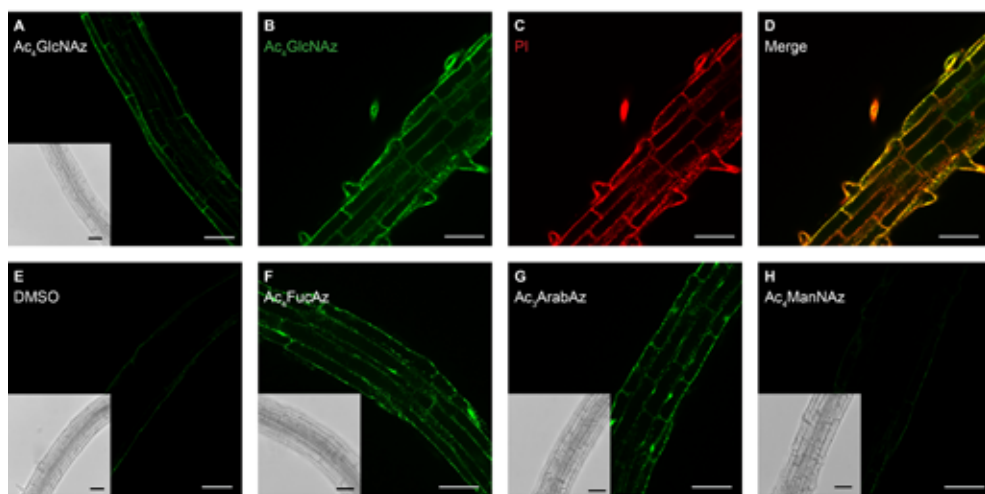


**Figure 3.** Optical sections of 4 day old Arabidopsis seedling roots incubated for 24 h with azido-monosaccharides. Seedlings were incubated with 25  $\mu\text{M}$   $\text{Ac}_4\text{GlcNAz}$  (a), followed by labeling through a copper-catalyzed click reaction with Alexa Fluor® 488 alkyne. Seedling roots treated with Alexa Fluor® 488 alkyne-labeled  $\text{Ac}_4\text{GlcNAz}$  (25  $\mu\text{M}$ , 24 h) (b, d) were counterstained; Propidium Iodide (PI, 0.05%) to visualize cell walls (c, d). Yellow color indicates overlap of the two dyes (d). Scale bars = 50  $\mu\text{m}$ . As a control, seedlings were treated with 0.01 % DMSO (e). Alternatively, seedlings were incubated with 25  $\mu\text{M}$   $\text{Ac}_4\text{FucAz}$  (f), 100  $\mu\text{M}$   $\text{Ac}_3\text{ArabAz}$  (g), or 25  $\mu\text{M}$   $\text{Ac}_4\text{ManNAz}$  (h).

To determine the subcellular localization of  $\text{Ac}_4\text{GlcNAz}$ ,  $\text{Ac}_4\text{GlcNAz}$ -labeled roots (Fig. 3b) were counterstained with propidium iodide (Fig. 3c) (PI). This revealed that both signals showed overlap (Fig. 3d), indicating a location of  $\text{Ac}_4\text{GlcNAz}$  in or at the cell walls. During these labeling experiments we focused on studying the transition zone because strong labeling was observed in this region. Directly above this region a decline in labeling was observed, while the meristem zone showed only a slight decrease in labeling.

Encouraged by these results we decided to investigate incorporation and visualization of sugar analogues of L-arabinose and L-fucose. Both of these monosaccharides are commonly found in oligosaccharides of plants. More specifically, L-arabinose - mainly present in Arabidopsis as L-arabinofuranose - is one of the most common O-glycan sugars and an important constituent of plant cell wall polysaccharides.<sup>27-30</sup> Furthermore, an alkynylated fucose analog was the first successful metabolically incorporated sugar in Arabidopsis cell

walls.<sup>22</sup> Hence, we investigated whether the azido-analogues of L-fucose and L-arabinose may be metabolically incorporated into glycans by Arabidopsis seedling roots. To that end, the two corresponding azido analogues of these sugars were synthesized; Ac<sub>3</sub>ArabAz and Ac<sub>4</sub>FucAz (Fig. 2). Ac<sub>4</sub>FucAz was prepared by acetylating commercially available 6-azido-L-fucose, while the novel Ac<sub>3</sub>ArabAz was prepared according to an adapted procedure of 5-azido-D-arabinose by Smellie and co-workers.<sup>31</sup> With both azido-monosaccharides in hand, the feasibility of the incorporations of these compounds was investigated. Similar to the investigation of Ac<sub>4</sub>GlcNAz the optimal incorporation was determined by using different concentrations of Ac<sub>4</sub>FucAz (Appendix E, Figure S4) and Ac<sub>3</sub>ArabAz (Appendix E, Figure S5). Clear incorporation of Ac<sub>4</sub>FucAz was observed at the 25  $\mu$ M range (Fig. 3f), whereas reliable incorporation of Ac<sub>3</sub>ArabAz was only observed after incubation at a concentration of 100  $\mu$ M (Fig. 3g). This is most likely due to the relatively high abundance of naturally occurring L-arabinose compared to N-acetylglucosamine and L-fucose. As such, the relatively high concentration of L-arabinose would compete during incorporation of Ac<sub>3</sub>ArabAz at low concentrations of this probe.

L-Arabinofuranosyl residues are incorporated into plant arabinogalactan from UDP-Araf by glycosyltransferases. This nucleotide sugar donor is believed to be biosynthesized exclusively from the thermodynamically more stable pyranosyl form of the same donor; UDP-Arap. However, ArabAz is not able to convert to its pyranose configuration meaning that the corresponding pyranosyl UDP-ArabAz cannot exist. This raises the question how ArabAz is incorporated. Fincher and coworkers recently reported on the catalytic properties of an UDP-arabinose mutase (UAM) enzyme in Barley that catalyzes the multistep reversible UDP-Arap  $\rightarrow$  UDP-Araf reaction.<sup>32</sup> They state that a key step in this reaction presumably includes cleavage of the arabinosyl residue from UDP-Arap, which allows opening of the pyranosyl-ring, formation of the furanose ring, and reconnection of the arabinofuranosyl residue to the UDP molecule. Similar UDP-mutase enzymes (RGP) have been reported in other plant species, including Arabidopsis.<sup>33</sup> Consequently, ArabAz may be recognized by these enzymes and converted to UDP-ArabAz and thus enable metabolic incorporation.

Next, the results obtained with the three azido-monosaccharides were compared with an azido analog of N-acetyl-D-mannosamine; Ac<sub>4</sub>ManNAz (Fig. 3h and Appendix E, Figure S6). Ac<sub>4</sub>ManNAz differs in only one chiral centre compared to Ac<sub>4</sub>GlcNAz, however, no evidence exists in literature that the corresponding monosaccharide (ManNAc) is incorporated in Arabidopsis glycans. In addition, no evidence exist that mannosamine can be used as a precursor for the biosynthesis of other sugar derivatives in plants.<sup>34</sup> Indeed, Arabidopsis seedlings incubated with Ac<sub>4</sub>ManNAz showed no labeling. This confirms that Ac<sub>4</sub>ManNAz is indeed not present in Arabidopsis cell walls and supports the experiments described above that indicated that Ac<sub>4</sub>GlcNAz, Ac<sub>4</sub>FucAz and Ac<sub>3</sub>ArabAz incorporation is mediated by active metabolism.

### Azido-monosaccharide incorporation is time-dependent and mediated by passive or active transport

To investigate if active cellular metabolism is necessary for incorporation of azido-monosaccharides, whole seedlings were killed and fixated by 4% paraformaldehyde. These fixated seedlings could then be used to distinguish between two scenarios, one where incorporation takes place via an active glycan salvage pathway,<sup>12</sup> or alternatively, a scenario where azido-monosaccharides are passively absorbed onto external cell walls. Fixation resulted in slightly more background fluorescence, but the intensity of fixated seedlings incubated with Ac<sub>4</sub>GlcNAz was equal to fixated DMSO control seedlings (Appendix E, Figure S7). This suggests that Ac<sub>4</sub>GlcNAz is actively incorporated through the plant cell metabolism rather than through non-specific absorption of the azido-monosaccharide to the plant cell wall. Similar results have been reported for alkyne-monosaccharides and a different azido-monosaccharide in Arabidopsis.<sup>18-19, 22</sup>

Next, the optimal incubation time of Arabidopsis seedlings in MS with 25  $\mu$ M Ac<sub>4</sub>GlcNAz was determined (Fig. 4 & Appendix E, Figure S8). Visible incorporation (Fig. 4b) was observed after 4 h of incubation with 25  $\mu$ M Ac<sub>4</sub>GlcNAz, while no incorporation was observed after 2 h (Fig. 4a).

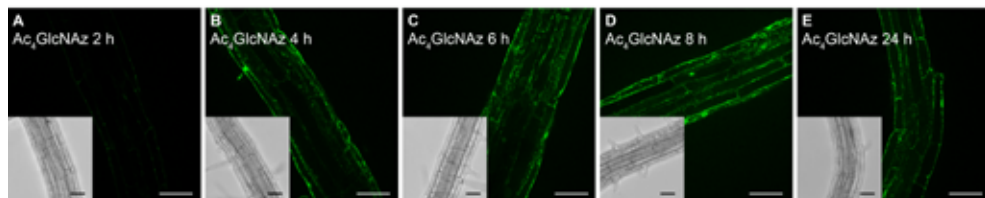


**Figure 4.** Optical sections of 4 day old Arabidopsis seedling roots incubated for 2 (a), 4 (b), 6 (c), 8 (d) and 24 h (e) with 25  $\mu$ M Ac<sub>4</sub>GlcNAz, followed by labeling through a copper-catalyzed click reaction with Alexa Fluor® 488 alkyne. Scale bars = 50  $\mu$ m.

The brightest fluorescence was observed after 6 and 8 h of incubation (Fig. 4c-d & Appendix E, Figure S8). This supports the idea that an active glycan salvage pathway is required for incorporation of Ac<sub>4</sub>GlcNAz. In a scenario involving passive adsorption weak fluorescence would already be expected after 2 h of incubation. Fluorescence decreased after 24 h incubation, which is most likely due to spreading of Ac<sub>4</sub>GlcNAz through the whole Arabidopsis root or an increased competition with natural *N*-acetyl-D-glucosamine synthesized by the plant itself. The time-dependent incorporation was also investigated for Ac<sub>4</sub>FucAz and Ac<sub>3</sub>ArabAz. In contrast to Ac<sub>4</sub>GlcNAz, incorporation of Ac<sub>4</sub>FucAz and Ac<sub>3</sub>ArabAz was visible after 2 h, but the best incorporation was observed after 24 h (Appendix E, Figure S9+10).

It is generally believed that the more hydrophobic acetylated monosaccharide probes, compared to their more polar non-acetylated version, end up inside plant cells via passive uptake.<sup>17-19</sup> Roberts et al. reported that root tissues of higher plants rapidly take up D-Glucosamine from

aqueous medium for incorporation into root tissue.<sup>35</sup> They also observed active uptake of *N*-acetyl-D-glucosamine, albeit 10 times slower, via the same pathway.<sup>35</sup> Since this indicated that *N*-acetylglucosamine – not acetylated at any of the hydroxyl groups – is actively taken up by the roots of Arabidopsis, we wondered whether the corresponding non-acetylated GlcNAz could also be incorporated similar to the fully acetylated analog, Ac<sub>4</sub>GlcNAz. To investigate this, Arabidopsis seedlings were incubated for 24 h with either 25  $\mu$ M Ac<sub>4</sub>GlcNAz or 25  $\mu$ M GlcNAz (Fig. 5a and b).

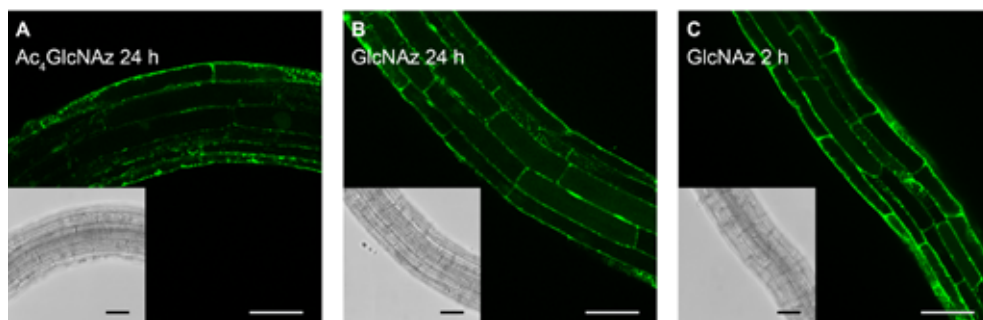


**Figure 5.** Optical sections of 4 day old Arabidopsis seedling roots incubated for 24 h with 25  $\mu$ M acetylated Ac<sub>4</sub>GlcNAz (a) or non-acetylated GlcNAz (b), followed by labeling through a copper-catalyzed click reaction with Alexa Fluor® 488 alkyne. Early incorporation with GlcNAz was observed with seedlings incubated for 2 h with 25  $\mu$ M GlcNAz (c). Scale bars = 50  $\mu$ m.

Incorporation was visible for both Ac<sub>4</sub>GlcNAz and GlcNAz with an almost similar fluorescent strength. This can indicate a maximum uptake for both sugar analogues after 24 h. It also suggests that GlcNAz is actively taken up via a cell membrane transport system as its polarity makes passing the fatty non-polar cell membranes via passive transport implausible. Non-acetylated GlcNAz uptake and incorporation was already visible after 2 h (Fig. 5c), this is in line with previous observations,<sup>35</sup> although GlcNAz is not directly comparable with *N*-acetyl-D-glucosamine. To determine the location of Ac<sub>4</sub>GlcNAz and GlcNAz incorporation the seedlings were stained with propidium iodide (PI) after the copper-catalyzed click reaction. Overlap of both incorporated monosaccharides with PI was observed, indicating cell wall labeling (Appendix E, Figure S11+12), and no differences in labeling pattern between Ac<sub>4</sub>GlcNAz and GlcNAz were observed. Taken together, this indicates that Arabidopsis is capable of active uptake of GlcNAz and it is probably salvaged and incorporated via the same pathway as Ac<sub>4</sub>GlcNAz.

### **Incorporation of Ac<sub>4</sub>GalNAz indicates GalNAc is metabolised in Arabidopsis**

*N*-Acetylgalactosamine (GalNAc) is not documented to be present in Arabidopsis glycans,<sup>12</sup> while GalNAc is found in several other higher plants<sup>36–37</sup> and in *N*-glycans of algae.<sup>38</sup> Glycosylation with GalNAc in Arabidopsis has only been documented in genetically engineered plant cell systems of this plant species.<sup>39</sup> Still, while it is not known whether GalNAc is incorporated into glycans, there is evidence for a UDP-GlcNAc nucleotidyltransferase in Arabidopsis that

is capable of converting GalNAc-1-P into its corresponding UDP-GalNAc.<sup>40</sup> In addition, a transporter was recently discovered in Arabidopsis that is capable of transporting both UDP-GlcNAc and UDP-GalNAc.<sup>21</sup> The presence of both an UDP-GalNAc transporter and the GalNAc-compatible transferase indicates that GalNAc might be salvaged or metabolized by Arabidopsis. For this reason, we investigated if this glycan metabolism could potentially be studied with a GalNAc-derived azido-monosaccharide, *N*-azidoacetyl-galactosamine ( $\text{Ac}_4\text{GalNAz}$ ).  $\text{Ac}_4\text{GalNAz}$  was prepared according to a procedure described by Bertozzi et al.<sup>26</sup> and then co-incubated with Arabidopsis seedlings for 24 h using different concentrations (2.5–100  $\mu\text{M}$ ; Appendix E, Figure S13). An incorporation signal for  $\text{Ac}_4\text{GalNAz}$  was observed after 24 h (Appendix E, Figure S13). However, the incubation time was prolonged because we observed lower fluorescence compared to the other azido-monosaccharides that we studied using the same incubation time. Increasing the incubation time to 48 h indeed improved the incorporation (Fig. 6).

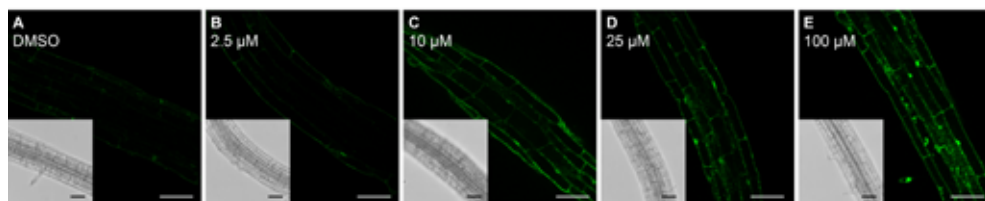


**Figure 6.** Optical sections of 4 day old Arabidopsis seedling roots incubated for 48 h with 2.5  $\mu\text{M}$  (b), 10  $\mu\text{M}$  (c), 25  $\mu\text{M}$  (d), and 100  $\mu\text{M}$  (e)  $\text{Ac}_4\text{GalNAz}$ , followed by labeling through a copper-catalyzed click reaction with Alexa Fluor® 488 alkyne. As a control, seedlings were treated with 0.01 % DMSO (a). Scale bars = 50  $\mu\text{m}$ .

This might indicate that salvage and incorporation of  $\text{Ac}_4\text{GalNAz}$  - compared to the monosaccharide analogs known to be present in Arabidopsis glycans - takes place via a lengthier pathway. The pathway may include an unknown epimerase that converts *N*-acetylgalactosamine, or a derivative thereof, to the corresponding *N*-acetylglucosamine epimer. An epimerase has been discovered in barley that reversibly interconverts UDP-GalNAc and UDP-GlcNAc and of which a homolog exist in Arabidopsis.<sup>41</sup> Maximum incorporation with 25  $\mu\text{M}$   $\text{Ac}_4\text{GalNAz}$  was observed in a time-frame of 24 h (Appendix E, Figure S13d), whereas 100  $\mu\text{M}$   $\text{Ac}_4\text{GalNAz}$  was required (Fig. 6e) to reach saturation with an incubation time of 48 h. The relative high concentration required after 48 h, is consistent with the other lengthier time incubation experiments with azido-monosaccharides.

### **Copper-free click reactions are good alternatives to label glycans in Arabidopsis roots**

A drawback of the studies reported until now that use monosaccharide probes to image plant glycans is that they all use a copper-catalyzed click reaction to attach the fluorescent reporter group to the metabolically incorporated glycans. The copper required to catalyze this reaction is known to be toxic to Arabidopsis and therefore might influence the outcome of the labeling



and imaging experiments in which it is used. This side effect is indeed also observed by us in the slightly inhomogeneous labeling after the copper-catalyzed click reaction, which damages the cell wall and in a few instances also caused minor internal labeling. The toxic effect that copper has on Arabidopsis seedlings was also observed by Anderson and coworkers,<sup>18,22</sup> who applied copper-catalyzed reactions to label alkyne-monosaccharides. To circumvent the use of copper ions, an alternative copper-free click reaction, the so-called strain-promoted alkyne-azide cycloaddition (SPAAC) has been developed, which is bio-orthogonal and can be applied to living cells.<sup>42</sup> It has not been applied towards azido-monosaccharide analog probes in Arabidopsis so far. This reaction is still rapid enough for biological applications, for instance when an azide-containing probe is reacted with an aliphatic cyclooctyne (BCN)<sup>43</sup> or dibenzocyclooctyne (DBCO).<sup>44-45</sup> Labeling of azido-monosaccharides *via* SPAAC has an advantage compared to the copper-catalyzed click reaction, since it does not damage living cells. However, while the alkyne-monosaccharides reported earlier cannot utilize SPAAC, our azido-monosaccharide probes do have the potential to be labeled through this click reaction. To investigate copper-free labeling of plant glycans *via* SPAAC, seedlings were labeled after incubation with Ac<sub>4</sub>GlcNAz (25  $\mu$ M, 24 h), Ac<sub>4</sub>FucAz (25  $\mu$ M, 24 h), Ac<sub>3</sub>ArabAz (100  $\mu$ M, 24 h) or Ac<sub>4</sub>GalNAz (25  $\mu$ M, 24 h) with a solution containing 1  $\mu$ M DBCO-PEG4-ATTO-488 in MS for 1 h. The resulting metabolically-labeled seedlings showed bright fluorescence and low background (Fig. 7a-d). In contrast, seedlings incubated with 0.01% DMSO showed only background fluorescence (Fig. 7e).

Comparison of seedlings labeled with Ac<sub>4</sub>GlcNAz and Ac<sub>3</sub>ArabAz with propidium iodide-labeled seedlings showed excellent overlap, indicating incorporation of the azido-monosaccharides in the cell wall glycans (Fig. 7h-j and Appendix E, Figure S14). Experiments with a more apolar DBCO-fluorophore without a PEG-spacer and a BCN-derived fluorophore were not successful and extensive non-specific absorption of the fluorophore (also as micelles) to the cell wall was observed.

In addition to SPAAC, other bio-orthogonal copper-free click reactions are also known. The inverse electron demand Diels-Alder (invDA) reaction between tetrazines and strained alkenes/alkynes has gained popularity as a very fast and bio-orthogonal complementary reaction to SPAAC.<sup>46</sup> We investigated whether this reaction could also be used for labeling plant glycans. Tetrazines conjugated to a fluorescent reporter group are typically used for labeling and we choose the smallest possible tetrazine reaction partner, a methyl-cyclopropene, as a chemical handle on an *N*-acetylglucosamine derivative. Known GlcNAc derivative with a methyl-cyclopropene (GlcNCyc), was prepared via an adapted procedure of Prescher<sup>47</sup> and Wittmann and co-workers.<sup>48</sup> Arabidopsis seedlings incubated with GlcNCyc for 24 h showed bright fluorescence, when clicked with 15  $\mu$ M Tetrazine-ATTO-488 (Fig. 7g), while a DMSO control did not show appreciable fluorescence (Fig 7f). Besides, compared to the other clickable dyes used in this study, it was observed that Alexa® Fluor-tetrazine was less



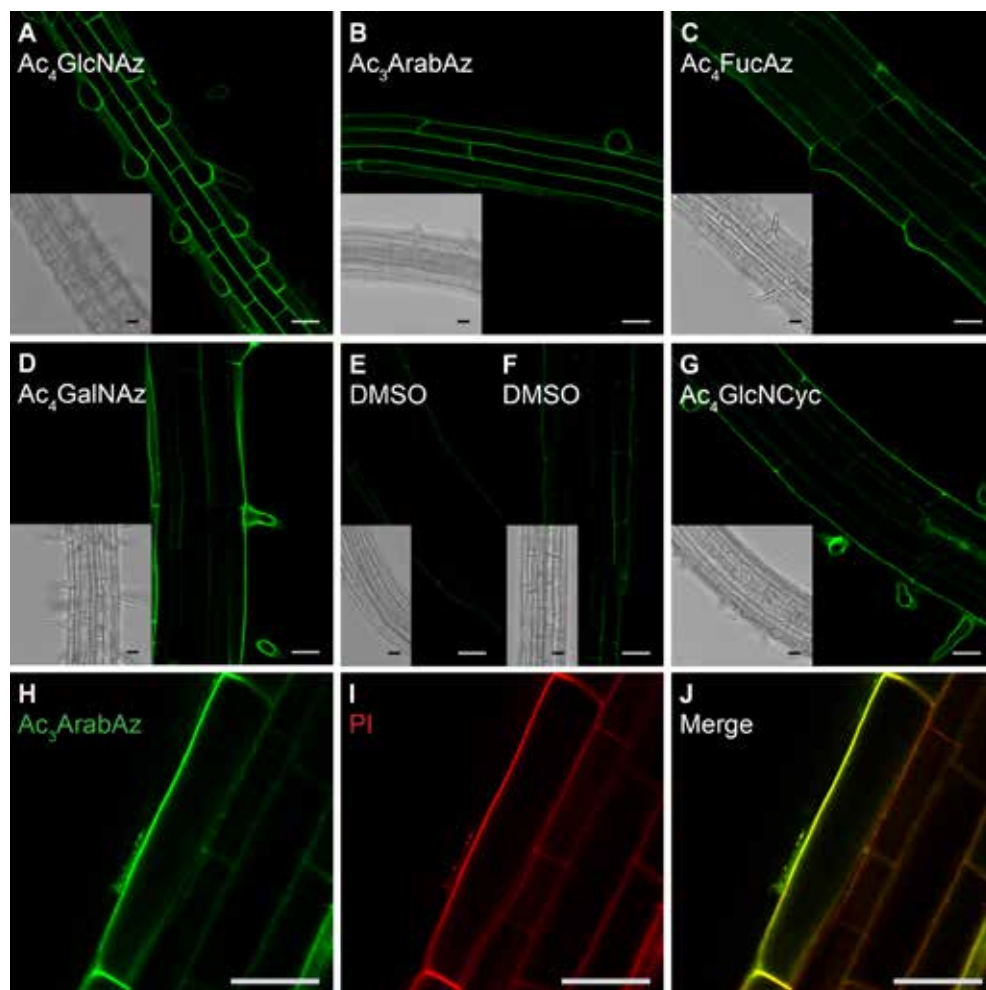


**Figure 7.** Optical sections of 4 day old *Arabidopsis* seedling roots incubated for 24 h with 25  $\mu$ M acetylated  $Ac_4$ GlcNAz (a), 100  $\mu$ M  $Ac_3$ ArabAz (b), 25  $\mu$ M  $Ac_4$ FucAz (c), 25  $\mu$ M  $Ac_4$ GalNAz (d) or 50  $\mu$ M GlcNCyc (g) followed by labeling through strain-promoted alkyne-azide cycloaddition with DBCO-PEG4-ATTO-488 (a-d) or an inverse electron demand Diels-Alder click reaction with Tetrazine-ATTO-488 (g). As a control, seedlings were treated with 0.01 % DMSO followed by labeling through strain-promoted alkyne-azide cycloaddition with DBCO-PEG4-ATTO-488 (e) or an inverse electron demand Diels-Alder click reaction with Tetrazine-ATTO-488 (f). Seedling roots treated with DBCO-PEG4-ATTO-488 labeled  $Ac_3$ ArabAz (100  $\mu$ M, 24 h) (f, j) counterstained Propidium Iodide (PI, 0.05%) to visualize cell walls (i, j). Yellow color indicates overlap of the two dyes (j). Scale bars = 25  $\mu$ m.

prone to stick to the cell wall and more water soluble than alkyne and DBCO dyes. This has the advantage that the fluorophore can be used at higher concentrations. These preliminary experiments with the SPAAC and invDA copper-free click reactions resulted in a more uniform staining. In addition, these mild labeling reactions do not require cytotoxic copper, which enables experiments that go beyond snapshot images of plant seedlings.

## Conclusions

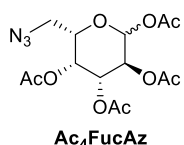
In this study, the toolbox of clickable monosaccharide analogs for glycan labeling in Arabidopsis seedlings has been expanded to allow the incorporation and direct visualization of five relevant plant monosaccharide analogs in complex cell wall-bound glycans. The clickable glycan analogs Ac<sub>4</sub>GlcNAz, Ac<sub>3</sub>ArabAz, Ac<sub>4</sub>FucAz and Ac<sub>4</sub>GalNAz were successfully metabolically incorporated and visualized in glycans of Arabidopsis seedling roots. The novel Ac<sub>3</sub>ArabAz for the first time allows for direct imaging of L-arabinose, one of the most common plant O-glycans and an important constituent of plant cell wall polysaccharides.<sup>27-30</sup> The incorporation of Ac<sub>4</sub>GalNAz we observe supports the possibility of an epimerase in Arabidopsis that converts GalNAz to GlcNAz. During the preparation of this manuscript Chen and coworkers reported on the metabolic incorporation and imaging of N-linked glycans in Arabidopsis with Ac<sub>4</sub>GlcNAz.<sup>24</sup> Our here reported results with this azido-monosaccharide are in correspondence with their work, and provide additional details on Ac<sub>4</sub>GlcNAz metabolic incorporation and imaging through the glycan salvage pathway. For example, we show that Ac<sub>4</sub>GlcNAz is already being incorporated after 4 h and that GlcNAz (non-acetylated) can also be salvaged, probably via active transport, within 2 h. Finally, earlier reports on the metabolic incorporation and imaging of monosaccharide analogs, including Ac<sub>4</sub>GlcNAz, rely solely on labeling through copper-catalyzed click chemistry. Although copper-catalyzed click reactions often work well, the toxicity of copper here led to damage of the cell wall, emphasizing the need for copper-free clickable analogs for long-term or spatiotemporal experiments. We here show for the first time that the strain-promoted azide-alkyne cycloaddition (SPAAC) and inverse electron demand Diels-Alder (invDA) click reactions allow for improved imaging of metabolic labeling with our azido-monosaccharides and a cyclopropene-GlcNAc derivative. The application of these improved copper free labeling methods can be generalized and extended to already existing and future click chemistry-enabled monosaccharide analogs in Arabidopsis. Taken together with the fact that the SPAAC and invDA reactions are bio-orthogonal *and* orthogonal with respect to each other, this will allow for *in vivo* and dual plant glycan labeling applications. Overall our results here and other recently published studies<sup>18-19,24</sup> promise a bright future for the Metabolic Oligosaccharide Engineering (MOE) methodology to enable the direct spatiotemporal imaging of complex glycans in living plants.<sup>16</sup>

## General information and methods

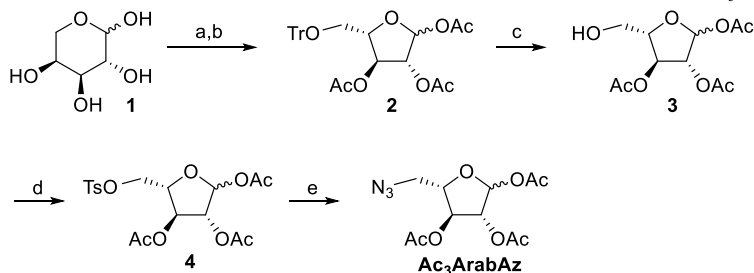
All moisture-sensitive reactions were carried out under an argon atmosphere, using oven-dried glassware, unless otherwise stated. Dichloromethane ( $\text{CH}_2\text{Cl}_2$ , Sigma-Aldrich, >99.8%) was purified over aluminum oxide under argon using a Pure Solv 400 solvent purification system (Innovative Technology, Amesbury, USA). Reagents were obtained from commercial sources and used without further purification unless stated otherwise. Analytical TLC was performed using prepared plates of silica gel (Merck 60 F-254 on aluminium) and then, according to the functional groups present on the molecules, revealed with UV light or using staining reagents: ninhydrin (5% in EtOH) for amines,  $\text{H}_2\text{SO}_4$  for monosaccharides or a basic solution of  $\text{KMnO}_4$  (0.75% in  $\text{H}_2\text{O}$ ) for general staining. Merck silica gel 60 (70–230 mesh) was used for flash chromatography.  $^1\text{H}$  NMR and  $^{13}\text{C}$  NMR spectra were recorded on a Bruker Avance III 400 spectrometer (observation of  $^1\text{H}$  nucleus 400 MHz, and of  $^{13}\text{C}$  nucleus 100 MHz). Chemical shifts are reported in parts per million (ppm), calibrated on the residual peak of the solvent, whose values are referred to tetramethylsilane (TMS,  $\delta_{\text{TMS}} = 0$ ), as the internal standard.  $^{13}\text{C}$  NMR spectra were performed with proton decoupling. Where indicated, NMR peak assignments were made using COSY and HSQC experiments.

## General information for synthesis

$\text{Ac}_4\text{GlcNAz}$ ,  $\text{Ac}_4\text{GalNAz}$  and  $\text{GlcNCyc}$  were prepared according to literature procedures.<sup>26</sup>  $\text{GlcNCyc}$  was prepared according to a literature procedure by Presher<sup>47</sup> and Wittmann et al.,<sup>48</sup> while the synthesis of one of the intermediates in this synthesis – the cyclopropane tag – has been adapted and is described below. The synthesis of  $\text{Ac}_4\text{FucAz}$ ,  $\text{Ac}_3\text{ArabAz}$  are described below.



**Synthesis of 1,2,3,4-tetra-O-acetyl-6-azido-L-fucose ( $\text{Ac}_4\text{FucAz}$ ).** 6-Azido-L-fucose (10.0 mg, 0.0448 mmol) was added to a mixture with pyridine (0.40 mL, 2.48 mmol, 100 equiv), acetic anhydride (0.20 mL, 2.12 mmol, 400 equiv) and 4-dimethylaminopyridine (0.1 mg, 0.008 mmol, 0.01 equiv). The mixture was stirred at room temperature for 24 hours under an argon atmosphere. The mixture was then cooled in an ice-bath for 1 hour and then extracted with dichloromethane (20 mL, 3×). The combined organic layers were washed with sat. aq.  $\text{NaHCO}_3$  (20 mL), brine (20 mL), dried ( $\text{MgSO}_4$ ) and then conc. *in vacuo*. The residue was purified by flash column chromatography (33% ethyl acetate in heptane) providing 1,2,3,4-tetra-O-acetyl-6-azido-D-fucose (10.3 mg, 0.0276 mmol, 62%) as a yellow oil.  $^1\text{H}$  NMR ( $\text{CDCl}_3$ , 400 MHz): 6.31 (s, 1H, H-1), 5.34 (s, 1H, H-3), 5.25 (d,  $J = 1.2$  Hz 2H, H-2, H-4), 4.14 (t,  $J = 6.8$  Hz 1H, H-5), 3.37 (dd,  $J = 5.2, 12.8$  Hz, 1H,  $-\text{CH}_2\text{N}_3$ ), 3.13 (dd,  $J = 7.2, 12.8$  Hz, 1H,  $-\text{CH}_2\text{N}_3$ ), 2.09–2.03 (m, 6H, 2x  $-\text{CO}-\text{CH}_3$ ), 1.96–1.92 (m, 6H, 2x  $-\text{CO}-\text{CH}_3$ ).  $^{13}\text{C}$  NMR ( $\text{CDCl}_3$ , 100 MHz): 89.7 (C-1), 70.3 (C-5), 68.3 (C-3), 67.5, 66.5 (C-2, C-4), 50.5 ( $\text{CH}_2\text{N}_3$ ), 20.9, 20.7, 20.7, 20.6 (4x  $\text{CH}_3$ ).

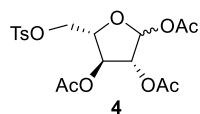
Overview of the synthesis route towards **Ac<sub>3</sub>ArabAz**.**Scheme 1.** Synthesis scheme for 1,2,3-tri-*O*-acetyl-5-azido-5-deoxy-L-arabinofuranose **Ac<sub>3</sub>ArabAz**.

Reagents and conditions: (a) Tritylchloride, pyridine, 63 h; (b) acetic anhydride, pyridine, 16 h, 19% for a,b; (c) 80% aqueous acetic acid, 100 °C, 0.5 h, 36%; (d) tosyl chloride, pyridine, dichloromethane, 48 h, 65%; (e) sodium azide, DMSO, 80 °C, 24 h, 24%.

**Synthesis of 1,2,3-tri-*O*-acetyl-5-*O*-trityl-L-arabinofuranose (2).** L-Arabinose (**1**) (5.00 g, 33.5 mmol) was refluxed in pyridine (175 mL) until it was completely dissolved. The dissolved L-arabinose was allowed to cool to room temperature followed by the addition of trityl chloride (9.30 g, 33.5 mmol). The reaction was stirred for 63 h under an argon atmosphere. The reaction was quenched with methanol (12.5 mL). The solvents were removed *in vacuo*. The residual oily substance was dissolved in ethyl acetate (100 mL) and washed with demi water (600 mL). The organic layer was dried over MgSO<sub>4</sub> and the remaining solvent was conc. *in vacuo* and the sticky product 5-*O*-trityl-L-arabinose was purified by flash column chromatography (50%, 40–60 light petrol in ethyl acetate). The product was then directly dissolved in pyridine (20 mL) and cooled to 0 °C. Acetic anhydride (4.5 mL) was slowly added and the reaction was stirred for 16 h under an argon atmosphere while allowing the reaction warming to room temperature. Afterwards the solvent was removed azeotrope (50 % toluene in ethanol, 3 ×) and dissolved in DCM (25 mL). The solution was washed with saturated NaHCO<sub>3</sub> (50 mL, 2 ×), dried over MgSO<sub>4</sub> and conc. *in vacuo*. The crystal product was purified by flash column chromatography (20 % ethyl acetate in heptane) to obtain 1,2,3, Tri-*O*-acetyl-5-*O*-trityl-L-arabinofuranose **2** (3.10 g, 6.15 mmol) as white crystals. Yield over two steps was 19%. <sup>1</sup>H NMR (CDCl<sub>3</sub>, 400 MHz): 7.48–7.45 (m, 6H, ArH), 7.32–7.22 (m, 9H, ArH), 6.38 (d, *J* = 4.8 Hz, 1H, H-1β), 6.22 (s, 1H, H-1α), 5.57 (t, *J* = 6.8 Hz, 1H, H-3β), 5.34 (dd, *J* = 4.8, 7.2 Hz, 1H, H-2β), 5.28 (d, *J* = 4.8 Hz, 1H, H-3α), 5.20 (d, *J* = 4.0 Hz, 1H, H-2α), 4.32 (dd, *J* = 4.8, 9.4 Hz, 1H, H-4α), 4.14 (dd, *J* = 5.2, 12.6 Hz, 1H, H-4β), 3.39–3.30 (m, 4H, H-5abα,β), 2.12–2.03 (6xs, 18H, 3x OAcα, 3x OAcβ). <sup>13</sup>C NMR (CDCl<sub>3</sub>, 100 MHz): 128.9–127.0 (15xC ArH), 99.5 (C-1α), 93.7 (C-1β), 83.6 (C-4β), 81.1 (C-2α), 80.7 (C-4β), 77.2 (C-3α), 75.6 (C-2β), 74.5 (C-3β), 64.4 (C-5β), 62.8 (C-5α), 21.1–20.5 (3x OAcα, 3x OAcβ).

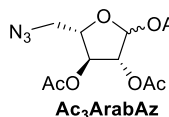
**Synthesis of 1,2,3-tri-*O*-acetyl-L-arabinofuranose (3).** 1,2,3-Tri-*O*-acetyl-5-*O*-trityl-L-arabinofuranose (3.10 g, 6.15 mmol) was stirred in refluxing (100 °C) 80% aqueous acetic acid (30 mL) for 30 minutes. After 30 minutes the solution was immediately cooled in an ice bath. The by product (trityl-alcohol) was filtered off and brine (30 mL) was added. The product was extracted with DCM (10 mL, 3 ×) and the combined layers were washed carefully with saturated NaHCO<sub>3</sub> (10 mL, 3 ×), dried over MgSO<sub>4</sub> and conc. *in vacuo*. Purification was done by silica chromatography (33% ethyl acetate in heptane) to obtain 1,2,3-tri-*O*-acetyl-L-arabinofuranose **3** (0.605 g, 2.19 mmol, 36%) as a transparent oil. <sup>1</sup>H NMR (CDCl<sub>3</sub>, 400 MHz):

6.38 (d,  $J = 3.6$  Hz, 1 H, H-1 $\beta$ ), 6.18 (s, 1 H, H-1 $\alpha$ ), 5.39 (d,  $J = 4.8$  Hz, 1H, H-2 $\beta$ ), 5.25 (s, 1H, H-2 $\alpha$ ), 5.12 (d,  $J = 5.2$  Hz, 1H, H-3 $\alpha$ ), 4.23 (dd,  $J = 4.0, 8.6$  Hz, 1H, H-4 $\alpha$ ), 3.90 (d,  $J = 12.4$  Hz, 1H, H-4 $\beta$ ), 3.82-3.74 (m, 4 H, H-5ab $\alpha,\beta$ ), 2.15-2.02 (6x s, 18H, 3x OAc $\alpha$ , 3x OAc $\beta$ ).  $^{13}\text{C}$  NMR ( $\text{CDCl}_3$ , 100 MHz): 99.2 (C-1 $\beta$ ), 93.4 (C-1 $\alpha$ ), 85.0 (C-4 $\alpha$ ), 82.5 (C-3 $\beta$ ), 81.0 (C-2 $\alpha$ ), 75.4 (C-3 $\alpha$ ), 74.4 (C-2 $\beta$ ), 63.3, 61.7, 60.4 (C-4 $\alpha$ , C-5 $\alpha$ , C-5 $\beta$ ), 21.0, 20.9, 20.8, 20.7, 20.6, 20.4 (3x OAc $\alpha$ , 3x OAc $\beta$ ).



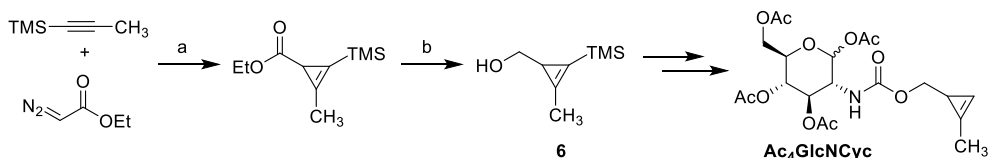
**Synthesis of 1,2,3-tri-O-acetyl-5-O-tosyl-L-arabinofuranose (4).** 1,2,3-Tri-O-acetyl-L-arabinofuranose (0.250 g, 0.905 mmol) was dissolved in 7.5 mL dry DCM and 0.75 mL pyridine followed by the addition of tosyl chloride (0.317 g, 1.6 mmol, 1.5 equiv). The reaction was stirred for 48 hours at room temperature under

an atmosphere of argon. Distilled water (20 mL) was added to the reaction mixture and the product was extract with DCM (10mL, 3 $\times$ ). The organic layers were combined and washed with 1M HCl (30 mL), sat.  $\text{NaHCO}_3$  (30 mL) and brine (30 mL) before drying with  $\text{MgSO}_4$  and conc. *in vacuo*. Purification was done by flash column chromatography (50% ethyl acetate in heptane) to obtain 1,2,3-tri-O-acetyl-5-O-tosyl-L-arabinofuranose **4** (0.253 g, 0.588 mmol, 65%) as a transparent, sticky oil.  $^1\text{H}$  NMR ( $\text{CDCl}_3$ , 400 MHz): 7.79 (d, 2H,  $J = 7.2$  Hz, ArH), 7.35 (d, 2H,  $J = 8.0$  Hz, ArH), 6.33 (d, 1H,  $J = 4.0$  Hz, H-1 $\beta$ ), 6.12 (s, 1H, H-1 $\alpha$ ), 5.31 (dd, 1H,  $J = 7.2, 7.2$  Hz), 5.16 (s, 1H, H-2 $\alpha$ ), 5.00 (d, 1H,  $J = 4.4$  Hz, H-3 $\alpha$ ), 4.33-4.13 (m, 7H, H-3 $\beta$ , H-4 $\alpha$ , H-5aa, H-5ab, H-4 $\beta$ , H-5aa, H-5b $\beta$ ), 2.45 (s, 3H,  $\text{H}_3\text{C-ArH}$ ), 2.11-2.05 (6x s, 18 H, 3x OAc $\alpha$ , 3x OAc $\beta$ )  $^{13}\text{C}$  NMR ( $\text{CDCl}_3$ , 100 MHz): 129.8 (ArH), 128.0 (ArH), 99.3 (C-1 $\alpha$ ), 93.3 (C-1 $\beta$ ), 80.2 (C-2 $\alpha$ ), 77.2 (C-3 $\alpha$ ), 74.3 (C-2 $\beta$ ), 82.5, 79.3, 75.0, 69.3, 68.0 (C-4 $\alpha$ , C-5 $\alpha$ , C-3 $\beta$ , C-4 $\beta$ , C-5 $\beta$ ), 20.9-20.4 (3x OAc $\alpha$ , 3x OAc $\beta$ ).



**Synthesis of 1,2,3-tri-O-acetyl-5-azido-5-deoxy-L-arabinofuranose (Ac<sub>3</sub>ArabAz).**

1,2,3-Tri-O-acetyl-5-O-tosyl-L-arabinofuranose (0.100 g, 0.24 mmol) and sodium azide (0.064 g, 0.91 mmol) were heated to 80  $^\circ\text{C}$  in DMSO (1.5 mL) and stirred for 24 hours. Upon cooling of the reaction after 24 hours, the reaction mixture was diluted with DCM (10 mL) and washed with demi water (40 mL). The organic layer was dried over  $\text{MgSO}_4$  and concentrated. Purification was done by wet column chromatography (33 % ethyl acetate in heptane). Fractions containing product were conc. *in vacuo*. The concentrated material was purified further by flash column chromatography (20 % ethyl acetate in heptane) to obtain 1,2,3-tri-O-acetyl-5-azido-5-deoxy-L-arabinofuranose **Ac<sub>3</sub>ArabAz** (0.017 g, 0.056 mmol, 24%) as a colourless sticky oil.  $^1\text{H}$  NMR ( $\text{CDCl}_3$ , 400 MHz): 6.41 (d, 1H,  $J = 7.6$  Hz, H-1 $\beta$ ), 6.22 (s, 1H, H-1 $\alpha$ ), 5.37 (dd, 1H,  $J = 4.4, 8.0$  Hz), 5.22 (d, 1H,  $J = 1.2$  Hz, H-2 $\alpha$ ), 5.05 (d, 1H,  $J = 4.4$  Hz, H-3 $\alpha$ ), 4.29 (dd, 1H,  $J = 4.0, 8.0$  Hz, H-4 $\alpha$ ), 4.14-4.09 (m, 1H, H-3 $\beta$ ), 3.68 (dd, 1H,  $J = 3.2, 13.4$  Hz, H-5 $\alpha$ ), 3.49-3.43 (m, 1H, H-5 $\beta$ ), 2.14, 2.12, 2.12, 2.11, 2.10, 2.09 ((6xs, 18H, 3x OAc $\alpha$ , 3x OAc $\beta$ )  $^{13}\text{C}$  NMR ( $\text{CDCl}_3$ , 100 MHz): 99.2 (C-1 $\alpha$ ), 93.5 (C-1 $\beta$ ), 84.1 (C-4 $\alpha$ ), 80.8 (C-3 $\beta$ ), 80.6 (C-2 $\alpha$ ), 77.2 (C-3 $\alpha$ ), 74.8 (C-2 $\beta$ ), 75.1 (C-4 $\beta$ ), 53.0 (C-5 $\beta$ ), 51.3 (C-5 $\alpha$ ), 21.0-20.4 (3x OAc $\alpha$ , 3x OAc $\beta$ ).

**Adapted synthesis of 3-hydroxymethyl-2-methyl-trimethylsilylcyclopropene (6).****Scheme 2.** Synthesis scheme for 3-hydroxymethyl-2-methyl-trimethylsilylcyclopropene (6).

Reagents and conditions: (a) Rhodium(II) acetate dimer, DCM, 12 h; (b) DIBAL-H, Et<sub>2</sub>O, 2 h, 96% over two steps. Intermediate **6** was converted into Ac<sub>4</sub>GlcNCyc using previously reported procedures.<sup>47,48</sup>

An oven-dried 50 mL round bottom flask was placed under vacuum and backfilled with argon. Rhodium(II) acetate dimer (15 mg, 0.034 mmol) was added to the flask under an argon flow. Next, trimethyl silyl propyne (4 mL, 27.01 mmol) was added and the resulting suspension was stirred slowly. A solution of ethyl diazoacetate (1.1 mL, 13% in DCM, 9.06 mmol) was diluted with 15 mL anhydrous DCM into a separate oven dried round bottom flask under argon. This solution was transferred to a 20 mL syringe and very slowly added over roughly 12 h to the roundbottom flask containing the suspension using a syringe pump (20  $\mu$ L/min, NE-1000 Multi-Phaser™) under a gentle argon flow. During the addition period the observed colour of the reaction mixture went from a colourless solution with a dark purple solid to a dark green reaction mixture and towards the end to a yellow-greenish reaction mixture. After the addition, the rhodium catalyst was separated by passing the reaction mixture over a silica gel plug (40 mL) and flushing with 100 mL DCM. The collected eluent was gently concentrated under a reduced pressure at room temperature to yield the crude intermediate as an oil that was used in the next reaction without further purification ( $R_f$  0.8 in 3:7 EtOAc:PE, KMnO<sub>4</sub> stain).

Di-isobutyl aluminium-hydride (18 mL, 1M in THF, 18 mmol) was added to anhydrous diethyl ether (15 mL) in an oven-dried roundbottom flask and cooled to 4 °C under an argon atmosphere. The complete crude ethyl TMS-cyclopropene acetate product from the previous reaction was dissolved in anhydrous diethyl ether (5 mL) and added dropwise over 5 min to the DIBAL-H containing flask. The reaction mixture was stirred for 2 hours at 4 °C under an argon atmosphere. Conversion to **6** was monitored by TLC ( $R_f$  ethyl TMS-cyclopropene acetate = 0.8;  $R_f$  **6** = 0.6, in 30:70 EtOAc: PE, KMnO<sub>4</sub> stain), and shown to be incomplete. Accordingly, additional DIBAL-H (7 mL; 7 mmol) was slowly added to the reaction mixture at 4 °C, after which TLC indicated complete conversion in under ten minutes. The reaction mixture was quenched by addition of a saturated aqueous solution of Rochelle's salt (300 mL) under vigorous stirring. A white gel formed in the aqueous layer. The biphasic system was separated and the water layer was extracted with EtOAc (50 mL, 3 $\times$ ). The combined organic layers were dried (NaSO<sub>4</sub>), filtered and gently evaporated under reduced pressure at room temperature. The resulting residue was purified using flash silica gel column chromatography (eluent: 10  $\rightarrow$  30% EtOAc in PE) to provide **6** in 96% yield over two steps (1.37 g, 8.76 mmol) as a pale yellow liquid with a pine-like odour. <sup>1</sup>H NMR (CDCl<sub>3</sub>, 400 MHz): 3.46 (q, 2H), 2.19 (s, 3H), 1.54 (t, 1H), 0.15 (s, 9H). Characterization is in agreement with previously reported <sup>1</sup>H NMR spectrum.<sup>47</sup>

**Growth of Arabidopsis Thaliana**

Wild type *Arabidopsis thaliana* (Col-0) seeds were surface sterilized in a mixture of commercial bleach and ethanol (v/v; 1/4) for 15 minutes followed by washing with ethanol (2 times) and drying. First a cold shock was applied on all sterilized seeds by placing them in a fridge (5 °C) for at least 2 days with a

maximum of one week while on filter paper, pre-wetted with 2 mL Milli-Q water, in a petri dish. Seeds were grown on half Murashige and Skoog medium (MS)<sup>49</sup> with vitamins in a petri dish (0.8 % plant agar) in a climate room on the shelf lit by Philips 36W/840 lamps (120  $\mu\text{mol}/\text{m}^2 \text{ sec}$ ) under long-day conditions (16h light/8h dark) at 22 °C. Young seedlings of 4 or 5 days old were used for incubation experiments.

### Incubation of *Arabidopsis*

Five young seedlings were put together in single well of a 24-well plate containing click-compatible azido-monosaccharide in half MS. After incubation time, 5 wells were filled with 2 mL half MS medium containing 0.05% Tween 20. Plants were dipped in each well for 15 seconds to wash away the excess of azido-monosaccharide. The seedlings were directly transferred to a new 24-well plate for labeling through either a 1) copper-catalyzed click-labeling 2) a SPAAC labeling or 3) a Diels alder-cycloaddition labeling.

### Copper-catalyzed click-labeling

Click-iT cell reaction kit (supplier: Invitrogen) was used for all copper-catalyzed “click” reactions. The labeling was carried out according to the procedure in the manual of Invitrogen except for the reaction time that was prolonged to 45 minutes. For the Alexa-fluor 488 fluorophore a concentration of 0.1  $\mu\text{M}$  was found to be the most optimal. The excess of fluorophore was removed by washing the seedlings 4× in 2 mL half MS containing 0.05% Tween 20. Duration of the sequential washings steps were respectfully 5, 10, 5 and 10 minutes. After washing the seedlings were stored for with a maximum time of 2 h in half MS (not containing Tween 20) before visualization by confocal microscopy.

### SPAAC labeling

SPAAC reactions were performed in 2 mL of 1  $\mu\text{M}$  DBCO-PEG4-ATTO-488 in half MS medium. Reaction time was 1 hour. Washing and storage was similar to the copper-catalyzed click reaction described above. The washing times were prolonged to 4 × 10 minutes.

### Diels-Alder cycloadditions

Reactions were performed in 1 mL of 15  $\mu\text{M}$  Tetrazine-ATTO-488 in half MS medium. All other procedures were similar to the SPAAC reactions described above.

### Seedling fixation with paraformaldehyde

As a negative control, seedlings were fixated in 4% paraformaldehyde solution in PBS (commercially available). Five seedlings were put together in 2 mL of the paraformaldehyde solution for 30 minutes. Afterwards seedlings were washed two times in 2 mL 0.5 MS before incubation with click-compatible azido-monosaccharides as discussed before.

### Toxicity test

Toxicity tests were performed based on growth of the plant. Agar plates containing the described azido-monosaccharides analogs were used for the growth experiments with young *Arabidopsis* seedlings for 8 days. Azido-monosaccharides were added after sterilization of the medium, when it was cooled down

to approximately 60 °C and before pouring the medium in a petri dish. *Arabidopsis* seedlings were subsequently germinated and grown on agar plates containing the different azido-monosaccharide solutions in ½ MS with 0.8% plant agar. After 8 days of growth, the white part of the root was measured from leaves till root tip.

### **Microscopy and image analysis**

Roots of seedlings were imaged with a Leica TCS SP8 confocal microscope (488 nm laser excitation, 534-571 emission filter and 600-650 emission filter for PI) using a 40X water immersion objective. Image J was used to process images. All images within the same experiment were adjusted to the same color balance. Mean fluorescence was calculated in Image J ([rsbweb.nih.gov/ij](http://rsbweb.nih.gov/ij)) using freehand tool to select the cell boundary of epidermal cells and to measure the mean pixel intensity. The standard deviation was determined based on the difference in the fluorescence intensity throughout the cells of a seedling. Data of those cells were collected from 3-4 seedlings per treatment and imaged using identical exposure settings.



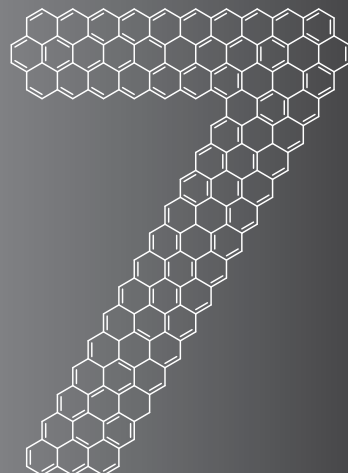
## References

1. Apweiler, R., Hermjakob, H., and Sharon, N. *Biochim. Biophys. Acta* **1999**, 1473, 4.
2. Gabius, H.J., Andre, S., Kaltner, H., and Siebert, H.C. *Biochim. Biophys. Acta* **2002**, 1572, 165.
3. Rolland, F., Baena-Gonzalez, E., and Sheen, J. *Annual review of plant biology* **2006**, 57, 675.
4. Nguema-Ona, E., Coimbra, S., Vicré-Gibouin, M., Mollet, J.-C., and Driouich, A. *Annals of Botany* **2012**, 110, 383.
5. Bais, H.P., Weir, T.L., Perry, L.G., Gilroy, S., and Vivanco, J.M. *Annual review of plant biology* **2006**, 57, 233.
6. Grobelak, A., Napora, A., and Kacprzak, M. *Ecol. Eng.* **2015**, 84, 22.
7. Chesson, A., Gardner, P.T., and Wood, T.J. *J. Sci. Food Agric.* **1997**, 75, 289.
8. Rapoport, T.A. *Nature* **2007**, 450, 663.
9. Boundy, J.A., Wall, J.S., Turner, J.E., Woychik, J.H., and Dimler, R.J. *J. Biol. Chem.* **1967**, 242, 2410.
10. Kalb, A.J. *Biochim. Biophys. Acta* **1968**, 168, 532.
11. Nguema-Ona, E., Vicre-Gibouin, M., Gotte, M., Plancot, B., Lerouge, P., Bardor, M., and Driouich, A. *Frontiers in plant science* **2014**, 5, 499.
12. Bar-Peled, M. and O'Neill, M.A. *Annual review of plant biology* **2011**, 62, 127.
13. Reiter, W.-D. and Vanzin, G.F. *Plant Molecular Biology* **2001**, 47, 95.
14. Rostovtsev, V.V., Green, L.G., Fokin, V.V., and Sharpless, K.B. *Angew. Chem. Int. Ed.* **2002**, 41, 2596.
15. Presolski, S.I., Hong, V., Cho, S.H., and Finn, M.G. *J. Am. Chem. Soc.* **2010**, 132, 14570.
16. Sminia, T.J., Zuillhof, H., and Wennekes, T. *Carbohydr. Res.* **2016**, 435, 121.
17. Sawa, M., Hsu, T.L., Itoh, T., Sugiyama, M., Hanson, S.R., Vogt, P.K., and Wong, C.H. *Proc. Natl. Acad. Sci. USA* **2006**, 103, 12371.
18. McClosky, D.D., Wang, B., Chen, G., and Anderson, C.T. *Phytochemistry* **2016**, 123, 16.
19. Dumont, M., Lehner, A., Vauzeilles, B., Malassis, J., Marchant, A., Smyth, K., Linclau, B., Baron, A., Mas Pons, J., Anderson, C.T., Schapman, D., Galas, L., Mollet, J.C., and Lerouge, P. *The Plant journal : for cell and molecular biology* **2016**, 85, 437.
20. Kajiura, H., Tanaka, R., Kato, K., Hamaguchi, Y., Seki, T., and Fujiyama, K. *Plant Biotechnology* **2012**, 29, 489.
21. Niemann, M.C.E., Bartrina, I., Ashikov, A., Weber, H., Novak, O., Spichal, L., Strnad, M., Strasser, R., Bakker, H., Schmulling, T., and Werner, T. *Proc. Natl. Acad. Sci. USA* **2015**, 112, 291.
22. Anderson, C.T., Wallace, I.S., and Somerville, C.R. *Proc. Natl. Acad. Sci. USA* **2012**, 109, 1329.
23. Kunito, T., Saeki, K., Oyaizu, H., and Matsumoto, S. *Ecotoxicol. Environ. Saf.* **1999**, 44, 174.
24. Zhu, Y., Wu, J., and Chen, X. *Angew. Chem. Int. Ed.* **2016**, 55, 9301.
25. von Schaewen, A., Sturm, A., O'Neill, J., and Chrispeels, M.J. *Plant Physiology* **1993**, 102, 1109.
26. Laughlin, S.T., Agard, N.J., Baskin, J.M., Carrico, I.S., Chang, P.V., Ganguli, A.S., Hangauer, M.J., Lo, A., Prescher, J.A., and Bertozzi, C.R., *Metabolic Labeling of Glycans with Azido Sugars for Visualization and Glycoproteomics*, in *Methods Enzymol.* 2006, Academic Press. p. 230.
27. Burget, E.G., Verma, R., Mølhøj, M., and Reiter, W.-D. *The Plant Cell* **2003**, 15, 523.

28. Tan, L., Varnai, P., Lampport, D.T.A., Yuan, C.H., Xu, J.F., Qiu, F., and Kieliszewski, M.J. *J. Biol. Chem.* **2010**, *285*, 24575.
29. Saito, F., Suyama, A., Oka, T., Yoko-o, T., Matsuoka, K., Jigami, Y., and Shimma, Y. *J. Biol. Chem.* **2014**, *289*, 20405.
30. Carpita, N.C. and Gibeaut, D.M. *The Plant journal : for cell and molecular biology* **1993**, *3*, 1.
31. Smellie, I.A., Bhakta, S., Sim, E., and Fairbanks, A.J. *Org. Biomol. Chem.* **2007**, *5*, 2257.
32. Hsieh, Y.S.Y., Zhang, Q., Yap, K., Shirley, N.J., Lahnstein, J., Nelson, C.J., Burton, R.A., Millar, A.H., Bulone, V., and Fincher, G.B. *Biochemistry* **2016**, *55*, 322.
33. Rautengarten, C., Ebert, B., Herter, T., Petzold, C.J., Ishii, T., Mukhopadhyay, A., Usadel, B., and Scheller, H.V. *The Plant Cell* **2011**, *23*, 1373.
34. Castilho, A., Pabst, M., Leonard, R., Veit, C., Altmann, F., Mach, L., Glossl, J., Strasser, R., and Steinkellner, H. *Plant Physiol* **2008**, *147*, 331.
35. Roberts, R.M. *Plant Physiol* **1970**, *45*, 263.
36. Wold, J.K. and Hillestad, A. *Phytochemistry* **1976**, *15*, 325.
37. Hori, H. *Plant and Cell Physiology* **1978**, *19*, 501.
38. Lenucci, M., Leucci, M.R., Andreoli, C., Dalessandro, G., and Piro, G. *Eur J Phycol* **2006**, *41*, 213.
39. Yang, Z., Bennett, E.P., Jorgensen, B., Drew, D.P., Arigi, E., Mandel, U., Ulvskov, P., Levery, S.B., Clausen, H., and Petersen, B.L. *Plant Physiology* **2012**, *160*, 450.
40. Yang, T., Echols, M., Martin, A., and Bar-Peled, M. *Biochem. J* **2010**, *430*, 275.
41. Zhang, Q., Hrmova, M., Shirley, Neil J., Lahnstein, J., and Fincher, Geoffrey B. *Biochem. J* **2006**, *394*, 115.
42. Agard, N.J., Prescher, J.A., and Bertozzi, C.R. *J. Am. Chem. Soc.* **2004**, *126*, 15046.
43. Dommerholt, J., van Rooijen, O., Borrmann, A., Guerra, C.F., Bickelhaupt, F.M., and van Delft, F.L. *Nat. Commun.* **2014**, *5*.
44. Debets, M.F., van Berkel, S.S., Schoffelen, S., Rutjes, F.P.J.T., van Hest, J.C.M., and van Delft, F.L. *Chem. Commun.* **2010**, *46*, 97.
45. Yao, J.Z., Uttamapinant, C., Poloukhine, A., Baskin, J.M., Codelli, J.A., Sletten, E.M., Bertozzi, C.R., Popik, V.V., and Ting, A.Y. *J. Am. Chem. Soc.* **2012**, *134*, 3720.
46. Devaraj, N.K., Weissleder, R., and Hilderbrand, S.A. *Bioconjugate Chem.* **2008**, *19*, 2297.
47. Patterson, D.M., Jones, K.A., and Prescher, J.A. *Molecular BioSystems* **2014**, *10*, 1693.
48. Späte, A.-K., Bußkamp, H., Niederwieser, A., Schart, V.F., Marx, A., and Wittmann, V. *Bioconjugate Chem.* **2014**, *25*, 147.
49. Murashige, T. and Skoog, F. *Physiol. Plant.* **1962**, *15*, 473.



## Chapter 7



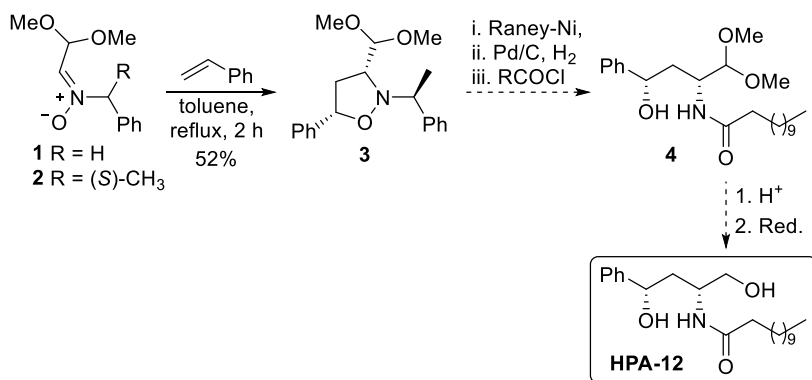
## General Discussion



The previous chapters described the synthesis of glycomimetic building blocks through the nitron-olefin [3+2] cycloaddition, and the application thereof towards the synthesis of an activity-based probe to study mammalian neuraminidases. Furthermore, this thesis concerns the application of molecular probes towards the study of plant glycans. The current chapter highlights key aspects of the previous chapters and discusses future prospects for each section.

**Chapter 2** describes the development of a novel masked aldehyde-containing nitron **1**. This nitron can be easily prepared through a facile one-step procedure and undergoes a [3+2]-thermal cycloaddition with a wide range of dipolarophiles. This nitron-olefin [3+2] cycloaddition reaction affords acid-stable isoxazolidine cycloadducts that are suitable for versatile post-cycloaddition modifications. These modifications include acetal hydrolysis under mildly basic conditions and the efficient one-pot procedure to give amine-protected  $\gamma$ -alcohols. Nevertheless, this chapter did not show an application towards total synthesis. However, the synthesis of several natural products could be undertaken that utilize the novel masked-aldehyde-containing nitron, e.g. the synthesis of HPA-12 as shown in Scheme 1.

**Scheme 1.** Proposed synthetic pathway towards HPA-12 *via* a nitron-olefin [3+2] cycloaddition with chiral nitron **2**.

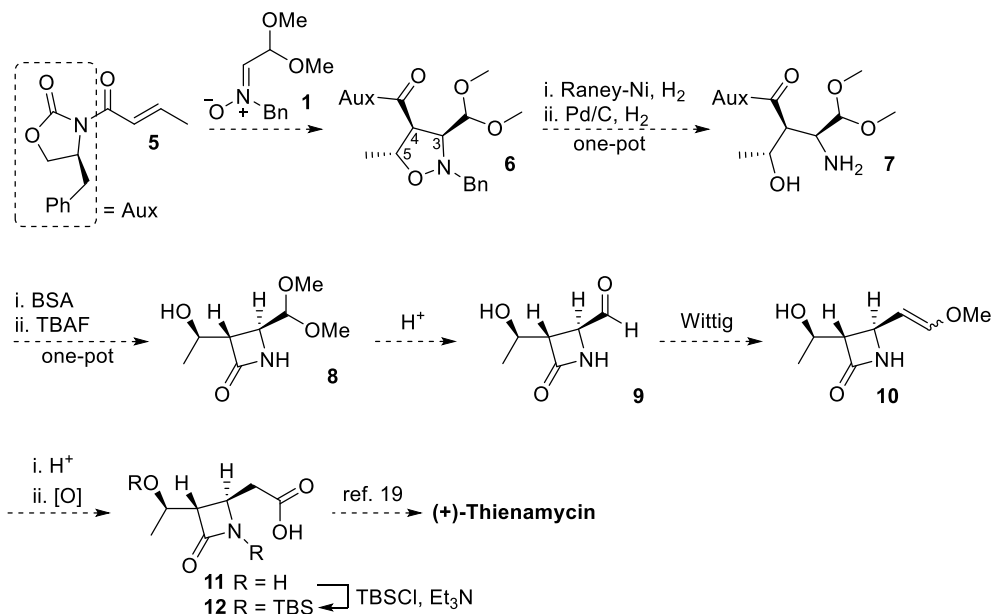


HPA-12, was identified as a potential drug<sup>1-5</sup> that inhibits synthesis and trafficking of sphingomyelin and ceramide, respectively, two classes of lipids in mammalian cells. Targeting the structural motif of these lipids led to the discovery of analogous HPA-12 as an inhibitor in the metabolism of these lipids. The synthesis of HPA-12 would involve the application of *N*-(1-phenylethyl)hydroxylamine as a chiral mediator to prepare nitron **2**, which is especially favorable since both (*R*)- and (*S*)-enantiomers are commercially available, meaning that both enantiomers of HPA-12 could be prepared. The synthesis of chiral nitron **2** is described in chapter 2 in addition to the subsequent enantioselective cycloaddition reaction providing the desired *anti*-diastereomer **3** in 52%. It was already shown in chapter 2 that the subsequent staged one-pot hydrogenolysis procedure is an efficient methodology to cleave the N-O-bond and liberate the primary amine. The only alteration to this procedure would involve replacing a protecting group with dodecanoyl chloride to give intermediate **4**. Finally, acidic hydrolysis of the acetal and subsequent reduction would provide HPA-12 in only 5 steps starting from

*N*-(1-phenylethyl)hydroxylamine. This short route enabled by nitron 2 would effectively compete with known procedures towards HPA-12, as these routes are lengthier (6 or 7 steps) and require expensive starting materials<sup>6, 7</sup> or reagents.<sup>8, 9</sup> Furthermore, in contrast to other synthetic pathways, this short route is ideally suited to enable a library synthesis of HPA-12 analogous as the route involves a nitron-olefin [3+2] cycloaddition. This reaction with nitron 1-2 accepts a variety of electron-poor to electron-rich olefins, while a library of HPA-12 analogs could be further diversified by the introduction of different acyl chlorides after the hydrogenation step.

Other stereospecific total synthesis applications could involve the reaction of achiral nitron 1 with chiral olefins. For example, a chiral olefin was discussed at length in chapter 4, but this olefin has unfortunately not been used in the scope study. This olefin, locostatin 5, bears an oxazolidinone more commonly known as an Evans auxiliary. This auxiliary can be used to control the stereochemical outcome of many transformations including the nitron-olefin [3+2] cycloaddition reaction.<sup>10</sup> Accordingly, using chiral alkene 5 in a thermal [3+2] cycloaddition reaction with nitron 1 could lead to cycloadduct 6 (Scheme 2).

**Scheme 2.** Proposed formal total synthesis of (+)-Thienamycin *via* isoxazolidine 5, the key intermediate resulting from a thermal [3+2] cycloaddition reaction between nitron 1 and locostatin. BSA: (*N,O*-bis(trimethylsilyl)acetamide).

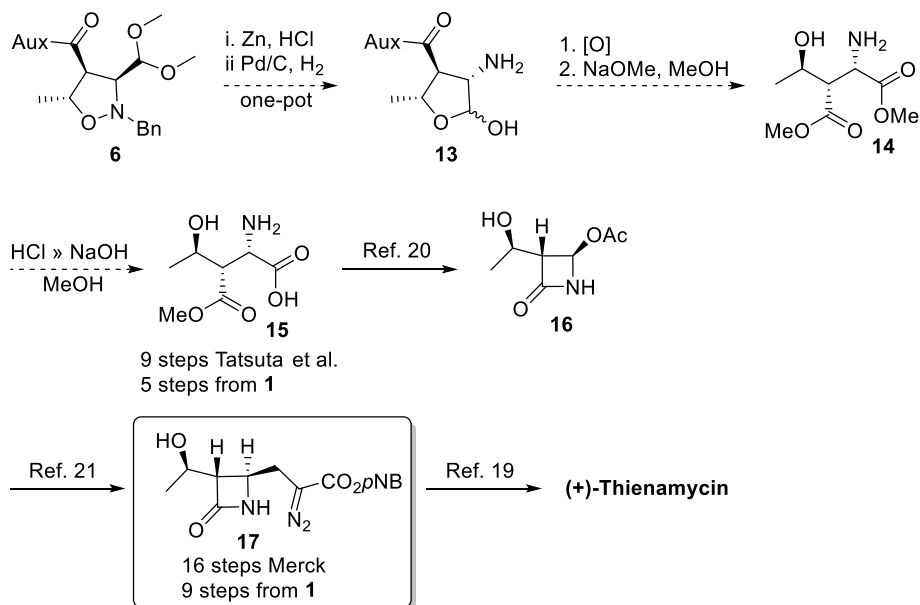


It is likely that this diastereomer is selectively formed as the C4-C5 stereochemistry (*trans*) is predetermined by the alkene geometry. Furthermore, the reaction would probably provide the desired C3-C5 *Anti*-product as observed for a cycloaddition involving similar substrates,<sup>10-12</sup> while the enantioselectivity of the reaction can be controlled, since both *R*- and *S*-enantiomers of the auxiliary are readily available. *Anti*-product 6 could be a good precursor to

(+)-Thienamycin. This natural product is one of the most potent naturally produced antibiotic thus far and the high interest in this molecule has led to the development of several synthetic routes. A novel formal synthesis towards (+)-Thienamycin may be undertaken by using cycloadduct **6**. Hydrogenation of this intermediate could provide free amine **7**. This intermediate may then be immediately ring-closed to the  $\beta$ -lactam, through a well-established silylation and fluoride-catalyzed cyclization procedure to provide intermediate azetidinone **8**.<sup>13-16</sup> The synthetic pathway leading up to intermediate **7** used masked-aldehyde nitrone **1**, which should enable a facile acidic hydrolysis at this stage to provide aldehyde **8**. This intermediate should exist solely in the open-chain form, as the structural limitations imposed by the  $\beta$ -lactam prevent formation of an hemiacetal. The open-chain-form of aldehyde **9** could undergo a Wittig reaction to give methoxy-alkene **10**. Successful hydrolysis of this intermediate would provide an isomeric mixture of the corresponding aldehyde that may be directly oxidized to carboxylic acid **11**. This intermediate may be derivatized to intermediate **12**, which was the key intermediate in the first stereocontrolled total synthesis by the Merck laboratories.<sup>17</sup> The same group later reported an alternative, more practical and scalable route to Thienamycin involving intermediate **12**.<sup>18,19</sup> The synthesis of intermediate **12** as described above and depicted in Scheme 2 would provide an alternative entry towards this intermediate in 8 steps. In comparison, the same intermediate is prepared in 9 steps in the improved synthesis of (+)-Thienamycin by Merck scientists.

However, the synthesis route can be improved further by taking advantage of the synthetic routes that have been developed since the elegant route developed by Merck scientists. For instance, other approaches have been developed that target a more advanced intermediate (**16**) in the improved Merck (+)-Thienamycin synthesis. The key diazo-keto ester intermediate **16** by the Merck synthesis was approached in two papers that involved the synthesis of  $\beta$ -lactam acetate **15**, which could be obtained from linear intermediate **14** (Scheme 3).<sup>20,21</sup> This linear intermediate was synthesized in 9 steps, but the same intermediate may be synthesized in 5 steps by utilizing the nitrone-olefin [3+2] cycloaddition with nitrone **1** (Scheme 3). Performing the hydrogenation of cycloadduct **6** under acidic conditions may result in the immediate hydrolysis of the acetal upon N-O bond cleavage. Opening of the N-O bond and successful hydrolysis would then give intermediate **13**, which may be oxidized to a lactone, followed by the removal of the auxiliary under basic conditions to give intermediate **14**. This diester **14** may then be converted to intermediate **15** in one step through a transesterification with catalytic acid, providing a lactone *in situ*, which can then be hydrolyzed to intermediate **15** through addition of NaOH.<sup>20,22</sup> Carboxylic acid **15** can then be converted to lactam **16** through a procedure by Tatsuta et al.<sup>20</sup> This acetate intermediate can then be converted to key-intermediate **17** through a procedure developed by Reider and coworkers.<sup>21</sup> Synthesis of intermediate **17** according to this synthetic pathway would provide this intermediate in 9 steps, starting from achiral nitrone **1**. In contrast, the improved synthetic route developed by Merck scientists requires 16 steps.

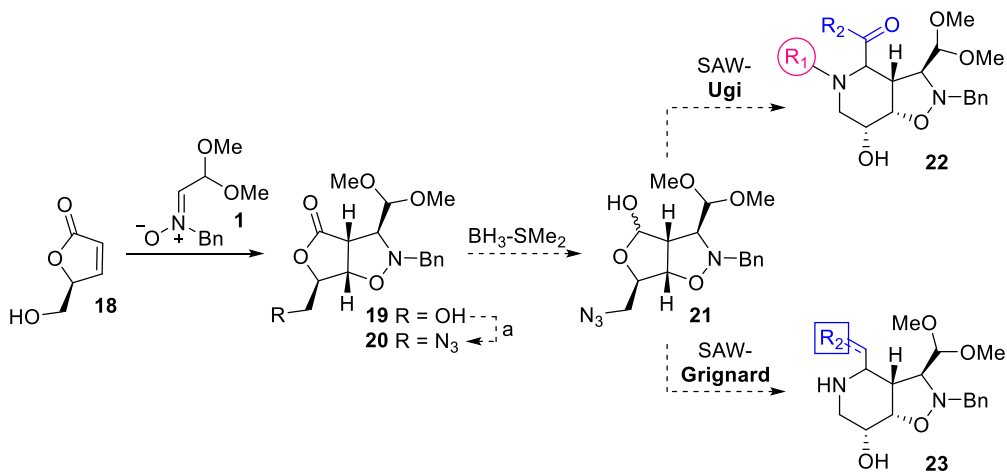


**Scheme 3.** Proposed synthetic pathway towards key-intermediate **17** for the formal synthesis of (+)-Thienamycin.

## Chapter 3

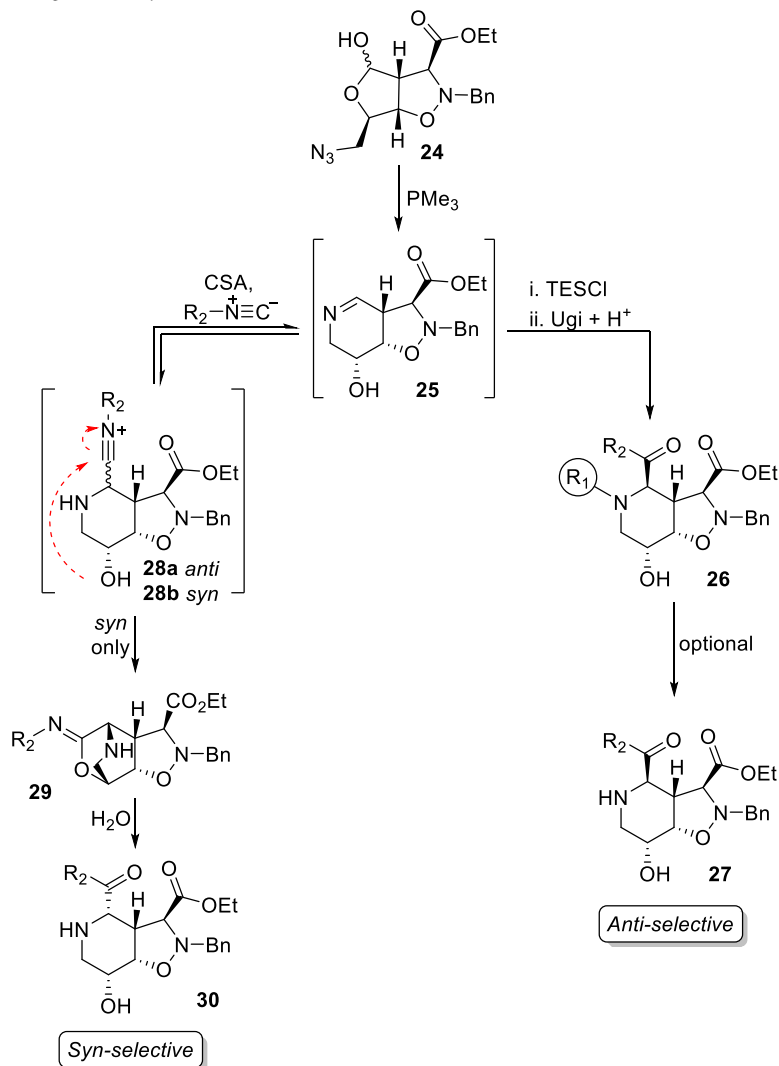
The novel masked aldehyde-containing nitrone **1** could also be employed for the library synthesis of iminosugars as described in **Chapter 3**. This chapter describes the selective modification of bicyclic isoxazolidines to enable the synthesis of complex glycomimetics building blocks, like iminosugars, *via* multicomponent chemistry. More specifically, a multicomponent one-pot Staudinger/aza-Wittig/Ugi (SAWU) reaction was used to synthesize a library of pipercolic acid derivatives. The key intermediate that enabled this library synthesis was derived from an ester-containing nitrone. However, the synthetic pathway towards this ester-containing key intermediate may accommodate an acetal instead of an ester to give acetal-containing intermediate **6** as shown in Scheme 4. The resulting azido-hemiacetal **21** could then be used to produce a novel library *via* the SAWU methodology. Notably, acetal intermediate **21** would also be a more versatile compared to its ester analog, since an acetal intermediate would enable application towards a Staudinger/aza-Wittig/Grignard reaction. This novel cascade reaction was recently reported<sup>23</sup> and should also be applicable on the azido-hemiacetal **6** and its ester analog. However, azido-hemiacetal **21** would be more suited towards this methodology as its ester analog may be susceptible towards competitive Grignard reactions.

**Scheme 4.** The synthesis of acetal-containing intermediate **21** may enable a more versatile derivatization of this intermediate through both Staudinger/aza-Wittig/Ugi and Staudinger/aza-Wittig/Grignard cascade reactions.

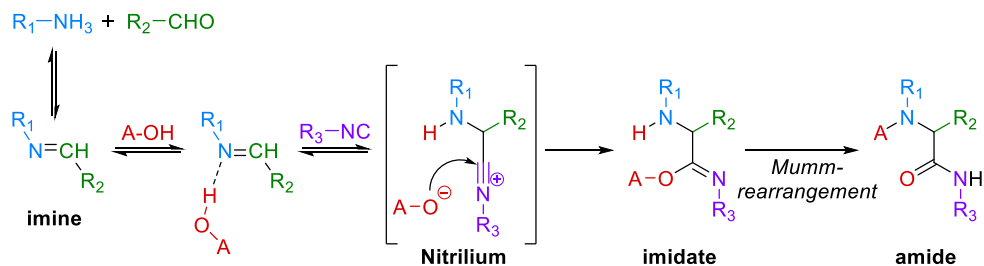


As discussed in chapter 3, the SAWU reaction provides both *syn*- and *anti*-products, but an approach for the selective *anti*-product formation was explored. This approach involved an *in situ* protection of the free hydroxy group of cyclic imine **25** after the initial Staudinger/aza-Wittig cascade, which prevents significant *syn*-attack of an isocyanide (Scheme 5). Consequently, the reaction could be controlled to provide mainly *anti*-product. However, the possibility of a *syn*-selective SAWU with azido-hemiacetal has not been explored in chapter 3. Still, the tendency of azido-hemiacetal **24** to form an cyclic imide (**29**) during a SAWU reaction could possibly be exploited to obtain only *syn*-products. An approach towards *syn*-selectivity would initially involve the formation of cyclic imine **25**. The formation of cyclic imine **25** would normally be succeeded by the addition of both a carboxylic acid and an isocyanide. However, replacing the carboxylic acid with a strong non-nucleophilic acid such as camphor sulfonic acid would prevent the trapping of *anti*-nitrilium ions **28a** by a carboxylate anion. Consequently, the *anti*-product amide cannot be formed. Instead, the *anti*-nitrilium ion **18a** may form an equilibrium with *syn*-nitrilium ion **18b**,<sup>24-28</sup> which ultimately would lead to complete *syn*-selectivity as the *syn*-nitrilium ions are immediately trapped as cyclic imide **29**. This intermediate can then be hydrolyzed as discussed in chapter 3 to obtain *syn*-iminosugar **30**.

**Scheme 5.** The *anti*-selective approach towards pipecolic acid derivative **26** and the proposed *syn*-selective approach towards iminosugar **30** via cyclic imidate **29**.

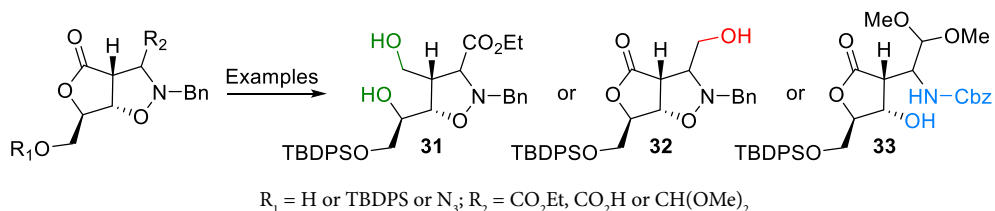


The potential of a *syn*-selective approach towards iminosugar **30** is supported by a recent publication by Fleurat-Lessard et al. showing evidence for the reversibility of the initial isocyanide attack.<sup>24</sup> This recent study challenges 50-year old established views of the reaction mechanism of the Ugi reaction (Scheme 6).

**Scheme 6.** The mechanism of the Ugi-reaction based on theoretical calculations by Fleurat-Lessard and coworkers.<sup>24</sup>

Conventional Ugi mechanisms considered the reaction to be reversible until the final irreversible Mumm-rearrangement, which provides the stable amide.<sup>25–28</sup> Fleurat-Lessard and coworkers challenged this view by performing extensive DFT calculations and concluded that “in the most probable mechanism the nitrilium formation does not proceed through an equilibrium”. However, closer inspection of this study shows that their theoretical calculations indicate that the formation of the imidate is irreversible rather than the formation of the nitrilium. The *syn*-selective synthetic pathway proposed in Scheme 5 does not involve a carboxylic acid that can attack the nitrilium ion, meaning that this approach is viable according to conventional<sup>25–28</sup> and new insights.<sup>24</sup> Furthermore, investigating a *syn*-selective approach towards iminosugar **30** would have the added advantage of resolving the ambiguity towards the Ugi mechanism.

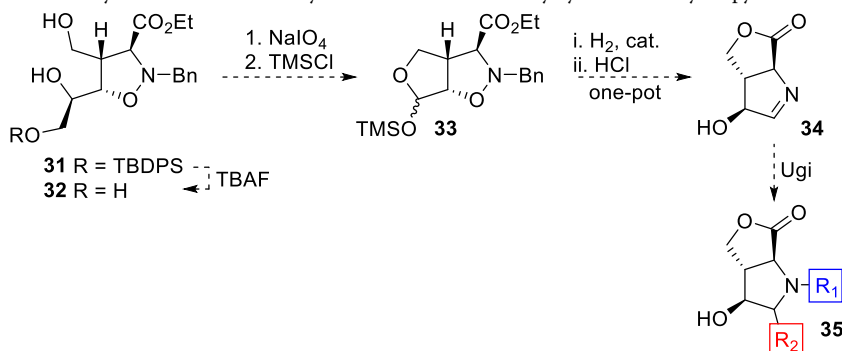
The synthesis of a library of pipecolic acid derivatives in Chapter 3 showed how the nitrone-olefin [3+2] cycloaddition reaction can be used to synthesize glycomimetics building blocks. The key intermediate of this cycloaddition reaction was a bicyclic isoxazolidine, but the chemistry of this chiral intermediate was not only explored to enable the synthesis of a library of pipecolic acid derivatives. In fact, this bicyclic intermediate was studied extensively to enable the versatile functionalization of every functional group. This exploration has led to the selective functionalization of the exocyclic ester, the N-O bond and the lactone (Scheme 7).

**Scheme 7.** Examples of products resulting from selective bicyclic isoxazolidine functionalization.

The selective modification of the versatile bicyclic isoxazolidine should enable the synthesis of other glycomimetics. For example, a library of pyrrolidine iminosugars can be synthesized. Pyrrolidine-based iminosugars are frequently isolated from natural sources and have therapeutic potential due to their ability to inhibit glycosidases.<sup>29</sup> This therapeutic potential

of pyrrolidines has resulted in the development of many synthesis strategies for this class of iminosugars, but these approaches typically involve long synthetic routes towards a single target.<sup>29-31</sup> The library synthesis of chiral pyrrolidines are less common,<sup>32-34</sup> while a library of these iminosugars could enable the discovery of novel glycosidases inhibitors. A novel entry towards the library synthesis of pyrrolidines would therefore be of interest and may be synthesized from diol intermediate **31** (Scheme 8).

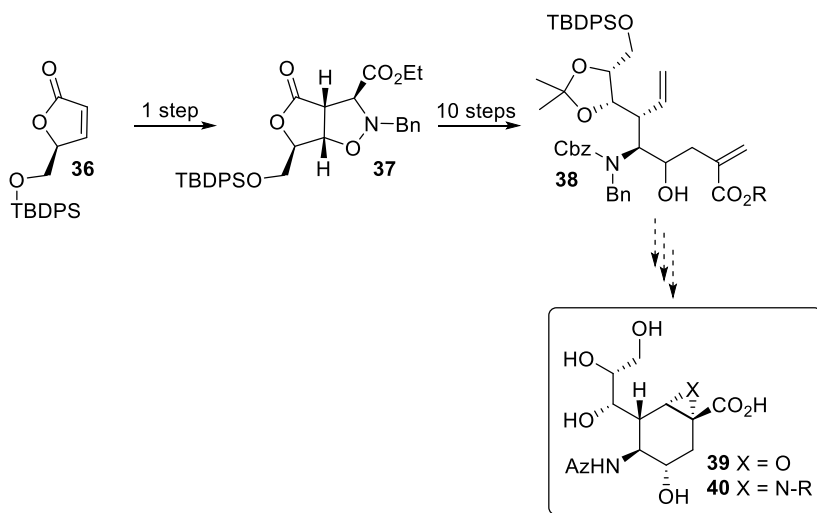
**Scheme 8.** A synthesis route towards cyclic imine **34** for the library-synthesis of bicyclic pyrrolidines (**35**).



This intermediate is the result of a selective reduction of the lactone in the bicyclic isoxazolidine precursor as described in chapter 3 and the resulting diol **31** may then be deprotected to give intermediate **32**. This intermediate possessing a vicinal diol could be cleaved with NaIO<sub>4</sub> to produce an aldehyde, which may be trapped as an acetal with a silyl-group to give intermediate **33**. This intermediate may then be hydrogenated to liberate the amine, followed by a cascade reaction, which includes TMS-removal, imine formation and transesterification to give cyclic imine **34**. This imine would be a good electrophile for a number of name reactions, including multicomponent reactions such as the Ugi reaction. Accordingly, the Ugi reaction may be used to synthesize a library of bicyclic iminosugars (**35**).

## Chapter 4

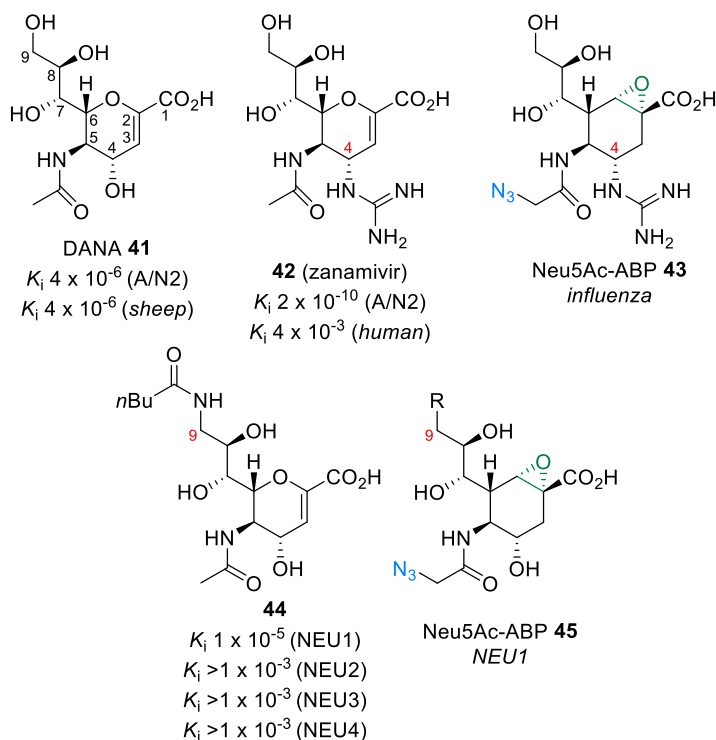
The previous section discussed the application of bicyclic isoxazolidines towards the synthesis of libraries. In contrast, **chapter 4** concerns the application of those intermediates towards a single target; a Neu5Ac-activity-based probe (ABP). As described in chapter 4, a synthetic pathway towards Neu5Ac-ABP **39** was investigated by starting with the nitrone-olefin [3+2] cycloaddition reaction, which provided intermediate **37** (Scheme 9).

**Scheme 9.** Overview of the synthesis route towards linear diene **38** as a key-intermediate towards Neu5Ac-ABP **39-40**

Selective functionalization of this intermediate led to the synthesis of a linear diene **38**. The synthetic pathway leading to this advanced intermediate, bearing 5 consecutive chiral centers, was generally high yielding and practical, requiring limited purification steps. As discussed in chapter 4, further investigations would involve the RCM of diene **38** or a derivative thereof to obtain a cyclohexene precursor that can then be used to obtain Neu5Ac-ABP **39** through an asymmetric Sharpless epoxidation. Still, epoxidation is not the only methodology to obtain an ABP from a cyclohexene-precursor. For example, instead of an epoxide an aziridine **40** can be installed at the carbocycle (Scheme 10). The installation of *N*-acyl- and *N*-alkyl-aziridines is typically used to install a clickable-handle (azide). Still, while the possibility of installing a clickable-handle *via* an aziridine is not crucial, as azidoacetamide-groups are commonly used on Neuraminic acid without impeding binding,<sup>35-37</sup> aziridines do have another advantage over epoxides. For instance, aziridines can be tethered with different *N*-acyl or *N*-alkyl groups, which enables the tuning of the reactivity of aziridine-based-ABPs. The tunability of aziridine-based ABP **40** could enable control over the activity towards neuraminidases.

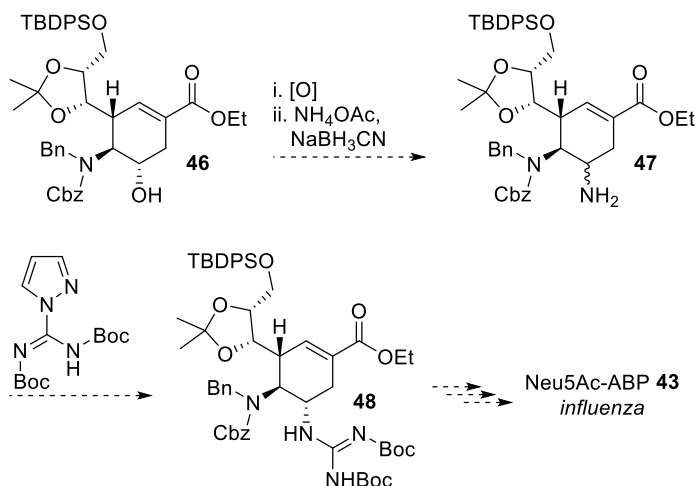
Another parameter of Neu5Ac-ABP **39** that could be addressed next to its activity is its selectivity. Neu5Ac-ABP **39** was presented in chapter 4 as an ABP towards mammalian neuraminidases. However, several pathogens are known to use neuraminidases to infect human cells.<sup>38</sup> For instance, influenza virus neuraminidase is essential for viral replication and infectivity; targeting this enzyme forms the basis of chemotherapies for influenza.<sup>39</sup> The high importance of this neuraminidase for therapeutics targeting influenza drove several groups to investigate the morphology of the catalytic site of this enzyme to enable rational design of novel inhibitors.<sup>40-42</sup> The structure of the active-site was determined via X-ray crystal structures of the enzyme with and without Neu5Ac-derived complexes. The crystal structure enabled predictive software to explore the enzyme's active site for its capacity to favorably

accommodate a range of functional groups.<sup>43</sup> The structure-based exploration revealed an anionic region that meant that the C-4 hydroxyl near this region may accommodate larger and positively charged groups (Figure 1), which could enhance affinity.<sup>44</sup>



**Figure 1.** An overview of existing neuraminidase inhibitors and the structure-based design of influenza- and NEU1-selective ABPs based on catalytic site modelling of NEU1 and influenza-neuraminidase enzymes.

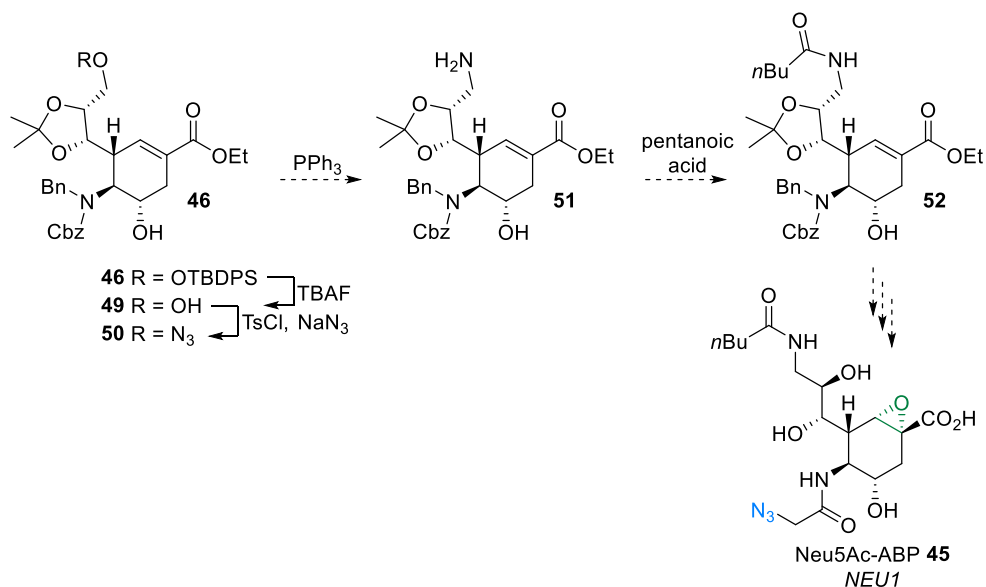
Consequently, a novel inhibitor was developed based on this principle, called zanamivir **42**.<sup>43, 45</sup> This inhibitor **42** has a potency four orders of magnitude stronger (i.e. 10,000 times) than DANA **41**, from which it was derived.<sup>46</sup> Furthermore, it was found that the installation of positively charged functionalities (at physiological pH) at the C-4 position of the parent compound DANA **41** resulted in increased selectivity towards the influenza virus neuraminidase compared to mammalian neuraminidases.<sup>43, 45</sup> In fact, the inhibition of human lysosomal neuraminidase with zanamivir is 7-fold less potent than the viral neuraminidases.<sup>43</sup> In comparison, DANA **41** shows no selectivity towards influenza virus neuraminidase compared to mammalian neuraminidases. Accordingly, similar structure-based design involving Neu5Ac-ABP **39** could lead to a derivative of this ABP that is selective towards influenza virus neuraminidase. For instance, Neu5Ac-ABP **43**, possessing a C-4 guanidine moiety could be a good potential target towards an ABP that is selective towards influenza. This derivative may be conveniently obtained from a precursor towards Neu5Ac-ABP **39**, by oxidizing the C-4 hydroxyl of intermediate **46**, followed by an *in situ* reductive amination to give intermediate **47** (Scheme 10).

**Scheme 10.** Proposed synthetic pathway to synthesize *Influenza* specific Neu5Ac-ABP **43** starting from precursor **46**.

This amine may then be converted into guanidine **48** using common reagents,<sup>47-49</sup> while further modifications towards ABP **43** most likely would involve the same reaction conditions used to obtain Neu5Ac-ABP **39** from precursor **46**.

In contrast to influenza, no viable treatments are known for the treatment of sialidosis patients. Therefore, it remains important to target the source of this disease; misfolded neuraminidase-1 enzymes (NEU1). Development of an NEU1-ABP towards this enzyme would enable small molecule library screening for leads that can bind the active site of a mutant NEU1 enzyme and promote better folding, thereby hopefully increasing lysosomal trafficking of NEU1 and its enzymatic activity. As discussed in chapter 4, this enzyme is one of the 4 known human neuraminidases. Consequently, to enable the discovery of selective inhibitors for NEU1, an ABP is required that is also selective towards NEU1 in the presence of NEU2-4. Neu5Ac-ABP **39** would probably not be selective towards NEU1, since DANA **41**, an inhibitor of NEU1, is equally or slightly more potent towards NEU2-4.<sup>50</sup> However, a structure-based design of an NEU1-selective ABP is possible, since the three-dimensional structures of NEU1, NEU3 and NEU4 have been modeled based on the crystal structure of NEU2.<sup>51</sup> The analysis of these structures allowed the identification of similarities and differences among the active sites, which can aid in the structure-based design of selective NEU1 inhibitors. For instance, it was found that glycerol binding group (C7-9) can be exploited to design selective inhibitors of NEU1.<sup>50</sup> Accordingly, replacing the C-9 hydroxyl of DANA **41** with an *N*-*n*-butyl amide resulted in increased binding towards NEU1, while NEU2-4 inhibition has decreased to the millimolar range (Figure 1). Similarly, replacing the C-9 hydroxyl group of Neu5Ac-ABP **39** with an *N*-*n*-butyl amide could lead to a highly active ABP (**45**) that is also very selective towards NEU1. For instance, Neu5Ac-ABP **45** may be obtained by using the same intermediate for both ABP **39** and *Influenza* ABP **46** as depicted in scheme 11.



**Scheme 11.** Proposed synthetic pathway towards NEU1 selective neuraminidase ABP **45** starting from intermediate **46**

Accordingly, the primary alcohol of intermediate **46** may be selectively deprotected with TBAF, followed by selective tosylation of the primary alcohol and substitution with NaN<sub>3</sub> to give intermediate **50**. This azide may be converted to an amine through a Staudinger reduction and subsequently coupled to pentanoic acid to give intermediate **52**, as a precursor to NEU1 ABP **45**. Consequently, Neu5Ac-ABP **39** may be used as a precursor towards both mammalian (NEU1) and viral (influenza A) neuraminidases. Consequently, the synthesis route towards Neu5Ac-ABP **39** may also be used to obtain selective mammalian (NEU1) and viral (influenza A) neuraminidase ABPs.

## Chapter 5

In Chapter 5 the synthesis and evaluation of locostatin-based chemical probes towards PEBP proteins was investigated. PEBP proteins are a family of phosphatidyl ethanolamine-binding proteins (PEBPs) comprising of over 400 members from a variety of organisms including mammals and plants. These PEBP proteins were studied to investigate the signaling of a plant-PEBP, FLOWERING LOCUS T (FT), that relays a signal from the leaves of a plant, traveling toward the growing tip of a plant to induce flowering. However, the effect of synthesized locostatin-based chemical probes on FT signaling could not be evaluated, since the evaluation of the probes showed that they are not selective and can also bind a multitude of non-PEBP proteins. In addition, the apparent toxicity of locostatin towards plants and lack of selectivity of locostatin-based probes towards FT indicate that locostatin is not a suitable lead compound towards novel small molecule binders of FT and flowering time-modulating compounds.

Nonetheless, in parallel, a small-molecule library screening was carried out to identify a flowering inducing agent mimicking FT function. The development of a novel library screening method and the subsequent screening of ~5000 compounds led to the discovery of a few flowering-inducing compounds, which will be reported in due time. Furthermore, the library screening also led to a serendipitous discovery of compound **47** (Figure 2) inducing an unexpected phenotype.

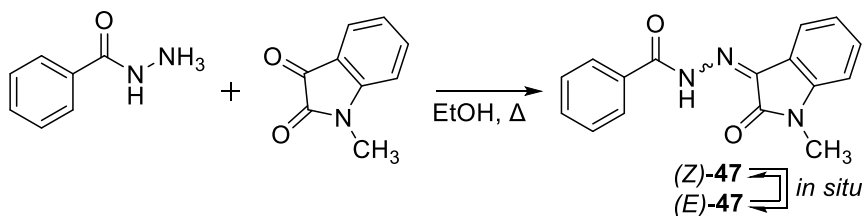


**Figure 2.** Condensation of 2-pyridinecarbohydrazide with methylisatin provides a geometrical mixture of **47**-isomers, which can be separated by column chromatography. Application of pure (*E*)-**47** or (*Z*)-**47** probably leads to isomerization *in situ*.

This phenotype involved a meristem termination, when *Arabidopsis thaliana* seedlings were grown on a medium with this compound (Figure 3). We observed that the compound **47** could exist as two geometrical isomers and were able to synthesize **47** and separate the respective *E*- and *Z*-isomers to separately evaluate their biological activity. However, we observed that the pure isomers seem to isomerize *in situ*, as both isomers seem to induce the same phenotype to the same extent.

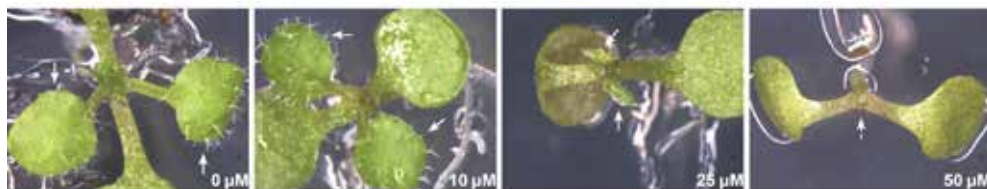


**Figure 3.** Phenotypic characterization of 10 day old *Arabidopsis* seedlings incubated with 0–50  $\mu\text{M}$  compound **47** for 10 d. The two pictures on the left are from *Arabidopsis* seedling on medium with 0 or 10  $\mu\text{M}$  compound **47**. Besides the two cotyledons, these seedlings have developed already two true leaves (indicated by white arrows). In contrast, the two seedlings shown on the right, which have been growing on medium containing compound 25–50  $\mu\text{M}$  **47**, show very limited until no leaf formation at all (most right picture).

The phenotype was therefore further studied with a mixture of both isomers. Seedlings exposed to different concentrations of compound **47** behave differently. For instance, as shown in Figure 3, all *Arabidopsis* seedlings develop their primary leaves as normal, but increasing concentrations of the compounds (10–50  $\mu\text{M}$ ) led to decreased and ultimately complete termination of the meristem. The termination of the meristem is evident from the lack of leaves that developed at the meristem flanks in the peripheral zone (Figure 4A). The cells in this zone are provided by divisions of undifferentiated meristematic cells in the central zone (Figure 4B).

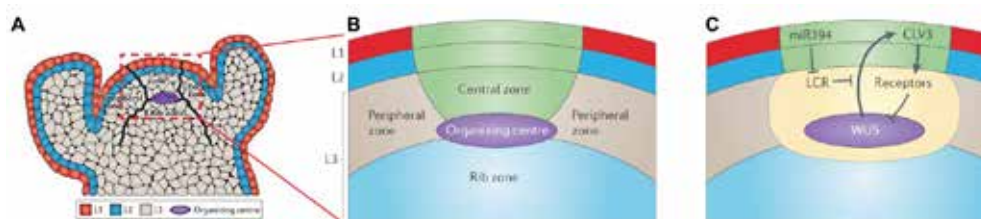


**Figure 4** Schematic representation of the Shoot Apical meristem of *Arabidopsis thaliana*. A, B) Organization of an apical meristem (growing tip) represented in different zones. C) Short-range signaling in meristem maintenance; WUSCHEL (WUS) is expressed in the organizing center situated below the central zone. WUS travels to the L1 and L2 layers to directly promote the expression of *CLAVATA3* (*CLV3*). Activation of the *CLV3*-dependent signaling pathway reduces the rate of stem cell proliferation and enhances organ initiation via a feedback loop that inhibits *WUS* expression. In *wus* mutants, stem cells are no longer maintained, and organ formation arrests prematurely.<sup>52-54</sup>

These stem cells provide plants the ability to continuously produce new organs from a small pool of stem cells, which are located close to the tip of the meristem.<sup>55</sup> The fate of this small pool of stem cells is regulated by *CLAVATA3* (*CLV3*), which initiates organ development, resulting in the reduced life-time of these stem-cells (Figure 4C). In turn, *CLV3* expression is controlled by *WUSCHEL* (*WUS*), a key regulator involved in localizing the stem cells close to the tip and essential for organization and maintenance of the stem cell population in the shoot apical meristem (Figure 4C).<sup>52-54</sup> Based on the observation of the phenotype it was hypothesized that compound **47** may affect *WUS* expression and cause the stems cells to differentiate, ultimately preventing the development of new organs. Indeed, inhibition of *Arabidopsis* seedlings with 25  $\mu$ M of compound **47** caused an increase in *WUS*-expression (Appendix F, Figure S1). Interestingly, further investigation showed that *WUS* is also ectopically expressed in the roots, where it is normally not expressed (Figure 5a-d).<sup>55</sup>

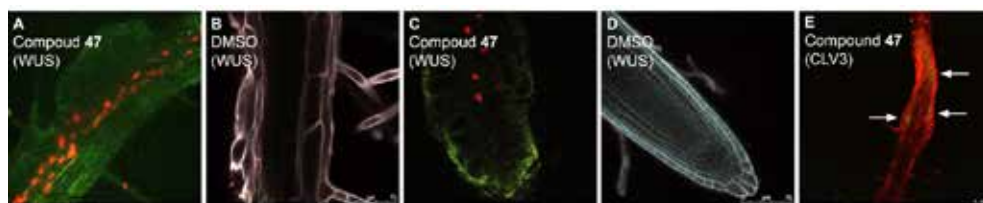


**Figure 5.** Visualization of *WUSCHEL* expression in the roots of 11 day-old *Arabidopsis* seedlings incubated with/without 25  $\mu$ M compound **47** since germination. A-D) pWUS::dsRED *Arabidopsis* seedlings incubated with 25  $\mu$ M compound **47** show *WUS* expression (red) in the root (A) and the root-tip (C), while seedlings incubated with DMSO do not show *WUS* expression in the root (B) or the root-tip (D). E) *WUS* expression in the root coincides with *CLV3* expression, as shown with a *CLV3*-GFP *Arabidopsis* seedling incubated with 25  $\mu$ M compound **47** and counterstained with propidium iodide (red); *CLV3*-expression is indicated by a green color (GFP).

The ectopic expression of *WUS* coincides with the expression of *CLV3*, a stem cell marker, in the roots, while *CLV3* expression is normally restricted to the shoot and floral meristem cells (Figure 5e).<sup>56</sup> This phenomenon has been reported by Sablowski and coworkers, who showed that *WUS*-expression in the roots leads to ectopic expression of *CLV3*, causing the ectopic

activation of stem cell functions.<sup>57</sup> These stem cells develop with the intrinsic shoot identity, which are responsive to developmental inputs that normally do not change root identity. Considering that compound **47** also induces ectopic expression of *WUS* and *CLV3* in the roots it would be interesting to determine if compound **47** can also induce shoots or embryos in the roots. Furthermore, this preliminary work shows that compound **47** may be the first non-transgenic agent that can influence *WUS* expression in plants. Accordingly, compound **47** may become a tool to study plant development, especially in plant species that propagate through vegetative reproduction.<sup>58</sup>

## Chapter 6

Different cellular structures in plants were investigated in chapter 6. This chapter describes the direct imaging of glycans in *Arabidopsis* roots *via* click-labeling of metabolically incorporated azido-monosaccharides. Accordingly, we were able to expand the toolbox of clickable monosaccharide analogs for glycan labeling in *Arabidopsis* seedlings with five glycan analogs. These clickable-monosaccharides; Ac<sub>4</sub>GlcNAz, Ac<sub>4</sub>GalNAz, Ac<sub>3</sub>ArabAz, Ac<sub>4</sub>FucAz and Ac<sub>4</sub>GlcNCyc were successfully metabolically incorporated and visualized in glycans of *Arabidopsis* seedling roots. In addition, techniques documented so far use toxic copper-catalyzed labeling, but we have shown that copper-free labeling reactions can be performed, which also leads to more uniform labeling. The mild nature of the copper-free labeling techniques should enable more complex spatiotemporal imaging, since the two copper-free labeling techniques discussed in chapter 6 are not only bio-orthogonal, but also orthogonal with respect to each other. This means that multiple unnatural sugars can be imaged at the same time using multicolor labeling experiments to allow the discrimination of temporally distinct glycan populations and analysis of their trafficking patterns during development.

The plant metabolism may also be studied on a different level by using the azido-monosaccharides probes. For instance, the incorporation of Ac<sub>4</sub>GalNAz we observe supports the possibility of a epimerase in *Arabidopsis* that converts Ac<sub>4</sub>GalNAz to Ac<sub>4</sub>GlcNAz. This GalNAc epimerase may be identified by using Ac<sub>4</sub>GalNAz, since a knock-out mutant of *Arabidopsis* not expressing this epimerase would not metabolically incorporate Ac<sub>4</sub>GalNAz.

In contrast to a possible GalNAc pathway, several reports discuss the presence of the GlcNAc salvage pathway in *Arabidopsis*. For example, recently a *N*-acetylglucosamine kinase (GNK) was identified, which is an essential enzyme for the salvage of GlcNAc.<sup>59</sup> Consequently, a knockout mutant - which does not express GNK - could be used as a negative control to unambiguously proof the incorporation of Ac<sub>4</sub>GlcNAz through the GlcNAc salvage pathway. Furthermore, while it was shown that Ac<sub>4</sub>GlcNAz is actively incorporated rather than passively by *Arabidopsis*, this has not been unequivocally proven for Ac<sub>4</sub>GalNAz, Ac<sub>4</sub>FucAz and Ac<sub>3</sub>ArabAz. Further investigations into these probes should also validate this, which should be

possible by evaluating if the unacetylated derivatives of these azido-monosaccharides are also incorporated. Accordingly, incorporation of unacetylated GalNAz, FucAz and ArabAz would provide evidence for an active mechanism, since passive incorporation of polar unacetylated azido-monosaccharides through the hydrophobic cell-membrane would be implausible

Furthermore, while the metabolic incorporation of Ac<sub>3</sub>ArabAz was observed, the exact mechanism of its incorporation remains obscure. Ac<sub>3</sub>ArabAz was chosen as a potential monosaccharide probe for metabolic incorporation in Arabidopsis, since Arabinose is mainly present in Arabidopsis as L-arabinofuranose (Araf) as one of the most common O-glycan sugars and an important constituent of plant cell wall polysaccharides (Figure 6).<sup>60-63</sup>

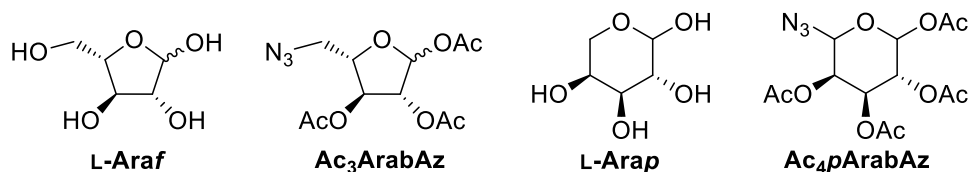


**Figure 6.** The different configurations of Arabinose (Ara) and the corresponding furanose- and pyranose- azido monosaccharides.

More specifically, L-Arabinofuranosyl residues are incorporated into the arabinogalactan of plants and transferred from UDP-Araf. However, this nucleotide is derived from the thermodynamically more stable pyranosyl form; UDP-Arap, while ArabAz is not able to convert to its pyranose configuration meaning that the corresponding pyranosyl UDP-ArabAz cannot be formed (Figure 7).<sup>64, 65</sup>

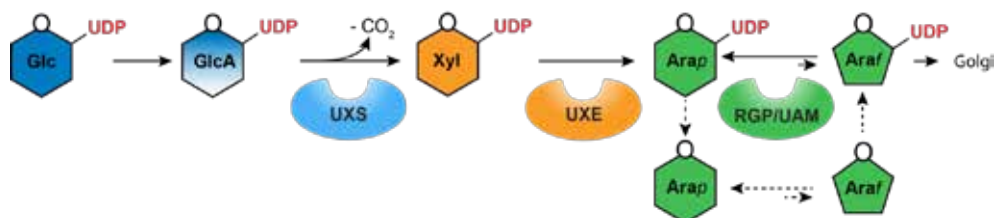


**Figure 7.** UDP-Araf is an important building block precursor for arabinoxylan biosynthesis and its precursor nucleotide sugar is considered to be UDP-D-Glc.<sup>64, 65</sup> This nucleotide can be oxidized to form UDP-D-glucuronate (UDP-GlcA), which can be converted into UDP-D-xylose (UDP-Xyl) through the essentially irreversible oxidative decarboxylation by UDP-Xyl Synthase (UXS). The UDP-Xyl can then act as a substrate for UDP-xylose 4-epimerase (UXE) for the biosynthesis of UDP- L-Arap. This Arap nucleotide is converted to UDP-Araf by the mutase Reversibly Glycosylated Protein (RGP) in *Arabidopsis Thaliana*<sup>66</sup> or by UDP-Ara mutase (UAM); the RGP analog in Barley reported by Finscher et al.<sup>67</sup> Fincher and co-workers proposed that the UAM-catalyzed interconversion of UDP-Ara involves several steps as depicted above. Finally, UDP-Araf enters the Golgi apparatus for arabinoxylan synthesis.

This raises the question how ArabAz is incorporated, since there is no known nucleotidyltransferase that is able to form UDP-L-Araf from arabinofuranose. Intriguingly, Fincher and coworkers recently reported on the catalytic properties of UDP-arabinose mutase (UAM) enzymes in Barley.<sup>67</sup> They show that these enzymes are involved in the reversible UDP-Arap → UDP-Araf reaction, but they also mention that this reaction probably involves several steps. These steps presumably include cleavage of the arabinosyl residue from the

UDP-Arap substrate, opening of the pyranosyl-ring, re-formation of the alternative ring form, and reconnection of the altered arabinosyl residue to the UDP molecule (Figure 7). Consequently, ArabAz may be salvaged by these enzymes and converted to UDP-ArabAz and thus enable metabolic incorporation into the cell wall. Similar UDP-mutase enzymes (RGP) have been reported in other plant species, including Arabidopsis,<sup>66</sup> which would provide a possible explanation for the observed metabolic incorporation of Ac<sub>3</sub>ArabAz. This hypothesis may be validated by working with a knockout mutant of Arabidopsis not expressing RGP, the enzyme responsible for UDP-Arap→UDP-Araf interconversion in this plant.<sup>66,68</sup> Furthermore a pyranose equivalent of Ac<sub>3</sub>ArabAz (Ac<sub>4</sub>-pArabAz; figure 6) may be synthesized to compare labeling with the furanosylic Ac<sub>3</sub>ArabAz. The synthesis of 5-azido-monosaccharides is not unprecedented,<sup>69-71</sup> but unacetylated pArabAz would partially exist as an α-azido alcohol, which are perceived as short-lived intermediates.<sup>72-74</sup> However, it was recently reported that α-azido alcohols can be prepared through a facile hydroazidation of aldehydes, which also showed that these compounds are stable enough for characterization.<sup>75</sup> Consequently, it may be possible metabolically incorporate Ac<sub>4</sub>-pArabAz, since it can be expected that the acetylated form is stable, while *in situ* hydrolysis towards pArabAz would give an azido-monosaccharide abiding mainly as a cyclic hemiacetal. In addition, incorporation of pArabAz in the cell wall as an arabinofuranose glycoconjugate, would prevent degradation, since a α-azido alcohol isomer can no longer be formed.

## References

1. Sakamoto, H., Okamoto, K., Aoki, M., Kato, H., Katsume, A., Ohta, A., Tsukuda, T., Shimma, N., Aoki, Y., Arisawa, M., Kohara, M., and Sudoh, M. *Nature Chemical Biology* **2005**, *1*, 333.
2. Elwell, C.A., Jiang, S., Kim, J.H., Lee, A., Wittmann, T., Hanada, K., Melancon, P., and Engel, J.N. *PLoS Pathog* **2011**, *7*, e1002198.
3. Swanton, C., Marani, M., Pardo, O., Warne, P.H., Kelly, G., Sahai, E., Elustondo, F., Chang, J., Temple, J., Ahmed, A.A., Brenton, J.D., Downward, J., and Nicke, B. *Cancer Cell* **2007**, *11*, 498.
4. Yasuda, S., Kitagawa, H., Ueno, M., Ishitani, H., Fukasawa, M., Nishijima, M., Kobayashi, S., and Hanada, K. *J. Biol. Chem.* **2001**, *276*, 43994.
5. Charruyer, A., Bell, S.M., Kawano, M., Douangpanya, S., Yen, T.-Y., Macher, B.A., Kumagai, K., Hanada, K., Holleran, W.M., and Uchida, Y. *J. Biol. Chem.* **2008**, *283*, 16682.
6. Ďuriš, A., Wiesenganger, T., Moravčíková, D., Baran, P., Kožíšek, J., Dařch, A., and Berkeš, D. *Org. Lett.* **2011**, *13*, 1642.
7. Snider, J.R., Entrekin, J.T., Snowden, T.S., and Dolliver, D. *Synthesis* **2013**, *45*, 1899.
8. Lalwani, K.G. and Sudalai, A. *Tetrahedron Lett.* **2016**, *57*, 2445.
9. Ueno, M., Kitagawa, H., Ishitani, H., Yasuda, S., Hanada, K., and Kobayashi, S. *Tetrahedron Lett.* **2001**, *42*, 7863.
10. Desimoni, G., Faita, G., Mella, M., Righetti, P., and Zema, M. *Tetrahedron* **1999**, *55*, 8509.

11. Fray, M.J., Jones, R.H., and Thomas, E.J. *J. Chem. Soc., Perkin Trans. 1* **1985**, 2753.
12. Casuscelli, F., Di Bella, M.R., Ficarra, R., Melardi, S., Romeo, G., Chiacchio, U., and Rescifina, A. *Gazz. Chim. Ital.* **1997**, 127, 367.
13. Burnett, D.A., Caplen, M.A., Browne, M.E., Zhau, H., Altmann, S.W., Davis Jr, H.R., and Clader, J.W. *Bioorg. Med. Chem. Lett.* **2002**, 12, 315.
14. Wang, Y., Zhang, H., Huang, W., Kong, J., Zhou, J., and Zhang, B. *Eur. J. Med. Chem.* **2009**, 44, 1638.
15. Sasikala, C.H.V.A., Reddy Padi, P., Sunkara, V., Ramayya, P., Dubey, P.K., Bhaskar Rao Uppala, V., and Praveen, C. *Organic Process Research & Development* **2009**, 13, 907.
16. Sova, M., Mravljak, J., Kovač, A., Pečar, S., Časar, Z., and Gobec, S. *Synthesis* **2010**, 2010, 3433.
17. Salzmann, T.N., Ratcliffe, R.W., Christensen, B.G., and Bouffard, F.A. *J. Am. Chem. Soc.* **1980**, 102, 6161.
18. Melillo, D.G., Shinkai, I., Liu, T., Ryan, K., and Sletzing, M. *Tetrahedron Lett.* **1980**, 21, 2783.
19. Melillo, D.G., Cvetovich, R.J., Ryan, K.M., and Sletzing, M. *J. Org. Chem.* **1986**, 51, 1498.
20. Tatsuta, K., Takahashi, M., Tanaka, N., and Chikauchi, K. *J. Antibiot.* **2000**, 53, 1231.
21. Reider, P.J. and Grabowski, E.J.J. *Tetrahedron Lett.* **1982**, 23, 2293.
22. Sedelmeier, G. and Bersier, J., *Process for the preparation of 4-acetoxy-3-hydroxyethyl-acetidinone*, Eur. Pat. Appl. EP 279,781, August 24, 1988.
23. Zoidl, M., Gonzalez Santana, A., Torvisco, A., Tysoe, C., Siriwardena, A., Withers, S.G., and Wrodnigg, T.M. *Carbohydr. Res.* **2016**, 429, 62.
24. Chéron, N., Ramozzi, R., Kaïm, L.E., Grimaud, L., and Fleurat-Lessard, P. *J. Org. Chem.* **2012**, 77, 1361.
25. Ugi, I. and Meyr, R. *Chem. Ber. Recl.* **1961**, 94, 2229.
26. Faggi, C., Garcia-Valverde, M., Marcaccini, S., and Menchi, G. *Org. Lett.* **2010**, 12, 788.
27. Barthelon, A., El Kaim, L., Gizolme, M., and Grimaud, L. *Eur. J. Org. Chem.* **2008**, 5974.
28. Domling, A. and Ugi, I. *Angew. Chem. Int. Ed.* **2000**, 39, 3168.
29. Stocker, B.L., Dangerfield, E.M., Win-Mason, A.L., Haslett, G.W., and Timmer, M.S.M. *Eur. J. Org. Chem.* **2010**, 2010, 1615.
30. Brandi, A., Cardona, F., Cicchi, S., Cordero, F.M., and Goti, A. *Chem. Eur. J.* **2009**, 15, 7808.
31. Felpin, F.-X. and Lebreton, J. *Eur. J. Org. Chem.* **2003**, 2003, 3693.
32. Chang, Y.-F., Guo, C.-W., Chan, T.-H., Pan, Y.-W., Tsou, E.-L., and Cheng, W.-C. *Molecular Diversity* **2011**, 15, 203.
33. Timmer, M.S.M., Risseuw, M.D.P., Verdoes, M., Filippov, D.V., Plaisier, J.R., van der Marel, G.A., Overkleeft, H.S., and van Boom, J.H. *Tetrahedron: Asymmetry* **2005**, 16, 177.
34. Bongers, K.M., Wennekes, T., de Lavoie, S.V.P., Esposito, D., van den Berg, R.J.B.H.N., Litjens, R.E.J.N., van der Marel, G.A., and Overkleeft, H.S. *QSAR Comb. Sci.* **2006**, 25, 491.
35. Laughlin, S.T., Baskin, J.M., Amacher, S.L., and Bertozzi, C.R. *Science* **2008**, 320, 664.
36. Laughlin, S.T., Agard, N.J., Baskin, J.M., Carrico, I.S., Chang, P.V., Ganguli, A.S., Hangauer, M.J., Lo, A., Prescher, J.A., and Bertozzi, C.R., *Metabolic Labeling of Glycans with Azido Sugars for Visualization and Glycoproteomics*, in *Methods Enzymol.* 2006, Academic Press. p. 230.



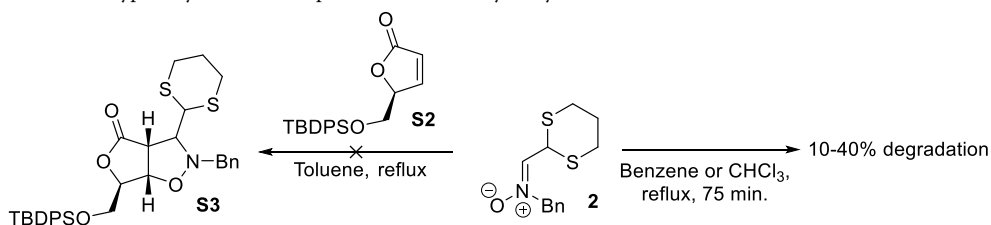
37. Zhao, X., Cai, L., Adogla, E.A., Guan, H., Lin, Y., and Wang, Q. *Bioconjugate Chem.* **2015**, 26, 1868.
38. Corfield, T. *Glycobiology* **1992**, 2, 509.
39. Müller, B. and Kräusslich, H.-G., *Antiviral Strategies*, in *Antiviral Strategies*, H.-G. Kräusslich and R. Bartenschlager, Editors. 2009, Springer Berlin Heidelberg: Berlin, Heidelberg. p. 1.
40. Colman, P.M., Varghese, J.N., and Laver, W.G. *Nature* **1983**, 303, 41.
41. Varghese, J.N., Mckimmbreschkin, J.L., Caldwell, J.B., Kortt, A.A., and Colman, P.M. *Proteins* **1992**, 14, 327.
42. Varghese, J.N., Laver, W.G., and Colman, P.M. *Nature* **1983**, 303, 35.
43. von Itzstein, M., Wu, W.Y., Kok, G.B., Pegg, M.S., Dyason, J.C., Jin, B., Phan, T.V., Smythe, M.L., White, H.F., Oliver, S.W., Colman, P.M., Varghese, J.N., Ryan, D.M., Woods, J.M., Bethell, R.C., Hotham, V.J., Cameron, J.M., and Penn, C.R. *Nature* **1993**, 363, 418.
44. von Itzstein, M., Dyason, J.C., Oliver, S.W., White, H.F., Wu, W.Y., Kok, G.B., and Pegg, M.S. *J. Med. Chem.* **1996**, 39, 388.
45. Holzer, C.T., Vonitzstein, M., Jin, B., Pegg, M.S., Stewart, W.P., and Wu, W.Y. *Glycoconjugate J.* **1993**, 10, 40.
46. von Itzstein, M., Wu, W.-Y., and Jin, B. *Carbohydr. Res.* **1994**, 259, 301.
47. Zaed, A.M. and Sutherland, A. *Org. Biomol. Chem.* **2010**, 8, 4394.
48. Wu, Y., Matsueda, G.R., and Bernatowicz, M. *Synth. Commun.* **1993**, 23, 3055.
49. Albiñana, C.B., Machara, A., Řezáčová, P., Páchl, P., Konvalinka, J., and Kožíšek, M. *Eur. J. Med. Chem.* **2016**, 121, 100.
50. Magesh, S., Moriya, S., Suzuki, T., Miyagi, T., Ishida, H., and Kiso, M. *Bioorg. Med. Chem. Lett.* **2008**, 18, 532.
51. Magesh, S., Suzuki, T., Miyagi, T., Ishida, H., and Kiso, M. *J Mol Graph Model* **2006**, 25, 196.
52. Laux, T., Mayer, K.F., Berger, J., and Jurgens, G. *Development* **1996**, 122, 87.
53. Muller, R., Borghi, L., Kwiatkowska, D., Laufs, P., and Simon, R. *Plant Cell* **2006**, 18, 1188.
54. Schoof, H., Lenhard, M., Haecker, A., Mayer, K.F., Jurgens, G., and Laux, T. *Cell* **2000**, 100, 635.
55. Mayer, K.F.X., Schoof, H., Haecker, A., Lenhard, M., Jürgens, G., and Laux, T. *Cell* **1998**, 95, 805.
56. Fletcher, L.C., Brand, U., Running, M.P., Simon, R., and Meyerowitz, E.M. *Science* **1999**, 283, 1911.
57. Gallois, J.-L., Nora, F.R., Mizukami, Y., and Sablowski, R. *Genes & development* **2004**, 18, 375.
58. Leeggangers, H.A., Moreno-Pachon, N., Gude, H., and Immink, R.G. *The International journal of developmental biology* **2013**, 57, 611.
59. Furo, K., Nozaki, M., Murashige, H., and Sato, Y. *FEBS Lett.* **2015**, 589, 3258.
60. Burget, E.G., Verma, R., Mølhøj, M., and Reiter, W.-D. *The Plant Cell* **2003**, 15, 523.
61. Tan, L., Varnai, P., Lampert, D.T.A., Yuan, C.H., Xu, J.F., Qiu, F., and Kieliszewski, M.J. *J. Biol. Chem.* **2010**, 285, 24575.
62. Saito, F., Suyama, A., Oka, T., Yoko-o, T., Matsuoka, K., Jigami, Y., and Shimma, Y. *J. Biol. Chem.* **2014**, 289, 20405.
63. Carpita, N.C. and Gibeaut, D.M. *The Plant journal : for cell and molecular biology* **1993**, 3, 1.
64. Rennie, E.A. and Scheller, H.V. *Curr. Opin. Biotechnol.* **2014**, 26, 100.



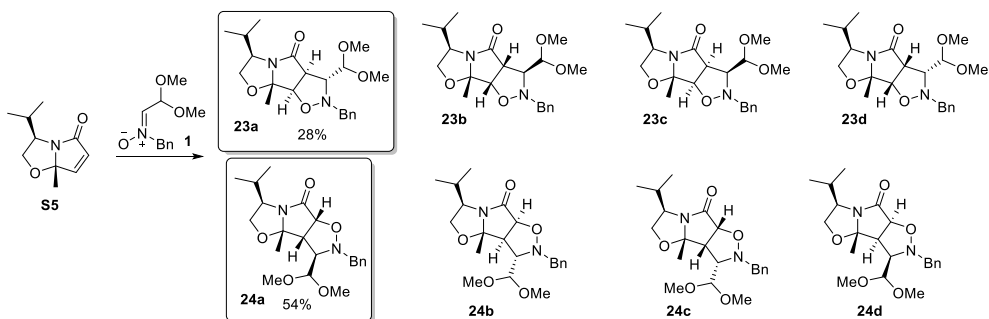
65. Bar-Peled, M. and O'Neill, M.A. *Annual review of plant biology* **2011**, 62, 127.
66. Rautengarten, C., Ebert, B., Herter, T., Petzold, C.J., Ishii, T., Mukhopadhyay, A., Usadel, B., and Scheller, H.V. *The Plant Cell* **2011**, 23, 1373.
67. Hsieh, Y.S.Y., Zhang, Q., Yap, K., Shirley, N.J., Lahnstein, J., Nelson, C.J., Burton, R.A., Millar, A.H., Bulone, V., and Fincher, G.B. *Biochemistry* **2016**, 55, 322.
68. Dugard, C.K., Mertz, R.A., Rayon, C., Mercadante, D., Hart, C., Benatti, M.R., Olek, A.T., SanMiguel, P.J., Cooper, B.R., Reiter, W.-D., McCann, M.C., and Carpita, N.C. *Plant Physiology* **2016**, 171, 1905.
69. Ha, V.T., Kien, V.T., Binh, L.H., Tien, V.D., My, N.T.T., Nam, N.H., Baltas, M., Hahn, H., Han, B.W., Thao, D.T., and Vu, T.K. *Bioorg. Chem.* **2016**, 66, 63.
70. Rye, C.S. and Withers, S.G. *J. Org. Chem.* **2002**, 67, 4505.
71. Wei, A. and Boulineau, F.P., *Enantiopure 4-deoxypentenoides, dihydropyrans and tetrahydropyrans and syntheses thereof*, 2003, Google Patents.
72. Richard, J.P., Amyes, T.L., Lee, Y.-G., and Jagannadham, V. *J. Am. Chem. Soc.* **1994**, 116, 10833.
73. Amyes, T.L. and Richard, J.P. *J. Am. Chem. Soc.* **1991**, 113, 1867.
74. Richard, J.P., Amyes, T.L., Jagannadham, V., Lee, Y.-G., and Rice, D.J. *J. Am. Chem. Soc.* **1995**, 117, 5198.
75. Banert, K., Berndt, C., Firdous, S., Hagedorn, M., Joo, Y.-H., Rüffer, T., and Lang, H. *Angew. Chem. Int. Ed.* **2010**, 49, 10206.

# **Appendix A**

## **Supporting Information for Chapter 2**

**Scheme S1.** Typical cycloaddition experiment and stability study of nitron 2

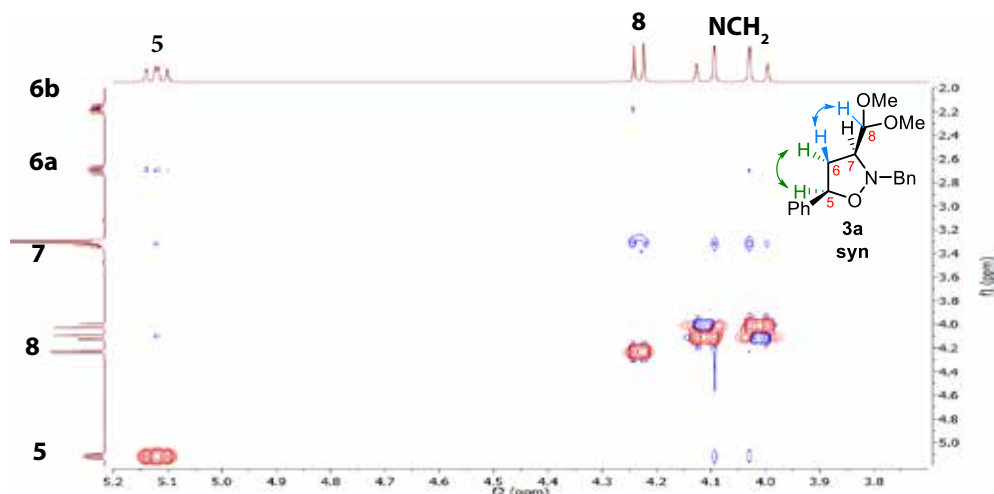
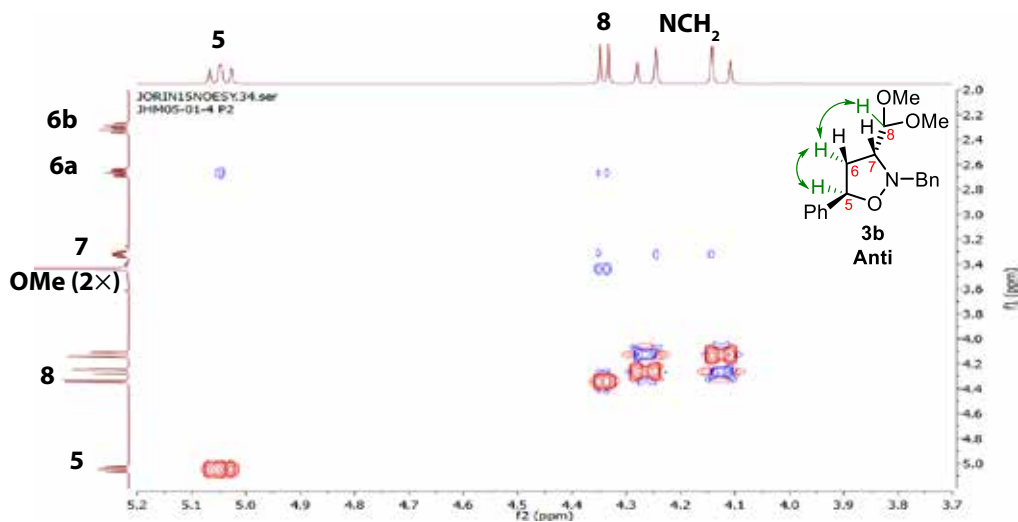
## Details for density functional theory calculations

**Scheme S2.** Cycloaddition of lactam S5 with nitron 1 providing eight theoretical regio- and stereo-isomers**Table S3.** Calculated lowest energies for compounds 3a-d and 4a-d<sup>a</sup>

Isomer	Total energy (in H)	Relative energies compared to 23a (in kcal/mol)
23a	-1303.881594	0.00
23b	-1303.880475	0.70
23c	-1303.878312	2.06
23d	-1303.875984	3.52
24a	-1303.880976	0.39
24b	-1303.875352	3.92
24c	-1303.868799	8.02
24d	-1303.855268	16.51

<sup>a</sup> The geometries of all 8 possible stereo- and regioisomers of the nitron reaction on lactam S5 were sequentially optimized by molecular mechanics MMFF94 calculations (in Chem3D) and density functional theory M11-L/6-311+G(d,p) calculations. This yielded the lowest energies for compounds 23a and 24a, which fits our experiments, and isomer 23b only slightly 1 kcal/mol higher than these. All other isomers were less stable, largely due to (significantly) increased steric hindrance.

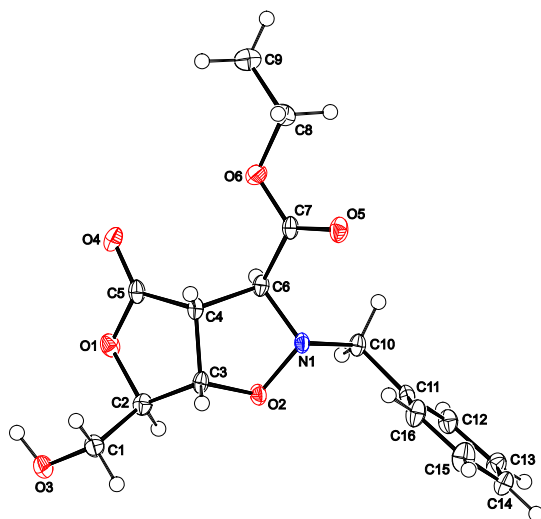
## Typical results of NOESY experiments

Figure S1. Typical example of syn/anti determination with cycloadduct **3a**.Figure S2. Typical example of syn/anti determination with cycloadduct **3b**.



## **Appendix B**

### **Supporting Information for Chapter 3**



**Figure S1.** Displacement ellipsoid plot of **6a** in the crystal (50% probability level).

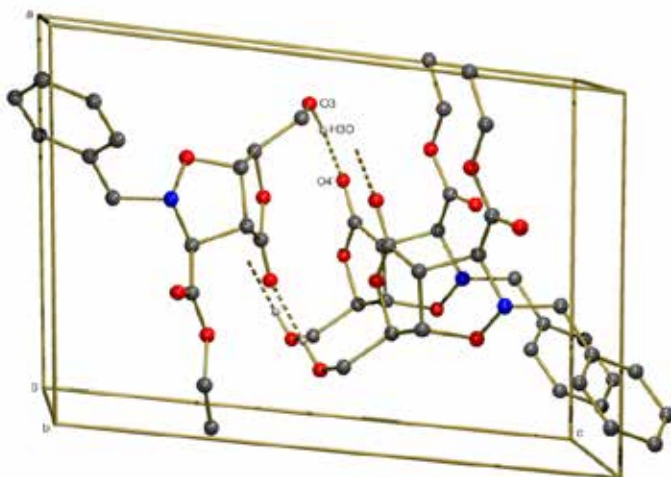


**Figure S2.** By hydrogen bonding, the molecules of **6a** are linked into one-dimensional chains along the b-axis. Symmetry code i: 1-x, y-0.5, 1-z. Geometry: O3-H3O 0.89(3) Å; H3O...O4<sup>i</sup> 1.97(3) Å; O3...O4<sup>i</sup> 2.838(2) Å; O3-H3O...O4<sup>i</sup> 163(3) °.

**Table S1.** Torsion angles [°] in the five-membered rings in **6a**, obtained from the X-ray crystal structure[\*]

O1-C2-C3-C4	4.5(2)	O2-N1-C6-C4	45.37(18)
C2-C3-C4-C5	-2.8(2)	N1-C6-C4-C3	-23.2(2)
C3-C4-C5-O1	-0.1(2)	C6-C4-C3-O2	-8.0(2)
C4-C5-O1-C2	3.2(2)	C4-C3-O2-N1	36.5(2)
C5-O1-C2-C3	-4.9(2)	C3-O2-N1-C6	-52.16(19)

[\*] Ring 1 is essentially planar, ring 2 is best described as envelope on N1.

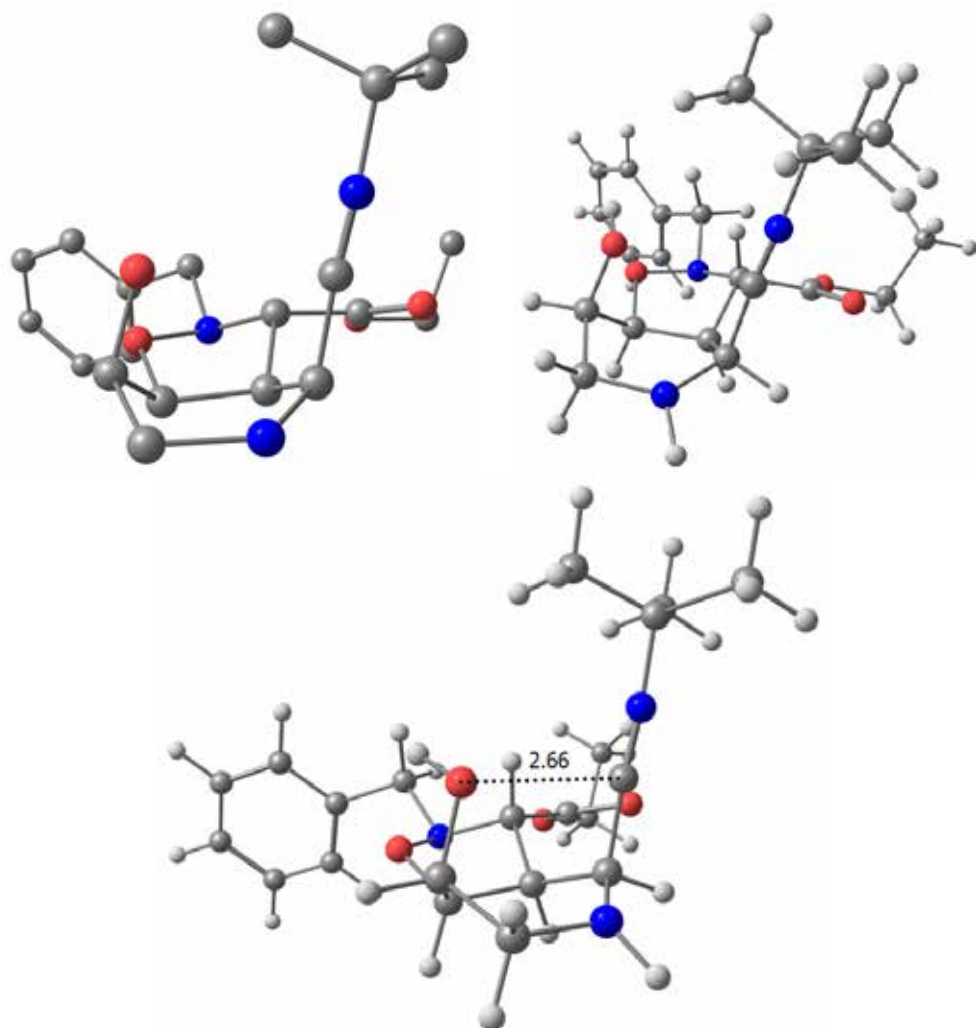


**Figure S3.** The pseudo-boat cation conformation **IV** as determined by M11/6-311+g(d,p) density functional calculations, which places the O-atom the hydroxyl group close to the partially positively charged C atom of the nitrilium ion.

**Table S2.** The absolute and relative energies of different conformations **IV** as determined by M11/6-311+g(d,p) density functional calculations

Conformer	E (hartree)	E <sub>rel</sub> (kcal/mol) <sup>a</sup>
semiboat	-1282.80431	0.0
boat	-1282.78789	10.3
chairOHax	-1282.79442	6.2
chairNHax	-1282.78586	11.6

<sup>a</sup> Relative energies based on the semiboat conformer

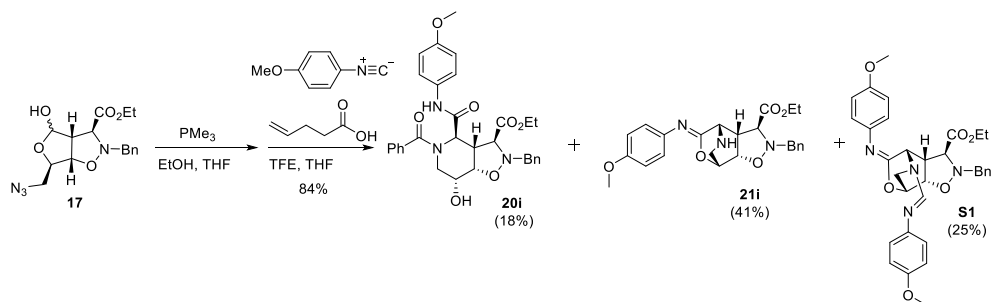
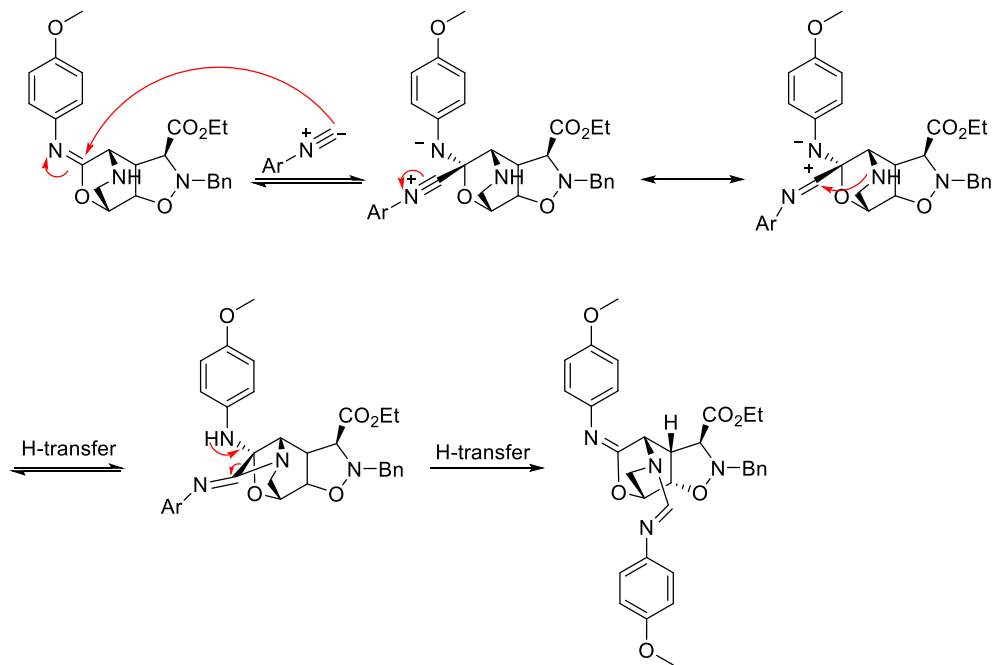


**Final energies semi boat (Energy= -1282.80437445 hartree )**

```

1\1\GINC-TIMO13\FOpt\RM11\6-311+G(d,p)\C21H30N3O4(1+)\ROOT\26-
Aug-2016  \0\# opt m11/6-311+g(d,p) freq\BOAT CATION IV\1,1\C,-3.0277088906,1
.6393287923,-0.2289544876\O,-0.2672250399,2.0824002167,0.281867365\C,
-0.504615233,2.3732228658,-1.0955801845\C,-1.0094563252,1.1104080988,
-1.7814993122\C,-2.3084568518,0.5941905454,-1.1188244676\O,-0.0488525405
,0.0837900349,-1.5616630764\N,-0.8020490813,-1.1364225779,-1.382826459
5\C,-1.8044446584,-0.6841728841,-0.4300245216\C,-1.5584569222,3.464326
0085,-1.1661980337\N,-2.8317538274,3.0035411929,-0.6061049576\H,-3.020
9124619,0.3076716601,-1.8996662031\C,-2.6758879111,1.4583457381,1.2169847639\N,
-2.4915690659,1.3371713604,2.3348592392\C,-2.1555722173,1.078458294,3.7389909486\
C,-2.6236661259,-0.3500496122,4.0322702846\C,-0.635415394,1.2205-
92499,3.8516933204\C,-2.8940210438,2.1124712615,4.5901092214\C,-2.9726747251,
-1.5948430077,-0.1143007934\O,-3.8756241132,-1.1695400935,0.5749960689\O,
-2.9076842524,-2.7973474995,-0.6366410191\C,-3.8754390658,
-4.3169987347,1.0194243599\C,-4.0205666055,-3.7037778785,-0.3591271194\
C,1.1851226904,-2.4910595189,-1.8734636449\C,0.7944397752,-2.8522493476,
-3.1610574075\C,1.7462280379,-3.22950651,-4.0974001803\C,3.0947033752,
-3.2507859354,-3.7540102124\C,3.4871684136,-2.8898332113,-2.4721721229\C,
2.5327389993,-2.5076467407,-1.5354759082\C,0.1432230108,-2.1112576728,-
0.8470761714\H,-4.1002648794,1.4051510623,-0.2339428356\H,0.4321651345,1.4-
180271229,0.3148297092\H,0.4169968436,2.723824795,-1.5790743392\H,-
1.1495494883,1.2767872914,-2.8585288619\H,-1.3230388568,-0.431819847,0.5365716596\
H,-1.1956428896,4.3355543332,-0.6077321115\H,-1.6816919144,3.7567681837,-
2.218872059\H,-3.6573841041,3.471146805,-0.9449830103\H,-2.3954813033,-0.5817-
606786,5.0783910518\H,-3.7026904936,-0.4511800436,3.874268627\H,-2.101735716,-
1.0717708705,3.3928130483\H,-0.3452423581,1.0298624307,4.890716555\H,
-0.3120754359,2.2294403894,3.5745835515\H,-0.1271367912,0.4902166692,3.2106548357\
H,-2.5809020521,3.1301711374,4.333965366\H,-3.9786347188,2.0235415667,
4.466599291\H,-2.6496167002,1.9289467669,5.6419770652\H,-4.6793329347,-
5.0435504767,1.1804346774\H,-2.9187857036,-4.8421950556,1.1118011194\H,
-3.9495478953,-3.5490226619,1.7964615047\H,-4.9494504541,-3.1329827324,-
0.457903537\H,-3.9549218076,-4.449906006,-1.1540485404\H,-0.2625526974,
-2.8273583538,-3.4232623217\H,1.4369683679,-3.5115775587,-5.1021101256\H,
3.8401979673,-3.5487705253,-4.4886808126\H,4.5407941865,-2.9021296264,-
2.1998264416\H,2.8431116656,-2.2200123682,-0.530760399\H,-0.4559454982,
-2.9869846145,-0.5686315867\H,0.6288185771,-1.7078112288,0.0611596314\
Version=EM64L-G09RevD.01\State=1-A\HF=-1282.8043054\RMSD=3.041e-09\
RMSF=2.834e-06\Dipole=-1.8957161,1.8853175,2.0613076\Quadrupole=
-8.6286931,0.854047,7.7746462,-3.3037374,-3.9313348,4.4783825\PG=C01 [X(C21H
30N3O4)]\@

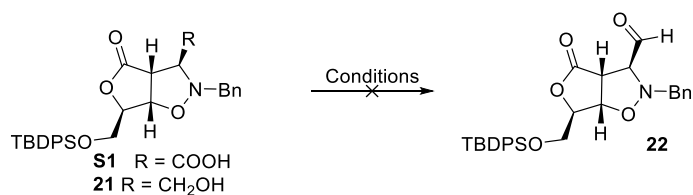
```

**Scheme S1.** The result of a SAWU-3CR between hemiacetal **17**, 4-pentenoic acid, and 4-methoxyisocyanide**Scheme S2.** Potential mechanism for the formation of formamidine **S1**



## **Appendix C**

### **Supporting Information for Chapter 4**

**Table S1.** Selected oxidation attempts to obtain aldehyde **22**

Entry <sup>a</sup>	Conditions <sup>b</sup>	Temperature (°C)	Result
1 (9)	1. (COCl) <sub>2</sub> , DMF	rt	Degradation
	2. Pd(PPh <sub>3</sub> ) <sub>4</sub> , <i>n</i> Bu <sub>3</sub> SnH	0→20 °C	
2 (10)	Swern ox.	-20	No conversion
3	Dess-Martin	20	No conversion
4	Dess-Martin <sup>c</sup>	20	Degradation <sup>f</sup>
5	PCC	0→20	Degradation, ≤10% yield
6	PDC	0→20	No conversion
7	Swern ox. <sup>d</sup>	-78	Degradation
8	Anelli's oxidation	0→20	Degradation <sup>f</sup>
9	Parikh-Doering	rt	Degradation <sup>f</sup>
10	Dess-Martin <sup>c</sup>	0→20	Degradation
11	PCC/NaOAc	rt	Degradation <sup>f</sup>
12	PCC/AcOH	rt	Degradation, ≤30% yield

<sup>a</sup>Reaction were generally carried out with alcohol **10** except for entry 1 (**9**). <sup>b</sup>Reactions were carried out in DCM.

<sup>c</sup>Dess Martin reagent was synthesized freshly. <sup>d</sup>Swern was carried out with large excess (5 equiv) of oxalyl chloride and DMSO (10 equiv). <sup>e</sup>A 0.3M solution of commercially available Dess-Martin periodane was used. <sup>f</sup>Still a lot of starting material left, but the formation of several spots (TLC-analysis/NMR) showed that complete degradation would occur over time.

**Table S2.** Attempted hydrogenations on isoxazolidine **7a**

Hydrogenation

Entry	Catalyst	H <sub>2</sub> -source	Solvent	<i>In situ</i> protection	Result <sup>b</sup>
1	Pd(OH) <sub>2</sub> /C	H <sub>2</sub> (1 bar)	THF	-	Slow/ degradation
2	Pd/C + HCl	H <sub>2</sub> (1 bar)	THF	-	Degradation
3	Pd/C	H <sub>2</sub> (1 bar)	THF (40 °C)	-	Slow/ degradation
4	Pd/C	H <sub>2</sub> (1 bar)	MeOH	-	Slow/ degradation
5	Pd/C	H <sub>2</sub> (1 bar)	AcOH	-	Degradation
6 <sup>a</sup>	Pd/C	NH <sub>4</sub> <sup>+</sup> HCO <sub>2</sub> <sup>-</sup>	MeOH (Reflux)	-	Degradation
7	Pd/C	NH <sub>4</sub> <sup>+</sup> AcO <sup>-</sup>	EtOH (Reflux)	-	No conversion
8	Raney-Ni	H <sub>2</sub> (1 bar)	EtOH	-	Fast conversion <sup>c</sup> , but degradation upon workup.
9	Pd/C	Cyclohexene	EtOH (reflux)	-	Good conversion, but degradation upon workup.
10	Conditions of entry 8 and 9 (sequential)	H <sub>2</sub> → Cyclohexene	EtOH	Ac <sub>2</sub> O, Py	Fast conversion <sup>c</sup> , but degradation upon protection.
11	Pd/C hydrogenation	Cyclohexene	EtOH	Boc <sub>2</sub> O, Py	Incomplete conv, and degradation upon protection.
12	Conditions of entry 8 and 9 (sequential)	H <sub>2</sub> → Cyclohexene	THF	Ac <sub>2</sub> O, Py	Clean conversion, but degradation upon protection.
13	Conditions of entry 8 and 9 (sequential)	H <sub>2</sub> (1 bar)	THF	TBDMSCl, imidazole <sup>d</sup>	Fast conversion <sup>c</sup> , but no protection
13	Conditions of entry 8 and 9 (sequential)	H <sub>2</sub> (1 bar)	THF	TMSCl, Et <sub>3</sub> N <sup>d</sup>	Fast conversion <sup>c</sup> , but no protection
14	Raney-Ni	H <sub>2</sub> (1 bar)	THF (-78-20 °C) <sup>e</sup>	TMSOTf, Lutidine	Fast conversion <sup>c</sup> , but no protection
15	Raney-Ni	H <sub>2</sub> (1 bar)	THF (-78-20 °C) <sup>e</sup>	TBDMSOTf, Lutidine	Fast conversion <sup>c</sup> , but no protection

<sup>a</sup>Reaction carried out with TBDPS-deprotected bicyclic isoxazolidine. <sup>b</sup>Complete conversion means N-O cleavage and N-Bn cleavage unless stated otherwise. <sup>c</sup>Selective N-O cleavage. <sup>d</sup>Protection step performed at rt. <sup>e</sup>Indicated temperature range was used for the protection step. The hydrogenation step was performed at rt.

**Table S3.** Selected failed reduction attempts on lactone **13a**

Entry	Reducing agent	Solvent	Temperature (°C)	Result <sup>a</sup>
1	DiBAL-H	THF	-78	≤33% (unreliable)
2	L-selectride	THF	-70	53% (combined)
3	NaBH <sub>4</sub>	EtOH	20	Diol + degradation
4	NaBH <sub>4</sub>	MeOH	20	Diol + degradation
5	NaBH <sub>4</sub>	THF	20	Degradation/product/diol/Sm1
6	NaBH <sub>4</sub>	Dioxane	20	Degradation/product/diol/Sm1
7	NaBH <sub>4</sub> , ZnCl <sub>2</sub>	MeOH	20	degradation
8	NaBH <sub>4</sub> , ZnCl <sub>2</sub> , Et <sub>3</sub> N	MeOH	20	degradation
9	BH <sub>3</sub> -SMe <sub>2</sub>	THF	20	78% hemiacetal + 16% diol
10	NaBH <sub>4</sub> , ZnCl <sub>2</sub>	THF	20	Similar as entry 9
				Yield/ratio not determined
11	NaBH <sub>4</sub> , ZnCl <sub>2</sub> , Et <sub>3</sub> N	THF	20	Similar as entry 9
				Yield/ratio not determined

<sup>a</sup>Reaction yield is the combined yield of hemiacetal **22** and diol **23** unless stated otherwise.

## **Appendix D**

### **Supporting Information for Chapter 5**



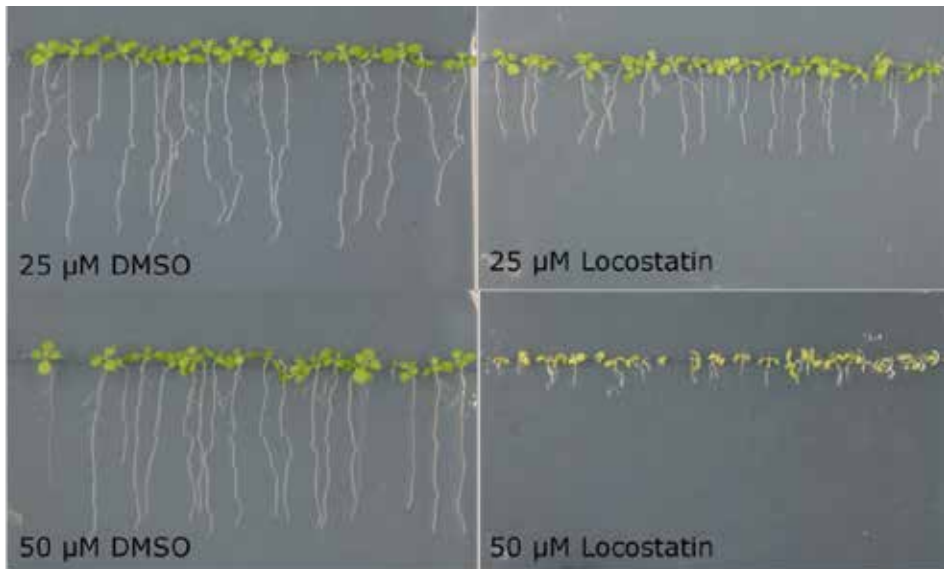


**Figure S1.** The effect of 25-50  $\mu$ M locostatin/ DMSO on the root development of *Arabidopsis thaliana*, grown for 10 days under LD conditions.

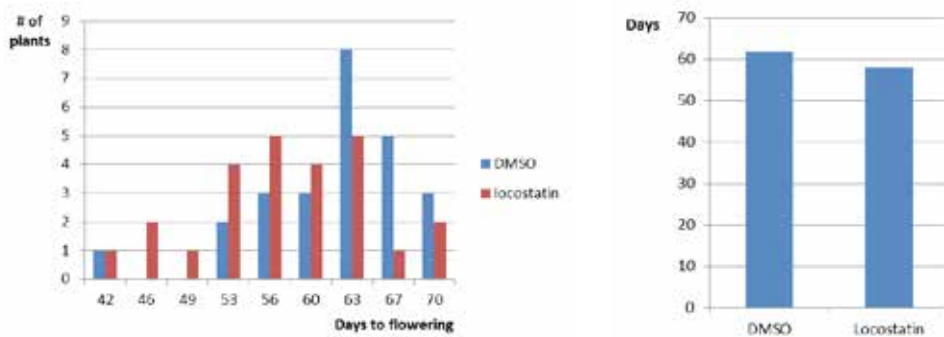


**Figure S2.** The effect of 25  $\mu$ M locostatin on the flowering time of *Arabidopsis thaliana*, grown under short day conditions (Left) and the average # days required for flowering (right).

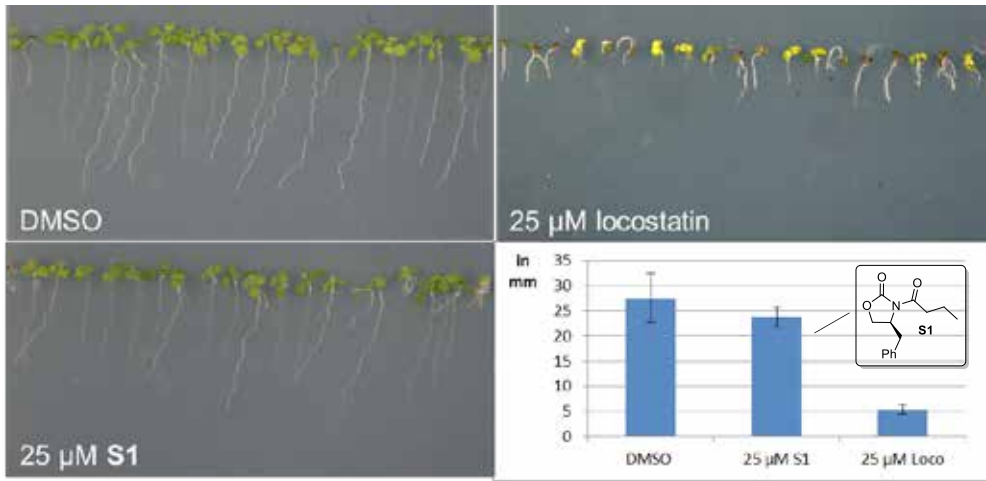


**Figure S3.** Effect of 25  $\mu\text{M}$  DMSO (Top left), 25  $\mu\text{M}$  saturated locostatin **S1** (bottom left), and 25  $\mu\text{M}$  locostatin (Top right) on root development of *Arabidopsis thaliana*, summarized in a chart (bottom right).

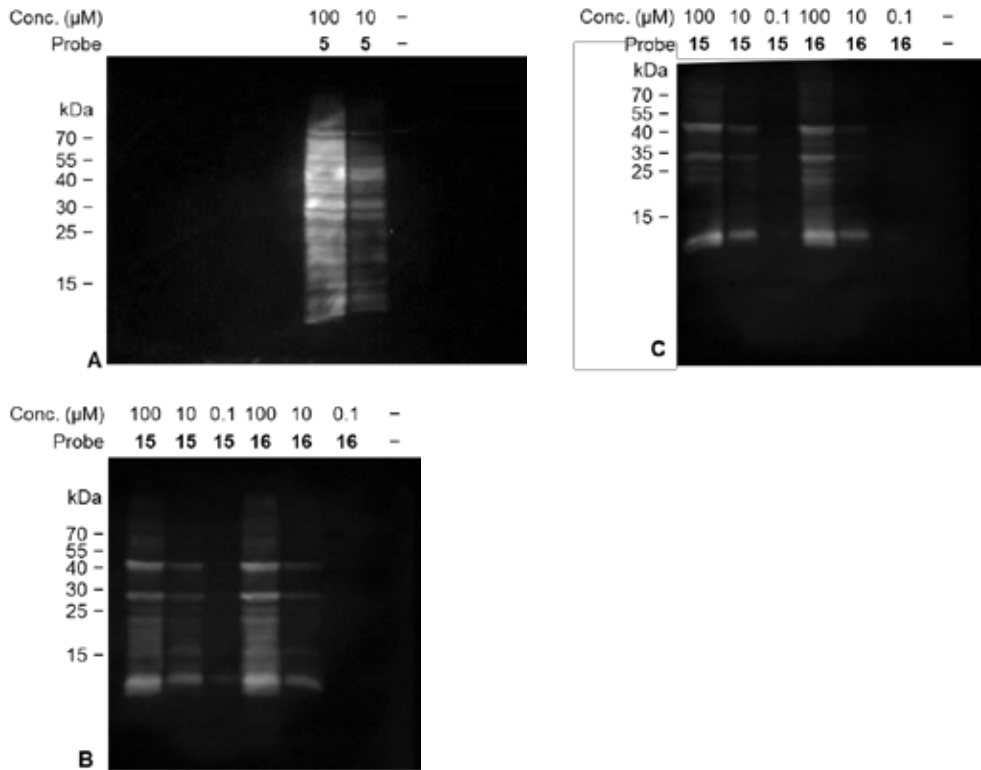


**Figure S4.** A) Binding of Probe 5 with in vitro expressed FT at 37 °C for 24 h; B) Binding of Probe 15&16 with in vitro expressed FT at rt for 2 h; C) Binding of Probe 15&16 with in vitro expressed FT at 4 °C for 2 h. [Note: Conc. ( $\mu\text{M}$ ) refers to the probe concentration].

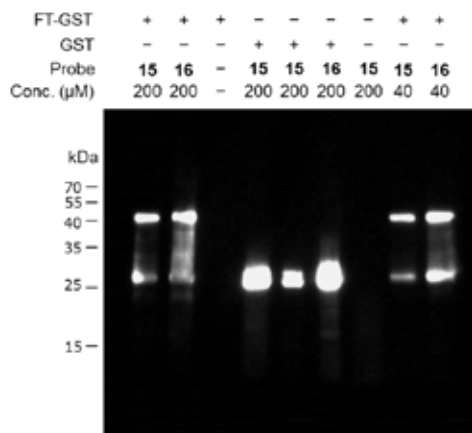


**Figure S5.** Binding of locostatin probes 15&16 with GST-FT + residual GST and binding of probe 15&16 with GST.

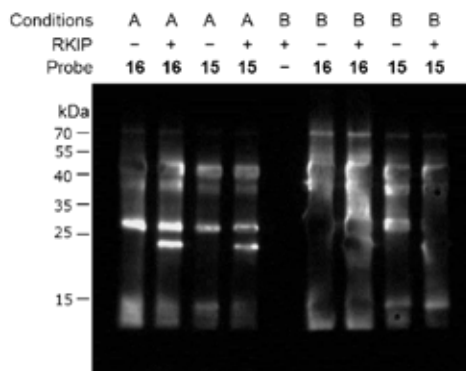


**Figure S7.** Evaluation of selectivity of locostatin probes 15&16 towards 5 reference proteins (2.38  $\mu$ M) with or without 2.38  $\mu$ M RKIP; Reference proteins: Ribonuclease A (13.7 kDa), Chymotrypsin A (25 kDa), Ovalbumin (45 kDa), Catalase (240 kDa (tetramer); 60 kDa monomer), Aldolase (158 kDa); Conditions: A) 20  $^{\circ}$ C, 1 h; B) 37  $^{\circ}$ C, 6 h.

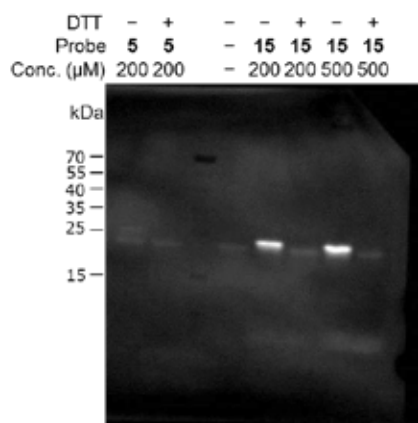


**Figure S6.** Binding of probe 5 and 15 with 2.38  $\mu$ M RKIP at 37  $^{\circ}$ C for 6 h with or without 2 mM DTT. Note that the presence of DTT prevents binding of locostatin-based probe 5 or 15.

## **Appendix E**

### **Supporting Information for Chapter 6**

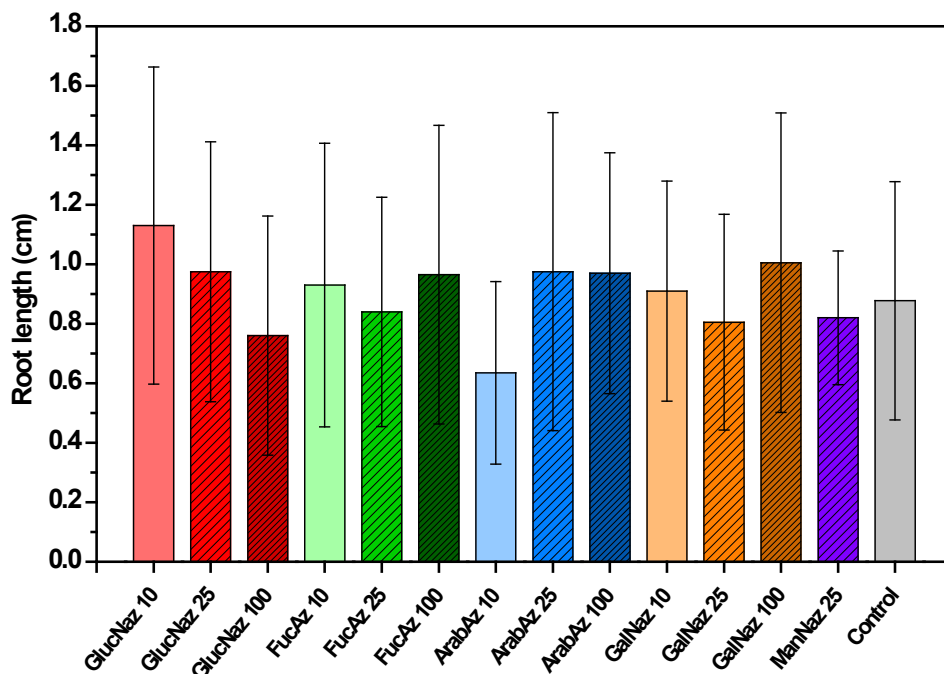


**Figure S1.** Arabidopsis growth on agar plate with various azido-monosaccharides. Arabidopsis seedlings were germinated and grown on agar plates containing the different azido-monosaccharide solutions in  $\frac{1}{2}$  MS with 0.8% plant agar. After 8 days of growth, the white part of the root was measured from leaves till root tip. Root length measured after 8 days of growth. Concentrations (10, 25 or 100) are in  $\mu\text{M}$ . Error bars represent standard deviations ( $n=20$  seedlings for each experiment,  $n=60$  for control experiments). No significant difference was observed (one-way ANOVA test,  $P<0.05$ ).

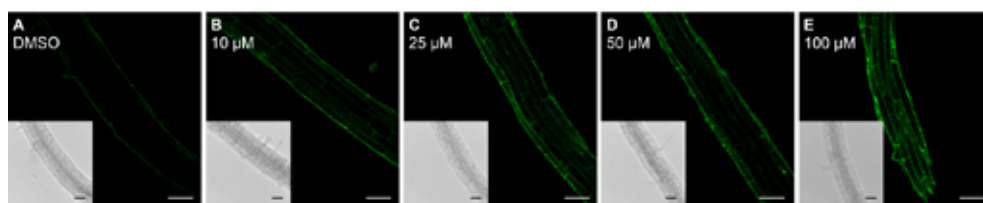


**Figure S2.** Concentration-dependent  $\text{Ac}_4\text{GlcNAz}$  incorporation. Optical sections of 4 day old Arabidopsis seedling roots incubated for 24 hours with 10  $\mu\text{M}$  (b), 25  $\mu\text{M}$  (c), 50  $\mu\text{M}$  (d), and 100  $\mu\text{M}$  (e)  $\text{Ac}_4\text{GlcNAz}$ , followed by labeling through a copper-catalysed click-reaction with Alexa Fluor® 488 alkyne. As a control, seedlings were treated with 0.01 % DMSO (a). Scale bars = 50  $\mu\text{m}$ .

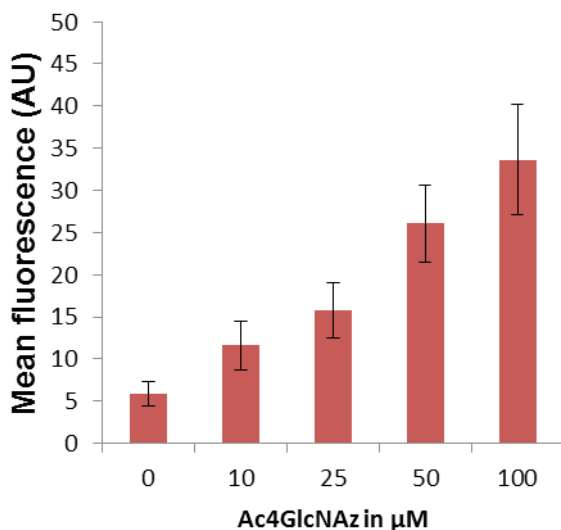


**Figure S3.** Mean fluorescence intensity of the epidermal cells of 4 day old Arabidopsis seedling roots incubated for 24 hours with 0-100  $\mu\text{M}$   $\text{Ac}_4\text{GlcNAz}$ . The error bars represent the S.D. in the fluorescent intensity throughout the cells of seedlings. Data of those cells were collected from 3-4 seedlings per treatment.

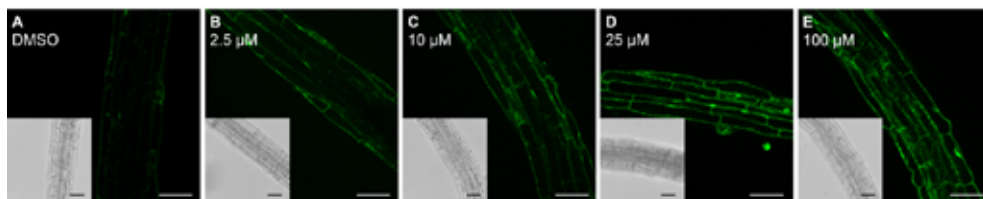


**Figure S4.** Concentration-dependent  $\text{Ac}_4\text{FucAz}$  incorporation. Optical sections of 4 day old Arabidopsis seedling roots incubated for 24 hours with 2.5  $\mu\text{M}$  (b), 10  $\mu\text{M}$  (c), 25  $\mu\text{M}$  (d), and 100  $\mu\text{M}$  (e) FucAz, followed by labeling through a copper-catalysed click-reaction with Alexa Fluor® 488 alkyne. As a control, seedlings were treated with 0.01 % DMSO (a). Scale bars = 50  $\mu\text{m}$ .

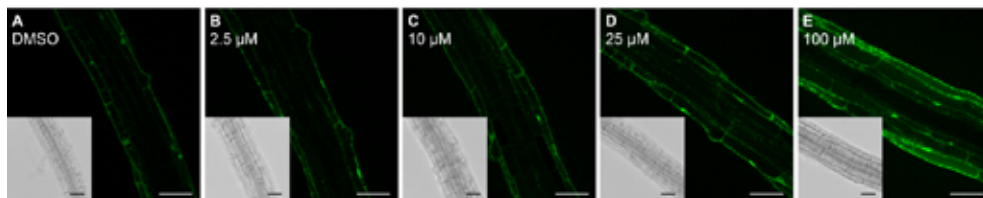


**Figure S5.** Concentration-dependent  $\text{Ac}_3\text{ArabAz}$  incorporation. Optical sections of 4 day old Arabidopsis seedling roots incubated for 24 hours with 2.5  $\mu\text{M}$  (b), 10  $\mu\text{M}$  (c), 25  $\mu\text{M}$  (d), and 100  $\mu\text{M}$  (e) ArabAz, followed by labeling through a copper-catalysed click-reaction with Alexa Fluor® 488 alkyne. As a control, seedlings were treated with 0.01 % DMSO (a). Scale bars = 50  $\mu\text{m}$ .

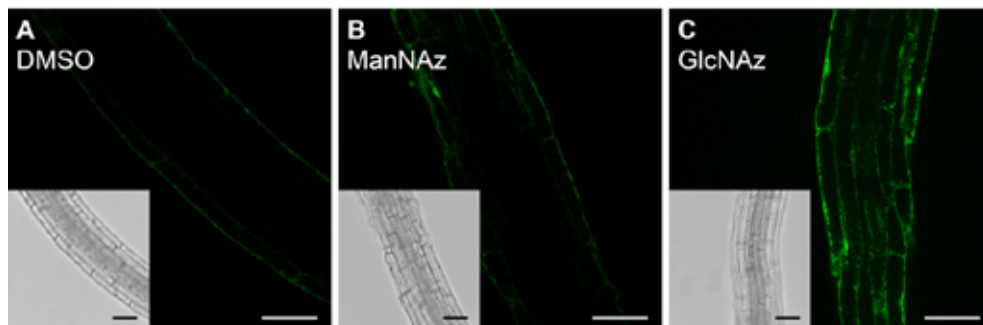


**Figure S6.** DMSO-incubated control for the corresponding ManNAz experiment. Optical sections of 4 day old *Arabidopsis* seedling roots incubated for 24 hours with 0.01 % DMSO as a control (a), 25  $\mu$ M ManNAz (b), or 25  $\mu$ M GlcNAz (c), followed by labeling through a copper-catalysed click-reaction with Alexa Fluor® 488 alkyne. Scale bars = 50  $\mu$ m.

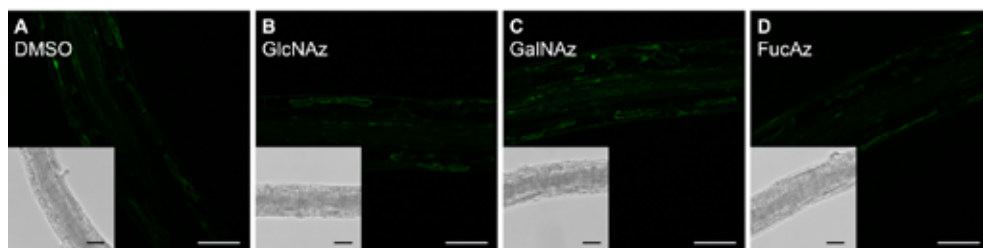


**Figure S7.** Azido-monosaccharide incorporation requires cell viability. Optical sections of 4 day old *Arabidopsis* seedling roots fixated in 4% paraformaldehyde solution in PBS incubated for 24 hours with 25  $\mu$ M GlcNAz (b), 25  $\mu$ M GalNAz (c), 25  $\mu$ M FucAz (d), followed by labeling through a copper-catalysed click-reaction with Alexa Fluor® 488 alkyne. As a control, seedlings were treated with 0.01 % DMSO (a). Scale bars = 50  $\mu$ m.

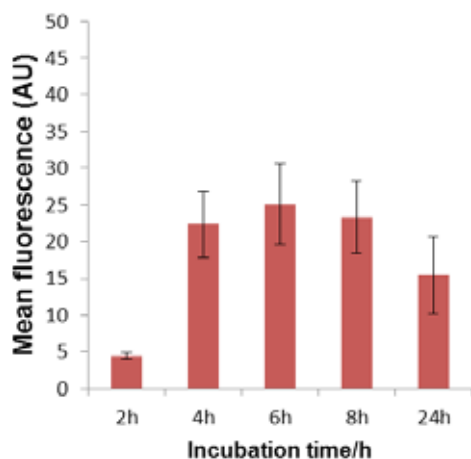


**Figure S8.** Mean fluorescence intensity of the epidermal cells of 4 day old *Arabidopsis* seedling roots illustrating the time-dependent uptake of 25  $\mu$ M Ac<sub>4</sub>GlcNAz. The error bars represent the S.D. in the fluorescent intensity throughout the cells of seedlings. Data of those cells were collected from 3-4 seedlings per treatment.

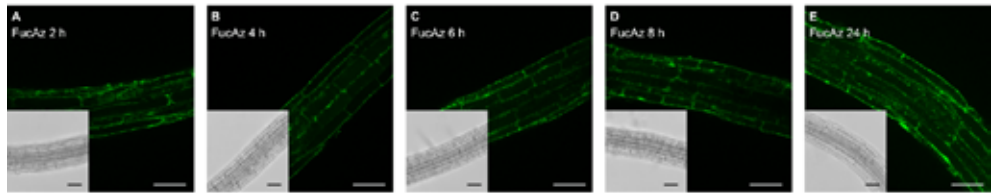


**Figure S9.** Time-course of  $\text{Ac}_4\text{FucAz}$  incorporation in elongating root cells. Optical sections of 4 day old Arabidopsis seedling roots incubated for 2 (a), 4 (b), 6 (c), 8 (d) and 24 hours (e) with  $25 \mu\text{M}$   $\text{Ac}_4\text{FucAz}$ , followed by labeling through a copper-catalysed click-reaction with Alexa Fluor® 488 alkyne. Scale bars =  $50 \mu\text{m}$ .

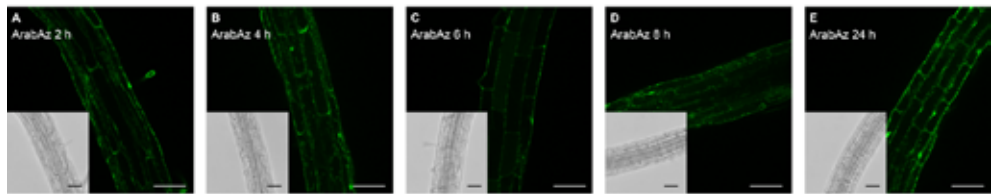


**Figure S10.** Time-course of  $\text{Ac}_4\text{ArabAz}$  incorporation in elongating root cells. Optical sections of 4 day old Arabidopsis seedling roots incubated for 2 (a), 4 (b), 6 (c), 8 (d) and 24 hours (e) with  $100 \mu\text{M}$  ArabAz, followed by labeling through a copper-catalysed click-reaction with Alexa Fluor® 488 alkyne. Scale bars =  $50 \mu\text{m}$ .

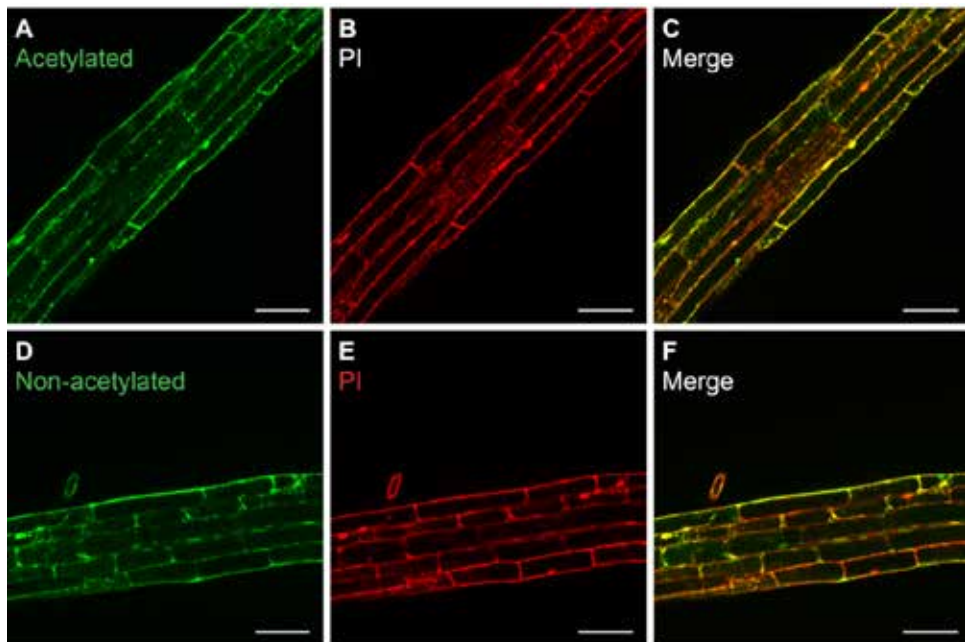


**Figure S11.** Comparison of non-acetylated and acetylated GlcNAz labeled seedlings with PI stain. Optical sections of 4 day old Arabidopsis seedling roots incubated for 24 hours with  $25 \mu\text{M}$  GlcNAz (a-c) or  $25 \mu\text{M}$  non-acetylated GlcNAz (d-f), followed by labeling through a copper-catalysed click-reaction with Alexa Fluor® 488 alkyne. Seedling roots treated with Alexa Fluor® 488 alkyne labelled GlcNAz ( $25 \mu\text{M}$ , 24 h) (a,c) were counterstained with Propidium Iodide (PI, 0.05%) to visualize cell walls (b,c). Similarly, seedling roots treated with Alexa Fluor® 488 alkyne labelled non-acetylated GlcNAz ( $25 \mu\text{M}$ , 24 h) (d,f) were counterstained with Propidium Iodide (PI, 0.05%) to visualize cell walls (e,f). Yellow colour indicates overlap of the two dyes (c,f). Scale bars =  $50 \mu\text{m}$ .



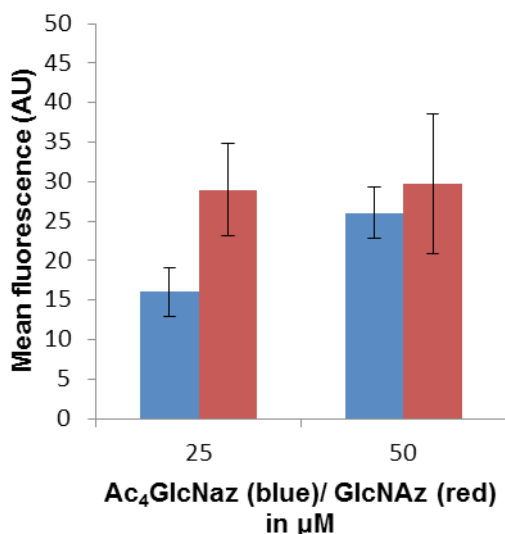


**Figure S12.** Comparison of the mean fluorescence of non-acetylated (GlcNAz) and acetylated (Ac<sub>4</sub>GlcNAz) labeled seedlings. Mean fluorescence intensity of the epidermal cells of 4 day old Arabidopsis seedling roots incubated for 24 hours with 25-50 acetylated Ac<sub>4</sub>GlcNAz or unprotected GlcNAz. The error bars represent the S.D. in the fluorescent intensity throughout the cells of seedlings. Data of those cells were collected from 3-4 seedlings per treatment.

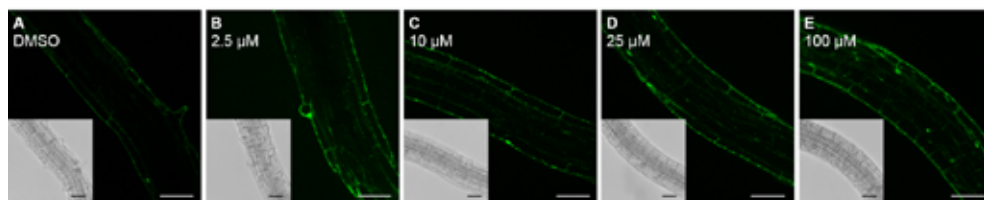


**Figure S13.** Concentration-dependent Ac<sub>4</sub>GalNAz incorporation (24 h incubation). Optical sections of 4 day old Arabidopsis seedling roots incubated for 24 hours with 2.5 μM (b), 10 μM (c), 25 μM (d), and 100 μM (e) GalNAz, followed by labeling through a copper-catalysed click-reaction with Alexa Fluor® 488 alkyne. As a control, seedlings were treated with 0.01 % DMSO (a). Scale bars = 50 μm.

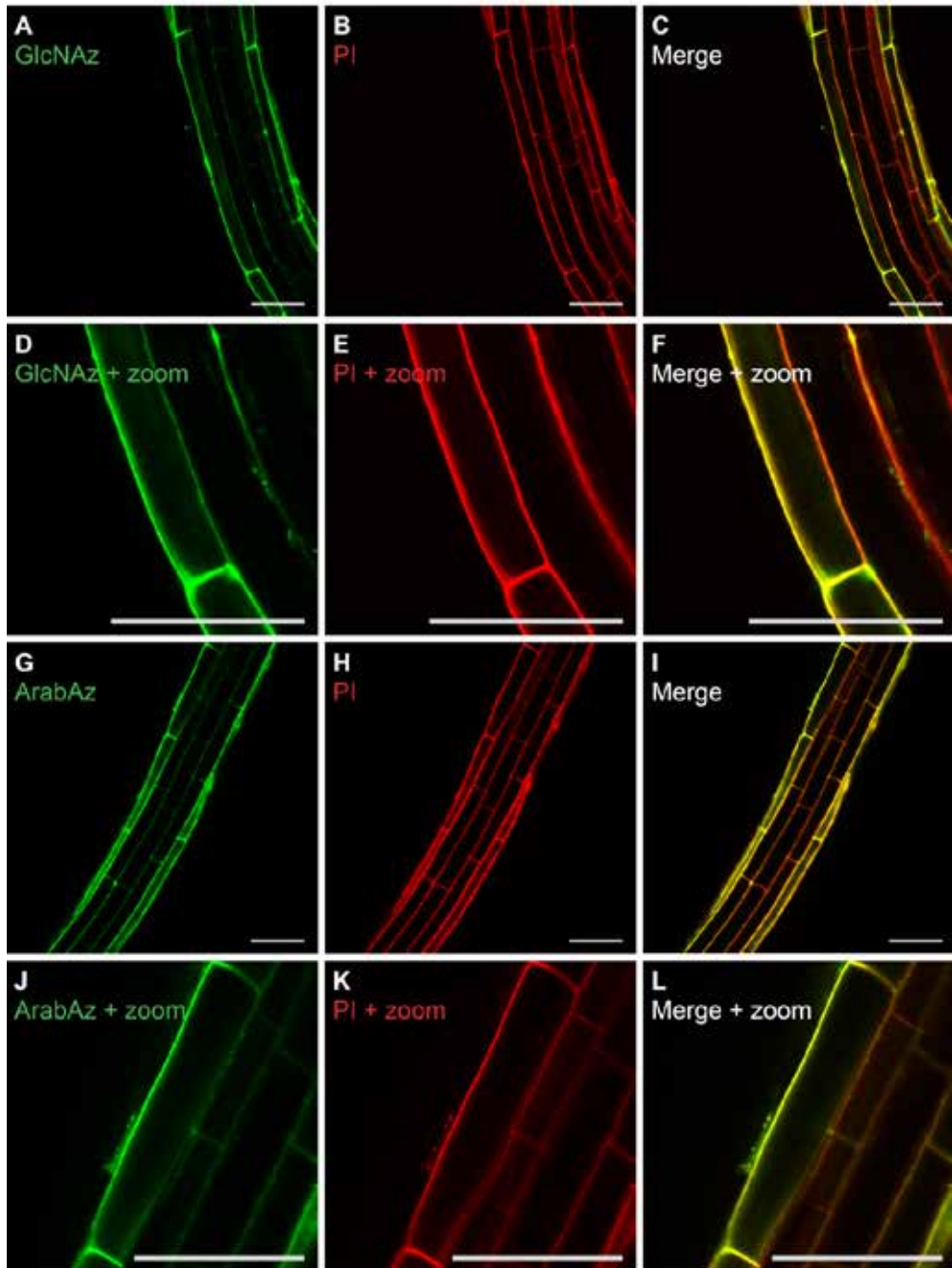


**Figure S14.** Comparison of  $Ac_4$ GlcNAz and  $Ac_3$ ArabAz labeled seedlings with PI stain. Optical sections of 4 day old *Arabidopsis* seedling roots incubated for 24 hours with 25  $\mu$ M GlcNAz (a-f) or 100  $\mu$ M ArabAz (g-l), followed by labeling through strain-promoted alkyne-azide cycloaddition with DBCO-PEG4-ATTO-488. Seedling roots treated with DBCO-PEG4-ATTO-488 labelled GlcNAz (25  $\mu$ M, 24 h) were counterstained with Propidium Iodide (PI, 0.05%) to visualize cell walls (b,c,e,f). Similarly, Seedling roots treated with DBCO-PEG4-ATTO-488 labelled ArabAz (100  $\mu$ M, 24 h) were counterstained with Propidium Iodide (PI, 0.05%) to visualize cell walls (h,i,k,l). Scale bars = 50  $\mu$ m.



## **Appendix F**

### **Supporting Information for Chapter 7**

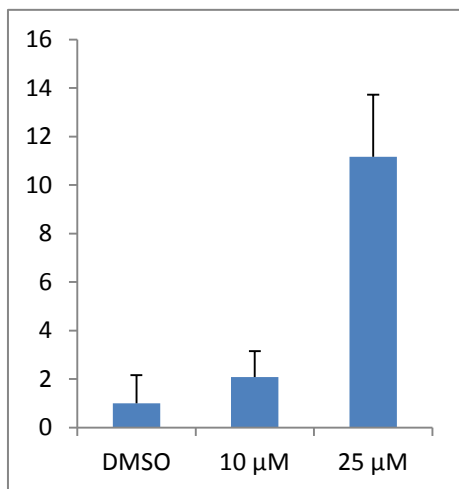


**Figure S1.** Relative WUS-expression based resulting from incubating Arabidopsis seedlings with 0-25 μM of compound 47.

# Summary

**Chapter 1** provides a perspective of synthetic organic chemistry as a discipline involved in the design, synthesis and evaluation of complex molecules. The reader is introduced with a brief history of synthetic organic chemistry, all the while dealing with different aspects of synthetic organic chemistry. These aspects include design, synthesis and evaluation of complex molecules, which are described with representative examples. For instance, chapter 1 described different strategies to design antibiotics like penicillin. Furthermore, efforts at the interface of chemistry and biology has led to the emerging of a new subdisciplines such as chemical biology. Although this discipline is relatively new, the scientific community has witnessed many breakthrough discoveries and some of these discoveries are highlighted in this chapter. After the general introduction presented in chapter 1, the following chapters of this thesis focus on the design, synthesis and evaluation of small molecular probes towards the study of proteins and glycans in plant and mammalian cells. Most of these probes are complex glycomimetic small molecules that in many instances are prepared with a nitron-olefin [3+2] cycloaddition as a key step.

In **chapter 2**, a novel nitron is presented for the nitron-olefin [3+2] cycloaddition reaction. This reaction is a powerful tool in synthetic organic chemistry for the synthesis of a wide range of complex molecules. The versatile nature of the reaction is illustrated by the synthesis of several classes of natural product such as vitamins and alkaloids – all complex molecules containing multiple neighboring chiral centers – through the nitron-olefin [3+2] cycloaddition. However, most nitrons that show good regio- and stereoselectivity are limited in their synthetic versatility, as subsequent synthetic modification of the cycloaddition products are limited. The nitron described in chapter 2 is a novel masked aldehyde-containing nitron. This nitron is prepared by a simple and scalable procedure and can be combined with a diverse set of olefins and other dipolarophiles to afford a broad range of cycloadducts. These cycloadducts can be considered as a masked form of amino-aldehydes, which makes them interesting from a synthetic point of view as illustrated by several postcycloaddition modifications.

The nitron-olefin [3+2] cycloaddition is also utilized in **chapter 3** for the synthesis of glycomimetic building blocks. Glycomimetics such as iminosugars and pipecolic acids are found in nature and possess a variety of biological activities. The potential of glycomimetics have led to the development of drugs for the treatment of diseases such as type 2 diabetes, Gaucher disease and HIV. Chapter 3 describes how glycomimetic building blocks can be obtained through a nitron-olefin [3+2] cycloaddition, providing different bicyclic isoxazolidines. These cycloadducts are synthetically versatile, as we report a set of reactions that allow selective modification at each functional position. Accordingly, these versatile bicyclic isoxazolidines enable the synthesis of different glycomimetic building blocks. For example, we were able to make a library of pipecolic acid derivatives – a popular drug-motif – via a one-pot Staudinger/aza-Wittig/Ugi three-component reaction.

The bicyclic isoxazolidines, discussed in chapter 3, are also reported in **chapter 4**. This chapter describes the development of a synthetic route towards an activity-based probe (ABP) to study the enzymatic activity of neuraminidases. Neuraminidases are a class of enzymes found in a range of organisms including mammals. The importance of neuraminidases is illustrated by the existence of a neuraminidase-related genetic disease, sialidosis. With no cure for this fatal disease being very limited, there is keen interest in the discovery of novel mechanisms to restore neuraminidase activity. The poor enzyme-activity of a different enzyme-related disease, Gaucher disease, could be improved through the identification of a small molecule that stabilizes and/or promotes the folding of the active enzyme. The validation of this small molecule was aided greatly by the development of a sensitive ABP targeting this disease specific enzyme. Accordingly, the development of a neuraminidase-ABP would provide a diagnostic tool to study the activity of neuraminidases and ultimately help identify small molecules that could increase the activity of mutant-neuraminidase molecules by stabilizing and/or promoting the folding of this enzyme. The synthesis of a carbocyclic neuraminidase ABP was the goal of chapter 4 and was approached by starting with the nitrone-olefin [3+2] cycloaddition as the key-step. This reaction provided a bicyclic cycloadduct that was used for the development of a synthetic route, which led to a high yielding and practical synthesis of an advance intermediate possessing the majority of the stereochemistry of the required carbocyclic neuraminidase ABP.

**Chapter 5** describes the synthesis and evaluation of chemical tools to study phosphatidyl ethanolamine-binding proteins (PEBPs). This family of proteins is found in a variety of organisms including mammals and plants. This family includes FLOWERING LOCUS T (FT), a signaling protein that acts as a vital flowering hormone in plants. No small molecule inhibitors for FT are known, but an inhibitor called locostatin has been reported to bind in the highly conserved ligand binding site of a structurally related protein. Based on this conservation and overall structural similarity with FT it was hypothesized that locostatin or derivatives thereof could covalently bind in the ligand binding pocket of FT and hence affect flowering. Chapter 5 reports on the synthesis of novel locostatin-based chemical PEBP probes, followed by evaluation for their ability and selectivity towards FT and a mammalian PEBP.

Chemical tools were also used to study plants in **chapter 6**, although different aspects of plants were investigated. This chapter describes the direct molecular imaging of carbohydrates (glycans) in *Arabidopsis thaliana*. Glycans play a crucial but not fully understood role in plant health and development. The formation of glycans is not genetically encoded, which makes it impossible to image them in vivo using genetically encoded fluorescent tags and related molecular biology approaches. A solution to this problem is the use of tailor-made glycans that are metabolically incorporated in plants via the roots, which may then be visualized with copper-catalyzed click labeling. However, this labeling-technique is toxic to plants and future applications would benefit from bio-orthogonal copper-free labeling techniques. Chapter 6



shows, for the first time in metabolic labeling and imaging of plant glycans, the potential of two copper-free click chemistry methods. These methods are bio-orthogonal and lead to more uniform labeling. Furthermore, this chapter also describes the metabolic incorporation of five novel monosaccharide probes in *Arabidopsis thaliana* roots and their imaging after (copper-free) fluorescent labeling.

Finally, **chapter 7** contains a general discussion, critically summarizing the body of this thesis along with additional ideas and recommendations for further research.

# Acknowledgments

Finally, acknowledgments. I have reached the point of my thesis that people will actually read. A PhD-thesis is read on average by 1.6 people according to often quoted (untrue?) statistics,<sup>1</sup> but the acknowledgments are the uncontested exception to that rule. So here goes!

There are no official rules to writing acknowledgements, but there are several examples illustrating how you shouldn't write acknowledgments.<sup>2,3</sup> For example, I am pretty certain that you shouldn't mention that the world will continue spinning if your supervisor is hit by a truck (especially if that supervisor turns out to become a Nobel prize winner).<sup>2</sup> Fortunately, I have had the honor and delight to be supervised by very good people during my PhD. Therefore, I would like to thank my promotor Han Zuilhof and Tom Wennekes. Han, as promotor, thank you for the opportunity to start my PhD at the Laboratory of Organic Chemistry (ORC) and for guiding me in becoming an independent professional scientist. Beyond that I enjoyed our discussions at the coffee-table, which involved numerous scientific and non-scientific topics. Tom, I would like to thank you most of all. You have been my daily supervisor for the duration of my PhD and the door to your office was always open. This I mean both in the literal sense and in the practical sense, as you were always available for questions, be it project-based or not. I enjoyed your enthusiasm, your commitment, your involvement in social activities in and around ORC and as an example of excellent science communication.

Of course I would like to thank all my colleagues and students at ORC who not only helped with figuring things out in the lab, but also in contributing to the lively and social atmosphere at ORC. With that I mean all the social gatherings during borrels, boardgame-nights, movie-nights and the lively conversations during coffee-breaks. So thanks (in no particular order), Maurice Franssen, Ton Marcelis, Marijn Schrage, Sweccha Joshi, Wilco Duvivier, Elly Geurtsen, Fred van Geenen, Bas van den Berg, Stefanie Lange, Digvijay Gahtory, Tjerk Sminia, Willem van Heugten, Satish Gangarapu, Radostina Manova, Teris van Beek, Bram Bielen, Jaime Garcia Hartjes, Wouter van der Schoot, Ai Nguyen, Aleida Ruisch, Frank Versluis, Nagendra Bhairamadgi, Esther van Andel, Milou Santbergen, Jorge Escorihuela Fuentes, Ester Roeven, Maarten Smulders, Rui Rijo da Costa Carvalho, Jorick Bruins, Jose Maria (Txema) Alonso Carnicero, Quyen (Christie) Nguyen, Erik van Rozendaal, Luc Scheres, Cees van Rijn, Aline Debrassi, Anne-Marie Franssen, Bauke Albada, Florine Duval, Alexandre Villela, Carel Weijers, Floris van Delft, Rickdeb Sen, Jacob Baggerman, Zhanhua Wang, Sjoerd Slagman, Fatima Garcia Melo, Umesh Chinnaswamy, Sidharam Pujari, Medea Kosian, Remco Regeling, Cees van der Haar, Hendra Willemen, Anke Trilling, Pepijn Beekman, Ian de Bus, Louis de Smet

And of course the technicians that keep the place running. For after all, there is no ORC without its technicians. So thank you Barend van Lagen and Pepijn Geutjes for all your help with NMR and IR measurements. Pepijn I would like to thank you specifically for your help with the development of the H2BC NMR-technique! Elbert van der Klift and Frank Claassen for your help with HPLC, GC and MS measurements and Jelmer van der Rijst for repairing and

inventing a plethora of equipment. Judith Firt for the synthesis of several key-intermediates that played a role in several chapters and publications.

Furthermore I would like to thank the different research groups and the researchers that became involved during my PhD. First of all, the people of Wageningen Plant Research. I especially would like to thank dr. Martijn Fiers and prof. Richard Immink who became involved right at the start of my PhD. Richard you were available from the beginning for all of my question about plant molecular biology. You took the time for my initial research plan and for every version of the locostatin-paper. Martijn thank you for your help with familiarizing myself outside an organic chemistry lab. Your help allowed me to become acquainted with plant molecular biology. In addition, your help with the first 'wild-west' experiments to image glycans in plant roots later formed the basis of chapter 6. Then, I would like to thank Jeroen de Keijzer for helping me with ImageJ and the people of the laboratory of molecular biology with special regard to Rene Geurts, Martinus Schneijderberg, Olga Kulikova and Rik Huisman for their help in and around the lab with the metabolic labeling experiments.

Special thanks to my students Sam Overduin, Jona Merx, Michiel Uiterweerd and Nathalja Berghuis. Each of you made significant contributions to this thesis. Jona, thank you for your perseverance in investigating nitron-olefin [3+2] cycloaddition reactions and the selective modification of the resulting cycloadducts. Your work showed that it is not trivial to find conditions to modify complex isoxazolidines, but your perseverance encouraged myself to keep looking for selective conditions to modify this substrate-class. Eventually, by utilizing unconventional reagents it became possible to selectively modify these bicyclic isoxazolidines, which is where Michiel Uiterweerd took over. Michiel your enthusiasm for synthetic organic chemistry was inspiring. At the start of the project we encountered an unexpected product, but your persevere, creativity and theoretical insight allowed us to make use of this unexpected sideproduct. This led to the development of a new synthetic route towards the desired carbocycle, which forms the foundation of chapter 4. Finally, Nathalja your hard efforts have led to the development of a new method to image metabolically incorporated glycans in plant-roots. You quickly showed that you could work independently in an interdisciplinary environment of both an organic chemistry and a plant molecular biology laboratory. Your efforts in these laboratories led to an excellent report that allowed me to write an article of which you are a proud co-first author.

During my time at ORC I was proud to witness the formation of several new and the continuation of old traditions. ORC has always known borrels and has loved game- and movie-nights, but I would like to thank several members of the usual suspects for their enthusiasm in organizing these events (Bas, Tjerk, Freddie, Jorick, Jaime and many others) and all the people who participated in Team Lutidine for a pubquiz at the Orion. I also would like to thank my fellow synthetic organic chemists at ORC and their enthusiasm in hosting several Food Science and Beer evenings (FSB-meetings). These infamous meetings continue

to this day and wouldn't be the same if not for these people: Tjerk, Jorick, Bas and Sjoerd.

Bas and Tjerk, you two are not only my paranymphs, but during my PhD you have become two of my closest friends. Bas you are always there to provide a helping hand, or lend a listening ear even if it was to one of my crazy ideas. Tjerk, you were always an enthusiastic participator in any event being organized, be it a flash BBQ, another escape room or as an actor in another wacky movie-scene for a defense-party. In addition, I enjoyed and still enjoy going for a run together in and around Wageningen.

Dan mijn ouders. Jullie hebben mij gesteund al lang voordat ik aan dit avontuur begon. Jullie hielpen mij bij het schrijven van mijn eerste sollicitatiebrieven en waren een steun in mijn rug tijdens mijn schooljaren, mijn studie en tijdens mijn tijd hier in Wageningen. Het blijft bijzonder dat twee gamma-ouders drie bèta-kinderen hebben gekregen, maar ik heb altijd ervaren dat jullie zeer betrokken waren tijdens mijn studie, mijn werk tot en met het lezen van mijn eerste (bèta-)artikel. Dank jullie daarvoor!

Marijn, ware het niet vanwege deze PhD, dan zou ik jou niet ontmoet hebben. We begonnen allebei op exact dezelfde dag op ORC, jij met je MSc-stage en ik voor deze PhD. Iedereen die een PhD doet heeft wel momenten dat hij/zij daarover twijfelt; "had ik hier wel aan moeten beginnen?". Die beslissing was altijd makkelijk te relativeren alleen al omdat ik anders jou nooit ontmoet zou hebben. Bovendien ben ik je zeer dankbaar voor alle steun, liefde en geduld de afgelopen jaren die ook voor jou niet altijd eenvoudig waren. Je bent geweldig en ik hou van je!

Jorin

## References

1. The past, present and future of the PhD thesis *Nature* **2016**, 535,(7). doi:10.1038/535007a
2. Schoonbeek, Franck S. (2001). Making it all stick together: The gelation of organic liquids by small organic molecules. [Groningen]: University of Groningen
3. Laughlin, Scott T. (2002). Chemical approaches to imaging glycans in living animals. [Berkeley]: University of California

# List of Publications

**A plant-based chemical genomics screen for the identification of flowering inducers**

M. Fiers, J. Hoogenboom, A. Brunazzi, T. Wennekes, G. Angenent, R. Immink

*Manuscript in preparation*

**Exploring the chemistry of bicyclic isoxazolidines for the multicomponent synthesis of glycomimetic building blocks**

J. Hoogenboom, H. Zuilhof, M. Lutz, T. Wennekes,

*J. Org. Chem.*, **2016**, 81, 8826-8836

**Direct imaging of glycans in Arabidopsis roots via click labeling of metabolically incorporated azido-monosaccharides**

J. Hoogenboom, N. Berghuis, D. Cramer, R. Geurts, H. Zuilhof, T. Wennekes,

*BMC Plant Biology*, **2016**, 16, 220

**Synthesis and evaluation of locostatin-based chemical probes towards PEBP-proteins**

J. Hoogenboom, M. Fiers, R. Immink, H. Zuilhof, T. Wennekes,

*Tetrahedron Lett.*, **2016**, 57, 2406

**Versatile Scope of a Masked Aldehyde Nitrone in 1,3-Dipolar Cycloadditions**

J. Hoogenboom, H. Zuilhof, T. Wennekes,

*Org. Lett.*, **2015**, 17, 5550

**Allylpalladium ( II ) Histidylidene Complexes and Their Application in Z-Selective Transfer Semihydrogenation of Alkynes**

R. M. Drost, D. L. J. Broere, J. Hoogenboom, S. N. de Baan, S.N. Lutz, B. de Bruin, C.J. Elsevier,

*Eur. J. Inorg. Chem.* **2015**, 982

## About the author



Jorin Hoogenboom was born on the 11<sup>th</sup> of February, 1988 in Haarlem, the Netherlands. After secondary HAVO education at the Schoter Scholengemeenschap in Haarlem, he started with a bachelor education in organic chemistry at the University of Applied Sciences in Leiden. As part of this study he conducted an 9-month internship at Syncom BV. During this internship he focused on the synthesis and chiral resolution of new families of  $\gamma$ -amino alcohols that can be used in (Dutch) resolutions. After obtaining his bachelor's degree in 2009, he decided to continue in the field of organic chemistry by starting the MSc program Molecular Design, Synthesis and Catalysis at the VU university Amsterdam. This MSc program included a 6 month internship conducted at the synthetic Organic Chemistry group of Prof. dr. H. Hiemstra and Prof. dr. J. H. van Maarseveen. This research under the supervision of dr. J. Rutters resulted in the master thesis 'A novel auxiliary-mediated approach towards peptide ligation'. While finishing his MSc, he conducted a second (4 month) internship at the University of Amsterdam where he worked under the supervision of Prof. dr. C. J. Elsevier and dr. R. Drost focusing on the synthesis of histidine derived NHC-Pd complexes. Almost directly after obtaining his MSc-degree in 2011 he returned to Syncom BV to work as a research chemist focused on custom synthesis for different international clients. In July 2012 he left Syncom to start his PhD at the Laboratory of Organic Chemistry at Wageningen University under the supervision of dr. Tom Wennekes and Prof. dr. Han Zuillhof, the results of this work are described in this thesis. Jorin currently works as a researcher at Synaffix BV, focusing on the development of antibody-drug conjugates.

## Overview of completed training activities

<b>Discipline-specific activities</b>	<b>Organizing institute</b>	<b>Year</b>
Synthesis School “New vistas in organic chemistry”	HRSMC	2013
Advanced Organic Chemistry	ORC	2012-2015
International Carbohydrate Symposium (presentation)	ACS	2016
Wageningen Symposium on Organic Chemistry (presentation)	KNCV	2013-2016
New Frontiers Symposium	NCMLS	2013
NWO CHAINS Conference (posters & presentation)	NWO	2014-2015
Van ‘t Hoff Symposium	KNAW/UU	2013
<b>General courses</b>		
Information Literacy	WUR	2012
PhD-week	VLAG	2012
ACS on Campus	ACS	2013
Advanced Course Guide to Scientific Artwork	WUR	2014
PhD Workshop Carousel	WIAS	2014
Scientific Writing	WUR	2015
Adobe Indesign	WUR	2016
<b>Optionals</b>		
Preparation of PhD research proposal	ORC	2012
NWO Organic Chemistry Conference (poster)	NWO	2012-2013
Organizing Committee PhD trip ORC to Germany/Switzerland	ORC	2013
PhD study trips Germany/Switzerland and Canada	ORC	2013-2015
NMR course - Mnova	Mestrelab	2015





The research presented in this thesis was financially supported by The Netherlands Organization for Scientific Research (NWO) via ChemThem Chemical Biology grant (728.011.105).

Financial support from Wageningen University for printing this thesis is gratefully acknowledged.

Cover design: Iliana Boshoven